Temporal evolution of the termini and subaqueous morphologies of lake-calving glaciers in *Aoraki*/Mount Cook National Park, New Zealand

A thesis presented in partial fulfilment of the requirements
for the degree of
Doctor of Philosophy in Geography
at Massey University, Palmerston North, New Zealand.

Clare Margaret Robertson

2012

This is for you Dad. I wish you were here to see it.

Abstract

The potential impact that subaqueous mass loss may have on glacier mass balance and volume reduction is unclear, primarily due to a lack of quantitative data. Therefore, in order to fully understand the potential contribution subaqueous calving and melting may make to glacier mass loss, it is important to understand how submerged extensions of glacier fronts ("ice ramps") are created and maintained. This study improves the understanding of the controls on subaqueous ice ramp development and evolution at debris-covered, lake-calving margins by investigating the temporal evolution and subaqueous morphology of the termini of lake-calving glaciers in *Aoraki*/Mount Cook National Park, New Zealand. These glaciers are in close proximity to each other, yet each represents different stages on the glacier retreat-proglacial lake development continuum. Through a combination of field-based data collection and remote sensing, the calving margins of Mueller, Hooker, Tasman, Murchison, Classen, Grey, Maud and Godley glaciers were examined over a variety of time scales (days to years). This research indicates that the evolution of subaqueous ice ramps is intrinsically linked to subaerial retreat and that temporal changes in subaqueous morphologies are driven by subaerial calving, subsequent subaqueous calving, and sedimentation. The study highlighted that it is vital to understand the subaqueous morphologies of glaciers, how these evolve over time and what controls this evolution. In addition, when predicting glacier retreat it is important to consider subaqueous morphologies, through the incorporation of quantitative data and waterline melt rates, in order to more accurately predict retreat and hence mass loss from a glacier. Glacier retreat and concurrent proglacial lake expansion were also found to vary significantly within a single mountain belt. The identification of subaqueous ice ramps extending from lake-calving debris-covered glaciers, along with the examination of controls on ice ramp development and evolution, contributes significantly to the understanding of subaqueous morphologies and potential mass loss from these sections of the glacier. These results also lead to a better understanding of how subaqueous sections influence overall glacier retreat.

Thesis structure and note on authorship

This thesis consists of traditional thesis-style chapters (chapters 1, 2 and 7) and manuscripts written for publication in scientific journals (chapters 3-6). As a result, there is some repetition in chapters 1 to 6, particularly in the introduction, methods and study area sections. Some journal specific restrictions, such as abstract length and key words, are retained in the thesis.

I completed all the field work at *Aoraki*/Mount Cook National Park, analysed data and wrote all the text in this thesis. Manuscripts are however co-authored to acknowledge the input of others into the PhD, as appropriate. My supervisors, Martin Brook, Ian Fuller, Douglas Benn, and Kat Holt, contributed to developing the project concept, editing manuscripts and providing general advice. Statements (Doctoral Research Committee form 16) regarding the contribution made by myself to chapters 3-6 and consent of the co-authors to include their work in the thesis are contained in the Appendices.

Clare Robertson

Acknowledgements

My PhD research would not have been possible without the support, guidance and advice of a number of people. Acknowledgements relating to individual chapters are included at the end of those chapters.

Firstly, I wish to thank my family. You lot have been my rock for the past 3 years. You may not have completely understood my ‘nerd-talk’ but you still listened, appeared interested, and encouraged me. Dad, I wish you were here to see the final product. You always knew I could do it and that helped me push through the obstacles. I finished this for you. John, you have listened to me complain for the past 3 years! I couldn’t have kept going if it wasn’t for your encouragement and support.

I would like to thank the Ryoichi Sasakawa Young Leaders Fellowship Fund for awarding me a fellowship. I could not have started or finished this work without this funding. I am also grateful for receiving the Harrette Jenkins Award from the Manawatu Branch of the New Zealand Federation of Graduate Women.

I could not have completed my fieldwork without the enthusiastic bunch of people that helped me. David Feek’s expertise and help were often the difference between success and failure in the field, while Rob Dykes often acted as a sounding board for field frustrations. John Appleby, Jess Costal, Jingjing Wang, Alastair Clement, Sam Benny and Rob Eastham all provide invaluable help on the lakes and shared in the suffering of carrying equipment to and from Mueller lake. I would like to thank Charlie Hobbs for being so enthusiastic about Mueller lake and this research. I knew I always had eyes on the lake when I wasn’t there. Thanks for all those hot chocolates too! Thanks to The Helicopter Line Mount Cook and Tekapo Helicopters who flew on the boundaries of

weather and weight limits to get my equipment where I needed it. Field accommodation help from The New Zealand Alpine Club was also greatly appreciated.

I wish to thank my supervisory team whose encouragement, guidance and patience through difficult times pushed me through to the end. In particular, I would like to thank Dr. Ian Fuller and Dr. Kat Holt who agreed to be a part of the team even though they were from different research areas, and Prof. Doug Benn, who provided invaluable advice and critical insight from the other side of the world and boosted my confidence in the process.

Table of Contents

Abstract iii

Thesis structure and note on authorship v

Acknowledgements vii

List of Figures xiv

List of Tables xxiii

Chapter 1: Introduction 1

1.1 Background 1

1.2 Aim, scope and objectives 3

1.3 Thesis structure 5

Chapter 2: Lake-calving glaciers 7

2.1 Introduction 7

2.2 The significance of calving glaciers 7

2.3 Influence of the proglacial water body 11

2.3.1 Development of proglacial lakes 12

2.3.2 Waterline melt 14

2.3.3 Subaqueous melt 15

2.3.4 Thermal regime 18

2.3.5 Circulation and convection 20

2.3.6 Lake level 22

2.4 Calving processes 23

2.4.1 The role of crevasses 23

2.4.2 Hierarchy of mechanisms that trigger calving 28

2.4.2.1 Stretching in response to large-scale velocity gradients 28
2.4.2.2 Force imbalances at unsupported ice cliffs 29
2.4.2.3 Undercutting by subaqueous melting 30
2.4.2.4 Torque arising from buoyant forces 30
2.4.2.5 Coseismic triggers 31
2.4.3 Calving types 31
2.4.3.1 Buoyant calving 32
2.4.3.2 Waterline melt-driven calving 32
2.4.3.3 Exploitation of crevasses created as a result of stretching of the front 33
2.4.4 Seismicity of calving 33
2.5 Glacier dynamics and calving 34
2.5.1 Calving as the 'master' 35
2.5.2 Calving as the 'slave' 35
2.6 Velocity 36
2.7 Calving laws and glacier models 38
2.7.1 Evolution of calving laws 38
2.7.2 The crevasse-depth calving criterion 42
2.7.3 Calving law derived from fracture-scale physics 43
2.7.4 Representation of calving in glacier models 44
2.8 Conclusions 44

Chapter 3: Glacier retreat and proglacial lake expansion in *Aoraki*/Mt Cook National Park, New Zealand 47

3.1 Introduction 47
3.2 Abstract 48
3.3 Introduction 49
3.4 Study area 51

3.4.1 Physical setting 51
3.4.2 Existing data on historical glacier fluctuations 56
3.5 Methods 58
3.6 Results: Glacier retreat and proglacial lake development 59
3.6.1 Mueller Glacier 64
3.6.2 Hooker Glacier 64
3.6.3 Murchison Glacier 66
3.6.4 Classen Glacier 66
3.6.5 Grey and Maud glaciers 66
3.6.6 Godley Glacier 67
3.7 Discussion 67
3.7.1 Retreat rates 67
3.7.2 Trends in lake expansion 71
3.7.3 Spatial and temporal evolution model 72
3.8 Conclusions 74
3.9 Acknowledgements 75

Chapter 4: Subaqueous calving margin morphology at Mueller, Hooker and Tasman glaciers in *Aoraki*/Mount Cook National Park, New Zealand 77
4.1 Introduction 77
4.2 Abstract 78
4.3 Introduction 78
4.4 Study area 81
4.4.1 Mueller Glacier 81
4.4.2 Hooker Glacier 83
4.4.3 Tasman Glacier 84
4.5 Methods 85

4.6 Results 86
4.6.1 Mueller Glacier and lake 86
4.6.2 Hooker Glacier and Lake 89
4.6.3 Tasman Glacier and Lake 91
4.7 Discussion 92
4.7.1 Calving and retreat rate 94
4.7.2 Debris on the ice ramps 95
4.8 Conclusion 97
4.9 Acknowledgements 98

Chapter 5: Temporal evolution of the calving terminus at Mueller Glacier, *Aoraki*/Mount Cook National Park, New Zealand 99
5.1 Introduction 99
5.2 Abstract 100
5.3 Introduction 101
5.4 Study area 102
5.5 Methods 104
5.6 Results 107
5.6.1 Terminus subaerial morphology 107
5.6.2 Subaqueous morphology and lake size 109
5.6.3 Vertical and horizontal terminus displacements 114
5.6.4 Water temperature 117
5.7 Discussion 118
5.7.1 Subaqueous morphology 118
5.7.2 Horizontal and vertical displacements on the terminus 120
5.8 Conclusion 122
5.9 Acknowledgements 123

Chapter 6: Calving retreat and proglacial lake growth at Hooker Glacier, Southern Alps, New Zealand 125

6.1 Introduction 125

6.2 Abstract 126

6.3 Introduction 126

6.4 Study area 128

6.5 Methods 130

6.6 Results 131

6.7 Discussion 139

6.7.1 Retreat rates 139

6.7.2 Retreat scenarios 140

6.8 Conclusions 143

6.9 Acknowledgements 144

Chapter 7: Synthesis and Conclusions 145

7.1 Introduction 145

7.2 Avenues for future research 149

7.3 Concluding remarks 153

Chapter 8: References 155

Chapter 9: Appendices 175

List of Figures

Figure 2.1: Icebergs produced from multiple calving events, grounded near the outlet of Tasman Lake, the proglacial lake adjacent to Tasman Glacier (source: C. Robertson, 2 April 2008). Englacial and some supraglacial debris has remained on the icebergs during calving and been transported down the lake. Calving permits much larger volumes of ice to be lost from the glacier than melting alone. 8

Figure 2.2: The rock avalanche from *Aoraki*/Mount Cook on 14 December 1991 (Photo: CN21503/11: D. L. Homer in Cox & Barrell, 2007). The avalanche descended 2720 m down the eastern side of *Aoraki*/Mount Cook and was deposited onto Tasman Glacier. The deposit formed closely spaced arcuate debris ridges on the glacier at the confluence of Tasman Glacier and the Hochstetter icefall (seen in the centre of the photo) which have elongated since deposition (Quincey & Glasser, 2009). The deposit caused the development of a 25 m high, debris-covered, ice ridge on the up-glacial edge of the deposit (Reznichenko *et al.*, 2011)..... 11

Figure 2.3: Sequence of retreat and subsequent proglacial lake development on a low-gradient glacier bound by the reverse slope of an outwash head (Figure 9 Kirkbride, 1993): 1) slow melting under a mantle of supraglacial debris; 2) collapse of conduits perforates the debris layer which allows rapid melting of exposed ice walls; 3) growth and coalescence of supraglacial ponds into a lake which may have an ice-cored floor. Subaqueous icebergs may calve from this floor; 4) disintegration of the ice-cored floor increases water depth and initiates rapid calving retreat. 13

Figure 2.4: A thermo-erosional notch (shown by the black arrow), formed at the waterline, at the terminal ice cliff of Mueller Glacier, New Zealand (source: C. Robertson, 20 November 2009). The rate of thermo-erosional notch development may directly control subaerial calving at some freshwater terminating glaciers, such as Tasman Glacier (Röhl, 2006). 15

Figure 2.5: Convection cell circulation patterns from laboratory experiments of ice melt in freshwater (after Figure 3 Eijpen *et al.*, 2003). Different subaqueous melt rates and hence geometries are created in different

freshwater temperatures. Circulation within the experimental tanks was minimised, however, in reality, circulation and convection in a proglacial lake is driven by a combination of glacial and non-glacial inflows and climatic parameters. Thus, circulation and convection patterns observed in this study may be markedly different from what occurs in a proglacial lake. 18

Figure 2.6: Factors that influence circulation and convection within a proglacial lake; water inflows, suspended sediment concentration, thermal regime, wind and solar radiation. The upper layers of a water body are mixed predominantly by waves and surface currents generated by wind. Mixing within the lake is influenced by the density of water entering the lake from precipitation, streams, meltwater streams from the glacier and meltwater delivered via englacial and subglacial conduits. Icebergs calving into the lake and melting will cool surrounding water. 21

Figure 2.7: Crevasses in the terminal ice cliff at Mueller Glacier (source: C. Robertson, 17 November 2009. The location, timing and magnitude of calving is determined by the location of crevasses which open in response to stresses and propagate to isolate blocks of ice from the glacier. 24

Figure 2.8: Three basic modes of ice fracture (Figure 3 Benn *et al.*, 2007b). Mode I describes tensile cracking where the walls of a fracture separate. Mode II occurs when fracture walls remain in contact but slide past each other. Mode III occurs when the fracture propagates at right angles to the direction of shear. If more than one mode of fracturing occurs it is termed mixed mode fracture. 26

Figure 2.9: Debris bands in the terminal ice cliff of Hooker Glacier, New Zealand (source: C. Robertson, 23 November 2009). Along with crevasses, the location, orientation and spacing of such weaknesses can control calving rates. 33

Figure 2.10: The relationship between calving rate and water depth for glaciers in different regions around the world (after Haresign, 2004). Calving rates for tidewater glaciers are larger than those at lake-calving termini. Data sources: New Zealand lakes: Warren & Kirkbride (2003), Tasman Glacier: Dykes & Brook (2010), Patagonian lakes: Rivera *et al.* (1997), Rott *et al.* (1998), Skvarca *et al*. (1995), Warren (1999), Warren *et al.* (1995b),

Warren *et al.* (2001), Breiðamerkurjökull: Björnsson *et al*. (2001), Mendenhall: Motyka *et al*. (2003c), European Alps (lakes): Funk & Röthlisberger (1989), Alaska (tidewater): Brown *et al.* (1982), Meier *et al.* (1985), Pelto & Warren (1991), West Greenland (tidewater): Carbonell & Bauer (1968), Svalbard (tidewater): Jania (1986), Pillewizer (1965), Wilhelm (1963). 41

Figure 3.1: Map showing the location of Mueller, Hooker, Murchison, Classen, Grey, Maud and Godley glaciers and their proglacial lakes. 52

Figure 3.2: Lower terminus and proglacial lakes in *Aoraki*/Mount Cook National Park: A) Mueller Glacier (source: C. Robertson, 28 January 2011). Mueller Glacier is on the left of the photo and Hooker River enters the lake in the top right-hand corner; B) Murchison Glacier (source: T. Chinn, 2011); C) Hooker Glacier (source: C. Robertson, 26 January 2011). 53

Figure 3.3: Lower terminus and proglacial lakes in *Aoraki*/Mount Cook National Park: A) Classen Glacier (source: T Chinn, 2011); B) Godley Glacier (far left of the photo) (source: S. Winkler, 2008). An enlarged image of the area in the red box is shown in C. C) Godley Lake is on the left with Godley Glacier retreating towards the right of the photo (source: T. Chinn). 2011); D) Grey (centre top of the photo) and Maud Glacier (on the right of the photo) entering Grey/Maud lake (source: T. Chinn, 2011). 54

Figure 3.4: Terminus positions of Mueller Glacier, 1986-2011 and Hooker Glacier, 1965-2011. 60

Figure 3.5: Terminus positions of Murchison Glacier, 1965-2010 and Classen Glacier, 1965-2008. 61

Figure 3.6: Terminus positions of Grey and Maud glaciers, 1965-2008 and Godley Glacier, 1965-2008. 62

Figure 3.7 (previous page): Retreat rate (u_r, m a^{-1}) and proglacial lake surface area (km^2) for A) Mueller Glacier, 1986-2011, B) Hooker Glacier, 1979-2011, C) Murchison Glacier, 1965-2010, D) Classen Glacier, 1965-2008, E) Grey and Maud glaciers, 1965-2008, and F) Godley Glacier, 1965-2008. Black diamonds on the lake surface area graphs represent values calculated in this study. Grey diamonds represent data from other studies: Mueller lake (Watson, 1995; Röhl, 2005), Hooker Lake (Warren &

Kirkbride, 1998), Grey/Maud lake (Warren & Kirkbride, 1998) and Godley lake (Warren & Kirkbride, 1998). 64

Figure 3.8: A four-stage model of spatial and temporal evolution of *Aoraki*/Mount Cook proglacial lakes. Stage 1: the appearance and growth of supraglacial lakes and/or meltwater channels on the lower ablation areas of glaciers. Stage 2: transition between supraglacial lakes and meltwater channels and a coalesced single lake. Stage 3: stable expansion of a single coalesced lake. Stage 4: slowing of retreat caused by shoaling as the valley's bedrock profile comes closer to lake level as retreat proceeds. Classen, Grey and Maud glaciers transited through stages 1 and 2 prior to 1965, although the transition between stage 1 and 2 is not constrained. Two distinct retreat phases between 1986 and the late 1990s, and 2006 and 2008, are superimposed on the four-staged model. All six glaciers are currently in stage 3, although the Godley Valley glaciers may be approaching stage 4. 73

Figure 4.1: Location of Mueller, Hooker and Tasman glaciers and their proglacial lakes. The Main Divide of the Southern Alps is highlighted by black dots..... 80

Figure 4.2: Mueller, Hooker and Tasman glaciers and their proglacial lakes: (A) the terminus of Mueller Glacier (on the left of the photo) and proglacial lake (source: C. Robertson, 28 January 2011). Hooker River can be seen entering the lake in the upper right-hand corner. The photo is taken from the south-western side of Mueller lake looking north-east. Hooker Glacier and Lake are behind the lateral moraine in the centre of the photo; (B) Hooker Glacier and Lake looking north-east towards Mount Cook (source: C. Robertson, 23 November 2009). Hooker Glacier can be seen flowing down valley, terminating in Hooker Lake. Eugenie Stream crosses an alluvial fan and enters the lake in the bottom left of the photo; (C) looking north-east up Tasman Lake to Tasman Glacier (source: C. Robertson, 25 November 2009)..... 82

Figure 4.3 (next page): Subaqueous terminus morphology and bathymetry of Mueller lake: A) November 2009. Lines A-A' and B-B' show the location of sub-bottom profile images in Figure 4.4; B) April 2010; C) the relative change in lake depth between November 2009 (A) and April 2010 (B). Negative values (red) show a decrease in depth and positive values (blue) show an increase in depth. 87

Figure 4.4: Sub-bottom profile images and interpretation from Mueller lake April 2010. Profile locations are shown in Figure 4.3. The box shows the approximate distal end of the ice ramp. 89
Figure 4.5: Subaqueous terminus morphology and bathymetry of Hooker Lake in November 2009. Line A-A' shows the location of the sub-bottom profile image. 90
Figure 4.6: Subaqueous terminus morphology of Tasman Lake in 2008. Line A-A' shows the location of the sub-bottom profile image. 92
Figure 5.1: A) Location of Mueller Glacier and the surrounding area. The black box shows the location of Figures 5.2, 5.3 & 5.4. The inset image shows the location of the lake mooring which collected lake temperature data, the weather station, and the depth data logger B) Mueller lake, with ice debris from a large collapse of subaerial ice cliffs ~100 m up-glacier of the terminus, (source: C. Robertson, 7 February 2011). Mueller Glacier is on the left of the photo. A swollen Hooker River can be seen entering the lake in the top right-hand corner. The photo is taken from Kea Point on the south-western side of Mueller lake looking north-east. 103
Figure 5.2: Subaerial morphology of the terminus of Mueller Glacier, February 2011. Fine-grained, glacio-fluvial sediment and coarse-grained, avalanche-derived sediment can be seen on the terminus. Exposed ice cliffs can be seen adjacent to Mueller lake, along the meltwater river and near the grey pond. 'Blue water' ponds can be seen on the SW of the terminus, which is lower in elevation than the rest of the terminus. 108
Figure 5.3: Variation in the terminus position of Mueller Glacier between November 2009 and February 2011, and the horizontal displacement of five prisms (numbered 1-5) on the terminus. The horizontal displacement (m) of each prism between the first and last survey, between 23 January and 18 February 2011, are shown by the black arrows (a 1 m scale arrow is shown in the legend). The location of the Trimble S6 automatic total station, used to survey the prisms, is also shown. Lines A-A' and B-B' show the location of sub-bottom sonar profiles shown in Figures 5.6 and 5.7. 109
Figure 5.4: The bathymetry of Mueller lake between November 2009 and February 2011. The approximate outline of the subaqueous ice ramp in

November 2009 and April 2010 is shown in (A) and (B). A DEM of difference between November 2009 and February 2011 is shown in Figure 5.5. Ice ramp data are not available for January and February 2011. 111
Figure 5.5: DEM of difference for Mueller lake between November 2009 and February 2011. Negative values (red) show a decrease in depth and positive values (blue) show an increase in depth. 112
Figure 5.6: Sub-bottom profile image A-A' and interpretation from Mueller lake, April 2010. The location of the image is shown in Figure 5.3. The images show ice at the bottom of the lake, which is overlain with fine-grained sediment (as identified by the thin laminations). Debris bands can be seen in the ice. Sediment on the lake side's slopes down and overlaps the ice. 113
Figure 5.7: Sub-bottom profile image B-B' and interpretation from Mueller lake April 2010. The location of the image is shown in Figure 5.3. The images show the lake floor near the terminus, which is underlain with ice. A thick layer of sediment (~5-7 m) covers the ice and debris bands can be seen within the ice. 114
Figure 5.8: Relative lake level, precipitation (from the climate station on the south-western side of the lake, shown in Figure 5.1), water temperature (at depth data logger, shown in Figure 5.1) and the vertical displacement of the five prisms on the lower terminus of Mueller Glacier, between 23 January to 18 February 2011. The symbols for each prism represent survey dates..... 116
Figure 5.9 (previous page): Lake temperature and precipitation in Mueller lake from 22 November 2009 to 30 April 2010. The first five graphs show water temperature at different depths approximately 100 m in front of the terminus and the bottom graph shows precipitation (mm d^{-1}) recorded at *Aoraki*/Mount Cook Village. Strong cooling typically occurred following a large precipitation event. The two grey lines show periods where a 1˚C drop in temperature was not associated with a large precipitation event..... 117
Figure 6.1: Map showing the location of Hooker Glacier and Lake in the central Southern Alps, New Zealand. Black dots denote the Main Divide of the Southern Alps. Sheila, Empress and Noeline glaciers, tributaries of Hooker Glacier, are also shown. 129

Figure 6.2: Hooker Glacier terminating into Hooker Lake (view to the northeast). Hooker River exits the lake near the bottom of the photo (source: C. Robertson, 26 January 2011). 130
Figure 6.3: Terminus positions of Hooker Glacier, 1965 to 2011. Supraglacial and ice-marginal ponds, which developed between 1965 and the early 1980s, coalesced in 1982. Since 1965 the terminus of Hooker Glacier has retreated 2.14 km up-valley from its LIA terminal moraine. The 1996 terminus position is from Hochstein *et al.* (1998). 132
Figure 6.4: Surface area of Hooker Lake between 1965 and 2011. Growth in lake surface area has followed a steadily increasing trend after the coalescence of supraglacial and ice-marginal ponds in 1982 and subsequent high retreat rates. 133
Figure 6.5: Ice cliff at the terminus of Hooker Glacier (source: C. Robertson, 23 November 2009). Note the layers of debris in the subaerial ice cliff which provide pre-existing weaknesses in the glacier which can be exploited to result in calving. The calving terminus is comprised of a vertical subaerial ice cliff (approximately 30 m high), which then forms a low gradient subaqueous ice ramp sloping away from the terminus into the lake. 133
Figure 6.6: Hooker Lake bathymetry and the location of an ice ramp which was identified in 2009 (Chapter 4). 134
Figure 6.7: Retreat rates and calving rates of Hooker Glacier between 1986 and 2011. U_r is retreat rate (mean retreat along the terminus multiplied by time), U_c is calving rate, $U_c + U_m$ is calving rate + melt at the calving cliff. Values are reported in Table 6.1. 137
Figure 6.8: Predicted retreat scenarios for Hooker Glacier. The profiles have a vertical exaggeration of approximately 12. The subglacial bedrock profile (dashed line) is inferred from Hochstein *et al.*'s (1998) ice thickness data, and is measured at 3 km and 4.8 km up-valley of the Hooker Lake outlet. The fast retreat scenario is based on waterline melt from Röhl (2005) and predicts the glacier terminus will stabilise > 3 km up-valley of the current lake outlet after 2028, when ice velocity equals calving rate. The slow retreat scenario, based on the calving rate-water depth relationship (established by Funk & Röthlisberger, 1989; Warren *et al.*, 1995b),

predicts the glacier will retreat ~4.8 km up-valley where it will stabilise as bedrock outcrops at lake level by 2096. 138
Figure 9.1: The EdgeTech 216S sub-bottom profiler being towed approximately 20 m behind the boat in Tasman Lake (source: C. Robertson, 2 April 2008). A RTK-dGPS rover attached to the top of the profiler to locate the survey. 181
Figure 9.2: The EdgeTech 216S sub-bottom profiler being towed approximately 10 m behind the boat in front of the terminus ice cliff of Hooker Glacier (source: R. Dykes, 29 November 2009). 182
Figure 9.3: EdgeTech 216S sub-bottom profiler towed beside the boat in Mueller lake (source: C. Robertson, 15 April 2010). The ballast (green tubes) which was attached to the profiler can be seen sitting above the water. The minicomputer and Toughbook used in conjunction with the profile can also been seen. Figure 9.4 shows a more detailed view of these components. 182
Figure 9.4: Minicomputer and Toughbook laptop used with the EdgeTech 216S sub-bottom profiler (source: C. Robertson, 15 April 2010). The profiler is attached to the yellow box (minicomputer) by a cable, with the minicopter then being connected to the Toughbook laptop. A profiler image can be seen on the Toughbook screen. The minicomputer is powered by batteries contained in the green plastic box. 183
Figure 9.5: An example of a sub-bottom profiler image from Hooker Lake which shows a considerable amount of acoustic blanking (shown by the arrows), the result of the signal being blocked by gas in the water column or lake bed. 184
Figure 9.6: An example of a sub-bottom profiler image from Mueller lake which shows acoustic scattering (the heavily lined part of the image) caused by gas in the water column or water inhomogeneities. Acoustic scattering prevents the image being analysed and interpreted due to the quality of the image. 185
Figure 9.7: The two buoys of the stationary lake mooring which 5 Onset Tidbit temperature loggers were attached to in Hooker Lake (source: C. Robertson, 28 November 2009). 188

Figure 9.8: The plastic basket the Onset U20-001-01 HOBO Depth Data Logger was deployed in to protect it from impacts (source: C. Robertson, 18 February 2011). This photograph was taken after the logger had been recovered in February 2011. Fine sediment can be seen on the basket from where it sunk into the sediment on the lake floor. 190
Figure 9.9: The Trimble S6 automatic total station (black box) established on Kea Point, ~150 m above Mueller Glacier, from where the photograph is taken (source: C. Robertson, 5 January 2011). 191
Figure 9.10: The Trimble S6 automatic total station established on Kea Point, ~150 m above Mueller Glacier (source: A. Clement, 21 January 2011). 192
Figure 9.11: The author beside a reflective prism that has just been attached to a large, stable, flat boulder on the surface of Mueller Glacier (source: A. Clement, 20 January 2011). The reflective face of the prism is directed towards Kea Point. The photograph is taken looking up-glacier. 193
Figure 9.12: An example of a photograph taken from a camera attached to the Lighter-than-air-Helikite (source: C. Robertson, 22 November 2009). The image contained a GCP (orange cross in the lower right hand corner) and could also be located (due to the inclusion of the boat and pond). The orange boat is approximately 3 m long. 195
Figure 9.13: An example of a photograph taken from the Lighter-than-air-Helikite that did not contained a GCP and therefore could not be located (source: C. Robertson, 22 November 2009). The large boulders in the upper and lower centre of the photograph are approximately 5 m in diameter. 196
Figure 9.14: An example of a photograph taken from the Lighter-than-air-Helikite that contained two GCPs (orange cross in the upper right corner and blue tarpaulin in the lower left corner) (source: C. Robertson, 22 November 2009). The photo could not be located as it was unclear what GCP the two are in the photo. The large boulder in the upper right of the photograph is approximately 5 m in diameter. 196

List of Tables

Table 3.1: Characteristics of glaciers and their proglacial lakes in *Aoraki*/Mount Cook National Park. Debris cover (%) gives the percentage of the glacier subaerial surface covered with debris. 55

Table 3.2: Retreat rates calculated in other studies for Mueller, Hooker, Classen, Grey, Maud, Godley and Tasman Glaciers. No additional retreat rate data for Murchison Glaciers have been published. Data for Grey Glacier are separated into Grey east and Grey west following Kirkbride (1993). While it is unclear in Kirkbrides (1993) study exactly what part of the glacier Grey east and Grey west refer to, it is assumed that rates for Grey east refer to the eastern boundary of Grey/Maud Glacier (when they were confluent) and Grey west rates refer to the western boundary of Grey/Maud Glacier (when they were confluent). Retreat rates for Tasman Glacier are incorporated for comparison purposes. 57

Table 3.3: Surface areas (km^2) of Mueller, Hooker, Murchison, Classen, Grey/Maud and Godley lakes calculated from aerial photographs, satellite images and field-based surveys. 66

Table 1.1: Physical characteristics of Mueller, Hooker and Tasman glaciers and their proglacial lakes. Supraglacial debris cover (%) refers to the percentage of the glacier surface area that is covered by debris ..... 83.

Table 1.2: Horizontal (H) and vertical (V) displacement (m) of prisms on the terminus of Mueller Glacier between 23 January and 18 February 2011 Data is non-cumulative and displacement is relative to the previous location. * is the first survey. 115

Table 6.1: Hooker Glacier full width retreat data between 1979 and 2011. ∂L_{max} is maximum retreat, ∂L_{mean} is mean retreat, U_r is retreat rate (∂L_{mean} multiplied by t to determine the annual rate), U_c is calving rate, $U_c + U_m$ is calving rate + melt at the calving cliff, D_w is water depth. Negative values indicate a width-averaged advance of the glacier. 135

Chapter 1: Introduction

1.1 Background

The recession of freshwater-terminating glaciers due to calving has become a widespread phenomenon in mountain glacier systems in recent decades, affecting glaciers in Patagonia (Warren, 1999; Warren & Aniya, 1999; Warren *et al.*, 2001; Haresign, 2004), the Himalaya (Benn *et al.*, 2001; Watanabe *et al.*, 2009; Thompson *et al.*, 2012), the European Alps (Diolaiuti *et al.*, 2005; Diolaiuti *et al.*, 2006) and New Zealand (Kirkbride, 1993; Kirkbride & Warren, 1997; Warren & Kirkbride, 2003; Röhl, 2005; Dykes *et al.*, 2011). Calving can also permit much larger volumes of ice to be lost from the glacier than would be possible from surface ablation alone (van der Veen, 2002; O'Neel *et al.*, 2007). Debate has focused on which mechanisms are causing observed increases in the rates of mass loss from calving termini, along with how these may influence future calving prognoses. A complicating factor however is that calving glaciers can become partially decoupled from climate, which results in factors other than equilibrium line altitudes (ELAs) controlling spatial extents (Mercer, 1961; Mann, 1986; Meier & Post, 1987; Alley, 1991; Powell, 1991; Warren, 1991; Fischer & Powell, 1998; Vieli *et al.*, 2001; Elsberg *et al.*, 2003; Nick & Oerlemans, 2006; Benn *et al.*, 2007b; Nick *et al.*, 2007).

Subaqueous calving and melting have been identified as important processes at water-terminating margins and have the potential to make large contributions to glacier mass loss (Eijpen *et al.*, 2003; Motyka *et al.*, 2003a; Haresign & Warren, 2005). Unlike subaerial calving, which can be a readily observed process, understanding the contribution of subaqueous calving and melting to glacier mass loss, and interactions between calving terminus dynamics and lake effects, remains severely limited due to a lack of quantitative data (Benn *et al.*, 2007b). Quantifying these contributions is also difficult due to factors including a hazardous working environment and spatially variable supraglacial debris covers, which may reduce melting, and therefore limit buoyant forces acting on ice (Hunter & Powell, 1998; Purdie & Fitzharris, 1999).

Hence, the potential impact of subaqueous calving and melting on glacier mass balance and volume reduction is particularly uncertain.

In order to fully understand the potential contribution subaqueous calving and melting may make to freshwater glacier mass loss, it is important to understand how submerged extensions of glacier fronts ("ice ramps") are created and maintained. Quincey and Glasser (2009 p. 193) noted, in relation to Tasman Glacier (New Zealand), that "establishing the presence or absence of a projecting ramp at the terminus of the glacier, the degree to which this affects subaerial ablation processes, and whether this contributes to mass loss by subaqueous calving would still be a significant step towards making a quantitative mechanics-based prediction of future lake expansion and is a clear area for further research". Understanding subaqueous margin morphology and the processes that control lake-calving glacier margins is important because of the recent and continuing rapid retreat of such mountain glaciers globally.

The presence or absence of ice ramps extending from calving margin termini have been mentioned in literature since 1919 when Nansen observed that "far away from [the glacier], out at sea, huge masses of ice may suddenly dart up from the depths and annihilate both boat and crew" (Nansen, 1919, as described by Benn *et al.*, 2007b). Since this observation, a number of authors have discussed, albeit briefly, the possibility of an ice ramp extending from glaciers (e.g. Howarth & Price, 1969; Purdie, 1996; Kirkbride & Warren, 1997; Motyka, 1997; Hochstein *et al.*, 1998; Hunter & Powell, 1998; Warren & Kirkbride, 1998; Röhl, 2005; Benn *et al.*, 2007b; Dykes *et al.*, 2011). Although no studies have specifically examined ice ramps, the importance of such features for glacier mass loss and retreat has been highlighted (Quincey & Glasser, 2009).

1.2 Aim, scope and objectives

The primary aim of the study is to improve the understanding of the controls on subaqueous ice ramp development and evolution at debris-covered, lake-calving margins. In order to do this, the study investigates the temporal evolution and subaqueous morphology of the termini of lake-calving glaciers in *Aoraki*/Mount Cook National Park, New Zealand. Mueller, Hooker, Tasman, Murchison, Classen, Grey, Maud and Godley glaciers and their proglacial lakes are investigated, with a particular focus on Mueller, Hooker and Tasman glaciers, where fieldwork was carried out. All of the *Aoraki*/Mount Cook National Park glaciers are in close proximity to each other, yet each represent different stages on the glacier retreat-proglacial lake development continuum. For example, calving began at Classen Glacier between 1930 and 1961, after which the glacier retreated 1.43 km, at an average rate of 57 m a^{-1} (Kirkbride, 1993). In comparison, Tasman Glacier began calving in 1991 (Hochstein *et al.*, 1995), and then entered a period of rapid retreat between 2006 and 2008, with the surface area of the proglacial lake expanding by 86% between 2000 and 2008 (Dykes *et al.*, 2010). Hence, examining and surveying such calving margins over a variety of time scales (days to years) allows an evaluation of the processes controlling terminus evolution, with a specific focus on subaqueous morphology.

Aoraki/Mount Cook glaciers and their adjacent proglacial lakes have been the focus of a broad variety of previous glacier research (e.g. Hicks *et al.*, 1990; Kirkbride, 1993; Hochstein *et al.*, 1995; Watson, 1995; Hochstein *et al.*, 1998; Warren & Kirkbride, 1998; Kirkbride & Warren, 1999; Purdie & Fitzharris, 1999; Warren & Kirkbride, 2003; Röhl, 2006; Quincey & Glasser, 2009; Dykes & Brook, 2010). Although these studies enable a comparison to be made between contemporary processes and published data, such studies have typically focused on retreat rates, calving rates and lake evolution on a single glacier. The last study that reviewed data from across several calving glaciers was published almost a decade ago (Warren & Kirkbride, 2003), and was based on data collected between 1994 and 1997. Subsequent studies have generally looked at these glaciers in isolation or with reference to a neighbouring glacier (Röhl, 2006; e.g. Dykes *et al.*, 2011). In addition, no studies have specifically examined the subaqueous calving margin morphologies, the evolution of such morphologies or subaqueous calving at the termini of glaciers in *Aoraki*/Mount Cook National Park. Given the dramatic changes

recorded at individual glaciers in *Aoraki*/Mt Cook National Park over the last decade (e.g. Röhl, 2006; Quincey & Glasser, 2009), quantification and a systematic analysis of calving retreat (both subaqueous and subaerial) and coeval proglacial lake development across the calving glaciers in the region is propitious. Subaqueous morphology and thus subaqueous calving are intrinsically linked to calving retreat and therefore must be analysed alongside subaerial calving retreat.

In order to achieve the primary aim of the study, four specific objectives are addressed. These are to:

1. Compare absolute rates of terminus retreat and proglacial lake development, and identify the processes responsible for this retreat, at lake-calving termini in *Aoraki*/Mount Cook National Park (chapter 3);
2. Map the subaqueous termini of Mueller, Hooker and Tasman glaciers to identify key characteristics of each calving margin (chapter 4);
3. Determine what processes control the development and evolution of subaqueous termini (chapter 4);
4. Examine the temporal evolution of the terminus (subaerial and subaqueous sections) of Mueller Glacier and identify the key controls for observed changes (chapter 5);
5. Predict future retreat scenarios for Hooker Glacier (chapter 6).

These objectives are addressed through a combination of field measurements and observations, remote sensing, and comparison with published data. Field-based investigations were carried out at Mueller, Hooker and Tasman glaciers and proglacial lakes between April 2008 and February 2011. These field surveys collected data on glacier, lake and climatic variables. Glacier variables included topographical data and horizontal and vertical displacements. Lake variables included bathymetric and sub-bottom profile data, water temperature, and lake level. Mueller Glacier was the focus of a more detailed study over a 16 month period. This investigation was necessary in order to better understand the controls of subaqueous morphology and its relationship to glacier retreat. Mueller Glacier was chosen due to the apparent rapidity of changes

occurring at the margin at the time of the study, the range of active processes, along with ease of access.

The study attempts to address some of the outstanding issues surrounding lake-calving subaqueous terminal morphology, while emphasising how the interaction of a variety of components at different margins, over different timescales, can produce varying forms of subaqueous termini. Thus, the study aims to extend the understanding of processes which operate to control the development and evolution of the subaqueous morphology of debris-covered, lake-calving glaciers and the timescales over which these processes operate.

1.3 Thesis structure

This thesis consists primarily of 'in press' or submitted manuscripts; hence, there is some degree of repetition between chapters, particularly the introductory, methodology and study area sections. Following this introduction, a review of lake-calving glacier literature is presented in Chapter 2. The chapter reviews previous research on lake-calving glaciers, with a particular focus on calving processes and subaqueous margin morphology. Following a discussion of the significance of calving glaciers, the development of the proglacial water body and the influence it has on the adjacent glacier is examined. Calving processes and glacier dynamics are reviewed, followed by an examination of calving laws.

Chapter 3 focuses on lake-calving glaciers in *Aoraki*/Mount Cook National Park. The chapter is in review as a journal article in *Geomorphology*. In order to gain a better understanding of the lake-calving glaciers in *Aoraki*/Mount cook National Park and how subaqueous ice ramps might affect glacial retreat, the chapter examines the retreat and formation of proglacial lakes at Mueller, Hooker, Murchison, Classen, Grey, Maud and Godley glaciers. The terminus positions of these glaciers from 1965 to 2011 are mapped, glacier retreat rates are calculated, and lake surface areas are estimated.

Patterns in glacier retreat and lake expansion are discussed, in conjunction with the possible reasons for these trends.

Chapter 4 examines and contrasts the subaqueous calving margin morphology of Mueller, Hooker and Tasman glaciers. The chapter has been published in *Journal of Glaciology*. In the chapter, a combination of sub-bottom sonar profiling and echo-sounding is used to identify ice on the lake floor and to delineate the subaqueous terminal morphology of each glacier. This includes mapping of lake bathymetry and the subaqueous portions of the calving margins. Key characteristics of the subaqueous margins are thus identified, and the processes which control subaqueous morphological development at the three glaciers are discussed.

Chapter 5 presents a detailed study on the temporal evolution of the calving margin of Mueller Glacier. The chapter is in review as a journal article in *Geografiska Annaler*. In order to increase the understanding of how subaqueous ice ramps fit into the wider picture of glacial retreat and proglacial lake expansion, the chapter examines recent (2009-2011) changes in the subaqueous and subaerial terminus morphology of Mueller Glacier. The temporal evolution of the terminus is constrained from a sequence of four field surveys over 2 years. The effect water temperature has on calving and the presence of a subaqueous ice ramp is discussed and the factors that control terminus buoyancy are identified.

Chapter 6 presents future retreat scenarios for Hooker Glacier. The chapter has been accepted for publication in *New Zealand Geographer*. The chapter predicts potential retreat scenarios and proglacial lake enlargement based on retreat rate and proglacial lake growth calculations from chapter 3, and subaqueous terminal morphology data from 2009 presented in chapter 4, and assesses the limitations of these retreat scenarios. Other factors that may affect the future retreat of the calving margin are also identified. A synthesis of the work is presented in Chapter 7, along with a discussion of avenues that warrant further, focused research, followed by concluding remarks.

Chapter 2: Lake-calving glaciers

2.1 Introduction

The termini of lake-calving glaciers are complex systems affected by glacier dynamics, the geographic and climatic environment, calving processes, properties of the water-body into which the glacier calves, and in some cases, debris cover. This chapter reviews previous research on lake-calving glaciers, with a particular focus on calving processes and subaqueous margin morphology. Calving from tidewater glaciers is also considered in places to provide context. The review is subdivided into five sections. The first section (2.2) discusses the significance of calving glaciers. The influence the proglacial water body has on the glacier through processes such as waterline melt, subaqueous melt, thermal regime, circulation and convection and lake level are discussed in section 2.3. Calving processes, the role of crevasses and key calving triggers are examined along with the main types of calving in section 2.4. Section 2.5 reviews the relationship between glacier dynamics and calving processes and a key debate as to whether calving losses are the cause or consequence of flow acceleration (the 'slave or master' hypothesis). Section 2.6 discusses glacier velocity and its role in calving. Section 2.7 reviews calving laws, how they have evolved and the way in which calving is represented in glacier models. The chapter concludes by summarising the main findings of the literature review.

2.2 The significance of calving glaciers

Calving is a significant ablation process for the mass balance of many glacier systems, at times allowing rapid mass transfer from the cryosphere to lakes and oceans (Figure 2.1). Calving can permit much larger volumes of ice to be lost from the glacier than would be possible from surface ablation alone (van der Veen, 2002; O'Neel *et al.*, 2007). In particular, large proportions of mass may be lost via calving from many major glacier systems, including the Greenland Ice Sheet (Hagen *et al.*, 2003; Rignot & Kanagaratnam, 2006; Straneo *et al.*, 2011), with the majority of mass loss from the

Antarctic Ice Sheet being via this process (Jacobs *et al.*, 1992). Calving is likely to have had a strong control on the growth and retreat of large ice sheets which terminated into the sea or lakes during the Pleistocene, including the Laurentide, Fennoscandian, British-Irish and Patagonian ice sheets (Cutler *et al.*, 2001; Hughes, 2002; Hulton *et al.*, 2002; Zweck & Huybrechts, 2003; Mangerud *et al.*, 2004; Siegert & Dowdeswell, 2004; Stokes & Clark, 2004). As Clarke *et al.* (1999) highlighted, a better understanding of calving processes is required in order to unravel the complex interactions between climatic, oceanographic and glaciological causes and effects of major calving episodes such as 'Heinrich Events' in the North Atlantic.

Figure 2.1: Icebergs produced from multiple calving events, grounded near the outlet of Tasman Lake, the proglacial lake adjacent to Tasman Glacier (source: C. Robertson, 2 April 2008). Englacial and some supraglacial debris has remained on the icebergs during calving and been transported down the lake. Calving permits much larger volumes of ice to be lost from the glacier than melting alone.

Mass loss via calving from glaciers and ice caps has contributed significantly to present-day global mean sea level rise (SLR), although the magnitude is not fully constrained (Glasser *et al.*, 2011). Calving glaciers can respond quickly to initial climate signals via rapid retreat (Post, 1975; Meier, 1997) and therefore have the potential to contribute disproportionally to sea level rise (Meier & Post, 1987; Rignot *et al.*, 2003). However,

calving glaciers can also become partially decoupled from climate-forcing, which results in factors other than equilibrium line altitudes (ELAs) controlling spatial extents (Alley, 1991; Benn *et al.*, 2007b). Hence, it is important to understand calving processes, as glaciers and ice sheets are expected to continue making a significant contribution to SLR in the twenty-first century (Jenkins, 2011). The magnitude of such contributions has been the focus of many studies (e.g. Glasser *et al.*, 2011; Paul, 2011; Radić & Hock, 2011; Scherler & Strecker, 2011; Jacob *et al.*, 2012), with debate focusing on the forcing behind the rapid increase in mass loss from calving termini, and whether the mass loss will continue in the near future and, if so, at what rate. The effect calving may have on oceanographic systems is also important, as variations in iceberg fluxes and routing may influence the wider climate system (Kenneally & Hughes, 2006).

Calving rates of freshwater glaciers are typically an order of magnitude lower than calving rates at tidewater glaciers (Bindschadler, 1980; Funk & Röthlisberger, 1989). Tidewater-freshwater calving rate differences have been attributed to variations in water density, upwelling rates and associated turbulent heat transfer, subaqueous melt rates, along with frontal oversteepening and longitudinal strain rates (Funk & Röthlisberger, 1989; Warren *et al.*, 1995b; van der Veen, 2002). Hence, it is important to understand the processes that control these widely differing calving rates, as this may assist in understanding contemporary glacier settings, palaeoglaciological records (Benn *et al.*, 2007b), and in predicting future global mean sea level rise (Shepherd *et al.*, 2010).

Calving glaciers and the water bodies into which they calve may also present a significant hazard to users of that environment (e.g. Tinti *et al.*, 1999). Glacier lake outburst floods (GLOFs) may be caused when a lake-damming moraine or ice ‘dam’ is breached, and can present a significant hazard to people and infrastructure when lake water then flows down-valley (e.g. Vuichard & Zimmermann, 1987; Yamada & Sharma, 1993; Richardson & Reynolds, 2000; Vincent *et al.*, 2010). Where proglacial lakes are used for, or contribute to hydro-electric power storage (e.g. Norway (Theakstone & Knudsen, 1986; Kennett *et al.*, 1997), Switzerland (Haeberli, 1977; Bindschadler, 1983b; Funk & Röthlisberger, 1989) and New Zealand (Purdie &

Fitzharris, 1999)), GLOFs can cause considerable damage. Avalanches of both ice and/or sediment into proglacial lakes also pose a hazard if the avalanche is large enough to generate waves and/or displace large quantities of water (Kershaw *et al.*, 2005; Harrison *et al.*, 2006; McKillop & Clague, 2006; Canassy *et al.*, 2011). Avalanche material may be sourced from surrounding mountain ranges, valley walls or lateral moraines (Quincey *et al.*, 2005). Rock avalanches onto glaciers and their effect on glacier behaviour has been described in a number of locations (e.g. Huggel *et al.*, 2004; Hubbard *et al.*, 2005; Shulmeister *et al.*, 2009) including *Aoraki*/Mount Cook National Park, New Zealand (Figure 2.2) (e.g. McSaveney, 2002; Cox *et al.*, 2008; Allen *et al.*, 2009; Cox & Allen, 2009; Reznichenko *et al.*, 2011). Furthermore, lateral moraine collapse and degradation has long been an issue at glaciers in *Aoraki*/Mount Cook National Park, due to rapid glacier downwasting and retreat since the end of the Little Ice Age (Blair, 1994).

Figure 2.2: The rock avalanche from *Aoraki*/Mount Cook on 14 December 1991 (Photo: CN21503/11: D. L. Homer in Cox & Barrell, 2007). The avalanche descended 2720 m down the eastern side of *Aoraki*/Mount Cook and was deposited onto Tasman Glacier. The deposit formed closely spaced arcuate debris ridges on the glacier at the confluence of Tasman Glacier and the Hochstetter icefall (seen in the centre of the photo) which have elongated since deposition (Quincey & Glasser, 2009). The deposit caused the development of a 25 m high, debris-covered, ice ridge on the up-glacial edge of the deposit (Reznichenko *et al.*, 2011).

2.3 Influence of the proglacial water body

Any proglacial water body adjacent to a calving glacier has a significant influence on glacier behaviour and how glacier retreat may proceed (e.g. Hart *et al.*, 2011; Tsutaki *et al.*, 2012). A water body can affect glacier dynamics by altering the stress regime operating on the glacier and influencing calving processes at the terminus (Kirkbride, 1993; Chinn, 1996). Glaciers that calve into water typically flow faster than those that terminate on land (Sugiyama *et al.*, 2011). This is a result of enhanced basal ice motion where basal water pressure is high. Tsutaki *et al.* (2011) found that glacier velocity nearly tripled as a result of proglacial lake formation and development on Rhonegletscher, Switzerland. Significant components operating at the water

body/glacier terminus boundary include: waterline melt, subaqueous melt, thermal regime, circulation patterns, and lake level fluctuations.

2.3.1 Development of proglacial lakes

Glacier thinning and recession since the Little Ice Age has resulted in an increasing number of proglacial lakes and an expansion of existing proglacial lakes globally. Proglacial lakes have been studied at glacier termini in Patagonia (Warren *et al.*, 1995a; Warren & Aniya, 1999; Skvarca *et al.*, 2002), Alaska (Reid & Callender, 1965; Gustavson, 1975a; Boyce *et al.*, 2007), the Himalayas (Sakai *et al.*, 2001; Salerno *et al.*, 2012; Thompson *et al.*, 2012), New Zealand (Kirkbride, 1993; Hochstein *et al.*, 1995; Chinn, 1996; Hochstein *et al.*, 1998; Warren & Kirkbride, 1998; Chinn, 1999; Dykes *et al.*, 2010; Gjermundsen *et al.*, 2011), Antarctica (Chinn & Woods, 1984; Bronge, 1999), Greenland (Warren, 1991), Norway (Duck & McManus, 1985; Theakstone & Knudsen, 1986; Laumann & Wold, 1992), Iceland (Derbyshire, 1974; Duck & McManus, 1985), Switzerland (Haeberli & Roethlisberger, 1976) and the Italian Alps (Diolaiuti *et al.*, 2005; Diolaiuti *et al.*, 2006; Diolaiuti *et al.*, 2009).

Proglacial lakes develop from a range of processes including: retreat of a glacier through an overdeepened trough (Warren & Aniya, 1999); glacial retreat up-valley from a terminal moraine (McKillop & Clague, 2007) or outwash head (Kirkbride, 1993) (Figure 2.3); and, downwasting. On debris-covered glaciers, Quincey *et al.* (2007) found that proglacial lakes form on glaciers with low long-profile surface gradients (of less than 2˚) and surface velocities of <10 m a^{-1}. The first stage of lake formation on debris-covered glaciers involves the removal or perforation of the supraglacial debris on the lower reaches of the glacier, commonly caused by the collapse of englacial conduit tunnels as a result of glacier thinning (Kirkbride, 1993). On low-gradient glaciers, disintegration is more likely to occur up-glacier of the terminus where internal drainage conduits are common, compared to steeper-gradient glaciers where disintegration is likely to occur closer to the margin due to thinner ice (Kirkbride, 1993). The disruption of the supraglacial debris cover increases melting of exposed ice surfaces due to removal of debris insulation and direct radiation exposure, and may lead to the development of supraglacial ponds or sinkholes. Expansion of these ponds is

predominantly by melting which may be enhanced by warmer pond water (Sakai *et al.*, 2000). Perched lakes show limited growth due to intermittent pond drainage (Benn *et al.*, 2001), while ponds connected to the englacial water system grow progressively (Röhl, 2008). The removal of supraglacial debris and subsequent exposure of bare ice cliffs marks the transition from melting and thinning under debris, to rapid melting and the development of proglacial lakes (Kirkbride, 1993), potentially through the coalescence of supraglacial ponds. Kirkbride (1993) proposes the second stage of proglacial lake evolution on debris-covered glaciers involves the development of a relatively straight terminal ice cliff (when observed in plan view), and rapid glacier retreat as a result of subaerial and subaqueous calving.

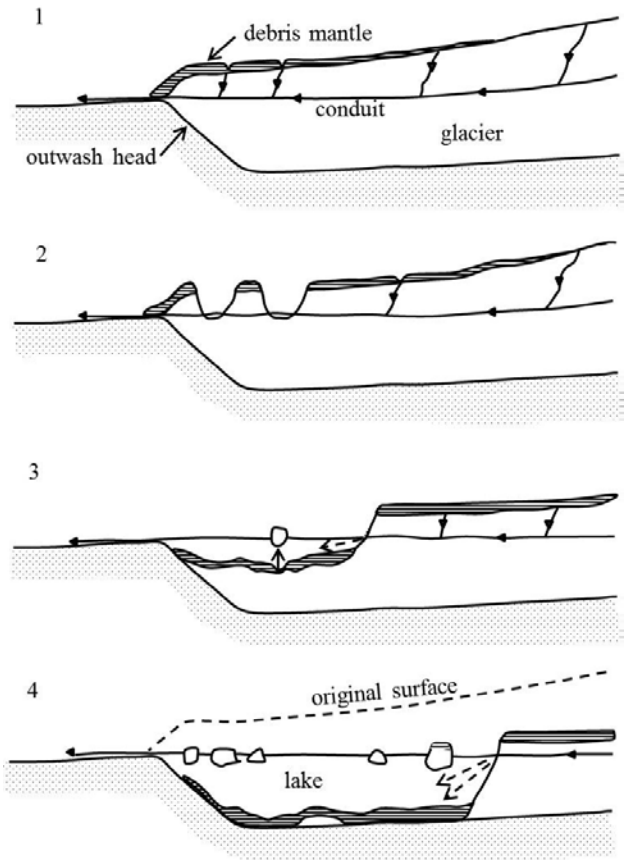

Figure 2.3: Sequence of retreat and subsequent proglacial lake development on a low-gradient glacier bound by the reverse slope of an outwash head (Figure 9 Kirkbride, 1993): 1) slow melting under a mantle of supraglacial debris; 2) collapse of conduits perforates the debris layer which allows rapid melting of exposed ice walls; 3) growth and coalescence of supraglacial ponds into a lake which may have an ice-cored floor. Subaqueous icebergs may calve from this floor; 4) disintegration of the ice-cored floor increases water depth and initiates rapid calving retreat.

2.3.2 Waterline melt

Melting of ice at the waterline ('thermo-erosional notching') is considered a significant influencing factor on calving rates at freshwater-terminating glaciers. If ice is in contact with water for a sufficient period of time, thermal erosion will occur at the waterline (Figure 2.4) as a result of energy transfer via warm surface water and water movement. Notches will form in the ice at the waterline as the melt proceeds faster than subaerial or subaqueous melting (Josberger, 1978). Thermal erosion and undercutting of ice cliffs have long been recognised as potentially important contributing factors at lake-calving glaciers (Tarr, 1909; Goldthwait *et al.*, 1963; Reid & Callender, 1965; Haeberli & Roethlisberger, 1976; Theakstone & Knudsen, 1986; Watson, 1995). Early studies looking at notch formation on icebergs in the Southern Ocean found notches up to 7-10 m deep and highlighted the importance of wave action in their formation (Martin *et al.*, 1978; Robe, 1978). Observations of thermo-erosional notches in proglacial lakes estimated a notch depth of up to 10 m at Tasman Glacier (Purdie & Fitzharris, 1999) and formation rates of 3-4 m over a few days at Maud Glacier (Kirkbride & Warren, 1997). Waterline melt in supraglacial ponds has also been found to be ~0.5 m d^{-1} at Ngozumpa Glacier, Khumbu Himal, Nepal (Benn *et al.*, 2001) and 0.8 m d^{-1} at Glacier León, Chilean Patagonia (Haresign & Warren, 2005). Although it is difficult to directly compare these observations, as some studies do not include water temperature measurements and others are based on short observation periods, it is clear that waterline melt and thermo-erosional notches are significant controls on calving rates at some lake-calving glacier margins (Kirkbride & Warren, 1997; Röhl, 2006; Diolaiuti *et al.*, 2009).

In particular, Röhl (2006) identified that the calving rate at Tasman Glacier is directly controlled by the rate of thermal undercutting of the subaerial portion of the ice cliff. The study highlighted the importance of separating ice melt at the waterline from notch formation, which eventually leads to calving. Ice melt at the waterline occurs when water is in contact with the ice and proceeds at higher rates than subaerial or subaqueous melting (Josberger, 1978). Notch formation is defined as the actual speed at which an ice cliff is undercut, or the change in notch depth, and proceeds more slowly than waterline melt (Röhl, 2006). Notch formation in turn is controlled by water temperature, circulation, cliff geometry, debris supply and lake-level fluctuations. To

separate waterline melt and notch formation, Röhl (2006) introduced an effective melt rate which incorporates changes in lake level and distinguishes the speed of waterline melt. Water temperatures within the lake could not be used to estimate notch formation due to the complex interaction of all influencing components. Although thermal undercutting was identified as a controlling factor at Tasman Glacier, the influence of this process at other lake-calving glacier margins may vary depending on glaciological factors such as ice velocity and surface gradient, together with limnological factors such as water temperature and water movement (Röhl, 2006).

Figure 2.4: A thermo-erosional notch (shown by the black arrow), formed at the waterline, at the terminal ice cliff of Mueller Glacier, New Zealand (source: C. Robertson, 20 November 2009). The rate of thermo-erosional notch development may directly control subaerial calving at some freshwater terminating glaciers, such as Tasman Glacier (Röhl, 2006).

2.3.3 Subaqueous melt

Historically, subaqueous ice melt at a calving terminus has been inferred or indirectly calculated, and as a result has generally been considered as negligible (Theakstone & Knudsen, 1986; Laumann & Wold, 1992; Hochstein *et al.*, 1998; e.g. Fitzharris *et al.*, 1999). Melt has often been incorporated into the calving rate of a glacier. However, where calving rates are low, subaqueous ice melt may make a significant contribution to

ice loss. This is in contrast to glaciers with high calving rates, where ice loss via subaqueous melt may be one or two magnitudes lower than losses via calving (Syvitski, 1989). The uncertainties surrounding calculated rates of subaqueous ice melt have also been high, making it difficult to justify their use (Warren *et al.*, 1995b; Haresign & Warren, 2005). More recently, a number of studies have suggested that subaqueous melt rates at tidewater termini are higher than first suspected (Warren *et al.*, 1995a; e.g. Haresign & Warren, 2005), with 57% of the estimated total ice loss at LeConte Glacier, Alaska, attributed to subaqueous melt alone (Motyka *et al.*, 2003a).

A number of studies have gone some way to quantifying subaqueous melt rates at tidewater glaciers in Greenland (e.g. Rignot *et al.*, 2010; Xu *et al.*, 2011; 2012) yet subaqueous melt rates in proglacial lakes remain poorly defined, although a number of recent studies estimated rates via calculations based on glacier and lake variables, or laboratory studies. Hochstein *et al.* (1998) calculated an 'apparent specific downmelting rate' for Hooker Lake of 9 m a^{-1} for the period 1986-1996 and 8 m a^{-1} for Tasman Lake from 1982-1993 (Hochstein *et al.*, 1995). The specific ice melting rate described "the removal of a given volume of ice by melting associated with a representative melt contact area for a given period" (Hochstein *et al.* 1998, p. 214). The calculations were based on 40 x 10^6 m^3 of ice being removed by melting between 1982 and 1993, mainly from a melt area of approximately 0.4-0.5 km^2. Although equation 2.1 was designed for application to saline water, Hochstein *et al.* (1998) found that it provided realistic melt rates at freshwater margins. Subsequently, Röhl (2008) calculated subaqueous melt rates for supraglacial ponds on Tasman Glacier, New Zealand using Russell-Head's (1980) equation:

$$V_m = 1.8 \times 10^{-2}(T_w + 1.8)^{1.5} \qquad 2.1$$

where V_m is the melt rate in m d^{-1} and T_w is the water temperature. The calculation gave a melt rate of 4.7 m a^{-1} for an annual average water temperature of 0.8˚C or a volume ice loss of ~35,000 m^3 a^{-1}. These values were considered to be a minimum estimate as ice melt by convection was expected to be higher.

Alternative equations for calculating melt rates have also been applied. Neshyba and Josberger (1980) use water temperature as a single variable:

$$V_m = 2.78T_w + 0.47\ T_w^2 \qquad 2.2$$

Flow velocity is included in Weeks and Campbell's (1973) equation for melt rates at the sea water/glacier ice interface for icebergs:

$$V_m = 6.74 \times 10^{-6} v^{0.8} \Delta T / x^{0.2} \qquad 2.3$$

where V_m is the melt rate, v the water current velocity, ΔT the temperature difference between ice and water, and x the length of the side of the iceberg. Results from this equation are substantially higher than those derived from equation 2.1.

Eijpen *et al.* (2003) used laboratory investigations to study the effect that water temperature and salinity has on subaqueous melt rates. Melt rates of between 43 and 64 mm d^{-1} at the base of an ice block, and between 29 and 50 mm d^{-1} in the middle of a block were recorded when a block of ice was submerged in water between 2 and 4˚C. The study also found that thermo-erosional notches form more quickly in water temperatures >4˚C. Although the study was carried out in a temperature-controlled laboratory (1-10˚C), frozen distilled water was used instead of glacier ice which has different ice density and debris content properties. Circulation within the experimental tanks was also minimised so convection patterns produced by ice melt could be observed (Figure 2.5). In reality, however, circulation and convection in a proglacial lake is driven by a combination of glacial and non-glacial inflows and climatic parameters. Thus, the circulation and convection patterns observed in the laboratory study may be markedly different from what occurs in a proglacial lake.

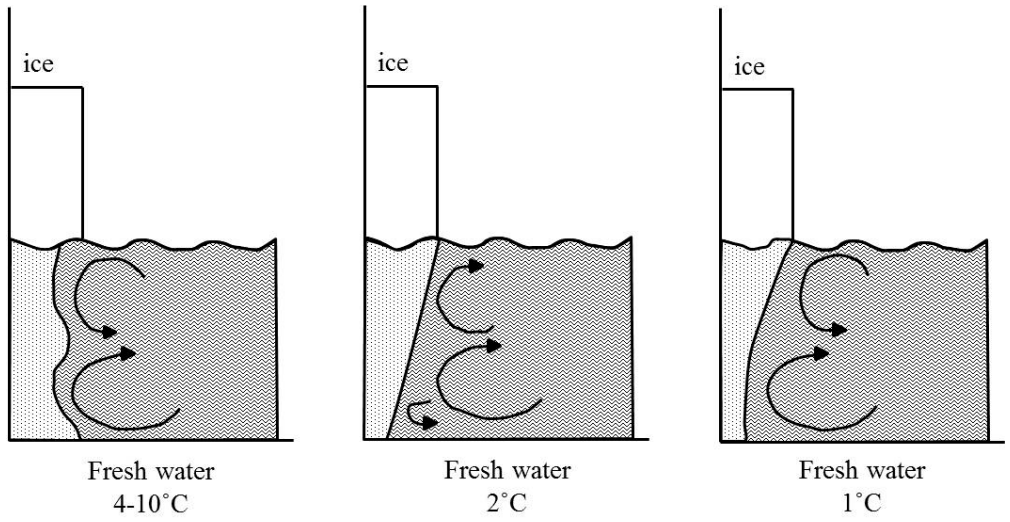

Figure 2.5: Convection cell circulation patterns from laboratory experiments of ice melt in freshwater (after Figure 3 Eijpen *et al.*, 2003). Different subaqueous melt rates and hence geometries are created in different freshwater temperatures. Circulation within the experimental tanks was minimised, however, in reality, circulation and convection in a proglacial lake is driven by a combination of glacial and non-glacial inflows and climatic parameters. Thus, circulation and convection patterns observed in this study may be markedly different from what occurs in a proglacial lake.

2.3.4 Thermal regime

The thermal regime of a proglacial lake is influenced by both climatic and glacial variables. Lake temperature is predominantly the product of solar warming (Ashley, 1995), yet can fluctuate with variations in incoming shortwave radiation, wind and rainfall. The absorption of incoming solar radiation in summer by a lake increases surface temperatures, while a large amount of solar radiation is reflected in winter if the lake freezes over (Björnsson *et al.*, 2001; Schomacker, 2010). Wind can force mixing of lake waters and as a result, alter the thermal stratification of a lake (Harris, 1976). Glacial variables, and particularly input of meltwater or supraglacial streams, are important components in determining the thermal regime of a proglacial lake. The location where the meltwater enters the lake is particularly important in terms of thermal stratification and circulation, and is discussed further in section 2.3.5. Calving also influences lake temperature as icebergs have a cooling effect on the surrounding water due to latent and sensible heat exchange (Kenneally & Hughes, 2006; Benn *et al.*,

2007b). Also, icebergs may contribute cool water to the lake via melt, and can promote a more uniform temperature distribution in the lake (Churski, 1973).

Consistent with the above observations and variability, actual temperature measurements from proglacial lakes show a wide range of thermal conditions which vary both temporally and spatially. Indeed, the large range of thermal regimes in proglacial lakes are the result of variations in latitude, altitude, climate, glacial influence, fluvial and sediment input (Warren & Kirkbride, 1998). In particular, temperatures have been found to be as low as –0.3˚C (Fleisher *et al.*, 1993) and as high as 11˚C on the surface (Röhl, 2005), with some lakes having a wide range in temperature (e.g. Gilbert & Desloges, 1987; Röhl, 1999). In contrast, others show little variation with depth or distance from the ice margin (e.g. Hicks *et al.*, 1990; Fleisher *et al.*, 1993; Warren, 1999). Some lakes have also been found to have thermoclines or are classified as being isothermal (Gilbert, 1971; Liverman, 1987; Fleisher *et al.*, 1993; Hochstein *et al.*, 1998). Although common patterns of temperature can be identified, direct comparison of lake temperatures can be difficult due to differences in data collection methods. For example, measurements taken in a lake in the early morning are likely to be different from measurements in the same lake taken in mid-afternoon, due to the warming effect of solar radiation. Similarly, temperatures collected in summer will be higher than those taken in winter. The location of repeat measurements can also hinder direct comparison as temperatures on the surface one metre from an ice cliff cannot be directly compared with temperatures taken at a depth of 20 m 10 m from the ice cliff.

Water temperature is an important control on thermo-erosional notch development, although the relationship between temperature and notching is not straightforward (Röhl, 2006). Nevertheless, such a relationship may explain the positive correlation between water temperature and calving rate found by Warren and Kirkbride (2003). Röhl (2006) also found that correlations between water temperature and notch formation can differ between survey locations and times. Questions also arise as to the most appropriate depth to take measurements: surface temperatures would appear to be the most relevant for waterline melt as the majority of heat transfer via waves occurs

here (Martin *et al.*, 1978), yet high surface temperatures are generally associated with warm, calm weather conditions with minimal wave movement, which reduces heat transfer to the ice cliff (Röhl, 2006). Temporal variation in calving rates at Tasman Glacier is thought to be largely affected by water temperature within thermo-erosional notches (Röhl, 2006). This is due to water movement towards, and within the notch, being a major control on waterline melt, notch formation and therefore calving rates.

2.3.5 Circulation and convection

Circulation and convection of water within a proglacial lake is driven by the thermal regime, water inflows, suspended sediment concentration, along with wind and solar radiation (Figure 2.6). Circulation patterns vary throughout the year with changes in driving factors, and can be used to classify lakes in terms of their mixing. Lakes that completely mix in spring and autumn are *isothermal*, glacier-fed lakes commonly turn over twice a year and are termed *dimictic*, while water bodies that completely mix once a year are *monomictic* (Ashley, 1995). The majority of lakes in contact with ice are thought to be *polymictic* near the ice margin, having no thermal stratification, which allows free circulation and convection (Reid & Callender, 1965; Churski, 1973; Harris, 1976; Ashley, 1995; Wetzel, 2001). However, *monomictic*, *dimictic* and *isothermal* conditions have been found in a number of different proglacial lakes and within the same lake at different times (e.g. Campbell, 1973; Gilbert & Desloges, 1987; Hochstein *et al.*, 1995; Hochstein *et al.*, 1998).

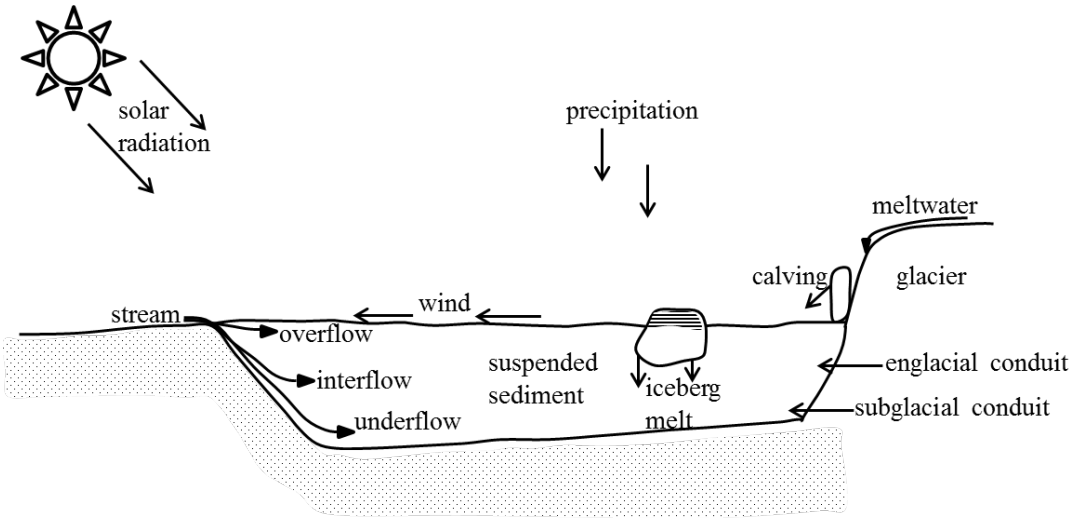

Figure 2.6: Factors that influence circulation and convection within a proglacial lake; water inflows, suspended sediment concentration, thermal regime, wind and solar radiation. The upper layers of a water body are mixed predominantly by waves and surface currents generated by wind. Mixing within the lake is influenced by the density of water entering the lake from precipitation, streams, meltwater streams from the glacier and meltwater delivered via englacial and subglacial conduits. Icebergs calving into the lake and melting will cool surrounding water.

The upper layers of a water body are mixed predominantly by waves and surface currents generated by wind, barometric pressure variations, and calving (Gustavson, 1975b; Martin *et al.*, 1978; Gilbert & Shaw, 1981). The degree to which waves mix surface waters depends on the lake orientation, wind direction and strength, shoreline orientation and fetch, with persistent katabatic winds enhancing the efficiency of mixing (Drewry, 1986). Water density and inflows have a strong influence on the mixing of deeper water. The density, and thus buoyancy of the water, will determine whether it sinks, rises, or spreads out where it enters the lake (Figure 2.6) and encourages mixing (Ashley, 1995). Water can enter the lake via sub- or englacial conduits, from supraglacial meltwater, streams and rainfall. If the inflowing water is a lower density than the lake water it will rise and spread out. This is known as an overflow and can occur where streams or supraglacial meltwater flow into a lake at lake level. An underflow occurs where the water flowing into the lake is a higher density and it sinks to the bottom of the lake. Where the inflowing water and lake are of a similar density, inflowing water will spread out at intermediate depths as an interflow or plume. Streams or meltwater entering a lake can also significantly influence the water body by

establishing thermal stratification close to the ice margin which may not exist otherwise (e.g. Gustavson, 1975a; 1975b). Circulation and convection are also influenced by icebergs melting in the lake and cooling surrounding water (Churski, 1973). Direct measurement of inflows from subaqueous sources is often difficult. However, flow conditions of these inflows is generally inferred by variables such as temperature distribution, suspended sediment concentration or transmissivity (e.g. Gustavson, 1975b; Hochstein *et al.*, 1995; Chikita *et al.*, 1999; Röhl, 1999).

2.3.6 Lake level

Lake level fluctuations are common in proglacial lakes (Röhl, 2006), and fluctuations can be very large, generally in response to changes in water inflow or outflow of the lake. Rises of up to 2 m have been recorded in Hooker Lake following heavy rainfall (Hochstein *et al.*, 1998), a 1.43 m rise in 33 hours was recorded in Tasman Lake (Röhl, 1999) and a 1.4 m rise was recorded in Tasman Lake over 8 days following 683 mm of rain (Kirkbride & Warren, 1997). Fluctuations in lake levels of 1.5-2.0 m have also been recorded at Mendenhall Glacier (Alaska) with small, rapidly occuring fluctuations triggering large calving events (Boyce *et al.*, 2007). Decreases in lake level can occur when there is a progressive or rapid emptying of a lake. For example, a marginal ice-contact lake at Miage Glacier in the Italian Alps is infrequently emptied. This is due to changes in the local subglacial drainage network routing water away from the ice cliff bounding the lake instead of towards it and into the lake, along with reversals in the ice-marginal equipotential surface (Diolaiuti *et al.*, 2005). Rapid emptying of a proglacial lake may also occur during a GLOF. Several lakes in the Nepal Himalaya have been identified as a high risk for GLOFs including Tsho Rolpa in Rolwaling and the Imja in the Khumbu Himal (Yamada, 1998; Reynolds, 1999; Richardson & Reynolds, 2000).

Lake level fluctuations are an important component in the formation of thermo-erosional notches, terminus buoyancy and glacier velocity. For example, variations in lake level influence the effectiveness of waterline melting (Röhl, 2006). If lake levels stay relatively constant, undercutting of the terminal ice cliff will be more effective as energy transfer, and thus melting, will be concentrated on a thin section of ice at the waterline, rather than spread over a wide area. Boyce *et al.* (2007) found that after the

terminus of Mendenhall Glacier became buoyant, minor but rapid perturbations in lake level (some resulting from rainfall events) were enough to trigger calving and the break-up of the terminus. Similar effects of rapid lake level changes were also noted at Austerdalsisen, Norway (Theakstone & Knudsen, 1986; Theakstone, 1989). Laumann and Wold (1992) also found that a rise in lake level resulted in increased glacier velocity due to increased sliding within 500 m of the terminus of Austdalsvatn, Norway.

2.4 Calving processes

Calving occurs from both subaerial and subaqueous sections of a glacier. Calving from the subaerial section can cause subaqueous calving as the overburden pressure on the subaqueous section is rapidly reduced and buoyant forces are increased (O'Neel *et al.*, 2007). Calving can materialise in different ways depending on pre-existing conditions.

2.4.1 The role of crevasses

Calving is a multifarious set of processes which result in the mechanical loss of ice from a glacier. It occurs in a variety of settings from tidewater to freshwater terminating glaciers to dry calving on land and from arid polar to sub-tropical regions (Smiraglia *et al.*, 2004; Benn *et al.*, 2007b). Calving is the result of fractures opening in response to stresses which propagate to isolate blocks of ice from the glacier (e.g. Figure 2.7). This propagation has been recorded at seismometers at Bench Glacier, Alaska (Mikesell *et al.*, 2012) as seismic waves are produced during the process (discussed further in section 2.4.4). Thus, the location, timing and magnitude of calving is determined by pre-existing weaknesses in the ice (Benn *et al.*, 2007b). Four key factors influence the degree to which any particular fracture will result in calving, including: 1) the ability of the fracture to enlarge, 2) the rate it enlarges, 3) how deep the fracture will propagate into the ice, and, 4) the orientation of the fracture.

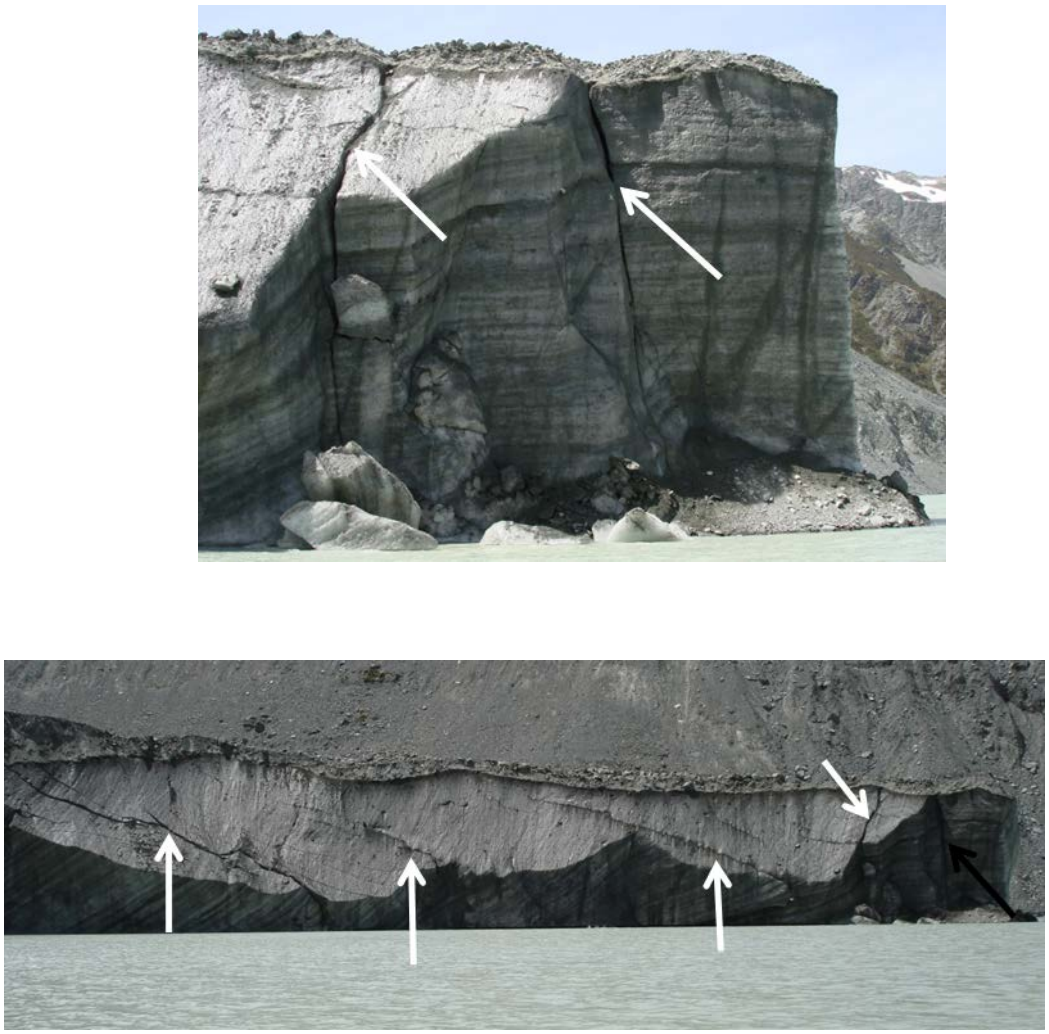

Figure 2.7: Crevasses in the terminal ice cliff at Mueller Glacier (source: C. Robertson, 17 November 2009. The location, timing and magnitude of calving is determined by the location of crevasses which open in response to stresses and propagate to isolate blocks of ice from the glacier.

The ability of a fracture to enlarge depends on failure criteria being met. These criteria have been identified from both observational field-based studies and laboratory studies, however results are often incompatible as they are presented in different terms by different workers. Field-based results are commonly expressed in terms of the threshold strain rate required for crevasse initiation (Meier, 1958; Hambrey & Muller, 1978) and do not allow for all stresses to be fully incorporated into calculations (Benn *et al.*, 2007b). In contrast, laboratory studies typically report results in applied stress at the point of failure, or fracture toughness (Nixon & Schulson, 1987; Rist & Murrell, 1994; Fischer *et al.*, 1995; Rist *et al.*, 1996; Weber & Nixon, 1996; Rist *et al.*, 1999). Results

from laboratory studies can be converted into threshold strain rates which field-based studies are presented in, and vice-versa, by inverting Glen's flow law for ice:

$$\dot{\varepsilon}_{ij} = A\tau_e^{n-1}\tau_{ij} \qquad 2.4$$

to yield:

$$\tau_{ij} = A^{-1/n}\dot{\varepsilon}_e^{1/n-1}\dot{\varepsilon}_{ij} \qquad 2.5$$

where $\dot{\varepsilon}_{ij}$ and τ_{ij} are strain rates and stress components, $\dot{\varepsilon}_e$ and τ_e are the effective strain rate and effective stress, and A and n are the flow law parameters. The use of this law in practice is difficult however, due to its reliance on assumed values of A and n, which can vary widely between damaged and undamaged ice.

Threshold strain rates for crevasse initiation from observed field-based studies cover a wide range. In Greenland, threshold strain rates of ~0.01 a^{-1} were found (Meier, 1958) while on White Glacier (Canada), crevasses were noted in areas of strain rates as low as 0.004 a^{-1}, but no crevasses were present in areas with a strain rate of 0.163 a^{-1} (Hambrey & Muller, 1978). From analysing observed threshold strain rates, Vaughan (1993) was able to calculate yield stresses for crevasse initiation of between 90 kPa and 320 kPa, which may reflect differences in ice rheology, crevasse spacing and the degree to which stress histories influence the regime. Tensile strength calculated from laboratory studies have also shown a moderate range of between 80 and 140 kPa at 0˚C, and between 100 and 130 kPa at –50˚C (Petrovic, 2003). Factors such as impurities in the ice may reduce the tensile strength of ice further. In addition, the loading rate as opposed to temperature may be more important in determining the level that stress failure will occur at, and therefore when crevasse propagation will be initiated (Nixon & Schulson, 1987; Rist & Murrell, 1994; Fischer *et al.*, 1995; Rist *et al.*, 1996; Weber & Nixon, 1996; Rist *et al.*, 1999). The application of these calculated thresholds to real glaciers and ice sheets is questionable however, as many of the laboratory studies have not used glacier ice (Benn *et al.*, 2007b).

Three types of fracturing have been identified by Benn *et al.* (2007b). These are shown in Figure 2.8 and include tensile cracking, sliding and tearing. *Tensile cracking* involves the wall of the fracture moving apart, and the fracture developing normal to the axis of maximum extension. *Sliding* occurs when the walls of the fracture slide past each other while staying in contact, and a fracture develops parallel to the shear plane. *Tearing* results in the fracture developing parallel to the shear plane but propagating at right angles to the direction of shearing. *Mixed mode fracture* can occur when more than one mode of fracturing acts to propagate a crevasse.

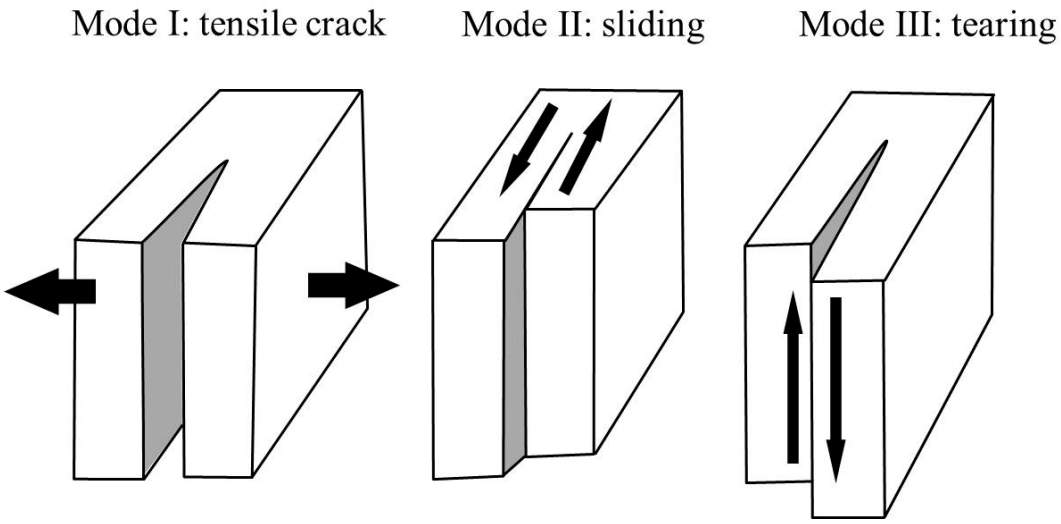

Figure 2.8: Three basic modes of ice fracture (Figure 3 Benn *et al.*, 2007b). Mode I describes tensile cracking where the walls of a fracture separate. Mode II occurs when fracture walls remain in contact but slide past each other. Mode III occurs when the fracture propagates at right angles to the direction of shear. If more than one mode of fracturing occurs it is termed mixed mode fracture.

Once fractures have developed in the glacier, the rate at which they propagate will depend on the stresses applied to them. The rate of crevasse propagation in some settings can control the rate of calving (c.f. Iken, 1977; Kenneally & Hughes, 2002;

Pralong & Funk, 2005). Fracture propagation rates can be calculated from a formula based on a creep fracture theory (Evans, 1984; Kenneally & Hughes, 2002):

$$\frac{\partial d}{\partial t} = \frac{1}{\varepsilon_f}\left(\frac{\sigma_n n}{(n+1)A}\right)^n (H-d)^{n/(n+1)} d_c^{n/(n+1)} \qquad 2.6$$

where d is crack depth, ε_f is the threshold fracture strain rate, d_c is a constant related to ice ductility, H is ice thickness, and σ_n is the net tensile stress normal to the plane of the crack. It has been used in combination with assumed crack spacing to calculate calving rates for specific glacier geometries. To consider fracture propagation in heavily broken areas of hanging alpine glaciers, Pralong *et al.* (2003) and Pralong and Funk (2005) developed an alternative approach based on continuum damage mechanics. Application of this approach was successful, with it predicting geometric evolution and block acceleration prior to failure.

The depth to which a fracture penetrates into the ice is a significant control on whether that fracture will result in calving and where the calving margin will be located. Benn *et al.* (2007a) have developed an alternative model to calculate theoretical crevasse depths for given stress conditions and to predict the position of calving margins. The model is based on the idea that a crevasse will penetrate into the ice until the forces acting to enlarge it are balanced exactly by forces opposing its penetration. Water is particularly important for maximum penetration of a crevasse (Weertman, 1973; Robin, 1974; van der Veen, 1998b; Alley *et al.*, 2005; Hart *et al.*, 2011). Water opposes cryostatic pressure and as a result allows a crevasse to penetrate deeper, potentially to the bed of the glacier if enough water is present. Water can enter crevasses via surface meltwater channels or where there is a connection to the glacier's proglacial water body. Scambos *et al.* (2000) found that surface meltwater ponds were a prerequisite for crevasse penetration and that crevasse propagation by meltwater was the primary mechanism for ice shelf weakening and subsequent retreat on the Antarctic Peninsula. Van der Veen (1998a) has identified that water is also important for the growth of basal crevasses.

Crevasses determine the geometry of the calving margin. Therefore, their orientation is an important factor to consider when examining calving margins. A number of equations have been defined to determine the relationship between crevasse orientation and stress fields on a glacier (Nye, 1952; Benn *et al.*, 2007b). Some equations only incorporate deformation by pure shear stress which results in transverse crevasses forming under longitudinal extension. Others include deformation via simple shear where crevasses will be orientating at 45˚ to the direction of shear. Where deformation is via a combination of pure and simple shear, intermediate orientations occur (Nye, 1952). However, most field-based studies have found that crevasses do not align perfectly with the principal stress axes, most probably due to the role of mixed mode fracture (as discussed above) (Kehle, 1964; Whillans *et al.*, 1993; van der Veen, 1999b; 1999a).

2.4.2 Hierarchy of mechanisms that trigger calving

As discussed above, calving is the result of crevasse propagation through ice in response to stresses. Benn *et al.* (2007b) have identified four situations where stresses are likely to be high enough to initiate crevasse propagation and result in calving and are therefore likely controls on calving processes. These include: 1) stretching in response to large-scale velocity gradients; 2) force imbalances at unsupported ice cliffs; 3) undercutting by subaqueous melting; and, 4) torque arising from buoyant forces. Coseismic events may also trigger calving once certain preconditions have been met (Dykes *et al.*, 2012).

2.4.2.1 Stretching in response to large-scale velocity gradients

Glaciers respond to velocity gradients by stretching which results in crevasse formation. These crevasses are a key first-order control on calving and terminus geometry as they form a preferential line of weakness along which calving can occur (Powell, 1983). On a glacier where surface velocity gradients are the primary control on crevasse propagation, calving will occur where the gradients are high enough to allow crevasses to penetrate the full depth of the glacier (discussed further in section 2.6). As discussed in section 2.4.1, meltwater on the surface of the glacier is a key control on calving processes, with water-filled crevasses growing downward without limitation. Thus, the

location of these crevasses will mark the calving margin. As mentioned by Benn *et al.* (2007b, p. 161), "the margin position will therefore be determined by the velocity distribution at the glacier surface (which controls crevasse depth), and the ice height above the waterline (which determines whether a crevasse of a given depth will reach the waterline)". Where a glacier stretches in response to large-scale velocity gradients, the key controls on calving are ice thickness, ice velocity and the components that influence these controls (Benn *et al.*, 2007b).

Longitudinal stretching associated with velocity gradients is considered a first-order control on calving in the hierarchy of calving controls. Velocity gradients determine the maximum depth of crevasses and therefore whether they will reach the waterline and result in calving. As discussed further in section 2.6, crevasses are more likely to reach the waterline if high velocity gradients are present, compared to low velocity gradients which encourage buoyancy and floating sections of ice (Benn *et al.*, 2007b). The position of the calving margin and, consequently, the maximum extent of the glacier, are also governed by velocity gradients.

2.4.2.2 Force imbalances at unsupported ice cliffs

Force imbalances at unsupported ice cliffs create a cyclic calving pattern. Unbalanced stresses at the terminus cause geometric changes in the ice cliff resulting in calving which reinstates the imbalance in stresses at the new calving margin (Reeh, 1968; Hughes, 1998; Hughes, 2002). Fracture propagation rates, the rate of terminus geometry evolution, and feedbacks between geometric changes and fracturing will determine the frequency of these calving events, while changes in the position of the terminus will be controlled by the magnitude of calving events and the length of the calving cycle (Benn *et al.*, 2007b). As outlined by Benn *et al.* (2007b, p. 161), "where fractures are generated and propagated entirely in response to unbalanced stresses at subaerial and/or subaqueous ice cliffs, calving is controlled by glacier margin geometry and ice rheology". Force imbalances at an ice cliff is a second-order control on calving, as it is superimposed on longitudinal stretching and operates within the boundaries established by glacier dynamics (Benn *et al.*, 2007b). Second-order processes like force imbalances

are particularly important and may be the key control of calving losses where longitudinal stretching is minimal.

2.4.2.3 Undercutting by subaqueous melting

Melting at the waterline destabilises the subaerial section of the terminal ice face and encourages calving. Melting is dependent on water level fluctuations, water stratification, circulation patterns and water temperature and for it to be effective needs to be concentrated on a narrow band of ice rather than spread over a wide range (Röhl, 2006). Where calving is driven by melting at or below the waterline, the rate at which the subaerial ice cliff is undermined by subaqueous melting is equal to that of the long-term calving rate (Benn *et al.*, 2007b). Subaqueous melting is a second-order control on calving losses as it has the ability to further erode the calving margin even after longitudinal stretching has determined its maximum extent (Benn *et al.*, 2007b).

2.4.2.4 Torque arising from buoyant forces

Buoyant forces may trigger crevasse propagation and calving when: 1) subaerial calving losses are greater than subaqueous losses, resulting in a subaqueous ice ramp which may break-up; and, 2) when surface lowering of a grounded glacier causes the ice to be below flotation thickness, resulting in the glacier becoming buoyant and calving (Benn *et al.*, 2007b). As a glacier is thinned by melting and becomes buoyant, it will attempt to maintain a constant ratio between surface and basal gradients. If this ratio is not achieved, the terminus will rotate in order to regain equilibrium either by slow ice creep or rapid crevasse propagation and calving (Howarth & Price, 1969; Holdsworth, 1973; Warren *et al.*, 2001). Subaqueous calving presents a significant hazard to users of proglacial lakes or fjords adjacent to the glacier, as was first documented in 1890 by Nansen (1919). Subaqueous calving events are generally larger in magnitude but less frequent than subaerial calving events (Warren *et al.*, 1995a; Motyka, 1997; O'Neel *et al.*, 2007). Subaqueous calving rates are connected to the rate of ice ramp development which is paced by subaerial cliff retreat and waterline melting. Pre-existing weaknesses in the subaqueous sections of the ice ramp are also thought to play an important role in the growth of basal crevasses and, therefore, the location and timing of subaqueous calving events (van der Veen, 1998b). Detachment of buoyant termini is classified as a

second-order process, while buoyant calving of a subaqueous ice ramp is considered a third-order process as it operates within and is paced by first- and second-order processes (Benn *et al.*, 2007b).

2.4.2.5 Coseismic triggers

Coseismic events or earthquakes may also be a potential trigger for calving through the generation of tsunami. Data from Antarctica show that the Honshu (Japan) tsunami (triggered by the Honshu Japan earthquake on 11 March 2011) triggered the detachment of a large iceberg from the Sulzberger Ice Shelf (Brunt *et al.*, 2011). However, Brunt *et al.* (2011) highlighted that the calving event was not purely a consequence of the strength of the earthquake but that additional 'enabling' conditions were met before the arrival of the tsunami. These conditions included a lack of fast and pack ice from the region north of the ice shelf. Coseismic triggers can also have an effect on closely proximal calving glaciers. Dykes *et al.* (2012) described the response of Tasman Glacier (New Zealand), to the M_w 6.3, 5.7 and 4.5 Christchurch 22 February 2011 earthquakes and the subsequent calving event. The large calving event that occurred on 22 February 2011 was in direct response to a resonance effect caused by shear (S-) waves oscillating the glacier terminus at the ice-water interface. However, Dykes *et al.* (2012) proposed that the magnitude of the calving event was amplified as prior to the earthquake, Tasman Glacier had reached a critical threshold for buoyancy-induced calving in relation to perturbations in lake level. This was evident prior to the event, as small to intermediate magnitude calving (and coeval terminus retreat) had been dominated by thermo-erosional notching at the waterline, destabilising the subaerial ice cliff above (Dykes *et al.*, 2012). Hence, in tectonically-active areas, coseismic-initiated calving can have an episodic, but major control on retreat, potentially destabilising a glacier system and leading to subsequent accelerated recession.

2.4.3 Calving types

Three key types of calving dominate: buoyant calving, waterline melt-driven calving and stretching of the glacier front activating crevasses. These are discussed, in turn, below.

2.4.3.1 Buoyant calving

Warren *et al*. (2001) found that buoyancy-driven calving was an important process at Glaciar Nef (Chilean Patagonia), caused by surface ice loss near the terminus resulting in large areas reaching flotation and bending upwards. Three stages were recognised when a glacier accommodates buoyancy-driven torque. First, ice at the terminus is slightly less than the ice thickness required for flotation, so the buoyant zone is confined to a small area at the terminus of the glacier. The buoyant terminus is held below hydrostatic equilibrium by non-buoyant ice upstream, as ice creep is minimal due to low torque and basal tensile stresses. Thermo-erosional notches form at the terminus. Second, surface melting thins the glacier causing the buoyant zone to migrate up-glacier. Increase torque causes the terminus to upwarp. Third, catastrophic failure occurs either at the up-glacier limit of the buoyant zone or where bottom topography introduced a local stress concentration. The section down-glacier of this point then moves away from the terminus as one or more icebergs. Boyce *et al.* (2007) also found evidence for buoyancy-driven calving at Mendenhall Glacier, southeast Alaska with uplift of the terminus resulting from ice thinning and lake level rise.

2.4.3.2 Waterline melt-driven calving

As discussed in section 2.3.2, waterline melt is an important process in the development of thermo-erosional notches. Thermal undercutting of the ice cliff and resultant notches destabilise the subaerial section of the ice cliff by removing ice at the waterline. This removal creates shear and tensile stresses in the overlying subaerial ice which is likely to lead to failure via calving (Röhl, 2006). Thermo-erosional notches have been identified as a rate-controlling mechanism during subaerial calving at a number of glaciers (Kirkbride & Warren, 1997; Benn *et al.*, 2001; Warren & Kirkbride, 2003; Diolaiuti *et al.*, 2005; Röhl, 2006; Benn *et al.*, 2007b). At Tasman Glacier, subaerial calving is directly controlled by, and is the result of, thermal undercutting. However, the form, frequency and magnitude of calving events is determined by pre-existing weaknesses in the ice (Röhl, 2006). Spatial variation in calving along the terminus at Tasman Glacier was the result of exposure to currents and waves while temporal variation was likely to be the result of water temperature (Röhl, 2006). Sakai *et al.* (2009) also found that thermal undercutting initiated calving on supraglacial lakes on debris-covered glaciers of the Nepal Himalaya.

2.4.3.3 Exploitation of crevasses created as a result of stretching of the front

Stretching of the glacier in response to velocity gradients can result in the formation of crevasses. These crevasses provide pre-existing weaknesses near terminal ice cliffs which can be exploited by calving. Benn *et al*. (2001) found that closely-spaced longitudinal crevasse traces near exposed ice cliffs allowed for the rapid expansion of supraglacial ponds on Ngozumpa Glacier, Khumbu Himal, Nepal. The study found that calving rates were controlled by the location, orientation and spacing of weaknesses in the ice such as crevasses and debris bands (e.g. Figure 2.9). Where pre-existing weaknesses were not present, waterline melting had a strong influence on calving rates. Near-terminus stretching was identified as a key component in a feedback cycle where stretching during rapid retreat drove thinning and bottom crevasse formation, which in turn caused rapid retreat (Venteris, 1999). Venteris (1999, p. 137) also argued that "more rapidly-flowing glaciers have larger stretching rates near the terminus, which increase calving/terminus retreat by thinning and fracturing".

Figure 2.9: Debris bands in the terminal ice cliff of Hooker Glacier, New Zealand (source: C. Robertson, 23 November 2009). Along with crevasses, the location, orientation and spacing of such weaknesses can control calving rates.

2.4.4 Seismicity of calving

Recently, work has been completed on detecting seismic signals that are produced during crevasse propagation and calving (e.g. Chen *et al.*, 2011; Veitch & Nettles, 2011; Dalban Canassy *et al.*, 2012; Kohler *et al.*, 2012; Mikesell *et al.*, 2012; Walter *et al.*, 2012). The area of research is still relatively new and a lot of work is needed to refine the methods used to track the location of these signals and discriminate between results

of crevasse propagation and icefalls (e.g. Dalban Canassy *et al.*, 2012). A number of studies have gone some way to refining these techniques including Mikesell *et al.* (2012), who analysed continuous seismic recordings from a series of seismometers placed on Bench Glacier, Alaska. They recorded and identified the propagation of a crevasse which propagated more than 200 metres in three hours and established that these events were likely the result of diurnal fluctuations in surface run-off and subglacial water pressure. Walder *et al.* (2012) also investigated seismic signals created during a large iceberg calving from Jakobshavn Isbræ, Greenland. These investigations found that seismic signals created during calving events (termed 'glacial earthquakes') may be more common with full-glacier thickness calving events from grounded termini than first reported.

2.5 Glacier dynamics and calving

Debate surrounding the relationship between glacier dynamics and calving losses has been fuelled by the abundant observations of glacier thinning, acceleration and rapid retreat worldwide. Discussions focus on whether calving losses are the cause or the consequence of flow acceleration, the so-called 'master versus slave debate'. One side of the debate sees calving as the 'master' with ice loss at the terminus triggering flow acceleration up-glacier (Hughes, 1986; Meier & Post, 1987; Meier, 1994; Hughes, 1996; Meier, 1997; Howat *et al.*, 2005). The opposing view theorises calving as the 'slave' to glacier dynamics, with ice loss the passive response to changes in the glacier system (van der Veen, 1996; Venteris, 1997; van der Veen, 2002). Both sides of the debate are based on the same comprehensive dataset from Columbia Glacier and have empirical support (Theakstone, 1989; Fischer & Powell, 1998; Kirkbride & Warren, 1999; Motyka *et al.*, 2003a; Joughin *et al.*, 2004). Statistical analysis of both the 'master' and 'slave' relationships explain a similar percentage of observational data, which emphasises the complex nature of this problem (Benn *et al.*, 2007b).

2.5.1 Calving as the 'master'

According to the 'calving as the master' side of the debate 'calving is the local driving process, and the ice dynamics changes in response to this driving' (Meier, 1997, p. 113). Calving losses cause a response in ice dynamics including accelerating flow up-glacier of the terminus. Increased flow is a direct response to the retreat of the calving-front due to increased effective stress which causes thinning of the glacier surface (Howat *et al.*, 2005). As thinning progresses up-glacier, the glacier surface steepens, which delays acceleration of the glacier trunk. Glacier thinning is also attributed to longitudinal stretching caused by increased calving rates (Meier, 1994). As the glacier thins it causes decreased effective basal pressure which increases flow and produces a negative feedback on retreat rates.

2.5.2 Calving as the 'slave'

In contrast, the 'calving as the slave' debate argues that flow acceleration and thinning control calving activity and thus calving is a more or less passive response to changes in other parts of the glacier system (van der Veen, 1996; Venteris, 1997; van der Veen, 2002). Geometric and dynamical changes in the system result in increased calving fluxes by causing the calving front to retreat, in turn, increasing the delivery of ice to that point (Benn *et al.*, 2007b). As glacier flow is intrinsically connected with basal sliding, which itself is controlled by effective pressure at the bed (Bindschadler, 1983a), any change in basal conditions or subglacial drainage will influence ice velocities. Van der Veen (1996) noted that increased calving rates at Columbia Glacier were associated with higher ice velocities, while Kirkbride and Warren (1999) also found that flow acceleration preceded increased calving rates at Tasman Glacier. More recent work on Tasman Glacier by Quincey and Glasser (2009) however, found that contemporary glacier dynamics data show a reduction in glacier velocity with widespread surface lowering and rapid retreat between 2002 and 2007, pointing to calving as the local driver. However, when data from after 2006 are examined, velocity appears to have increased (Quincey & Glasser, 2009). Thus, determining if calving is the master or slave of ice dynamics at any particular glacier is difficult.

2.6 Velocity

Glacier velocity is an essential control on calving rates with variations in space and time determining the behaviour of calving glaciers (Benn *et al.*, 2007b). A good correlation between calving rates and glacier speed should be expected as ice velocities at the terminus are usually larger than the rate of change of terminus position, except in periods of rapid retreat (van der Veen, 1996). Longitudinal and transverse velocity gradients determine both the depth of surface crevasses and rates of dynamic thickness variation. Velocity gradients and the tensile stresses associated with them are generally high enough to initiate the propagation of crevasses on glaciers and ice shelves. Crevasses create a point of weakness in the glacier where calving is more likely to occur. Thus, the location of crevasses exert a strong influence on the position and shape of the calving front, with arcuate crevasse patterns typically mirrored in the geometry of embayments in the terminus (Powell, 1983). Velocity gradients also play a crucial role in determining whether surface crevasses reach water level and where subaerial calving will occur. High velocity gradients result in crevasses being more likely to reach water level, compared to low gradients which promote buoyancy near the grounding line, and may support a floating ice tongue or ramp (Benn *et al.*, 2007b). High velocities and longitudinal strain rates are driven by basal motion; hence, factors that control motion are key components in the glacier dynamics/calving relationship.

Glacier velocity is driven by the balance of forces resisting ice flow such as basal drag, lateral drag and resistance from longitudinal stress gradients (van der Veen & Whillans, 1989), the magnitude of driving stresses, and variations in these forces in time and space. As long-term fluctuations in velocity require changes in resistance or driving stresses which result from large changes in glacier geometry, short-term temporal fluctuations often reflect variations in resisting stresses (e.g. Iken & Truffer, 1997). Basal drag resists ice flow by increasing friction between the glacier and its bed. It is a complex process which results from interactions of ice temperature, pressure, volume and distribution of subglacial water (e.g. Bartholomew *et al.*, 2012) and debris content (Benn *et al.*, 2007b). Where subglacial water is present the ice will move. However, where the glacier is above the pressure melting point and no water is present, movement will be negligible. Basal drag can be reduced by increasing the basal water pressure which decouples the ice from the bed and reduces friction (Iken, 1981; Iken &

Bindschadler, 1986; Schweizer & Iken, 1992; Cohen *et al.*, 2005; Willis *et al.*, 2012). When basal drag is decreased, ice flow accelerates (e.g. Pritchard & Vaughan, 2007). Where this occurs in conjunction with high stretching rates near the terminus, deeper crevasses are produced and calving is encouraged.

Lateral drag is similar to basal drag in that it opposes driving stresses, yet the proportion to which it resists flow varies in space and time. For example, lateral drag provides the majority of resistance to ice flow on the Whillans Ice Stream, West Antarctic (Whillans & van der Veen, 1997). In addition, lateral drag in combination with basal drag oppose flow to a similar degree along most of the Pine Island Glacier, West Antarctic (Payne *et al.*, 2004). In contrast, O'Neel *et al.* (2005) found that lateral drag was generally less than basal drag at Columbia Glacier (Alaska) but that lateral drag becomes increasingly significant at times of rapid retreat. Speeding-up of Jakobshavn Isbræ (Greenland) is attributed, in part, to a reduction in resistance at the lateral margins bounding the fast-moving ice stream (van der Veen *et al.*, 2011).

Where lateral drag has a significant effect on ice flow, sliding laws that are pressure-dependant, such as that introduced by Budd *et al.* (1979), fail to accurately predict ice velocity (Benn *et al.*, 2007b). Therefore, where these sliding laws are incorporated into calving laws and glacier models, ice velocity and its impact on calving and mass losses will be inaccurately modelled. Modelling of the effects of lateral drag on ice flow (e.g. Raymond, 1996; van der Veen, 1999a; 1999b) however, has shown that ice flow is strongly dependent on glacier channel width and is independent of ice thickness. Thus, small increases in channel width will cause large increases in velocity, and decreases in width will reduce velocity and encourage terminus stability (Benn *et al.*, 2007b). As a result, glacier termini tend to be located at widenings in embayments or fjords and where longitudinal strain rates are high. High longitudinal strain rates at these locations encourage crevasses to penetrate to the waterline making it more likely that the crevasse depth criterion will be met (discussed in section 2.7.2) (Benn *et al.*, 2007a). In contrast to ice flow modelling by Raymond (1996) and van der Veen (1999a; 1999b) that found ice velocity is independent of ice thickness, Hindmarsh (2012) proposes a simple boundary layer theory for ice shelf calving which relates ice velocity at the calving front

to ice thickness, shelf width and strain rate. The theory explains empirical relationships between ice shelf calving rates and glaciological parameters (Alley *et al.*, 2008) and although it is not designed to explain these relationships at lacustrine-calving glaciers, it provides insights into the stability of laterally resisted ice streams.

Longitudinal stress gradients are a function of spatial variation in basal drag, lateral drag, longitudinal stress and result from a glacier trying to achieve equilibrium via viscous stretching. At a vertical terminus, the drive to regain balance in these stress gradients is the consequence of outward-directed cryostatic pressure being greater than backward-directed hydrostatic pressure (Benn *et al.*, 2007b). Similar imbalances are present at the point between a grounded glacier and its floating, unconfined ice tongue or shelf. Where forces such as lateral drag resist flow, however, the imbalance may be offset which results in additional backward pressure (van der Veen, 1997). O'Neel *et al.* (2005) found that on Columbia Glacier, particularly up-glacier of trough narrowings, longitudinal stresses played an important role in resisting driving forces locally, and that when a glacier retreats from key attachment points such as terminal moraines and topographic 'pinning points' (e.g. Warren & Hulton, 1990), flow acceleration is likely. As longitudinal stresses carry the effects of lateral drag up-glacier, the removal of these constraints will result in flow acceleration (Benn *et al.*, 2007b).

2.7 Calving laws and glacier models

2.7.1 Evolution of calving laws

The first theoretical analysis of calving was based on floating polar glaciers where calving was the result of a stress imbalance induced by unbalanced hydrostatic forces at the terminus (Reeh, 1968). The stress imbalance causes bending with stresses peaking at a distance up-glacier corresponding to the ice thickness. Fastook and Schmidt (1982) expanded the theory by considering enhanced calving along water-filled crevasses. Iken (1977) considered slab calving from a grounded ice wall and concluded that the thickness of slabs calved off from the undercut cliff were equal to cliff height. The downward propagation of a crack behind the cliff after reaching a critical tensile stress

and subsequent development of an overhang prior to calving were important components. Hughes (1992) developed a bending creep mechanism concept where deformation at polar glaciers resulted in calving of slabs along shear bands which were caused by a bending moment at the base of the ice cliff. The calving mechanism is controlled by bending creep that causes an overhang of the ice cliff. The concept was further expanded by Hughes and Nakagawa (1989) who stated that the expanded version could be applied to all types of calving at all glaciers. Subsequent work by Hughes (2002) on subaerial calving and consequential calving from ice ledges resulted in the theory that slabs one-tenth the thickness of the subaerial height of the ice cliff calve along surface crevasses. The rate of subaerial calving controls the rate of block calving from the ice ledge, which occurs along bottom crevasses when the ledge is one-half the ice thickness below water. The forward-bending mechanism has been applied at a number of calving margins with observations being made of overhangs before major calving events (Theakstone & Knudsen, 1986). However, Kirkbride and Warren (1997) questioned the applicability of the mechanism to temperate, lake-calving glaciers, such as those in *Aoraki*/Mt Cook National Park. They reported that the full height of the ice cliff at Maud Glacier calved too frequently to allow bending creep to create shear bands and an overhang. Instead, overhangs were created by small-scale calving of the thermo-erosional notch roof in response to waterline melting.

Current methods for incorporated calving losses into glacier models involve a calving rate. Calving rate is defined as the difference between ice velocity at the glacier terminus and glacier length change over time:

$$U_C = \bar{U}_T - \frac{dL}{dt} \qquad 2.7$$

where $\bar{U}_T$ is the vertically-averaged glacier velocity, L is the glacier length and t is time (Benn *et al.*, 2007b). Motyka *et al.* (2003a) has expressed this equation in terms of mass fluxes per unit width which includes losses by melting:

$$Q_C - Q_M = H.\bar{U}_T - H.\frac{dL}{dx} \qquad 2.8$$

where Q_C is calving flux and Q_M is the melt rate at the terminal ice cliff.

Two approaches have been used to solve equation 2.7. The first involves estimating a calving rate from independent variables (e.g. water depth, ice velocity, stretching rate) and then combining that rate with ice velocity to predict changes in terminus position (e.g. Sikonia, 1982; Bindschadler & Rasmussen, 1983; Siegert & Dowdeswell, 2004). Using this technique, a relationship between calving rates and water depth was identified at tidewater margins (Brown *et al.*, 1982), and defined by Pelto and Warren (1991) as:

$$U_C = 70 + 8.33 D_W (\mathrm{m\,a^{-1}}) \qquad 2.9$$

Additional studies at freshwater margins showed that these calving rates were an order of magnitude lower than those at tidewater margins (Funk & Röthlisberger, 1989). The relationship between calving rates and water depth, however, is not straightforward. It can vary between regions (e.g. Figure 2.10, Haresign, 2004) and temporally for a single glacier (van der Veen, 1996; 2002). Variations of equation 2.9 have been developed (e.g. Sikonia, 1982), although the model must be altered to fit different glacier margins, thus limiting its applicability as a general calving rate predictor. Other disadvantages to the water-depth model include: (1) its application only to annual-averaged calving rates (Brown *et al.*, 1982); (2) its inability to explain seasonal fluctuations in calving rates (van der Veen, 2002); and (3) its invalidity during times of rapid retreat on grounded glaciers as the terminus approaches flotation (Meier & Post, 1987). Van der Veen (2002) argues that a calving rate – ice velocity relationship may be more appropriate as it can explain seasonal fluctuations and can be applied to tidewater and freshwater calving margins.

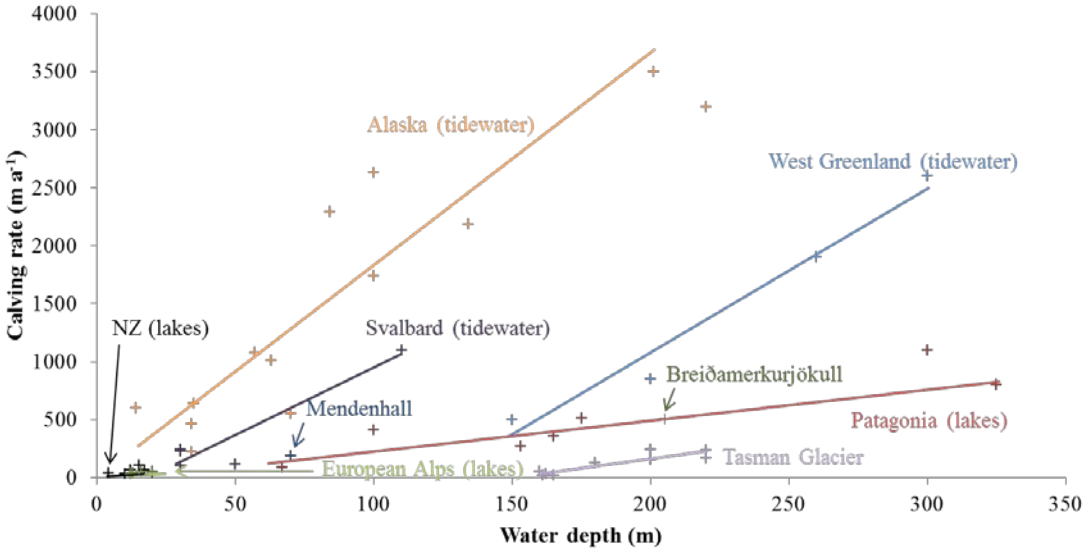

Figure 2.10: The relationship between calving rate and water depth for glaciers in different regions around the world (after Haresign, 2004). Calving rates for tidewater glaciers are larger than those at lake-calving termini. Data sources: New Zealand lakes: Warren & Kirkbride (2003), Tasman Glacier: Dykes & Brook (2010), Patagonian lakes: Rivera *et al.* (1997), Rott *et al.* (1998), Skvarca *et al.* (1995), Warren (1999), Warren *et al.* (1995b), Warren *et al.* (2001), Breiðamerkurjökull: Björnsson *et al*. (2001), Mendenhall: Motyka *et al*. (2003c), European Alps (lakes): Funk & Röthlisberger (1989), Alaska (tidewater): Brown *et al.* (1982), Meier *et al.* (1985), Pelto & Warren (1991), West Greenland (tidewater): Carbonell & Bauer (1968), Svalbard (tidewater): Jania (1986), Pillewizer (1965), Wilhelm (1963).

The second approach to solving equation 2.7 inverts the equation and uses ice velocity and terminus position changes to determine calving losses (e.g. van der Veen, 1996; Vieli *et al.*, 2001; van der Veen, 2002; Vieli *et al.*, 2002). Using the data set from Columbia Glacier, van der Veen (1996) argued that the calving front will retreat to a point where the height-above-buoyancy criterion is met (~50 m for Columbia Glacier). A modified version of the height-above-buoyancy model was used by Vieli *et al.*(2000; 2001; 2002) and was successful in modelling observed retreat of Hansbreen Glacier, Svalbard. The model works well at glaciers where the margin position is controlled by stretching and fracture growth as the glacier approaches floatation. Although there are also a number of disadvantages to this model: (1) it does not allow for the formation of ice shelves, (2) it does not explain how some glaciers can thin past flotation thickness

and develop ice shelves without calving, and (3), it cannot explain calving at glacier margins which are not floating (Benn *et al.*, 2007b).

Calving laws currently lack quantitative subaqueous data (Benn *et al.*, 2007b). Reasons for this include the inaccessibility of the environment in which data need to be collected, coupled with the hazardous nature of calving margins. However, as discussed in sections 2.2 and 2.3.3, subaqueous sections of a glacier have the potential to contribute large proportions of mass loss to the total glacier system. Therefore, to ensure that calving laws and models are accurate, subaqueous data must be included. Calving laws also tend to simplify nature in order to make models manageable. In doing so, key variables and relationships may be excluded and, therefore, the accurate prediction of what occurs in nature is lowered. Although van der Veen (2002) notes that it is illusory to expect a universally applicable calving law to exist, it has been highlighted that there is a need for a versatile and robust calving law that can be applied to a wide variety of glacier settings (Bassis, 2011).

2.7.2 The crevasse-depth calving criterion

A crevasse-depth calving criterion has been proposed by Benn *et al.* (2007a) as a simple way of parameterising first-order calving processes in ice sheet models. It is based on the theory that the down-glacier velocity gradient and ice elevation above the waterline are the main controls on glacier terminus position. The criterion explains both the water depth and buoyancy relationships and shows why they can be applied in some locations and not others. The criterion proposed that the position of the calving margin can be defined as the point where the depth of the surface crevasses, d, equals the glacier 'freeboard' above sea level, h;

$$x = L \text{ where } d(x) = h(x) \qquad 2.10$$

where x is the horizontal co-ordinate parallel to glacier flow, positive downstream. It is recommended that crevasse depths for time-evolving ice sheet models are calculated using the Nye (1957) formulation (shown in equations 2.10 and 2.11 in Benn *et al.*,

2007b) as it is not dependant on crevasse spacing (c.f. van der Veen, 1998b), it is computationally cheap, and it works just as well as more complex functions (Benn *et al.*, 2007b).

Although the criterion is more versatile than the water depth and height-above-buoyancy models, there are a number of drawbacks (Benn *et al.*, 2007b). First, where surface melt is negligible and no connection exists between crevasses and a proglacial water body, water may not enter surface crevasses but the crevasses may still propagate to, or below lake/sea water level. The crevasse will not penetrate the full thickness of the glacier or cause calving but if surface melting is increased, then calving could be 'switched on' (e.g. Scambos *et al.*, 2000). Secondly, the criterion does not incorporate crevasses in the transverse (*y*) direction. Thirdly, where second-order processes control calving, the crevasse-depth criterion may overestimate glacier length.

2.7.3 Calving law derived from fracture-scale physics

In the search for a universal calving law, Bassis (2011) has developed a method for deriving calving laws from an underlying mesoscopic theory of fracture. Bassis (2011) proposes that since iceberg calving is intrinsically linked to the fracturing of ice, calving laws should not be entirely independent of fracture physics. To this end, he has modified a differential master equation, which describes the rate of change of probability, to produce a macroscopic equation that describes how the terminus position of a glacier varies over large spatial and long temporal scales. The derived calving law is valid for any glaciological regime as it can reproduce different calving styles such as irregular detachment of large tabular icebergs from ice shelves and more frequent, lower magnitude calving from tidewater and outlet glaciers. The model may however fail to produce comprehensive calving laws for large ice shelves, such as those in Antarctica, due to their complex geometry and the inability of the model to consider these. Further testing of this model against calving datasets and comparison with calving rates calculated by remote sensing is needed.

2.7.4 Representation of calving in glacier models

Currently, calving rates incorporated into ice sheet models are based on poorly-tested empirical functions with little or no physical basis (Benn *et al.*, 2007b). Accurate quantification of mass loss from glaciers at marine and lacustrine settings is vital for the successful prediction of the way ice masses will respond to climate change. However, the sensitivity of ice sheet models is strongly influenced by the calving law that is incorporated into the model (Siegert & Dowdeswell, 1995) and at present there is not a satisfactory mathematical or physical model of calving processes (Bassis, 2011). Very few studies have applied and tested outputs from these models against real observations (e.g. Vieli *et al.*, 2002; Nick, 2006; Nick & Oerlemans, 2006).

2.8 Conclusions

To summarise the main points of this review:

- Understanding calving glaciers is important in accurate comprehension of the response of glaciers and ice caps to climate change and the resultant eustatic sea-level rise (SLR).
- Accurately quantifying mass loss from glaciers at tidewater and lacustrine settings is vital for the successful prediction of the way ice masses will respond to climate change.
- Calving glaciers and the water bodies into which they calve present a significant hazard to users of that environment, as well as causing distal downstream effects from GLOFs, which may also be caused by water displacement from avalanches or landslides into the proglacial water body.
- Three key calving types are: buoyancy-driven; melt at the waterline; and, stretching at the front activating crevasses.
- Although glacier dynamics and calving appear to be inextricable linked, the direction and strength of these linkages is highly debated.
- Proglacial water body fluctuations can affect glacier dynamics by altering the stress regime operating on the glacier and influencing calving processes at the terminus.

- Waterline melt and thermo-erosional notches are significant controls on calving rates at some lake-calving glacier margins with water temperature and circulation within the notch and lake level having a strong influence on ice melt.
- Subaqueous melt rates, in particular, remain poorly defined in lacustrine and tidewater environments.
- Four situations where stresses are likely to be high enough to initiate crevasse propagation and result in calving, and are therefore likely controls on calving processes, are: 1) stretching in response to large-scale velocity gradients: 2) force imbalances at unsupported ice cliffs: 3) undercutting by subaqueous melting: and, 4) torque arising from buoyant forces.
- Pre-existing weaknesses in ice such as crevasses and debris bands are vital to the location and rate of calving.
- Although it is illusory to expect a universally applicable calving law to exist, such laws have evolved from theories of bending creep and forward-bending mechanisms to water depth and height-above-buoyancy models. The final suite of calving models include those based around a crevasse-depth calving criterion, which explains both the water depth and buoyancy relationships, and shows why they are applicable at some locations and not others, and laws derived from fracture-scale physics.
- A particularly significant issue with calving laws is that they lack quantitative subaqueous data due to the hazardous nature and inaccessibility of the environment, and so such laws tend to simplify nature in order to make models manageable.

As this review has highlighted, there are still many gaps in calving theory and thus calving laws and models. One significant issue is the lack of quantitative subaqueous data. Thus, this study focuses on subaqueous margins at lake-calving glaciers in order to improve understanding of the controls on subaqueous ice ramp development and evolution. As was highlighted by Quincey and Glasser (2009) and discussed in Chapter 1, identifying subaqueous ice ramps and understanding how they affect glacier retreat and mass loss is a clear area for further research. Improving the understanding of subaqueous margin morphology and the processes which drive their evolution may also assist in defining subaqueous melt rates and how a glacier responds to altered stress

regimes as a result of proglacial water body fluctuations. Improving the knowledge of subaqueous margins will also improve hazard and risk assessment near calving glacier margins.

Chapter 3: Glacier retreat and proglacial lake expansion in *Aoraki*/Mt Cook National Park, New Zealand

3.1 Introduction

Chapter 2 reviewed previous research on lake-calving glaciers, with a particular focus on calving processes and subaqueous processes. Following a discussion of the significance of lake-calving glaciers, the way in which proglacial lakes form was examined, along with how these water bodies influence the adjacent glacier. The chapter examined processes of mass loss at the termini of lake-calving glaciers and introduced key laws and models on calving processes. The chapter highlighted that accurately quantifying mass loss from lake-calving glaciers is important in order to successfully predict the way ice masses will respond to climate change and thus to accurately predict resultant eustatic sea-level rise (SLR). The focus of this chapter is to examine and quantify glacier retreat and concurrent proglacial lake expansion in the central Southern Alps, New Zealand. Mueller, Hooker, Murchison, Classen, Grey, Maud and Godley glaciers within *Aoraki*/Mount Cook National Park provide an excellent example to examine variations in glacial retreat and lake expansion within a single mountain belt.

This chapter is contained within the manuscript: Robertson, C.M., Brook, M.S., Fuller, I.C., Holt, K.A. and Benn, D.I., Glacier retreat and proglacial lake expansion in *Aoraki*/Mount Cook National Park, New Zealand, which is in review in the journal *Geomorphology*. This manuscript examines glacier retreat and coeval proglacial lake expansion at seven glaciers in *Aoraki*/Mount Cook National Park. These glaciers have been the focus of previous studies, however the studies typically focused on a single glacier with few considerations of multiple glaciers. Firstly, glacier retreat data previously published for these glaciers is reviewed (section 3.4.2). Secondly, glacier retreat at each glacier between 1965 and 2011 is quantified along with proglacial lake expansion rates (section 3.6). Trends in retreat rates and lake growth rates are discussed

in relation to each other and with other proglacial lakes (sections 3.7.1 and 3.7.2). Lastly, a 4-stage model is proposed that explains the temporal and spatial evolution of glacial retreat and lake growth (section 3.7.3). This examination illustrates that there can be considerable temporal and spatial variations in retreat and lake expansion rates within the same mountain belt, and therefore that trends in glacier retreat within a small geographical area cannot be solely attributed to climate forcing. Therefore, in order to understand patterns of mass loss and thus improve predictions of sea level rise, data from multiple glaciers within a single mountain belt must be used.

3.2 Abstract

New Zealand glaciers, along with temperate glaciers worldwide, have undergone substantial changes during the twentieth and twenty-first centuries. Yet glacier retreat and associated processes of proglacial lake expansion remain relatively poorly understood at debris-covered, lake-calving glaciers. We present a systematic analysis of the retreat of debris-covered glaciers and formation of proglacial lakes at Mueller, Hooker, Murchison, Classen, Grey, Maud and Godley glaciers in *Aoraki*/Mount Cook National Park, New Zealand. Decades of downwasting and recession at these glaciers, since the Little Ice Age (LIA), has resulted in the formation of proglacial lakes during the latter half of the 20th century. Proglacial lakes had already formed at Classen, Grey and Maud glaciers by 1965, with proglacial lakes developing at Godley, Hooker and Murchison glaciers by 1986. A proglacial lake formed at Mueller Glacier in the early 1990s. Godley lake was the largest proglacial lake at 1.99 km^2 in 2011. The rates of calving retreat (ranging between –3 m a^{-1} and 157 m a^{-1}), in conjunction with proglacial lake development, are not consistent across time and space and can be divided into a four-staged model ranging from the appearance of supraglacial lakes through to the slowing of retreat caused by shoaling as retreat proceeds. All six glaciers examined in this study are currently in stage 3, although there is evidence that the glaciers in the Godley Valley may be approaching stage 4. The study highlights that trends observed at one glacier cannot be transferred to another glacier and that mass loss via glacier retreat at multiple glaciers within a single mountain belt (as opposed to a single glacier) must be incorporated into predictions of sea level rise and water availability.

Key words: glacier retreat, proglacial lake, calving glacier, New Zealand

3.3 Introduction

Understanding glacier response to climate change is a core focus of contemporary glaciological research. Fluctuations in glacier size and length on decadal to centennial scales, and relating these to climate, forms the basis of models aimed at understanding glacier response to climate change both in the past and future. According to simple modelling (Oerlemans, 2005), the change in length and timescale of a glacier's response to climate change are inversely proportional to the glacier's surface slope, and also dependent upon local climate and glacier size. However, this model cannot be applied to all glaciers worldwide. In particular, these variables alone do not adequately explain the variable recession rates observed across many debris-covered, lake calving glacier systems. Further to this, there is often a highly variable glaciological response to climate change even between glaciers within the same mountain belt, for example the Himalaya (e.g. Scherler & Strecker, 2011), and the New Zealand Southern Alps (e.g. Chinn *et al.*, 2005).

Debris cover and the presence of a proglacial lake are interpreted to exert a significant influence on mass loss of glaciers which possess them. Notable examples are located within the Himalaya (Watanabe *et al.*, 1995; Benn *et al.*, 2000; Benn *et al.*, 2001; Watanabe *et al.*, 2009; Thompson *et al.*, 2011), the European Alps (Haeberli *et al.*, 2001; Huggel *et al.*, 2002; Diolaiuti *et al.*, 2005; Diolaiuti *et al.*, 2006), and New Zealand (Kirkbride, 1993; Chinn, 1996; Warren & Kirkbride, 2003; Röhl, 2005; Quincey & Glasser, 2009; Dykes *et al.*, 2011). Glacier fluctuations in these areas occur in response to both changes in local and regional scale temperature and precipitation (Barry, 2006; Calmanti *et al.*, 2007), but also in response to the complicating effects of proglacial lake expansion and insulating debris cover. Such glaciers store a significant proportion of the world's freshwater (80-90%; van der Veen, 2002), and therefore understanding dynamics of mass loss at these glaciers is crucial for developing predictions of aspects of global importance, such as future water availability (Popovnin & Rozova, 2002) and global sea level rise (Raper & Braithwaite, 2005). Yet glacier retreat and associated processes of proglacial lake expansion remain relatively poorly

understood at debris-covered, lake-calving glaciers, and have thus been largely neglected in previous predictions relating to water availability and sea level rise.

New Zealand glaciers, along with most temperate glaciers worldwide, have undergone substantial retreat during the twentieth and twenty-first centuries. For New Zealand glaciers in particular, this recession has been spectacular. Although for some glaciers (e.g. Franz Josef Glacier), this general trend of long-term retreat has been punctuated by advances on decadal timescales (Chinn *et al.*, 2005), highlighting the importance of understanding glacier retreat at individual glaciers even within the same mountain belt. In this study we examine glacier retreat and concurrent proglacial lake formation at Mueller, Hooker, Murchison, Classen, Grey, Maud and Godley glaciers in *Aoraki*/Mount Cook National Park, New Zealand, in an effort to understand the temporal and spatial patterns of mass loss at the termini (via melting and calving) of debris-covered, lake-calving glaciers. These glaciers have undergone significant downwasting and recession during the last two centuries and provide an excellent example to examine variations in glacier retreat and lake expansion within a single mountain belt. Through mapping the terminus positions of these glaciers from 1965 to 2011, quantifying retreat rates and measuring lake surface areas during this time, we aim to identify temporal and spatial patterns in the retreat of debris-covered glaciers and proglacial lake expansion in *Aoraki*/Mount Cook National Park. The resulting data will shed light on how glaciers within a relatively small geographical area can respond differently to the same climatic signals and how proglacial lakes influence glacier retreat and mass lost at the terminus.

Previous studies of these glaciers (e.g. Hicks *et al.*, 1990; Kirkbride, 1993; Hochstein *et al.*, 1995; Watson, 1995; Hochstein *et al.*, 1998; Warren & Kirkbride, 1998; Kirkbride & Warren, 1999; Purdie & Fitzharris, 1999; Warren & Kirkbride, 2003; Röhl, 2006; Quincey & Glasser, 2009; Dykes & Brook, 2010) have typically focused on retreat rates, calving rates and lake evolution on a single glacier, with few considerations of multiple glaciers. The most recent study to review data across several calving glaciers was published almost a decade ago (Warren & Kirkbride, 2003), and was based on calving rates, water depths near the terminus and temperature data collected between

1994 and 1997. Subsequent studies have generally looked at these glaciers in isolation or with reference to a neighbouring glacier (Röhl, 2006; e.g. Tasman Glacier; Dykes *et al.*, 2011). Given the dramatic changes recorded at individual glaciers in *Aoraki*/Mt Cook National Park over the last decade (primarily Tasman Glacier, e.g. Röhl, 2006; Quincey & Glasser, 2009), quantification and a systematic analysis of calving retreat and coeval proglacial lake development across the calving glaciers in the region is propitious.

3.4 Study area

3.4.1 Physical setting

Mueller, Hooker, Murchison, Classen, Grey, Maud, and Godley glaciers are located in *Aoraki*/Mount Cook National Park on the eastern side of the central Southern Alps, New Zealand (Figures 3.1, 3.2 and 3.3). Climate of the area is dominated by westerly airflow which brings in moisture from the Tasman Sea. This, in conjunction with the topographic barrier of the Southern Alps, generates abundant precipitation to the west of the Alps, decreasing towards the east (Griffiths & McSaveney, 1983). Precipitation at *Aoraki*/Mount Cook Village ranges from 3000 to 5000 mm a^{-1} rising to 7000 mm a^{-1} at higher elevations in the Park (Anderton, 1975). South to southwest winds dominate (Hay & Fitzharris, 1988). All eight glaciers have been downwasting (thinning due to mass loss) since the late 19th century and all currently terminate into proglacial lakes which developed during the 20th century (Kirkbride, 1993; Chinn, 1996). Table 3.1 gives summary information on glacier length, area and terminal elevation and proglacial lake surface area, depth and volume, gleaned from a combination of previous work and the present study.

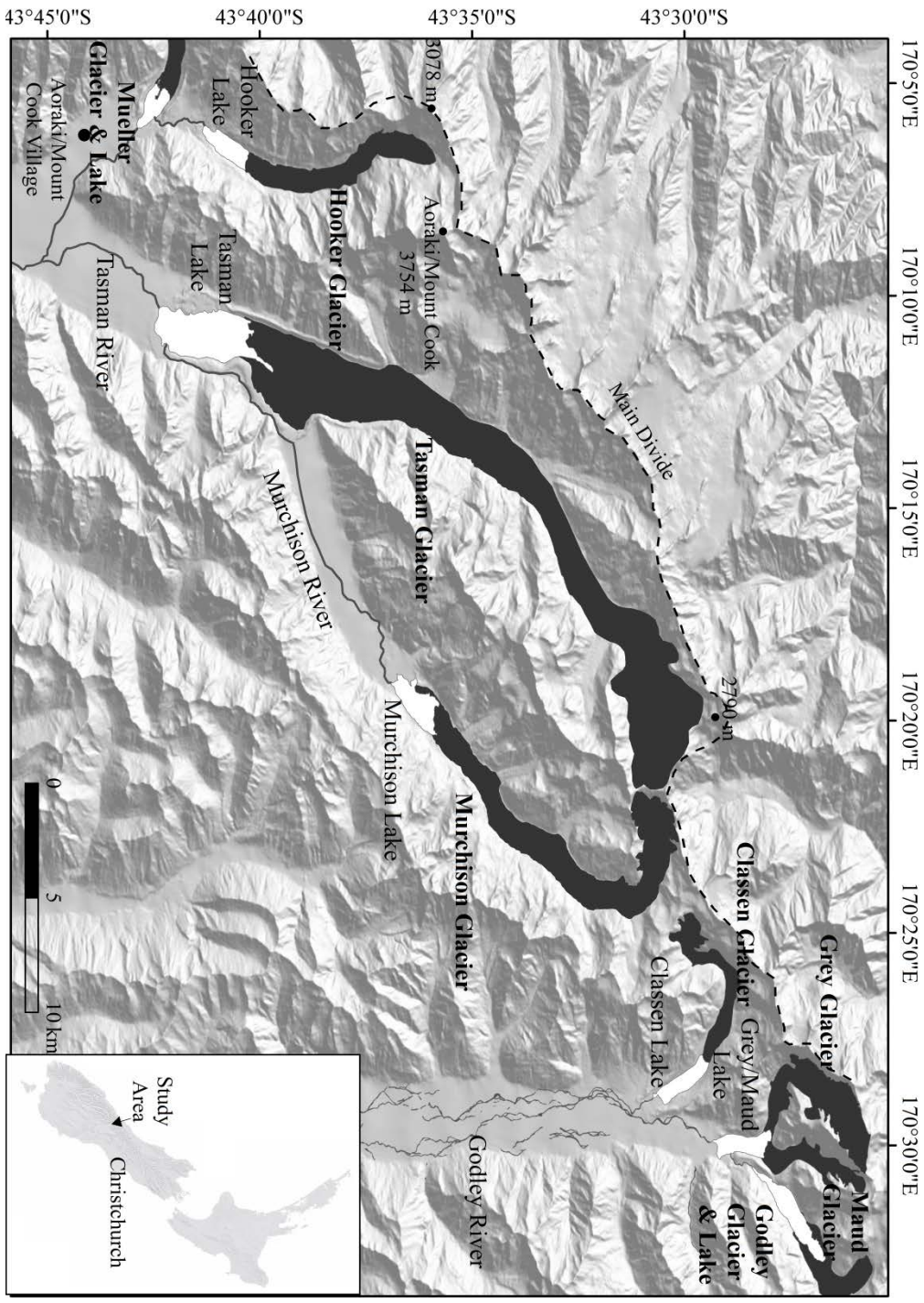

Figure 3.1: Map showing the location of Mueller, Hooker, Murchison, Classen, Grey, Maud and Godley glaciers and their proglacial lakes.

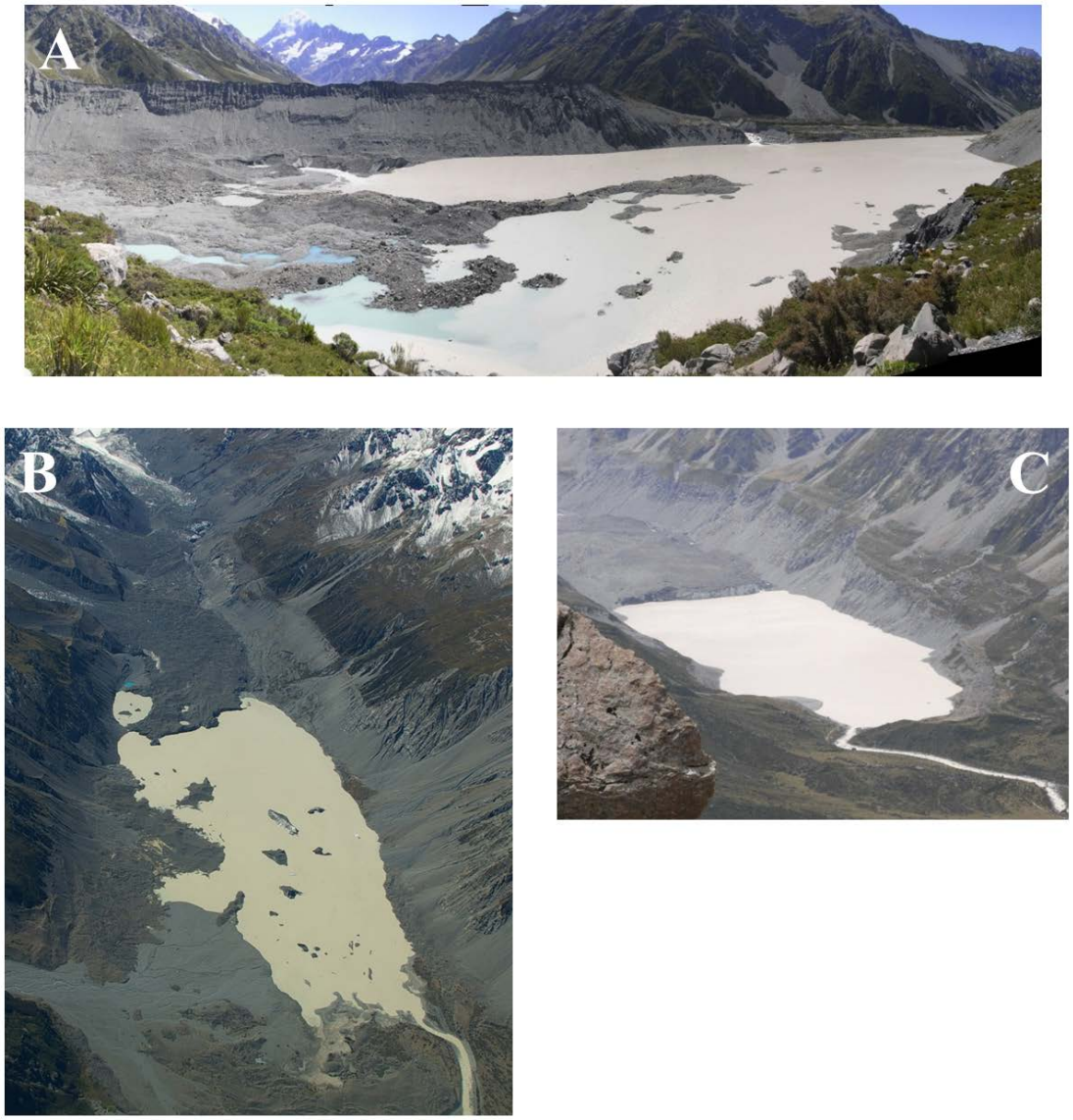

Figure 3.2: Lower terminus and proglacial lakes in *Aoraki*/Mount Cook National Park: A) Mueller Glacier (source: C. Robertson, 28 January 2011). Mueller Glacier is on the left of the photo and Hooker River enters the lake in the top right-hand corner; B) Murchison Glacier (source: T. Chinn, 2011); C) Hooker Glacier (source: C. Robertson, 26 January 2011).

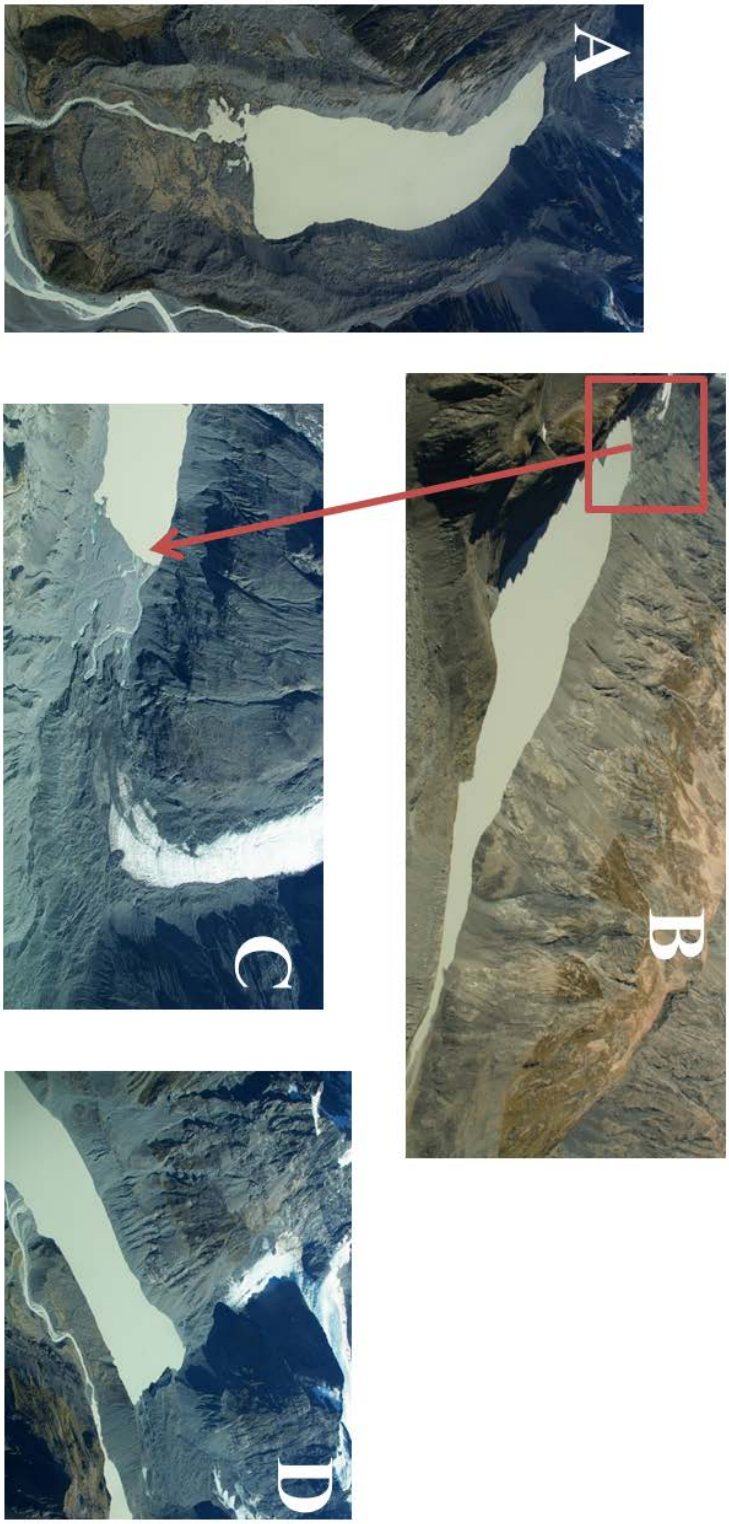

Figure 3.3: Lower terminus and proglacial lakes in *Aoraki*/Mount Cook National Park: A) Classen Glacier (source: T Chinn, 2011); B) Godley Glacier (far left of the photo) (source: S. Winkler, 2008). An enlarged image of the area in the red box is shown in C. C) Godley Lake is on the left with Godley Glacier retreating towards the right of the photo (source: T. Chinn). 2011); D) Grey (centre top of the photo) and Maud Glacier (on the right of the photo) entering Grey/Maud lake (source: T. Chinn, 2011).

Table 3.1: Characteristics of glaciers and their proglacial lakes in *Aoraki*/Mount Cook National Park. Debris cover (%) gives the percentage of the glacier subaerial surface covered with debris.

	Mueller	**Hooker**	**Murchison**	**Classen**	**Grey & Maud**	**Godley**
Length (km)	13.9	12.3	16.8	8.25	Grey ~6.8 Maud ~5	8.6
Area (km^2)	22.5	17	36.6	10.8	10.9	26.7
Debris cover (%)	37.2	25	30.5	28.9	20.9	30.3
Lake surface area (km^2)	0.97	1.28	1.85	1.76	1.40	1.99
Lake outlet (m a.s.l.)	765	876	1005	1005	~1020	1130
Maximum lake depth (m)	83	135	unknown	unknown	97	99
Lake formation	1993-1994	1982	Late 1980s to early 1990s	1920s-1930s or 1950s	Mid 1950s	Late 1960s
Last lake survey	2011	2009	1978	unknown	1995	1995
Sources	(This study; Chapter 4; Kirkbride, 1993; Watson, 1995; Winkler, 2004; Röhl, 2005)	(This study; Chapter 4; Hochstein *et al.*, 1998; Warren & Kirkbride, 1998)	(This study; Gellatly, 1985; Kirkbride, 1993; Chinn, 1996)	(This study; Kirkbride, 1993; Chinn, 1996)	(This study; Kirkbride, 1993; Hochstein *et al.*, 1998; Warren & Kirkbride, 1998)	(This study; Kirkbride, 1993; Warren & Kirkbride, 1998)

3.4.2 Existing data on historical glacier fluctuations

Mueller Glacier has been downwasting since the early 1900s at a rate of ~ 0.5 m a^{-1} in the terminal zone between 1879 and 1994 (Watson, 1995). By the end of the 1980s, Kirkbride (1993) noted that the glacier had retreated approximately 600 m from the 1890 terminal moraine. A series of melt ponds began forming on the terminus in the early 1980s and gradually grew in size and coalesced to form Mueller lake in the early 1990s (Watson, 1995). Subaerial calving from the terminal ice cliffs began prior to 1994 (Watson, 1995). Retreat rates estimated by Röhl (2005) are given in Table 3.2.

Downwasting of Hooker Glacier began in the late 20th century and ranged between 0.3 and 1 m a^{-1} along the centre flow line between 1915 and 1986 (Hochstein *et al.*, 1998). Between 1986 and 1996 downwasting decreased to approximately 0.3 m a^{-1} on the lower 3 km as a result of increased basal sliding due to melting (Hochstein *et al.*, 1998). Hooker Lake began forming in 1982, following rapid melting of the glacier behind the proximal ice-contact slope, formed of outwash 'head' (Kirkbride, 1993). Melting encouraged blocks of ice along the glacier margins to become buoyant which further enhanced melting and resulted in large melt channels (Kirkbride, 1993). These channels coalesced to form a proglacial lake which effectively 'drowned' the terminus (Kirkbride, 1993). By 1994, subaerial calving had commenced and downwasting rates had decreased (Hochstein *et al.*, 1998; Warren & Kirkbride, 1998). Retreat rates are given in Table 3.2. A minor glacier advance punctuated the progressive lake enlargement between 1983 and 1997 (Kirkbride & Warren, 1997; Chinn *et al.*, 2005).

Table 3.2: Retreat rates calculated in other studies for Mueller, Hooker, Classen, Grey, Maud, Godley and Tasman Glaciers. No additional retreat rate data for Murchison Glaciers have been published. Data for Grey Glacier are separated into Grey east and Grey west following Kirkbride (1993). While it is unclear in Kirkbrides (1993) study exactly what part of the glacier Grey east and Grey west refer to, it is assumed that rates for Grey east refer to the eastern boundary of Grey/Maud Glacier (when they were confluent) and Grey west rates refer to the western boundary of Grey/Maud Glacier (when they were confluent). Retreat rates for Tasman Glacier are incorporated for comparison purposes.

Glacier	**Study**	**Time period**	**Retreat rate (m a^{-1})**
Mueller	(Kirkbride, 1993)	1890-1980	retreat of 600 m
	(Röhl, 2005)	2000-2003	retreat of 0-210 m
Hooker	(Warren & Kirkbride, 1998)	Late 1970s	70
	(Hochstein *et al.*, 1998)	1982-1996	30
	(Warren & Kirkbride, 2003)	1995-1997	4
	(Hochstein *et al.*, 1998)	1998	30
Classen	(Kirkbride, 1993)	1920-1965	27.3
	(Kirkbride, 1993)	1965-1986	54.4
Grey east	(Kirkbride, 1993)	1920-1965	18.9
	(Kirkbride, 1993)	1965-1986	51.4
Grey west	(Kirkbride, 1993)	1920-1965	13.0
	(Kirkbride, 1993)	1965-1986	49.5
Grey	(Warren & Kirkbride, 2003)	1994-1995	13
Maud	(Warren & Kirkbride, 2003)	1994-1995	45 (advance)
	(Chinn, 1996)	1878-1978	66
Godley	(Kirkbride, 1993)	1965-1986	84.8
	(Kirkbride, 1993)	1974-1986	133
	(Warren & Kirkbride, 2003)	1994-1995	60
	(Röhl, 2005)	1994-2003	80
Tasman	(Dykes *et al.*, 2011)	2000-2006	54
	(Dykes *et al.*, 2011)	2002-2005	33
	(Dykes *et al.*, 2011)	2006-2008	144

Downwasting, retreat and proglacial lake formation at Murchison Glacier is poorly documented. Gellatly (1985) observed that the glacier surface lowered by approximately 60 m between 1900 and 1982 and that a proglacial lake formed at some stage during this period. The down-valley extent of this proglacial lake is constrained by terminal moraines and an outwash head (Kirkbride, 1993), with the lake estimated to have enlarged at ~0.14 km^2 a^{-1} between April 2000 and February 2003 (Röhl, 2005). Retreat of Classen Glacier prior to the 1950s (rates given in Table 3.2) led to the formation of a proglacial lake, with estimates for the inception of the lake ranging from the 1920s or 1930s (Kirkbride, 1993) to the 1950s (Chinn, 1996). The proglacial lake at the termini of the Grey and Maud glaciers began to form in the late 1950s when the glaciers were still confluent (Kirkbride, 1993; Warren & Kirkbride, 1998). Grey and Maud glaciers ceased to be confluent from 1990 onwards, and both now terminate into the lake via separate calving fronts (Chinn, 1996; Warren & Kirkbride, 1998). At Godley Glacier, a proglacial lake developed in the 1960s after the glacier (which was once also confluent with Grey and Maud glaciers) retreated up a narrow valley (Chinn, 1996). Retreat rates for the Godley Glacier are shown in Table 3.2.

3.5 Methods

Terminus positions and lake extent data for the glaciers described above were acquired from field-based surveys, along with aerial photographs and satellite image digitalisation. Field-based surveys were undertaken at Mueller lake in November 2009, April 2010, January 2011 and Hooker Lake in November 2009 using handheld GPS with an accuracy of ± 5 m (Garmin Ltd, 2007). All other terminus positions for Mueller, Hooker, Murchison, Classen, Grey, Maud and Godley glaciers were acquired from 14 aerial photographs covering 1965 to 1986 and 12 multispectral satellite images covering 2001 to 2011. The satellite images were sourced from 2 satellite sources, the Advanced Spaceborne Thermal Emission and Reflection Radiometer (ASTER) and Landsat. The images were geo-referenced using ground control points (stable, recognisable features present in all images) to register the selected images against topographic data from Land Information New Zealand Topo50-BX15, BX16, BX17, BY15, BY16 maps (New Zealand Transverse Mercator 2000). The images were registered using the rotation,

sampling and translation warping (RST) method, resulting in the root mean square error for each image being smaller than a single pixel (Jensen, 1997). Terminus positions and lake areas were generated from these geo-referenced images by manual digitisation in ESRI ArcMap software.

Rates of retreat between the terminus positions were calculated by measuring the distance between terminus profiles parallel to the flow axis (as shown in Figure 3.4, 3.5 and 3.6) at multiple locations along the terminus front; for example, the distance between the 2009 and 2010 terminus position. These measurements were averaged to give the mean rate of change between each terminus position. Distances were measured parallel to the flow axis to distinguish glacier retreat from local retreat (which would be measured perpendicular to the local ice margin). Convoluted ice margins have high local ice-wall retreat rates. As an ice cliff straightens, local ice-wall retreat rates are effectively converted to glacier retreat. Retreat rates were calculated for the periods between which data were available for each glacier (for example, 1986-2004, 2004-2006, 2006-2008, 2008-2009, 2009-2010, and 2010-2011 for Mueller Glacier; Figure 3.7).

3.6 Results: Glacier retreat and proglacial lake development

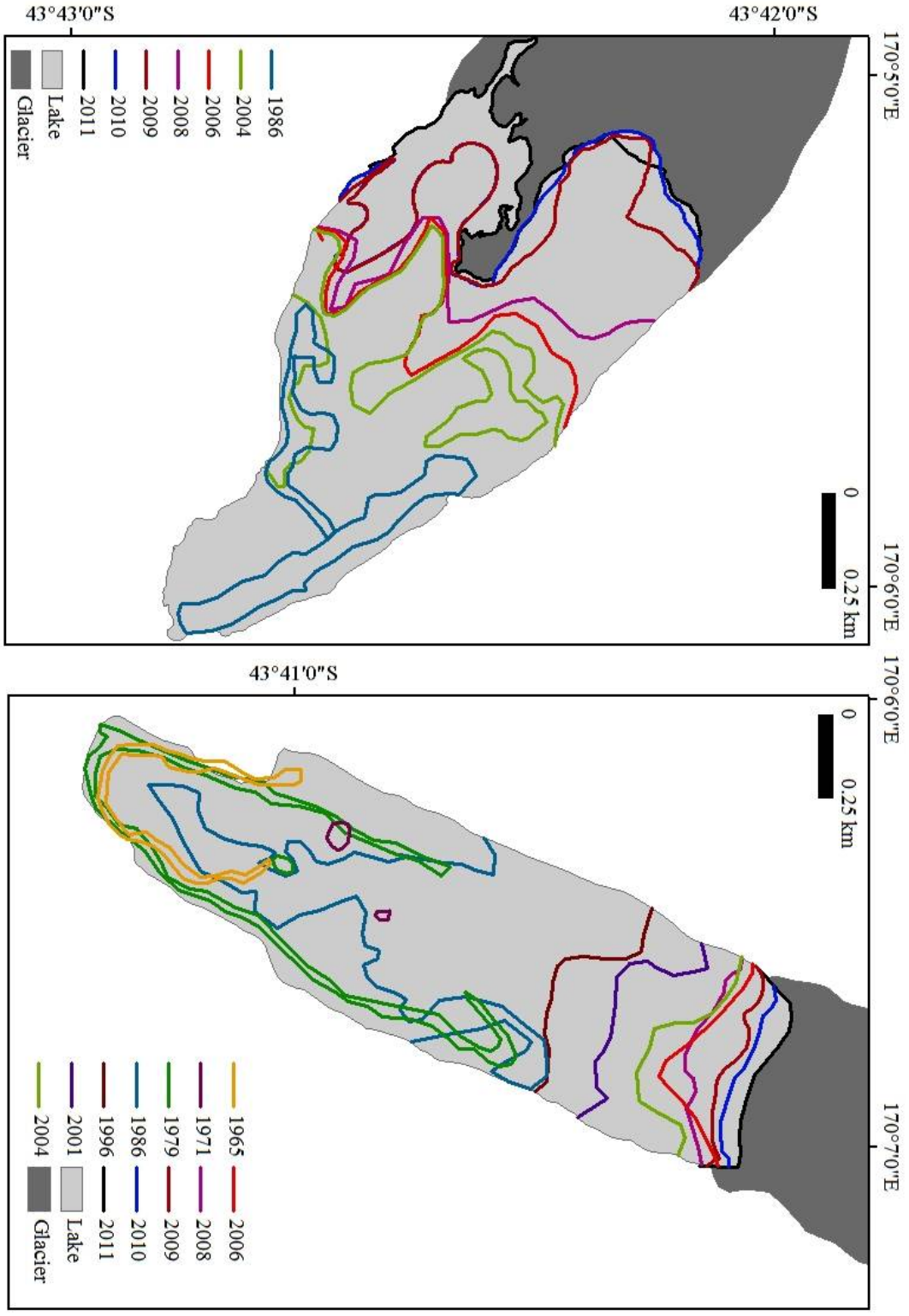

Figure 3.4: Terminus positions of Mueller Glacier, 1986-2011 and Hooker Glacier, 1965-2011.

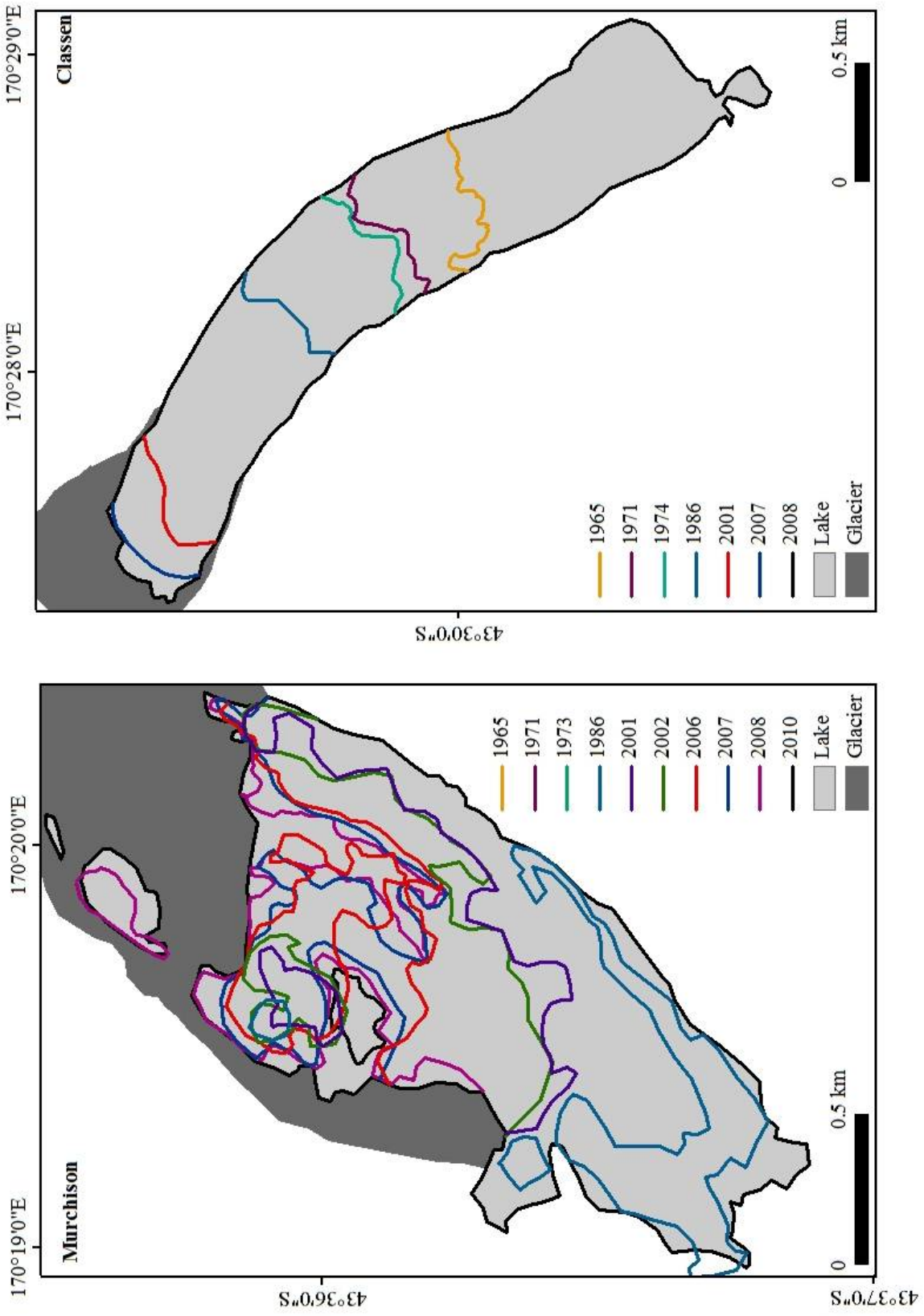

Figure 3.5: Terminus positions of Murchison Glacier, 1965-2010 and Classen Glacier, 1965-2008.

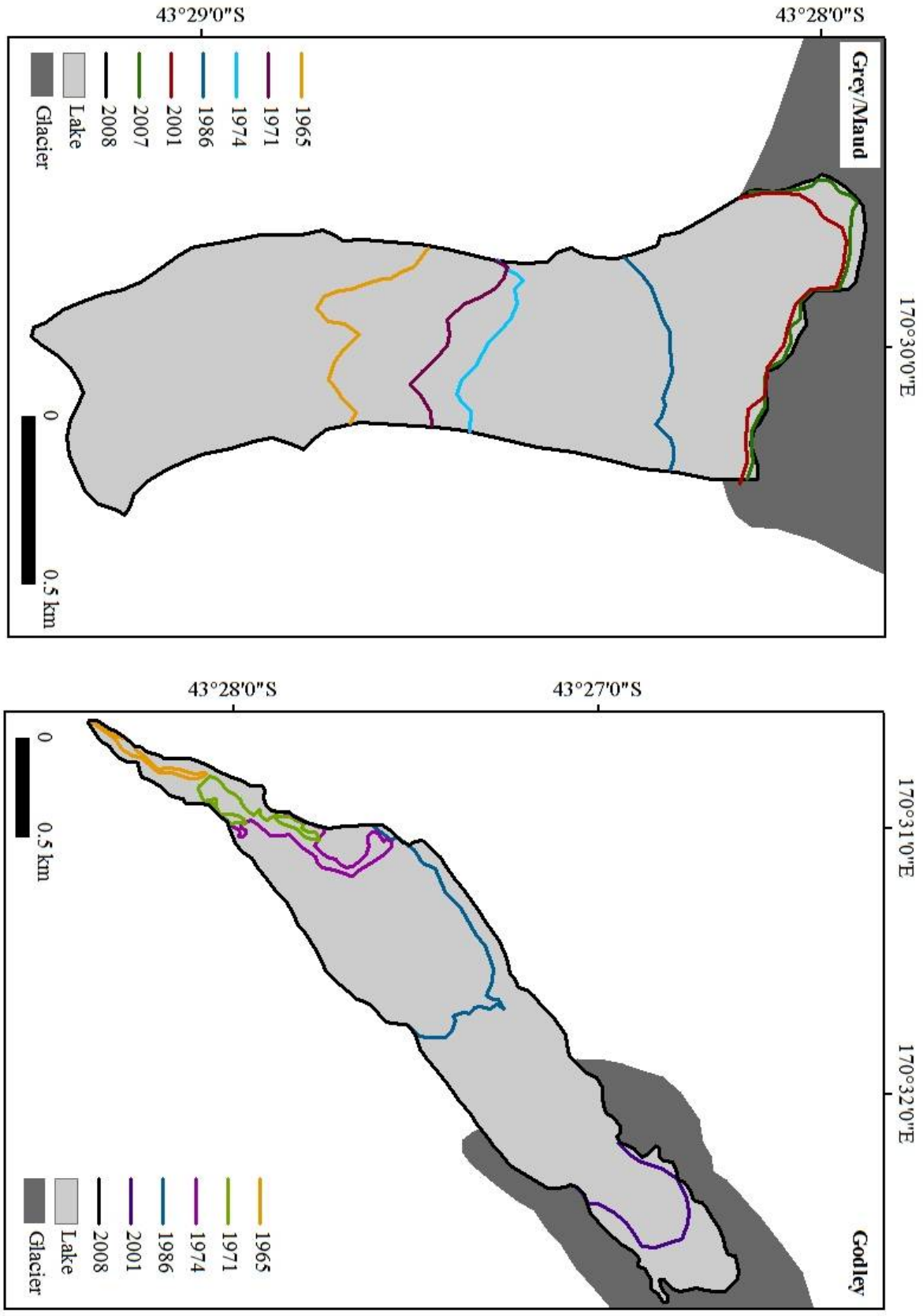

Figure 3.6: Terminus positions of Grey and Maud glaciers, 1965-2008 and Godley Glacier, 1965-2008.

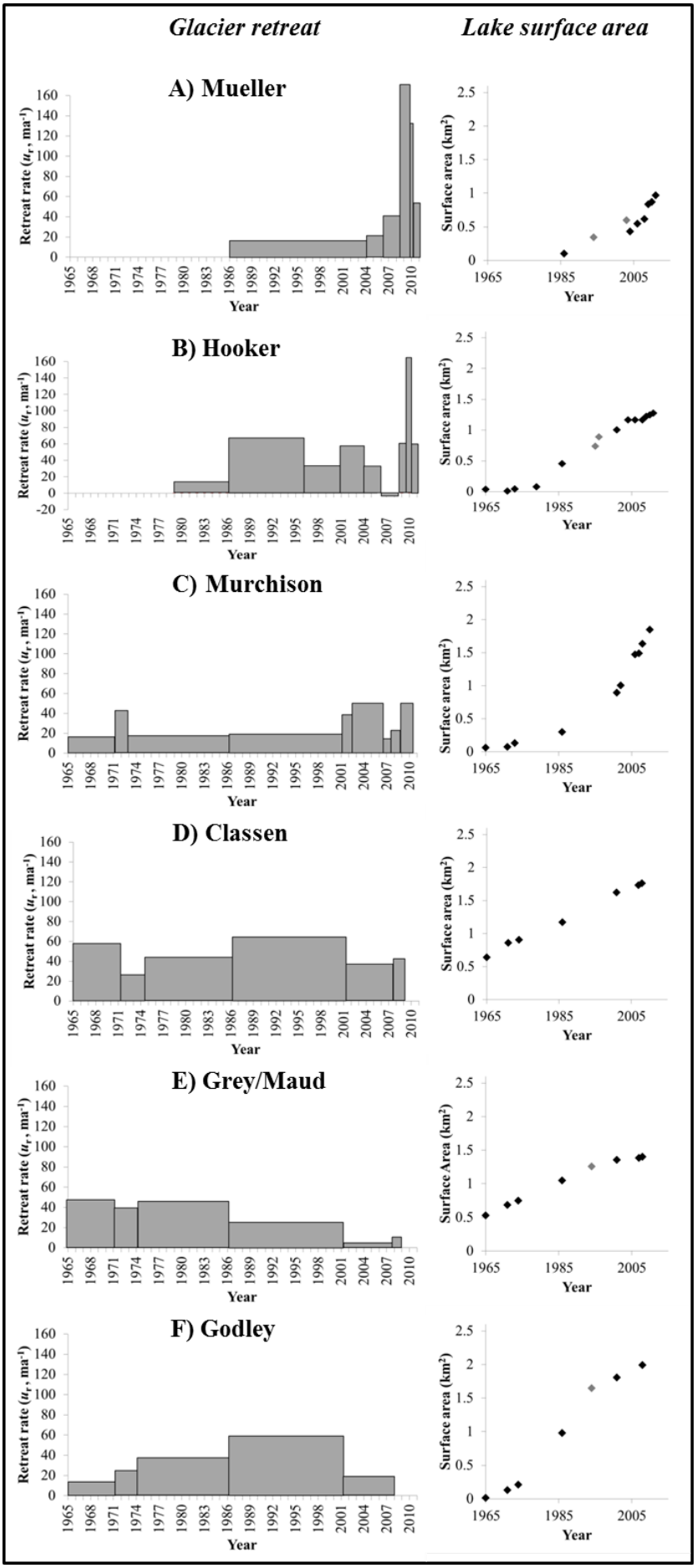
Glacier retreat
Lake surface area
A) Mueller
B) Hooker
C) Murchison
D) Classen
E) Grey/Maud
F) Godley
Retreat rate (u_r, ma^{-1})
Surface area (km^2)
Surface Area (km^2)
Year

Figure 3.7 (previous page): Retreat rate (u_r, m a^{-1}) and proglacial lake surface area (km^2) for A) Mueller Glacier, 1986-2011, B) Hooker Glacier, 1979-2011, C) Murchison Glacier, 1965-2010, D) Classen Glacier, 1965-2008, E) Grey and Maud glaciers, 1965-2008, and F) Godley Glacier, 1965-2008. Black diamonds on the lake surface area graphs represent values calculated in this study. Grey diamonds represent data from other studies: Mueller lake (Watson, 1995; Röhl, 2005), Hooker Lake (Warren & Kirkbride, 1998), Grey/Maud lake (Warren & Kirkbride, 1998) and Godley lake (Warren & Kirkbride, 1998).

3.6.1 Mueller Glacier

Terminus positions of Mueller Glacier between 1986 and 2011 are shown in Figure 3.4. In 1986, ponds had developed adjacent to the terminus along the south-western margin and between the Hooker River inflow and outflow. Figure 3.7A shows the retreat rate of Mueller Glacier from this period to 2011 and the resultant increase in lake surface area. Röhl's (2005) estimated 2004 lake surface area is not consistent with surface areas calculated in this study. This difference is attributed to Röhl (2005) having included gravel islands within the lake whereas the areas calculated in this study do not include these subaerial features. As the glacier retreated between 1986 and 2004 a peninsula developed in the centre of the terminus which extended into the lake. The glacier has maintained this peninsula as retreat has proceeded. Retreat rates increased rapidly from 15-38 m a^{-1} between 1986 and early 2008 to 157 m a^{-1} between May 2008 and November 2009 and 123 m a^{-1} between November 2009 and April 2010, leading to a lake surface area of 0.97 km^2 in February 2011 (Table 3.3).

3.6.2 Hooker Glacier

Glacier terminus positions for the period between 1965 and 2011 are shown in Figure 3.4, with retreat rates and proglacial lake area expansion between 1965 and 2011 reported in Figure 3.7B. Supraglacial ponds and meltwater channels were first evident on the terminus in 1965 and fluctuated in size during the 1970s. By 1986 these ponds and meltwater channels had increased in size to create a lake of approximately 0.45 m^2 (Table 3.3). The lake continued to increase due to glacier retreat (at rates of between 29 and 62 m a^{-1}) until rates of lake expansion slowed between 2004 and 2008. This slowing coincided with an advance of the terminus between May 2006 and May 2008, which was most pronounced in the centre of the terminus, where the glacier was advancing at a

rate of 3 m a^{-1}. Subsequently, the glacier retreated between 2009 and 2010 at a rate of 152 m a^{-1} before recession slowed to 55 m a^{-1} between 2010 and 2011. As the glacier retreated between 1996 and 2011, the terminus began to develop a more linear calving front. In February 2011 the lake had a surface area of 1.28 km^2, making it the second smallest lake out of the six studied.

Table 3.3: Surface areas (km^2) of Mueller, Hooker, Murchison, Classen, Grey/Maud and Godley lakes calculated from aerial photographs, satellite images and field-based surveys.

	Mueller	**Hooker**	**Murchison**	**Classen**	**Grey/Maud**	**Godley**
1965		0.03	0.06	0.64	0.53	0.02
1971		0.01	0.07	0.86	0.69	0.13
1973		0.04	0.13			
1974				0.90	0.75	0.21
1979		0.08				
1986	0.10	0.45	0.30	1.17	1.05	0.98
1994	0.35*				1.26*	1.65*
1995		0.74*				
1996		0.89				
2001		1.00	0.89	1.62	1.36	1.81
2002			1.00			
2003	0.60*					
2004	0.43	1.16				
2006	0.55	1.16	1.47			
2007			1.49	1.73	1.38	
2008	0.61	1.17	1.63	1.76	1.40	1.99
2009	0.83	1.22				
2010	0.87	1.24	1.85			
2011	0.97	1.28				
*source	(Watson, 1995; Röhl, 2005)	(Warren & Kirkbride, 1998)			(Warren & Kirkbride, 1998)	(Warren & Kirkbride, 1998)

3.6.3 Murchison Glacier

The retreat of Murchison Glacier between 1965 and 2001 was relatively slow compared with Hooker and the Godley Valley glaciers (Figure 3.7), and involved the development, enlargement and coalescence of many supraglacial ponds (Figure 3.5). After 2001, retreat rates doubled to around 46 m a^{-1}, except for the short period between 2006 and 2007, when retreat slowed to just 13 m a^{-1} (Figure 3.7C). Coeval with retreat rates, lake surface area increased rapidly post-2001, compared with lake growth between 1965 and 2001 (Table 3.3). By 2010, these preceding decades of glacier retreat had increased the lake surface area to 1.85 km^2.

3.6.4 Classen Glacier

Terminus positions from 1965 to 2008 for Classen Glacier are shown in Figure 3.5, with retreat rates and lake surface areas reported in Figure 3.7D. By 1965 the glacier had retreated from its terminal moraine and a proglacial lake had formed between the glacier snout and the terminal moraine, with a lake surface area of 0.64 km^2. The glacier continued to retreat at a rate of 24 to 59 m a^{-1} up until 2009. This moderate retreat rate caused a gradual increase in lake surface area, with no clear phases of either acceleration or deceleration of growth rates. By 2008, the lake had a surface area of 1.76 km^2 (Table 3.3).

3.6.5 Grey and Maud glaciers

By 1965, Grey and Maud glaciers, which both flowed into a single glacier tongue, had retreated up-valley from the terminal moraine, and a proglacial lake, with a surface area of 0.53 km^2, had formed. Terminus positions between 1965 and 2008 are shown in Figure 3.6. Between 1965 and 2007 combined retreat rates for the two glaciers decreased from 43 m a^{-1} to 3 m a^{-1} (Figure 3.7E). Subsequently, combined retreat rates then increased to 10 m a^{-1} between 2007 and 2009. However, when the retreat of each glacier is analysed individually (following the separation of Grey and Maud glaciers), results show that Grey Glacier retreated twice as fast as Maud Glacier between 2001 and 2008 at rates of 6 m a^{-1} and 3 m a^{-1}, respectively. Growth of the surface area of the lake appears to have been reasonably constant between 1965 and 2001, after which

growth slowed (Figure 3.7E and Table 3.3), with the lake reaching a surface area of 1.4 km^2 in 2008.

3.6.6 Godley Glacier

A small channel which drained the glacier had formed on the terminus of Godley Glacier by 1965. Further terminus melting and disintegration enlarged this channel and created a proglacial lake with a surface area of 0.13 km^2 by 1971. Between 1971 and 1974, glacier retreat was focused on the northwest section of the terminus, with the lake advancing up a narrow arm (Figure 3.6). The surface area of the lake increased significantly between 1974 and 1986 from 0.21 km^2 to 0.98 km^2 (Table 3.3) and again between 1986 and 1994. Lake area expansion then slowed, reaching a surface area of 1.99 m^2 in 2009. Phases of rapid lake expansion were mirrored by increased rates of calving retreat, which increased from 14 m a^{-1} to 59 m a^{-1} between 1965 and 2001, before decreasing to 18 m a^{-1} between 2001 and 2009 (Figure 3.7F).

3.7 Discussion

Glacier retreat and proglacial lake expansion in the *Aoraki*/Mount Cook area has varied both temporally and spatially. By 1965, large proglacial lakes had already formed at the termini of Classen, Grey and Maud glaciers. Between 1965 and 1986, supraglacial lakes and meltwater channels began forming and enlarging on Godley, Mueller, Hooker and Murchison glaciers, with Mueller Glacier being the last to enter this stage of disintegration in the late 1980s. Since the early 1990s, all the glaciers have continued to retreat from their LIA moraines and their proglacial lakes have steadily expanded. Lake expansion at the Godley Valley lakes however, now appears to be slowing, while Mueller and Murchison lakes continue to expand rapidly.

3.7.1 Retreat rates

With the general trend of retreat across all the glaciers since 1965 (Figures 3.4, 3.5, 3.6 and 3.7), two distinctive phases can be discerned. The first period from 1986 to the late

1990s was characterised by increased rates of retreat at all the glaciers except the Grey/Maud system (where rates actually slowed, possibly due to an advance of a few tens of metres between 1995 and 1997 (Warren & Kirkbride, 1998)) (Figure 3.7). The increase in retreat rates was greatest at Hooker Glacier, where rates increased from 12 m a^{-1} between 1979 and 1986 to 62 m a^{-1} between 1986 and 1996 (Figure 3.7). Lake surface areas also increased rapidly during this time (Figure 3.7 and Table 3.3) with the largest increase at Godley lake, which increased from 0.98 km^2 in 1986 to 1.81 km^2 in 2001. The second phase occurred between approximately 2006 and mid-2008, and was characterised by a slowing of terminus retreat at Hooker, Murchison, Classen, Grey, Maud and Godley glaciers (Figure 3.7). In particular, the decrease in retreat rate was more marked at Murchison Glacier, where the retreat rate decreased from 46 m a^{-1} to 13 m a^{-1}. Hooker Glacier actually advanced during this second phase at a rate of 3 m a^{-1} (Figure 3.7). The decrease in retreat rates actually began earlier (2001) at the Godley Valley glaciers (Classen, Grey, Maud and Godley glaciers). In contrast, while the retreat of all the other glaciers at least slowed, Mueller Glacier's retreat accelerated over the same period (Figure 3.7).

The primary driver of the increase in retreat rates after 1986 was the transition from melting to calving as the dominant mass loss process at the termini of these glaciers (Kirkbride, 1993). This transition involved the disruption of supraglacial debris cover which caused thermokarst erosion of ice margins and englacial conduits, resulting in rapid retreat via calving and a period of exponential lake growth (Kirkbride, 1993; Chinn, 1996). The decrease in retreat rate at Grey and Maud glaciers during the same period can be attributed to the separation of the two glaciers in 1990 (Warren & Kirkbride, 1998), after which Grey Glacier continued to retreat while Maud Glacier advanced between 1994 and 1995 (Warren & Kirkbride, 1998). The rock avalanches from Mt Fletcher in May and September 1992 may also have reduced the retreat of Grey and Maud glaciers due to the input of several million cubic metres into the glacier system (Warren & Kirkbride, 1998).

There are a number of possible explanations for the phase of decelerating retreat between 2006 and 2008 at the Hooker, Murchison and Godley Valley glaciers. The

glaciers may have retreated up-valley onto an adverse bedrock slope, creating a shoaling effect, which resulted in a decrease in calving retreat rates (e.g. Brown *et al.*, 1982; Hanson & Hooke, 2000). However, this hypothesis can be rejected for Hooker Glacier at least, where post-2008 bathymetry indicates (Chapter 4) that the terminus actually retreated into a bedrock overdeepening and thus deeper water after 2004. Unfortunately, post-2008 bathymetry from the other glaciers is not available to investigate the validity of this theory further. A second explanation for the decrease in retreat rates between 2006 and 2008 is that this was possibly a period of regional positive mass balance. Terminus advances at Franz Josef and Fox glaciers, on the western side of the Southern Alps, from the mid-1980s until 2010 (Herman *et al.*, 2011) have been linked to mass gained during negative phases of El Niño-Southern Oscillation (e.g. Purdie *et al.*, 2008), which brings cold moist south-westerly airflow to the Southern Alps. Kirkbride (1993) found that reduced retreat at Classen and Grey glaciers in the late 1960s coincided with regional positive mass balance, also reflected in advances of Franz Josef and Fox glaciers and also at Stocking Glacier, on the eastern side of the Southern Alps (Hessell, 1983; Salinger *et al.*, 1983; Brazier *et al.*, 1992). It was proposed by Kirkbride (1993) that increased ice delivery to the terminus at Classen and Grey glaciers may have come close to replacing ice lost by calving during this time. However, whether or not late 20th-early 21st century mass gains in the Southern Alps accumulation zones led to a deceleration in calving retreat during 2006-2008 is questionable. This is because the calving glaciers in the present study are among the longest in the Southern Alps, and have low-gradient debris-covered tongues, leading to terminus response times in the order of several decades (Chinn *et al.*, 2005). This is in direct contrast to the steep, debris-free Franz Josef and Fox glaciers that have response times of around a decade (e.g. Purdie *et al.*, 2008). Hence, based on likely terminus response times of several decades, it is difficult to conclude that climate-driven positive mass balances during the 1990s and 2000s caused a deceleration in retreat (or advance) at Hooker, Murchison and the Godley Valley glaciers between 2006 and 2008.

The contrasting increase in retreat rate at Mueller Glacier during 2006-2008 coincides with the rapid retreat at Tasman Glacier during this period. Retreat rates at Tasman Glacier increased from 54 m a^{-1} to 144 m a^{-1} during 2000-2006 (Dykes & Brook, 2010), with Dykes and Brook (2010) proposing two potential reasons for this increase in

retreat. These were: (1) a change in the velocity regime towards the terminus, and (2) the growth of supraglacial ponds on the terminus. Dykes and Brook (2010) outlined how Quincey and Glasser's (2009) study on Tasman Glacier hinted at more rapid ice flow on the terminus after January 2006 and that this velocity increase may have been driving calving losses, with calving acting as the 'slave' to glacier dynamics (e.g. van der Veen, 2002). Whether or not this is the case is difficult to determine empirically. Further examination of Quincey and Glasser's (2009) study shows the subtle increases in glacier velocity between January 2002 and December 2007 coincided with widespread surface lowering and rapid retreat over the same period which may point to velocity acting as the 'slave'. Hence, it is difficult to determine if calving was acting as the local driver and 'master' to glacier dynamics (e.g. Meier, 1997) or not. Unfortunately, detailed velocity data during this period are not available for Mueller Glacier to confirm if fluctuations in ice flow up-glacier of the terminus was driving or acting in response to calving.

Dykes and Brook's (2010) second proposal to account for increased retreat at Tasman was the significant growth of supraglacial ponds on the terminus between 2000 and 2006. Likewise, at Mueller Glacier, supraglacial ponds formed on the terminus during this time, including a large (~0.02 km^2) pond in 2008 immediately up-glacier of the terminus. This pond expanded prior to 2006, with a large pond coalescing with the lake sometime between June 2009 and November 2009. Röhl (2008) highlighted the importance of supraglacial ponds in terminus disintegration, and once ponds become hydraulically connected to the englacial drainage system, pond expansion via melting and small-scale calving occurs. Rapid drainage of such ponds can then increase buoyancy of the terminus, leading to longitudinal extension and basal crevasse propagation (Benn *et al.*, 2007b). From aerial photographs, the coalescence of the large supraglacial pond into Mueller lake in 2009 appears to be a similar process to that which occurred at the terminus of Tasman Glacier in 2000 (Röhl, 2008). The consequence at Tasman Glacier was accelerated retreat (via calving) of the surrounding ice walls and main ice cliff. Likewise at Mueller Glacier, the coalescence of the large supraglacial pond with Mueller lake contributed to rapid calving retreat of the glacier between 2006 and 2008.

3.7.2 Trends in lake expansion

Since the initiation of proglacial lake development, all six lakes have expanded rapidly in conjunction with glacier retreat. After the initial rapid expansion of the Godley Valley proglacial lakes, lake surface area growth appeared to slow down relative to Mueller and Murchison lakes (Figure 3.7). Classen lake increased by 0.14 km^2, Grey/Maud lake increased by 0.04 km^2, and Godley lake increased by 0.18 km^2 between 2001 and 2008. The slowed expansion of these three proglacial lakes, in addition to the overall trend of decreasing retreat rates (Figure 3.7), may be a sign that the glaciers are retreating into shallower water due to a bedrock high (e.g. Brown *et al.*, 1982; Hanson & Hooke, 2000). Unfortunately, bathymetry data post-1995 are not available for the Godley Valley lakes to verify this idea.

The surface areas of Mueller and Murchison lakes have increased rapidly by 0.13 $km^2\ a^{-1}$ and 0.11 $km^2\ a^{-1}$, respectively, between 2008 and 2010. This is in comparison with Hooker Lake which increased by only 0.04 $km^2\ a^{-1}$ over the same period and Tasman Lake which increased very rapidly by 0.34 $km^2\ a^{-1}$ over an 8 year period, between 2000 and 2008 (Dykes & Brook, 2010). The rapid expansion of Mueller and Murchison lakes is likely to be in response to a combination of factors, including high calving rates and hence glacier retreat rates (Figure 3.7). Calving retreat into deeper water may also be one of these factors, following the calving rate-water depth relationship as discussed by Hanson and Hooke (2000). This relationship describes how calving rates increase as the water depth adjacent to the terminus increases due to the glacier retreating into deeper water. The subaqueous morphology at the terminus of the glaciers may, however, be a complicating factor in this relationship as the presence of an ice ramp extending from the terminus would reduce the effective water depth adjacent to the terminus. Although ice ramps have recently been identified extending from Mueller, Hooker and Tasman Glaciers (Chapter 4), the degree to which these ice ramps influence calving rates and hence retreat rates remains unclear.

3.7.3 Spatial and temporal evolution model

From our analysis we propose that the *Aoraki*/Mount Cook debris-covered glaciers and proglacial lakes have followed a four-stage model of spatial and temporal evolution (Figure 3.8):

- *Stage 1:* The disruption of supraglacial debris cover, followed by the appearance and growth of supraglacial lakes and/or meltwater channels on the lower ablation areas of the glacier. The disruption of the supraglacial debris cover encourages melting of the bare ice slopes. Classen, Grey and Maud glaciers experienced this stage prior to 1965. Godley Glacier went through this stage during the mid-1960s to the mid-1970s. Hooker and Murchison glaciers went through this stage during the mid-1960s to the early-mid 1980s while Mueller Glacier passed through the stage in the mid-1980s.
- *Stage 2:* This stage marks the transition between the development of supraglacial lakes and meltwater channels, and the coalescence of these into a single lake. This stage could be seen as the 'tipping point' between supraglacial pond development and proglacial lake enlargement. As with stage 1, Classen, Grey and Maud glaciers experienced this stage prior to 1965 as large proglacial lakes had developed at their termini by this time (Figure 3.5 and 3.6). Godley Glacier transitioned through this stage between 1974 and 1986. By 1986, Hooker Glacier had entered this stage. Mueller and Murchison glaciers passed through this stage between 1986 and 1994.
- *Stage 3:* The stable expansion of a single coalesced lake. By 1965, Classen, Grey and Maud glaciers had entered this stage. Godley glacier had entered this stage by 1986. Hooker Lake began a steady expansion shortly after 1986. Murchison and Mueller glaciers entered stage 3 much later, just prior to 1994. The distinctive retreat between 1986 and the late 1990s can be characterised as this stage of lake evolution. The period was characterised by an increase in retreat rates leading to the stable expansion of the proglacial lakes at the majority of the glaciers. This stage could be further split into 1) steady lake growth, 2) rapid or accelerating lake growth and 3) decelerating lake growth.
- *Stage 4:* Stage 4 is characterised by slowing lake expansion rates due to slowing retreat, caused by shoaling, as the valley's bedrock profile comes closer to lake level as retreat proceeds. Thus, the timing of when a glacier may enter stage 4 is controlled by the bedrock profile under the glacier. The second distinctive phase

between 2006 and mid-2008 may fit into the beginning of this stage of proglacial lake evolution. The phase was characterised by a slowing of terminus retreat at Hooker, Murchison, Classen, Grey, Maud and Godley glaciers. The Godley Valley glaciers, and in particular Godley Glacier, may now be approaching or entering stage 4, as retreat rates and lake expansion have shown a steadily decreasing trend since 2001 (Figure 3.7). Photographs of the terminus of Godley Glacier (Figures 3.3B and 3.3C) show a delta is growing in between the lake and the glacier, which may indicate that Godley Glacier is retreating away from Godley lake. Hochstein *et al.* (1998) predicted that Hooker Glacier would continue to retreat until the bedrock under the glacier is at the same level as the lake outlet, 4.8 km up-valley. The glacier is currently 2.14 km from the lake outlet, so will presumably approach stage 4 in the future. Accurate bedrock topography data up-valley from the current termini are needed to predict when Mueller and Murchison glaciers may enter stage 4, and when the glaciers will become detached and retreat up-valley from their proglacial lakes.

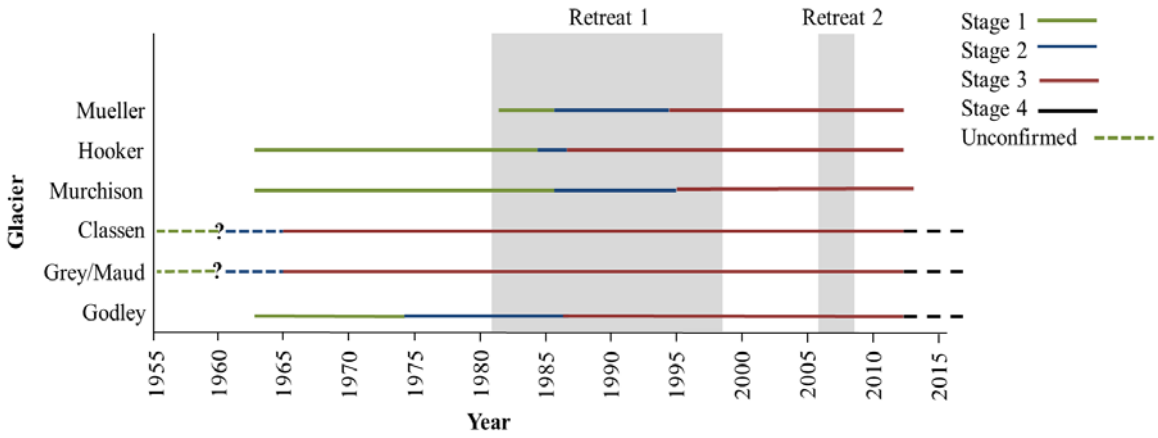

Figure 3.8: A four-stage model of spatial and temporal evolution of *Aoraki*/Mount Cook proglacial lakes. Stage 1: the appearance and growth of supraglacial lakes and/or meltwater channels on the lower ablation areas of glaciers. Stage 2: transition between supraglacial lakes and meltwater channels and a coalesced single lake. Stage 3: stable expansion of a single coalesced lake. Stage 4: slowing of retreat caused by shoaling as the valley's bedrock profile comes closer to lake level as retreat proceeds. Classen, Grey and Maud glaciers transited through stages 1 and 2 prior to 1965, although the transition between stage 1 and 2 is not constrained. Two distinct retreat phases between 1986 and the late 1990s, and 2006 and 2008, are superimposed on the four-staged model. All six glaciers are currently in stage 3, although the Godley Valley glaciers may be approaching stage 4.

A simpler 3-stage model has been postulated for the Bhutan Himalayas by Komori (2008). Proglacial lake evolution in this area was also characterised by the appearance and growth of supraglacial lakes, the coalescence of these lakes into a single lake, followed by, stable expansion of the single lake. Komori (2008) found that it took at least 40 years for the glacier and proglacial lake systems in the Bhutan Himalayas to pass though stages 1 and 2 and enter stage 3. This is substantially longer than the six glaciers in *Aoraki*/Mount Cook region that took between 8 and 30 years to enter stage 3. This temporal variability in proglacial lake evolution may be the result of differences in: calving retreat rates between the two regions (e.g. Yamada, 1998; Sakai *et al.*, 2000; Komori, 2008); glacier velocity (e.g. Hochstein *et al.*, 1998; Warren & Kirkbride, 1998; Kääb & Reichmuth, 2005; Röhl, 2005), glacier gradients, and; precipitation, due to higher altitudes and the continental climate in Bhutan. Thus, these conditions result in the glaciers of the central Southern Alps of New Zealand being more dynamic than those in the Bhutan Himalayas.

3.8 Conclusions

Glacier retreat and proglacial lake expansion in the *Aoraki*/Mount Cook area has varied both temporally and spatially. By 1965, large proglacial lakes had already formed at the terminus of Classen, Grey and Maud glaciers. Between 1965 and 1986, supraglacial lakes and meltwater channels began forming and enlarging on Godley, Mueller, Hooker and Murchison glaciers, with Mueller Glacier being the last to enter this stage of disintegration in the late 1980s. Since the early 1990s, all the glaciers have continued to retreat from their LIA moraines and their proglacial lakes have steadily expanded. Lake expansion at the Godley Valley lakes however now appears to be slowing, while Mueller and Murchison lakes continue to expand rapidly.

The temporal and spatial evolution of the glaciers and proglacial lakes in *Aoraki*/Mount Cook National Park can be divided into four stages, including: (1) the appearance and growth of supraglacial lakes and/or meltwater channels on the lower ablation areas of glaciers; (2) transition between supraglacial lakes and meltwater channels and a

coalesced single lake; (3) stable expansion of a single coalesced lake; and, (4) slowing of retreat caused by shoaling as the valley's bedrock profile comes closer to lake level as retreat proceeds. All six glaciers examined in this study are currently in stage 3, although some glaciers, particularly the Godley Valley glaciers, may be approaching stage 4. The glaciers are also more dynamic than their continental counterparts in the Bhutan Himalayas. Superimposed upon this four-staged evolution have been two distinct periods of retreat in the timeline of overall retreat since 1965. The first retreat, which falls into stage 3, occurred between 1986 and the late 1990s, and saw retreat rates at the majority of the glaciers increase, resulting in the rapid expansion of the proglacial lakes. This period of retreat was caused by the transition from melting to calving as the primary process of mass loss at the terminus. The second period of distinctive retreat occurred between 2006 and mid-2008, and was characterised by the slowing of retreat rates at the majority of glaciers. Mueller Glacier was the only glacier where retreat rates continued to increase during this time. This second retreat may be an indication that the glaciers are approaching or entering stage 4 of proglacial lake evolution.

Our study has shown that there can be considerable temporal and spatial variations in glacier retreat and proglacial lake expansion rates within the same mountain belt, and therefore that trends observed at one glacier cannot necessarily be used to infer response of another glacier, even in the same region. Fluctuations in glacier length on decadal scales can also not be attributed to climate forcing, as glaciers within a small geographical area will transition through the same glacial retreat stage at different times. In order to understand and incorporate patterns of mass loss via glacier retreat into predictions of sea level rise and water availability, data from multiple glaciers within a single mountain belt must be used.

3.9 Acknowledgements

This work was funded by the Ryoichi Sasakawa Young Leaders Fellowship Fund. We would like to thank the Department of Conservation for allowing field-based work and Rob Dykes, Jess Costall, Jingjing Wang, Rob Eastham, Alastair Clement, Sam Benny

and David Feek for field assistance. Satellite images and aerial photographs were generously provided by Trevor Chinn, Stefan Winkler and Wolfgang Rack.

Chapter 4: Subaqueous calving margin morphology at Mueller, Hooker and Tasman glaciers in *Aoraki*/Mount Cook National Park, New Zealand

4.1 Introduction

Chapter 3 quantified glacier retreat and lake expansion rates within a single mountain belt and proposed a 4-stage model of evolution of proglacial lakes in *Aoraki*/Mount Cook National Park. The chapter illustrated that there can be considerable temporal and spatial variations in retreat and lake expansion rates within a small geographical area. It also highlighted the importance of understanding patterns of mass loss at multiple glaciers within a single mountain belt in order to improve predictions of glacier retreat. A lack of quantitative subaqueous data in calving laws and models of glacier retreat however was highlighted in Chapter 2. Therefore, the focus of this chapter is to examine subaqueous morphologies at three calving margins in the central Southern Alps, New Zealand. Mueller, Hooker and Tasman glaciers provide an excellent opportunity to examine subaqueous morphologies of glaciers that are within the same stage of glacier retreat and proglacial lake expansion (chapter 3) and within a single mountain belt.

This chapter is contained within the manuscript: Robertson, C.M., Benn, D.I., Brook, M.S., Fuller, I.C. and Holt, K.A., 2012, Subaqueous calving margin morphology at Mueller, Hooker and Tasman glaciers in *Aoraki*/Mount Cook National Park, New Zealand, *Journal of Glaciology*, 58(212), 1037-1046. This manuscript examines the subaqueous morphologies of Mueller, Hooker and Tasman glaciers, in New Zealand's Southern Alps. The study uses a unique combination of high-resolution sub-bottom seismic sonar and bathymetric data (section 4.5). Firstly, the subaqueous morphologies, including subaqueous ice ramps identified extending from the three termini are described (section 4.6). These morphologies are discussed in relation to subaerial calving and retreat rates (section 4.7.1), and then the effect of debris on the subaqueous ice ramps is examined (section 4.7.2). Controls on subaqueous ice ramp evolution are also identified (section 4.7). The examination illustrates that subaqueous ice ramps are

transient features that can be sustained at freshwater calving glaciers. In addition, due to their highly changeable nature, it is important to improve our understanding of the controls on subaqueous margins in order to fully understand the potential contribution subaqueous calving may make to glacier mass loss.

4.2 Abstract

The subaqueous margins of calving glaciers have the potential to make significant contributions to glacier mass loss. However little is known currently about their morphology and development. A unique combination of sub-bottom sonar and bathymetric data collected between 2008 and 2010 in proglacial lakes at Mueller, Hooker and Tasman glaciers, in New Zealand's Southern Alps, reveal subaqueous ice ramps extending up to 510 m from the terminus of each glacier. Ice ramp surfaces are undulating and covered by up to 10m of poorly sorted sediment derived from supraglacial and englacial debris, lateral moraines, and deltaic deposits. A cyclic calving pattern, relatively stable lake level, and debris cover appear to control the development and maintenance of these ice ramps. High subaerial retreat rates generally correspond to high subaqueous calving rates, although the highest subaerial retreat rates are not associated with the largest ice ramp. Debris mantling the subaqueous ice ramp surfaces insulates the ice from melting and also reduces buoyant forces acting on the terminus. Comparisons with previous studies show that the ice ramps evolve over time with changes in glacier dynamics and water-body properties.

4.3 Introduction

Subaqueous calving and melting have been identified as important processes at water-terminating margins and have the potential to make large contributions to glacier mass loss (Eijpen *et al.*, 2003; Motyka *et al.*, 2003a; Haresign & Warren, 2005). Recent observations show that ice losses from calving glaciers can be strongly influenced by processes operating below the waterline, particularly subaqueous melting and

buoyancy-driven calving (e.g. Venteris, 1999; Motyka *et al.*, 2003a; Boyce *et al.*, 2007; Nick *et al.*, 2012). However, due to a lack of quantitative data, the potential impact of these two forms of ice mass loss on glacier mass balance and volume reduction remains uncertain (Benn *et al.*, 2007b). Quantifying these contributions is made particularly difficult by various factors, including the presence of debris cover which is known to reduce both melting and buoyant forces acting on ice (Hunter & Powell, 1998; Purdie & Fitzharris, 1999), along with the inherently hazardous working environment of the calving glacier terminus. Subaqueous calving also poses a significant hazard to users of water-bodies into which these glaciers calve (Benn *et al.*, 2007b). In order to fully understand the potential contribution that subaqueous calving and melting may make to glacier mass loss it is necessary to understand: (1) how submerged extensions of glacier termini ("ice ramps") are created and maintained; (2) the effect debris cover has on ice ramp evolution; and (3), how ice ramps contribute to mass loss at subaqueous termini. Establishing the presence or absence and, if present, the extent of such ice ramps will assist in predicting future lake expansion at lacustrine calving margins (Quincey & Glasser, 2009).

In this study, we have applied a unique combination of sub-bottom sonar profiling and echo-sounding to identify ice on the lake floor and to examine the subaqueous terminus morphology of the proglacial lakes of Mueller Glacier, Hooker Glacier and Tasman Glacier in *Aoraki*/Mount Cook National Park, in New Zealand's central Southern Alps (Figure 4.1). These glaciers are all debris-covered lake-calving glaciers which have undergone significant downwasting and recession in recent decades. The aims of this study are three-fold: (1) to map the subaqueous morphology of these lakes near the calving face; (2) to identify key characteristics of the subaqueous morphology of the termini of these three glaciers; and (3), to determine what processes control the development and evolution of subaqueous termini.

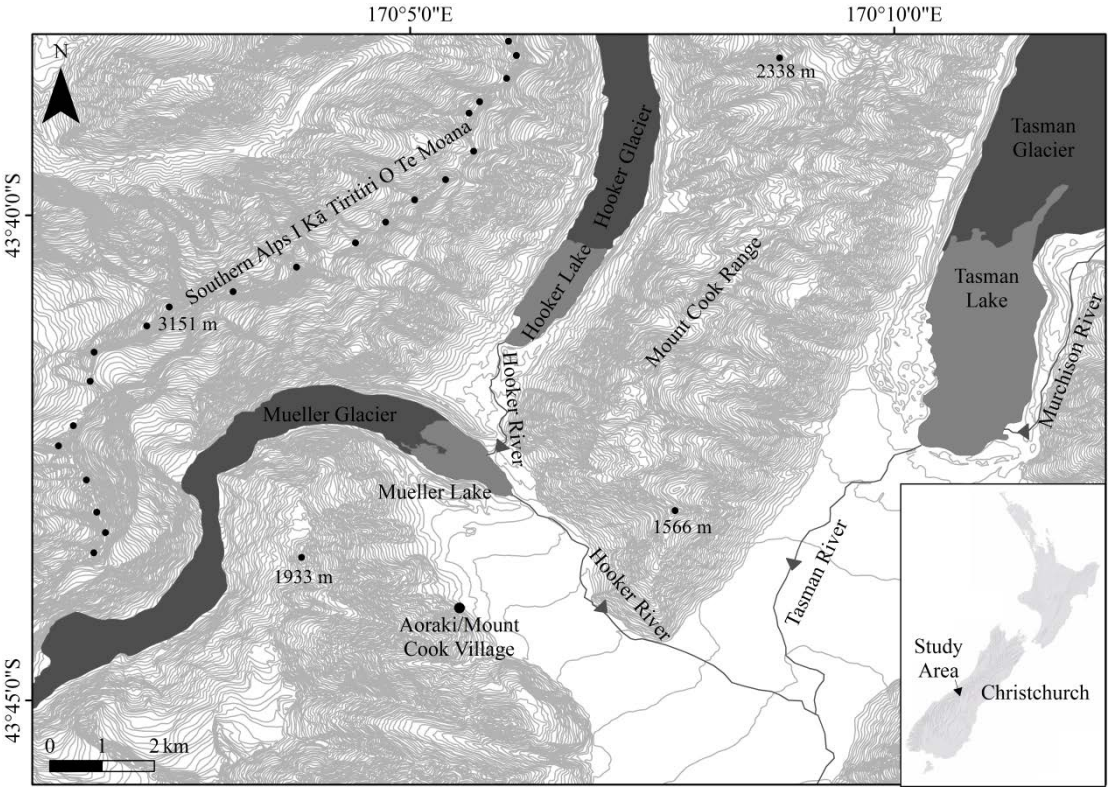

Figure 4.1: Location of Mueller, Hooker and Tasman glaciers and their proglacial lakes. The Main Divide of the Southern Alps is highlighted by black dots.

In this study, we use high-resolution CHIRP (Compressed High Intensity Radar Pulse) seismic sonar to identify the location and characteristics of subaqueous ice ramps extending from the termini of three freshwater calving glaciers. CHIRP seismic profilers remotely determine the acoustic attenuation of lake floors, with individual features giving varied acoustic returns (Jakobsson, 1999; Duck & Herbert, 2006; Lafferty *et al.*, 2006; Zhou *et al.*, 2007). The varying acoustic returns allow the identification and delineation of the spatial extent of subaqueous ice ramps, allowing, for the first time, observations on ice ramp morphology and temporal development.

4.4 Study area

Mueller, Hooker and Tasman glaciers are located on the eastern side of the Main Divide of the central Southern Alps, in *Aoraki*/Mount Cook National Park (Figure 4.1). Since reaching their Little Ice Age (LIA) maximum in the mid-late 19th century, the three glaciers have progressively downwasted (Gellatly, 1985; Blair, 1994; Kirkbride & Warren, 1999; Purdie & Fitzharris, 1999; Gjermundsen *et al.*, 2011), with the development of proglacial lakes and calving termini in the late 20th century (Kirkbride & Warren, 1999). All these glaciers now terminate in proglacial lakes (Figure 4.2), but there is a paucity of research on the calving processes active at each glacier. Only subaerial calving processes have previously been studied in any detail, with the focus typically being at Tasman Glacier (e.g. Röhl, 2005). Like most freshwater calving glaciers around the world, very little data exist on the subaqueous terminus morphology at these glaciers.

4.4.1 Mueller Glacier

The terminus of Mueller Glacier has been downwasting at a rate of ~0.5 m a^{-1} since the early 1900s (Watson, 1995). The glacier is 13.9 km long and descends from ~2000 to 765 m a.s.l (Table 1). A series of melt ponds formed on the terminus in the early 1980s and coalesced in the early 1990s to form what is now Mueller lake, with subaerial calving commencing just prior to 1994 (Watson, 1995). In 2010, the lake had a surface area of 0.87 km^2 and a maximum depth of 83 m (Table 1). Since 1994, lake area has increased by 141% while lake volume has increased by 842%. Röhl (2005) estimated that the amount of retreat varied between 0 and 210 m between April 2000 and February 2003 at different points along the terminus. The actively-calving section of the terminus retreated 150 m between November 2009 and February 2011.

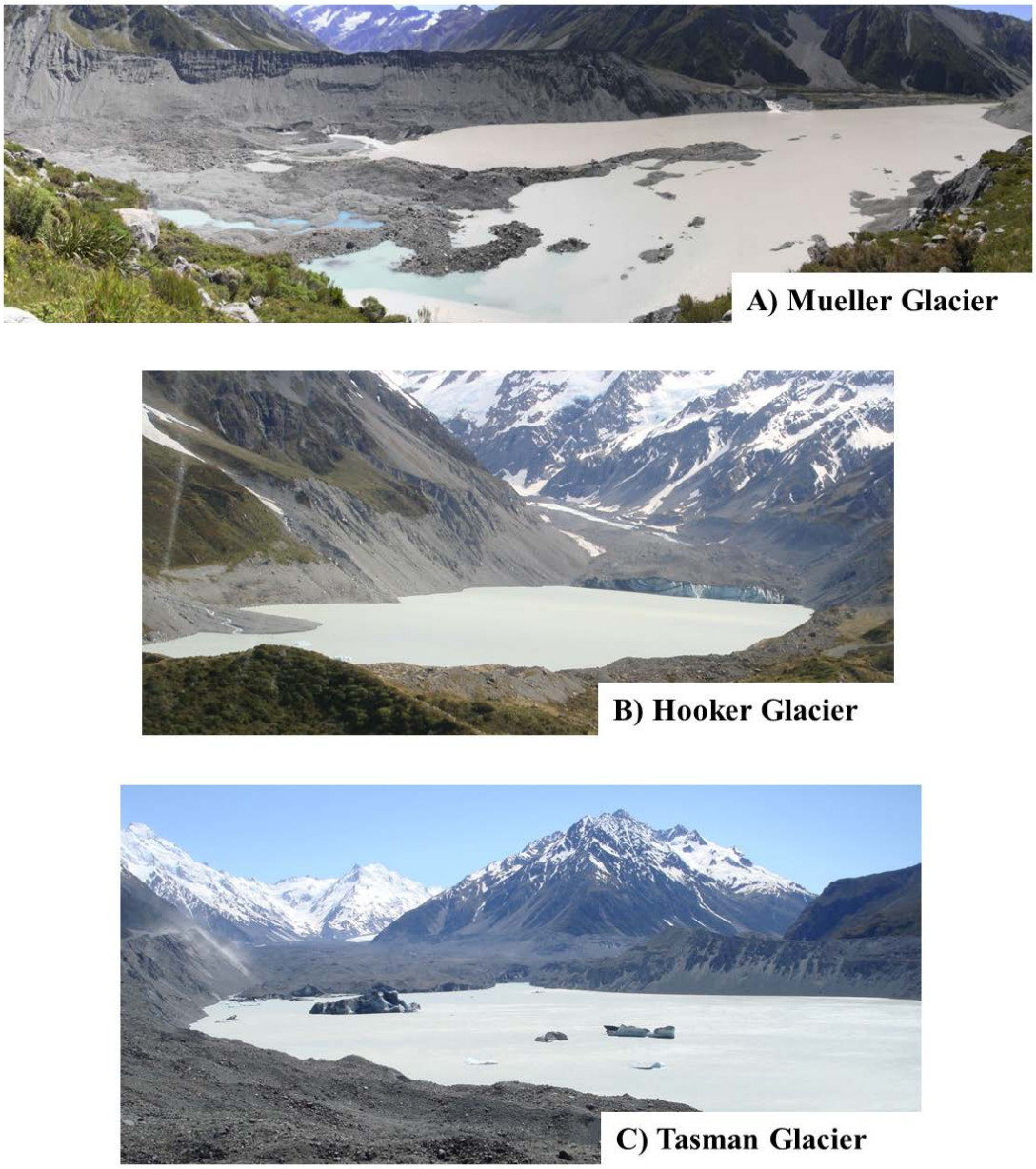

Figure 4.2: Mueller, Hooker and Tasman glaciers and their proglacial lakes: (A) the terminus of Mueller Glacier (on the left of the photo) and proglacial lake (source: C. Robertson, 28 January 2011). Hooker River can be seen entering the lake in the upper right-hand corner. The photo is taken from the south-western side of Mueller lake looking north-east. Hooker Glacier and Lake are behind the lateral moraine in the centre of the photo; (B) Hooker Glacier and Lake looking north-east towards Mount Cook (source: C. Robertson, 23 November 2009). Hooker Glacier can be seen flowing down valley, terminating in Hooker Lake. Eugenie Stream crosses an alluvial fan and enters the lake in the bottom left of the photo; (C) looking north-east up Tasman Lake to Tasman Glacier (source: C. Robertson, 25 November 2009).

Table 4.1: Physical characteristics of Mueller, Hooker and Tasman glaciers and their proglacial lakes. Supraglacial debris cover (%) refers to the percentage of the glacier surface area that is covered by debris.

	Mueller	**Hooker**	**Tasman**
Glacier			
Area (km^2)	22.5	17	99
Length (km)	13.9	12.3	28.5
Elevation range (m a.s.l)	~2000-765	~3000-876	2400-717
Surface slope	3.7º lower 2 km	3.5º lower 1.5 km	<1.5º lower 10 km
Supraglacial debris cover (%)	37.2	25	31.8
Supraglacial debris thickness (m)	2-3	0.5	1-3
Lake			
Area (km^2)	0.87	1.22	5.96
Volume (km^3)	0.02	0.05	0.51
Max. depth (m)	83	140	240
Sources	(This study, Chinn, 1996; Röhl, 2005)	(This study, Chinn, 1996; Hochstein *et al.*, 1998; Hambrey & Ehrmann, 2004; Röhl, 2005)	(Hochstein *et al.*, 1995; Chinn, 1996; Kirkbride & Warren, 1999; Röhl, 2005; 2008; Dykes *et al.*, 2011)

4.4.2 Hooker Glacier

Hooker Glacier is the fourth largest glacier in the National Park with an area of 17 km^2 (Table 1). Between 1915 and 1986, the glacier downwasted along the centre flow line at rates of up to 1 m a^{-1}, with downwasting progressing at ~0.3 m a^{-1} on the lower 3 km between 1986 and 1996 (Hochstein *et al.*, 1998). By 1994, subaerial calving was active

(Hochstein *et al.*, 1998; Warren & Kirkbride, 1998), and Kirkbride (1993) theorised that the development of an unconfined aquifer on the lower terminus, in conjunction with thinning, increased the buoyancy of blocks of ice along the glacier margins. This induced fracturing, enhancing melting by allowing further water infiltration, resulting in the development of large meltwater channels (Kirkbride, 1993). These channels coalesced to form a proglacial lake which effectively 'drowned' the terminus (Kirkbride, 1993). Retreat rates actually decreased between the early 1980's and 1996 from 70 m a^{-1} to 30 m a^{-1} (Hochstein *et al.*, 1998; Warren & Kirkbride, 1998), but then increased between 2001 and 2003 with rates of 79 m a^{-1} reported (Röhl, 2006). In 2009 the lake had a surface area of 1.22 km^2 and a maximum depth of 135 m. Published subaqueous terminal morphology data are limited to bathymetric maps created in 1995 (Warren & Kirkbride, 1998), 1996 (Hochstein *et al.*, 1998) and 2002 (Röhl, 2005). From this bathymetry and lake growth data, Hochstein *et al.* (1998) were able to approximate a subaqueous "downmelting rate", based on the vertical lowering of an area of lake floor, of approximately 5 m a^{-1} for the period between 1982 and 1986 and approximately 9 m a^{-1} between 1986 and 1996. Mass loss due to melt and calving were undifferentiated in their approximation.

4.4.3 Tasman Glacier

Tasman Glacier is the longest glacier in New Zealand at 28.5 km. Downwasting at a rate of 1.2 m a^{-1} resulted in ~1.4 km of retreat from the terminal moraine between 1972 and 1982 (Hochstein *et al.*, 1995). This is less than the downwasting rate of 1.9-4.2 m a^{-1} reported between 1986 and 2007 by Quincey and Glasser (2009). Proglacial Tasman Lake formed by the coalescence of thermokarst ponds which appeared on the glacier surface in the late 1950s (Kirkbride, 1993; Kirkbride & Warren, 1999; Röhl, 2008). The small thermokarst ponds had developed from the collapse of englacial channels (resulting from downwasting) and consequential melting of exposed ice. Retreat rates have varied from 41 m a^{-1} during 1994 and 1995 (Purdie & Fitzharris, 1999), 22 m a^{-1} between 2001 and 2003 (Röhl, 2006), 54 m a^{-1} during 2006 and 144 m a^{-1} during 2006 and 2008 (Dykes *et al.*, 2010). This recession meant that by 2008 the lake had enlarged to a surface area of 5.96 km^2 (Table 1). Hochstein *et al.* (1998) estimated a mean subaqueous melt rate, based on the vertical lowering of an area of lake floor, of 8 m a^{-1} for the period 1982-1993.

Although quantifying subaqueous calving rates for these glaciers was not possible in the present study due to our inability to measure all calving events, observations and unpublished reports (C. Hobbs, pers. comm. 2010) point to a higher subaqueous calving rate on Tasman Glacier than on Mueller and Hooker glaciers. Local tourist operators on Tasman Lake often report observing subaqueous calving events which produce icebergs that are usually very large (10s to 100s of metres across) and white to blue in colour. Röhl (2005) also reported witnessing subaqueous calving events in Tasman Lake. These events produced the largest icebergs present in the lake – larger than those from subaerial events. Subaqueous calving is thought to occur from a submerged ice ramp, and is sometimes preceded by subaerial calving, although this is not always the case. Subaqueous calving events have also been observed on Mueller (C. Hobbs, pers. comm. 2010, Röhl, 2005) and Hooker glaciers (Hochstein *et al.*, 1998; Warren & Kirkbride, 1998). In particular, Röhl (2005) observed a large subaqueous calving event at Mueller Glacier in February 2005. The calving occurred over three minutes and was captured in a series of photographs which shows a group of large subaqueous icebergs rising out of the lake and rolling. The frequency of these sightings at Mueller and Hooker lakes are lower than at Tasman Lake, but whether this is due to higher visitor numbers at Tasman Lake or more subaqueous calving events at Tasman Glacier, is unknown.

The climate in the National Park is dominated by westerly airflow from the Tasman Sea. The Southern Alps enhance orographic precipitation (Cox & Barrell, 2007) resulting in high precipitation to the west of the Main Divide (up to 12,000 mm at Remarkable Peak (Griffiths & McSaveney, 1983)), decreasing eastward. Precipitation in higher elevation areas is approximately 7000 mm a^{-1} decreasing to between 3000 to 5000 mm a^{-1} at Mount Cook Village (Anderton, 1975; Röhl, 2006).

4.5 Methods

The morphology of the subaqueous calving margins of Mueller, Hooker and Tasman glaciers was surveyed using a CHIRP sub-bottom profiler and echo-sounder. Subaqueous morphology and bathymetry data were obtained from both Mueller and

Hooker lakes in November 2009, with Mueller Lake resurveyed in April 2010. Tasman Lake was surveyed in April and October 2008.

High-resolution CHIRP seismic data of the subaqueous morphology in the three lakes were collected with an EdgeTech 216S sub-bottom profiler. The profiler operates by remotely determining the acoustic attenuation of lake sediments by transmitting an FM (frequency modulation) pulse (also known as CHIRP or Klauder wavelets) linearly over an area (Schock *et al.*, 1989; EdgeTech, 2005). The sonar works on a frequency range of 2-16 kHz and gives a vertical resolution of 60-100 mm (EdgeTech, 2005). Data were collected over intersecting transects ~100 m apart throughout the lakes with particular focus on the lake floor within 750 m of the termini. Data sampling was limited to calm lake conditions as rough water causes interference with the sub-bottom signal (Pantin & Wright, 1994; Black Laser Learning, 2006; Duck & Herbert, 2006). The quality of the recorded data was high so post-processing could be limited to video gain (dB) and time varied gain (TVG) (dB/100M) alteration on individual profiles in EdgeTech Discover software. The displayed vertical scales on the sub-bottom profiles are based on an assumed sound-wave velocity of 1500 m s^{-1} (Mullins & Halfman, 2001; Lafferty *et al.*, 2006). Individual acoustic units were identified and described according to accepted concepts in seismic stratigraphy (e.g. Lafferty *et al.*, 2006). Mueller lake and Hooker Lake surveys were located via handheld GPS with an accuracy of ± 5 m (Garmin Ltd, 2007), while a Trimble Real-Time Kinematic differential Global Positioning System (RTK-dGPS) was utilised in Tasman Lake giving horizontal (x, y) and vertical (z) precision of ± 60 mm. Data were interpolated using triangular irregular network (TIN) modelling from which smoothed bathymetric contours were produced in ERSI ArcMap.

4.6 Results

4.6.1 Mueller Glacier and lake

In April 2010, Mueller lake had a surface area of 0.87 km^2, and a volume of 0.02 km^3. The morphology of the subaqueous calving margin in November 2009 and April 2010 is shown in Figure 4.3. The lake floor sloped at an average of ~18˚ away from the glacier

in the NW to the deepest point of the lake (83 m) approximately 600 m from the terminus, while lake depth in the SW was considerably shallower (Figure 4.3). Sub-bottom data (Appendix 2B) reveal a large fine-grained sediment-filled basin in the SW and an ice ramp underlying a thick cover of sediment (~5-10 m) on the sloping lake floor in the NW (Figure 4.4). The basin increased in depth by up to 25 m (Figure 4.3) between November and April. In November 2009 this ice ramp extended ~325 m (± 5 m) from the NW terminus into the lake and had a surface area of approximately 0.16 km^2. Subaerial calving on the NW of the terminus during the 2009/2010 summer increased the length of the ramp to ~370 m and the area to 0.23 km^2. The longest section of the ice ramp in April 2010 was 510 m (± 5 m). Lengthening of the ramp in the south (Figure 4.3B) is an artefact of data collection. It is the result of ice being distinguishable in sub-bottom sonar data in this area in 2010 but not 2009. The ice ramp contains a large number of debris bands similar to those observed in the exposed terminal ice cliff in the NW (similar to the terminus ice cliff of Hooker Glacier; Figure 4.2). The surface of the sediment on the ramp is undulating and pockmarked with small depressions. The ice ramp measured in April 2010 was 60m shorter in the N than measurements in November 2009. This may have been due to subaqueous calving.

Figure 4.3 (next page): Subaqueous terminus morphology and bathymetry of Mueller lake: A) November 2009. Lines A-A' and B-B' show the location of sub-bottom profile images in Figure 4.4; B) April 2010; C) the relative change in lake depth between November 2009 (A) and April 2010 (B). Negative values (red) show a decrease in depth and positive values (blue) show an increase in depth.

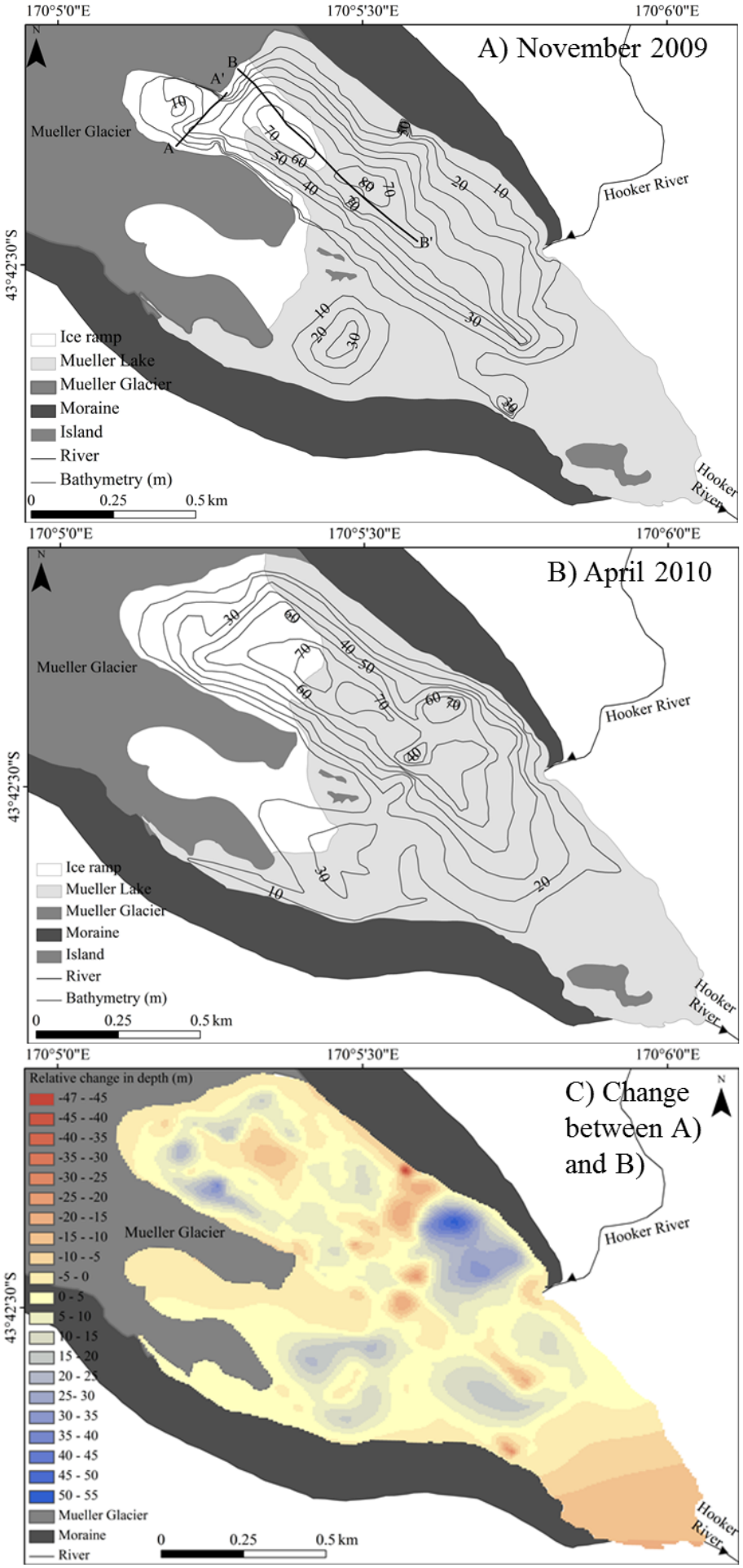
170°5'0"E
170°5'30"E
170°6'0"E
43°42'30"S
N
A) November 2009
B) April 2010
C) Change between A) and B)
Mueller Glacier
Hooker River
Ice ramp
Mueller Lake
Mueller Glacier
Moraine
Island
River
Bathymetry (m)
0
0.25
0.5 km
Relative change in depth (m)
-47 - -45
-45 - -40
-40 - -35
-35 - -30
-30 - -25
-25 - -20
-20 - -15
-15 - -10
-10 - -5
-5 - 0
0 - 5
5 - 10
10 - 15
15 - 20
20 - 25
25- 30
30 - 35
35 - 40
40 - 45
45 - 50
50 - 55

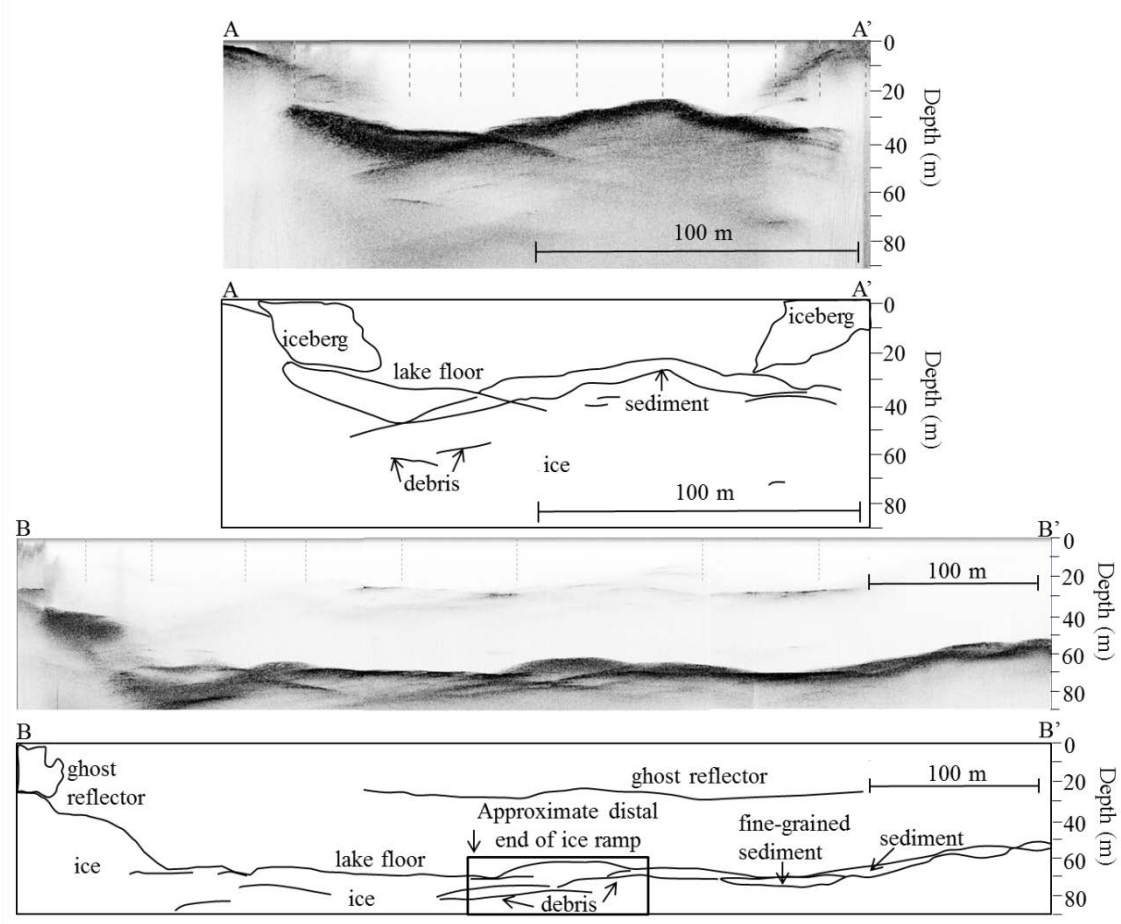

Figure 4.4: Sub-bottom profile images and interpretation from Mueller lake April 2010. Profile locations are shown in Figure 4.3. The box shows the approximate distal end of the ice ramp.

4.6.2 Hooker Glacier and Lake

The bathymetry and morphology of the Hooker Glacier calving margin and lake is shown in Figure 4.5. In 2009 the lake had a surface area of 1.22 km^2 filling a steep-sided U-shaped glacial valley which shallows towards its outlet, Hooker River. From the deepest point in the lake (140 m, 390 m in front of the terminus) the lake floor shallows rapidly towards the terminus at an angle of approximately 20˚. On either side of this deep basin, within 150 m of the terminus, the lake floor slopes at approximately 30˚ towards the terminus. Towards the centre of the lake, the lake floor is relatively flat with a change in elevation of 20 m over 270 m. Sub-bottom data along the terminus show an ice ramp, covered with a thick layer of sediment (>10 m), extending 320 m into the

lake, with a surface area of approximately 0.13 km^2 (Figure 4.5). Within 25 m of the terminal ice cliff the surface of the ice ramp is uniform and relatively smooth, beyond which the surface is undulating. The ice ramp abuts the lateral moraine on both sides of the glacier and material displaced from subaerial sections of these moraines mantles the edges of the ramp. Debris bands can also been seen in the ice (Figure 4.5).

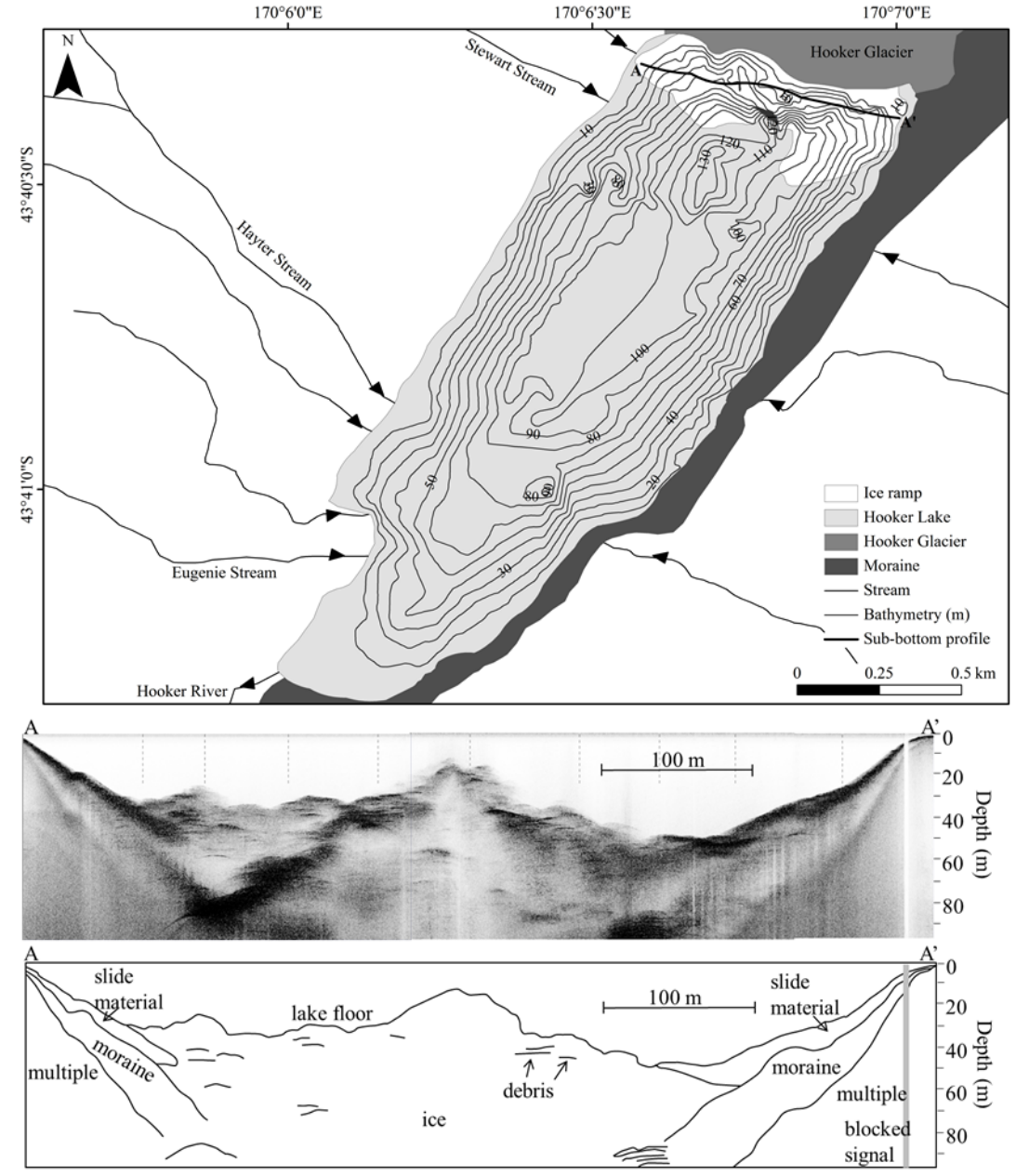

Figure 4.5: Subaqueous terminus morphology and bathymetry of Hooker Lake in November 2009. Line A-A' shows the location of the sub-bottom profile image.

4.6.3 Tasman Glacier and Lake

Bathymetric data, described by Dykes *et al.* (2011), were collected at the same time as the sub-bottom data contained herein. The sub-bottom data show ice overlain by a layer of sediment (5-10 m, Figure 4.6) sloping away from the terminus into the lake for approximately 400 m. The approximate surface area of this ice ramp is 0.49 km^2. The surface of the ramp adjacent to the subaerial section of the terminus is pockmarked with small depressions (<10 m) and ridges but these become less pronounced as the ramp extends further into the lake. Additional sub-bottom data (shown in appendix 2) show that the ice extends along the full face of the glacier and abuts the lateral moraines on both sides of the lake.

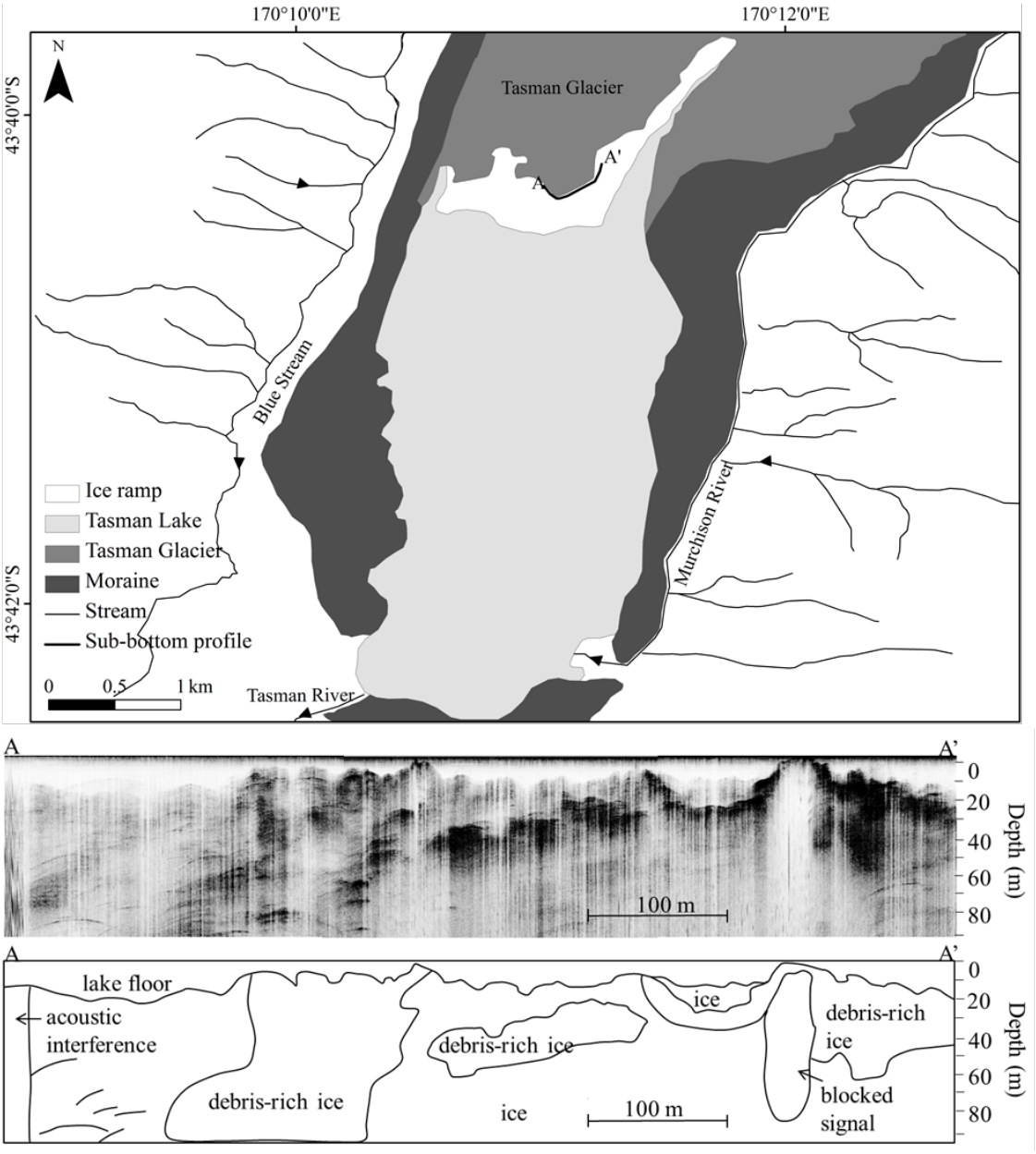

Figure 4.6: Subaqueous terminus morphology of Tasman Lake in 2008. Line A-A' shows the location of the sub-bottom profile image.

4.7 Discussion

Sub-bottom profile data from Mueller, Hooker and Tasman lakes show ice ramps extending from the calving termini of the three glaciers into their proglacial lakes. At 510 m, the ice ramp extending from Mueller Glacier is the longest of the three, as well as the largest in terms of the percentage of lake length (20%) and glacier length (2.6%).

There are no previous recorded observations of an ice ramp in the lake, although based on glacier thickness estimates of Watson (1995), Röhl (2005) suggested that the lake floor was likely to be ice-cored in 2003. Hence, the ice ramp mapped in 2009 and 2010 is likely part of what formed the 2003 ice-cored floor. A comparison of lake depths between 2005 and 2009 (not shown) indicates that the ice ramp has disintegrated in the SE of the lake, probably via subaqueous calving, (which commenced in 2005: Röhl, 2005), and now extends further up-valley to the NW due to continued subaerial calving retreat. Subaqueous calving is also likely to have removed 60 m on the distal end of the ice ramp that was detected in 2009 but not in 2010.

Based on bathymetry data, a small ice ramp has been recorded in Hooker Lake on two previous occasions. Hochstein *et al.* (1998 p. 213) found a 'small, protruding, basal ice tongue' extending from the bottom of the ice cliffs on the terminus of Hooker Glacier in 1996, as well as remnant ice along the margins of the lake. Warren and Kirkbride (1998) also reported a small, projecting ice ramp just below the waterline which sloped at a gradient of 20˚- 30˚ into the lake. This gradient is comparable to that measured in 2009, with steepening of up to 10˚ occurring on the SE section. In contrast to these observations, Röhl (2005) believed the subaqueous ice margin in Hooker Lake to be vertical or near-vertical between 2001 and 2003. There are two possible explanations for this variation: (1) the ice ramp observed prior to 2001 completely disintegrated via subaqueous calving and melting, creating a near-vertical ice margin: or, (2) the ice ramp was simply not detected. Given that the ice ramp reported by Warren and Kirkbride (1998) extended ~100 m from the terminus, and the closest data point Röhl (2005) collected was 100 m from the subaerial terminus, it would appear that Röhl's (2005) survey design precluded detection of an ice ramp between 2001 and 2003.

Disparities also exist amongst the data sets from Tasman Glacier. Indeed, Hochstein *et al.* (1995) concluded that the subaqueous ice cliff was near vertical in at least one location along the terminus in 1993. In contrast, Purdie (1996) and Röhl (2005) reported that an ice ramp extended along the majority of the terminus, except for a small section at the eastern end. Warren and Kirkbride (1998) also observed an ice ramp at the waterline, which was present along the full width of the terminus. After 1993, all

bathymetric surveys in the lake have suggested that an ice ramp extended from the glacier, albeit in varying locations. As illustrated by these fluctuations in ramp size and location, it is likely that the ice ramp has evolved in a cyclic pattern of growth and disintegration, in connection with subaerial retreat of the glacier (e.g. Röhl, 2005).

Ice ramps have been observed in the past at other glaciers in New Zealand including Maud, Grey, Godley and Ivory Glaciers (Warren & Kirkbride, 1998) and worldwide including Le Conte Glacier, south-east Alaska (Motyka, 1997), the margin of Breiðamerkurjökull terminating into Stemmárlón, south-east Iceland (Howarth & Price, 1969) and Muir and Johns Hopkins Glaciers, Alaska (Hunter & Powell, 1998). To understand the morphology and development of the subaqueous margins of Mueller, Hooker and Tasman glaciers, possible relationships between calving processes, retreat rate and debris cover are explored further below.

4.7.1 Calving and retreat rate

A cyclic calving pattern is common at water-terminating ice margins in *Aoraki*/Mount Cook National Park (Kirkbride & Warren, 1997; 1999), the Himalaya (Benn *et al.*, 2001) and Patagonia (Warren, 1999; Haresign & Warren, 2005). This cycle involves melting at the waterline which creates an overhanging subaerial cliff. The cliff calves progressively larger lamellae, by flaking and eventually full-height slab calving. As the destabilised subaerial ice cliff retreats, a subaqueous ice ramp will develop if mass losses per unit area above the waterline exceed those below. Eventually, the ice ramp will calve or melt away. The rate of ramp development is controlled by the difference between the rate of subaerial cliff retreat (by calving and melting), and subaqueous ramp retreat (by calving and melting). Therefore, a glacier with a high subaerial retreat rate will not necessarily have a large ice ramp. For example, Tasman Glacier has a higher subaerial retreat rate than Mueller Glacier (Röhl, 2006; Dykes *et al.*, 2010), yet its ice ramp is smaller. This is a consequence of higher relative subaqueous mass loss rates at Tasman Glacier. Subaerial retreat rates may be higher at Tasman Glacier than Mueller Glacier due to variations in the rate of thermal undercutting, as a result of differences in water temperature, water-level fluctuations and terminal ice cliff geometry (e.g. Röhl, 2006). In addition to the control which subaerial and subaqueous

retreat rates exert of ramp development, other factors must control the maximum extent of the ice ramp a given glacier can sustain. Potential controls may include debris cover and resultant buoyancy and properties of the water body (e.g. water temperature) into which the glacier terminates. In addition, where subaqueous calving is an important process, longitudinal strain rates are also a potential control as these rates influence fracture formation and propagation (Benn *et al.*, 2007b), along with pre-existing weaknesses such as crevasses and debris bands.

Subaerial calving at the three glaciers is predominantly driven by undercutting of the ice cliff, which is controlled by waterline melt. Röhl (2005; 2006) identified lake level stability as a crucial component in waterline melting. Constant lake levels cause energy transfer and thus melting to be concentrated on a thin section of ice at the waterline rather than spreading it over a wider vertical area. This energy concentration creates higher thermal-erosional notching rates, leading to high subaerial calving rates. Fluctuations in lake level of more than 0.15 m over 24 hours were enough to significantly retard the development of thermal notches on Tasman Glacier (Röhl, 2005).

4.7.2 Debris on the ice ramps

Sub-bottom data from Mueller, Hooker and Tasman lakes show that debris thicknesses on the ice ramps vary between 5 and 10 m. This sediment comprises unsorted sands, gravels and boulders. Isolated areas of undisturbed laminated lacustrine muds which fill small basins and depressions are also present in all three lakes. These areas are generally distal from the terminus, where subdued sediment and water movement allows fine sediment to settle out of suspension. Mueller lake is an exception, with fine sediment in-filling a large flat-bottomed basin in the SW part of the lake adjacent to the terminus. This delta was created by a supraglacial river which flowed into the area until 2006.

Sediment on the subaqueous ice ramps is derived from six potential sources: (1) transfer of supraglacial debris off the glacier terminus; (2) slumping from lateral moraines

bordering the lake margins; (3) iceberg fallout; (4) melting of the ramp; (5) fluvial deltaic deposition; and (6) englacial conduits. Sources 1-4 are present at all three glaciers, with fluvial deposition forming a delta on the ramp only at Mueller Glacier where a supraglacial river flows from the glacier surface into the lake. Sources one, two, five and six are likely to be the largest sources of debris on the glaciers.

Debris on subaerial ice can either retard or enhance melting depending on its thickness. Where debris is thicker than 30 mm it insulates the ice and impedes melting (Østrem, 1959; Mattson *et al.*, 1993; Hambrey *et al.*, 2008). On Tasman Glacier, Purdie and Fitzharris (1999) found a layer of supraglacial debris up to 3 m thick, which reduced ablation by 93%. Debris cover on subaqueous ice will also act in an insulating capacity, reducing the effectiveness of downward advection of water warmed at the lake surface. Röhl (2005) reported that melting of subaqueous ice under debris was minimal in Tasman Lake. With water temperatures of 1.5˚C, ice overlain with 2 m of debris melted between 0.02 and 0.14 m a^{-1}. Debris cover on the subaqueous ice ramps in Mueller, Hooker and Tasman lakes is considerably thicker therefore melt rates could be expected to be considerably smaller. The thick layer of sediment covering the ramps greatly reduces melting, minimising thinning of the ice, and also adding mass to the ice ramp, reducing the buoyant forces that act to break up the ramp (Hunter & Powell, 1998). Indeed, due to this added mass on the subaqueous ramp surface acting against buoyancy, it is likely that the ice ramp is maintained, rather than undergoing disintegration via subaqueous calving. Debris bands, observed in the CHIRP data, in Hooker and Tasman ramps are more clearly defined than those in the Mueller ramp. This may be because the debris is more evenly distributed within the Mueller ramp due to processes of entrainment and transport in the glacier and/or because of differences in debris composition which may result in a weaker reflective signal. Debris bands within all three ramps are very similar in appearance to debris seen in the exposed ice cliffs at the termini of the glaciers, and icebergs in the lakes.

Debris content and distribution may be important in ice ramp evolution in some instances. Hunter and Powell (1998), working at Muir Glacier in Alaska, suggest that the top of an ice ramp is more likely to develop at the boundary of sediment-rich,

stratified, basal ice, and overlying bubbly white ice above. They found that subaqueous-sourced icebergs contained a debris-rich ice layer which graded upward into relatively clean ice. People who have observed subaqueous calving events from ice ramps in Mueller, Hooker and Tasman lakes (C. Hobbs, per. comm. 2010; Röhl, 2005) report that the bergs commonly consist of bubbly white ice containing debris bands, and do not grade from debris-rich ice to clean ice. Thus, Hunter and Powell's (1998) theory does not appear to be relevant in our case.

4.8 Conclusion

Periods of constant water level and warm surface water temperatures adjacent to the ice cliffs allow thermo-erosional notches to develop vigorously. These notches destabilise the subaerial ice cliffs above. Thus, subaerial calving proceeds faster than subaqueous mass loss, resulting in the formation of ice ramps. The rate of ice ramp development is controlled by the difference between subaerial retreat and subaqueous mass loss (by calving and melting). The 'steady-state' situation would be one in which subaerial retreat was matched by retreat of the subaqueous ice ramp.

The subaqueous terminal morphologies of Mueller, Hooker and Tasman glaciers show ice ramps extending up to 510 m from the calving termini into their respective proglacial lakes, with the ice ramp extending from Mueller Glacier being the largest. The surfaces of these ice ramps are undulating and covered with a thick layer of unsorted sediment derived from supraglacial and englacial debris, lateral moraines and fluvial deltaic deposition. As with supraglacial debris on subaerial ice, sediment on the ice ramps reduces melting and therefore thinning of the ramps. It also counterbalances buoyant forces acting to disintegrate the ice ramps. The ice ramps are therefore able to remain intact hundreds of metres in front of the calving termini.

Ice ramps appear to be transient features of glacier margins terminating in freshwater. They evolve over time as variables including glacier dynamics and water-body properties change. It therefore cannot be assumed that if an ice ramp does not exist at a particular time, the glacier is unable to support such a feature. Due to the highly

changeable nature of ice ramps, it is important to improve our understanding of the controls on glacier termini undergoing subaqueous calving in order to fully understand the potential contribution subaqueous calving may make to glacier mass loss.

4.9 Acknowledgements

This work was funded by the Ryoichi Sasakawa Young Leaders Fellowship Fund (to CMR) with fieldwork at Tasman Glacier supported by Massey University Research Fund (to MSB). We would like to thank the Department of Conservation for allowing fieldwork in *Aoraki*/Mount Cook National Park, Charlie Hobbs and the New Zealand Alpine Club. Field assistance from John Appleby, Rob Dykes and David Feek was also greatly appreciated. Critical reviews from Roger LeB. Hooke and Robert McNabb significantly improved the manuscript and were greatly appreciated.

Chapter 5: Temporal evolution of the calving terminus at Mueller Glacier, *Aoraki*/Mount Cook National Park, New Zealand

5.1 Introduction

Chapter 4 examined the subaqueous morphologies of Mueller, Hooker and Tasman glaciers, in New Zealand's Southern Alps. Subaqueous ice ramps were identified extending from the termini of the three glaciers. The previous chapter illustrates that these subaqueous ice ramps are transient features and that it is therefore important to improve our understanding of the controls on subaqueous margins. Doing so will increase our understanding of the potential contribution subaqueous calving may make to glacier mass loss. Thus, the focus of chapter 5 is to examine the temporal evolution of the subaqueous ice ramp at Mueller Glacier in order to identify controls on its evolution.

This chapter is contained within the manuscript: Robertson, C.M., Brook, M.S., Fuller, I.C., Benn, D.I. and Holt, K.A., Temporal evolution of the calving terminus at Mueller Glacier, *Aoraki*/Mount Cook National Park, New Zealand, which is in review in the journal *Geografiska Annaler.* The manuscript examines the temporal evolution of the terminus of Mueller Glacier over a 16 month period. The subaerial and subaqueous morphologies are examined in order to identify the controls on the evolution of the subaqueous ice ramp. Mueller Glacier was the focus of this study due to the apparent rapidity of changes occurring at the margin at the time of the study, the range of active processes, along with ease of access. Firstly, the subaerial terminal morphology is described along with variations in the terminus position (section 5.6.1). Evolution in the subaqueous morphology, subaqueous ice ramp and lake size over the study period are then examined (section 5.6.2). Vertical and horizontal terminus displacements are also quantified (section 5.6.3), along with a brief description of lake temperature (section 5.6.4). Controls on the evolution of the subaqueous morphology are discussed (section 5.7.1) and correlations between terminus movements, precipitation and lake level are

identified (section 5.7.2). Controls on vertical terminus displacements are also identified (section 5.7.2). The study contributes to the quantitative dataset on subaqueous ice ramps, and identifies the dominant processes controlling their evolution in debris-covered, lake-calving glaciers. It illustrates that the development and maintenance of the extent of subaqueous ice ramps is intrinsically linked with subaerial retreat.

5.2 Abstract

The recession of freshwater-terminating glaciers, due to calving, has become a widespread phenomenon in mountain glacier systems in recent decades. Yet, our understanding of the processes responsible for, and contributing to, glacial retreat and proglacial lake development at debris-covered, lake-calving glaciers, remains somewhat limited. In addition, few observations have been made of the subaqueous sections of these glaciers, with the potential for subaqueous ice ramps to extend from the glaciers and how these may influence overall glacial retreat being poorly understood. Glacier and lake-based measurements at the terminus of Mueller Glacier, New Zealand between 2009 and 2011 allowed changes in the subaqueous morphology in conjunction with subaerial processes to be investigated. The calving front of Mueller Glacier retreated ~150 m over the 16 month study, with lake volume increasing by 32% and the area covered by the lake increased by 17%. A subaqueous ice ramp was identified extending up to 510 m from the terminus. Changes in the subaqueous morphology were found to be controlled by a combination of subaerial retreat and subsequent subaqueous calving, along with sedimentation. Subaqueous melting was minimal due to the effects of debris cover. Horizontal and vertical displacements of the glacier were driven by the terminus approaching flotation thickness. The development and maintenance of the extent of subaqueous ice ramps is intrinsically linked with retreat of the subaerial section at debris-covered, lake-calving glaciers.

5.3 Introduction

The recession of freshwater-terminating glaciers, due to calving, has become a widespread phenomenon in mountain glacier systems in recent decades, affecting glaciers in New Zealand (e.g. Kirkbride, 1993; Kirkbride & Warren, 1997; Warren & Kirkbride, 2003; Röhl, 2005), Patagonia (e.g. Warren, 1999; Warren & Aniya, 1999; Warren *et al.*, 2001; Haresign, 2004), the Himalaya (e.g. Benn *et al.*, 2001; Watanabe *et al.*, 2009; Thompson *et al.*, 2012), and the European Alps (e.g. Diolaiuti *et al.*, 2005; Diolaiuti *et al.*, 2006). Calving and melting has resulted in accelerated rates of ice loss (Warren & Aniya, 1999) and the growth of supraglacial and proglacial lakes which, in some cases, can pose significant risk of glacier lake outburst floods (GLOFS; Clague & Evans, 2000). Our understanding of the processes responsible for, and contributing to, glacial retreat and proglacial lake development at freshwater-terminating lake-calving glaciers, however, remains somewhat limited.

For example, predictions of lake growth rates are complicated by the fact that calving glaciers can become partially decoupled from climate-forcing, which allows factors other than surface mass balance, such as valley topography and lake bathymetry (Warren, 1991; 1992; Purdie & Fitzharris, 1999), to control rates of retreat or advance. Debris cover on these glaciers also complicates mass loss processes as debris can reduce surface melting, and thus thinning, stabilising the ice margin (Diolaiuti *et al.*, 2006). In addition, few observations have been made of the subaqueous sections of these glaciers, with the potential for subaqueous ice ramps to extend from the glaciers and how these may influence overall glacial retreat being poorly understood.

Where subaerial mass loss exceeds subaqueous mass loss an ice ramp will form. Therefore, as subaqueous morphology is intrinsically linked to subaerial calving, factors that influence subaerial calving may also influence subaqueous ice ramps. For example, work by Röhl (2006) at the calving margin of Tasman Glacier, New Zealand, highlighted that thermo-erosional notching drives subaerial calving and factors including water temperature, cliff geometry, debris supply and water-level fluctuations, control notch development. There are clear gaps in our knowledge on the processes operating at the subaqueous termini of lake-calving glaciers that need to be addressed

by further studies of such glaciers. This study seeks to address at least some of these gaps by investigating changes in the subaqueous morphology in conjunction with subaerial processes over time at an example of a lake-calving glacier in New Zealand.

Mueller Glacier is a debris-covered, lake-calving glacier, on the eastern side of the central Southern Alps, New Zealand, which has undergone significant downwasting (approximately 0.5 m a^{-1} since the early 1900s (Watson, 1995)) and recession in recent decades. In this paper we use a combination of sub-bottom sonar, echo-sounding, water temperature, lake level and high resolution topographic measurements to examine recent (2009-2011) changes in the subaqueous and subaerial terminal morphology of Mueller Glacier. This approach will allow us to investigate subaqueous ice ramps, the dominant processes controlling their evolution, and how subaqueous ice ramps influence glacier retreat. Our objectives are four-fold: 1) to map the subaerial and subaqueous morphology of the Mueller Glacier terminus to determine if and how changes in the two are connected; 2) identify the controls on subaqueous morphology evolution; 3) to understand horizontal and vertical glacier movement in relation to precipitation and lake level, and; 4) to identify controls on terminus uplift. In doing so, we will contribute to the understanding of glacial retreat and proglacial lake development at debris-covered, lake-calving glaciers.

5.4 Study area

Mueller Glacier is on the eastern side of the Main Divide of the central Southern Alps, in *Aoraki*/Mount Cook National Park (Figure 5.1). The glacier covers an area of ~22.5 km and extends ~13.9 km down the Mueller Valley, terminating at 765 m a.s.l into Mueller lake (the lake does not have an official New Zealand Geographical Board name). Thirty seven per cent of the glacier is covered with supraglacial debris, 2-3 m thick (Chinn, 1996). Mueller Glacier's gradient is very low (~3.7º on the lower 2 km; Röhl, 2005) and has been downwasting at a rate of ~0.5 m a^{-1} since the early 1900s (Watson, 1995). No mass balance data are available for the glacier.

A series of melt ponds formed on the terminus in the early 1980s. These ponds enlarged during the late 1980s to form a small lake along the margin of the terminus. The lake enlarged by subaerial and subaqueous melting and calving, particularly at small ice cliffs adjacent to the lake. In 1994 the lake area was ~3.46 x 10^5 m^2 with a volume of ~1.73 x 10^6 m^3; the maximum lake depth was 40 m (Watson, 1995). By 2003, Röhl (2005) reported that a number of small debris covered, ice-cored islands within the lake had disintegrated via subaqueous calving and estimated the lake area had increased to ~6 x 10^5 m^2 and was 1 km in length.

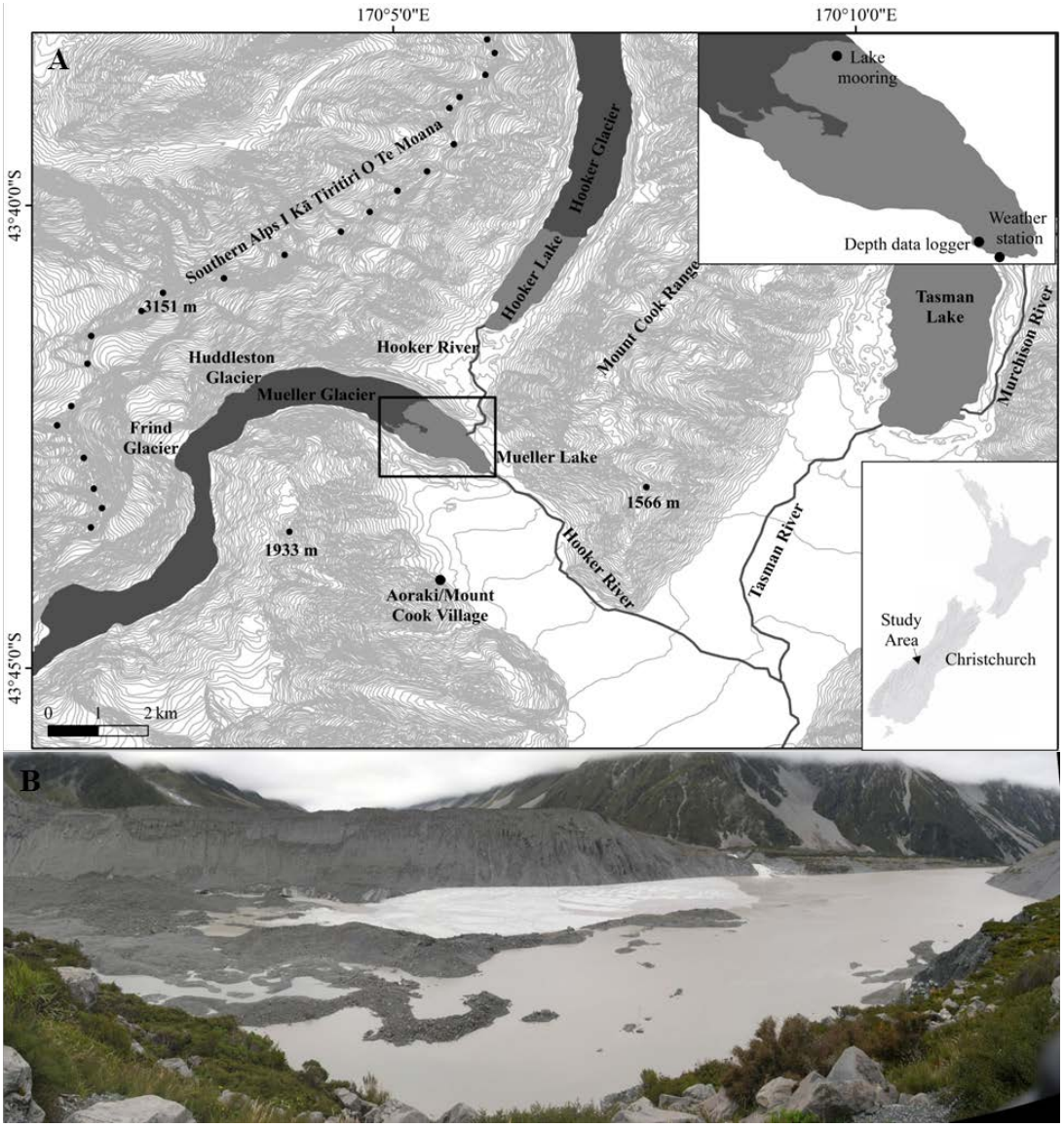

Figure 5.1: A) Location of Mueller Glacier and the surrounding area. The black box shows the location of Figures 5.2, 5.3 & 5.4. The inset image shows the location of the lake mooring

which collected lake temperature data, the weather station, and the depth data logger B) Mueller lake, with ice debris from a large collapse of subaerial ice cliffs ~100 m up-glacier of the terminus, (source: C. Robertson, 7 February 2011). Mueller Glacier is on the left of the photo. A swollen Hooker River can be seen entering the lake in the top right-hand corner. The photo is taken from Kea Point on the south-western side of Mueller lake looking north-east.

The climate in *Aoraki*/Mount Cook National Park is dominated by westerly airflows from the Tasman Sea that, in conjunction with the barrier created by the Southern Alps, results in orographic precipitation (Cox & Barrell, 2007). The net result is high precipitation to the west of the Main Divide of the Southern Alps (up to 12,000 mm at Remarkable Peak, Galena Range, Westland; Griffiths & McSaveney, 1983) decreasing towards the east. At Mount Cook Village (2 km south of Mueller lake) precipitation ranges from 3000 to 5000 mm a^{-1} (Anderton, 1975).

5.5 Methods

Three field campaigns were undertaken in November 2009, April 2010, and January and February 2011 at Mueller Glacier. Data collection consisted of glacier terminus surveys, subaqueous surveys, lake temperature and lake level measurements, along with precipitation measurements.

During January and February 2011, vertical (z) and horizontal (x, y) movement of the terminus of Mueller Glacier was also measured using a Trimble S6 automatic total station established on Kea Point, ~150 m above Mueller Glacier, and an array of five reflective prisms. The prisms were attached to large, stable boulders on the lower 400 m of the terminus and the distance and angles between the total station and prisms were measured. The prisms were surveyed at approximately 1000 hours on twelve different days during the study period. Daily surveys were not possible due to adverse weather conditions, difficulties in accessing the site during these conditions and strong heat shimmer on the glacier on sunny days, which prevented a reflection from the prisms being returned to the total station. Precision within 05” over a maximum distance of 919

m gave an error of 0.02 m in positional accuracy, at the farthest point. Each survey was locked into the same baseline by surveying 6 stationary features (e.g. information boards, wooden platform and a seat) at the beginning of each survey and fixing the total station over the same peg throughout the survey period. Electronic distance measurements were corrected with barometric pressure and temperature with data from the National Institute of Water and Atmospheric Research (NIWA) automatic climate station at Mount Cook Village (-43.736 ºS 170.096 ºE). Vertical angle observations had curvature and refraction corrections applied by the total station.

Topographic data were collected using the automatic total station to map the surface of the glacier terminus. 1500 data points (*x*,*y*,*z*) were collected at breaks in slope within and between morphological units, and geographic features in February 2011. The automatic total station and handheld GPS (accuracy of ± 5 m; Garmin Ltd, 2007) were used to survey terminus positions in 2009, 2010 and 2011. Errors associated with the handheld GPS in the *z* dimension are likely to be higher than ± 5 m. Ice thicknesses at the terminus were calculated by combining height data from the topographical dataset with lake depth data. An assumption was made (based on sub-bottom sonar data) that the deepest point in the lake (83 m) was the valley floor and that this point was not underlain with ice. The ice thickness at prism locations was calculated by combining this lake depth (83 m) with the height of the prism above lake level.

Subaqueous morphology and water depth surveys were completed on 18 November 2009, 15 April 2010, 21 January 2011 and 17 February 2011 using a sub-bottom sonar profiler and echo-sounder. An EdgeTech 216S sub-bottom profiler was used in November 2009 and April 2010 to penetrate lake floor sediment and collect high resolution sub-bottom data. The sonar worked on a frequency range of 2-16 kHz and gave a vertical resolution of 60-100 mm (EdgeTech, 2005). In January and February 2011, a Humminbird 323 DualBeam Plus dual frequency echo-sounder (frequencies of 200 kHz and 83 kHz) was used to collect subaqueous morphology data. The echo-sounder was calibrated against known depths within the lake to give an accuracy of less than 1 m. No difficulties were observed with ‘rogue’ readings of either the sub-bottom sonar or echosounder caused by reflections from steep valley sides or ice cliffs. More

than 500 data points were recorded during each echo-sounding survey and were located by handheld GPS with an accuracy of ± 5 m (Garmin Ltd, 2007). It was not possible to use RTK-dGPS due to the limited sky views in the valley. Both the sub-bottom profiler and echo-sounding surveys followed intersecting transects over the lake; the sub-bottom profile sampled continuous along these transects, while the echo-sounder sampled approximately every 50 m. Bathymetry data were interpolated using triangular irregular network (TIN) modelling from which smoothed bathymetric contours were produced in ESRI ArcMap. Volumetric changes were calculated by subtracting lake volumes calculated in ESRI ArcMap. It is important to note that the method of producing smoothed contour lines may affect perceived lake depth changes. Changes measured within the study though are however well outside of the errors that could have been produced via this method.

Lake temperature measurements were made to better understand how temperature may affect both the subaqueous and subaerial terminal morphologies and how the thermal structure of the lake changed over time. A stationary temperature profile attached to a lake mooring was located ~100 m from the terminus on the north-eastern side of the lake (Figure 5.1) in approximately 50 m of water. Onset Tidbit temperature loggers on the lake mooring at 2, 10, 20, 30, and 49 m recorded temperatures every 3 hours. These tidbits were calibrated in the laboratory to an accuracy of 0.2˚C over the range of O˚C to 50˚C.

Lake level was monitored to determine its influence on terminus movement. An Onset U20-001-01 HOBO Depth Data Logger monitored lake level and water temperature in approximately 1.5 m of water in a sheltered bay (to reduce the influence of wind-induced waves) in the SE of the lake (Figure 5.1). Data were recorded at 5 minute intervals from 20 April 2010 to 19 February 2011. Barometric corrections were made to the data from the NIWA automatic climate station at Mount Cook Village. Local precipitation data were taken from the NIWA climate station and a Campbell Scientific climate station established on the SE shore of the lake collected precipitation data in April 2011 (Figure 5.1).

5.6 Results

5.6.1 Terminus subaerial morphology

The terminus of Mueller Glacier is covered by two distinct types of supraglacial debris (Figure 5.2); fine-grained glacio-fluvial sediment deposited via an historic supraglacial meltwater stream and coarse-grained supraglacial debris derived predominantly from avalanche material (e.g. Cox *et al.*, 2008). The fine-grained glacio-fluvial sediment is ~5 m thick, compared with the coarse-grained, avalanche-derived debris which is 2-3 m thick and comprises large boulders (up to 10 m wide), gravel and coarse sand. The terminus surface is very hummocky with changes in elevation of up to 20 m. A large ridge along the northern margin of the glacier slopes down to a number of ponds which have formed along the boundary of the glacier and the northern lateral moraine and slopes south to ice cliffs along the meltwater stream exiting the glacier. This ridge terminates into the lake at large (~20 m) ice cliffs. In the centre of the glacier, adjacent to the lake, is a large, flat, fine-grained sediment delta which becomes flooded during and after high precipitation events. The south-western section of the terminus is lower in elevation than the west and northern sections and contains a number of ‘blue water’ supraglacial ponds.

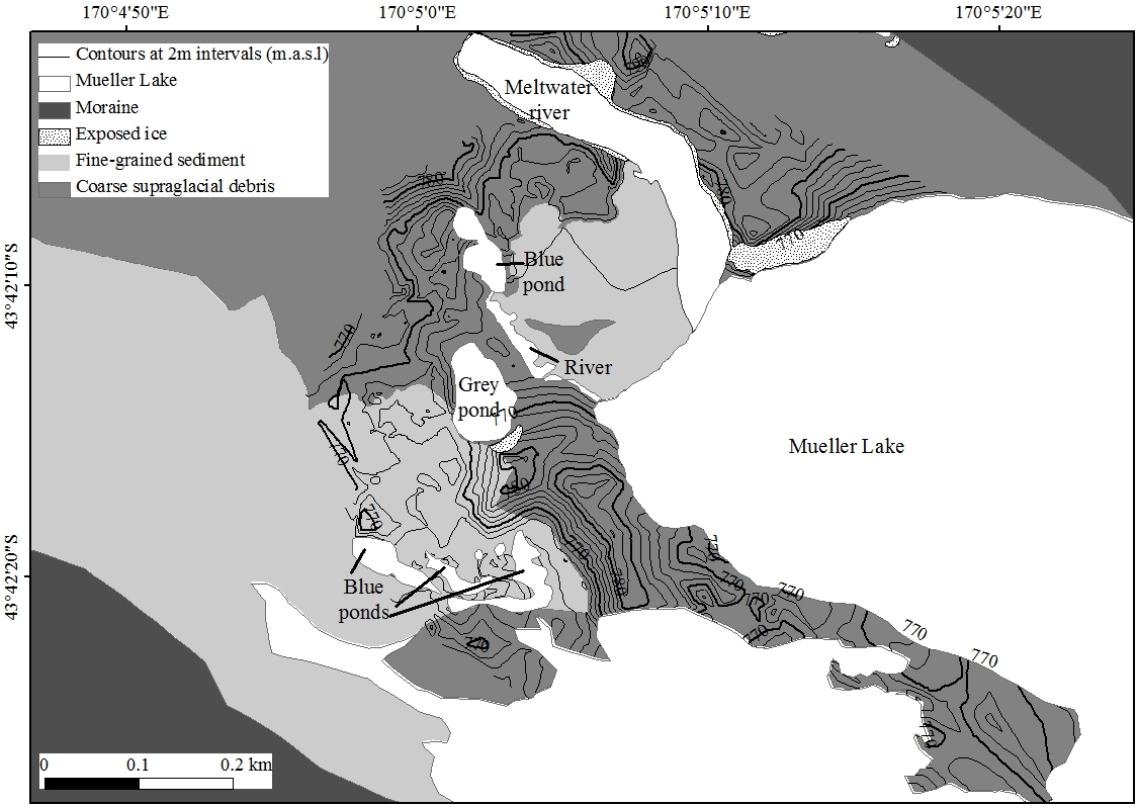

Figure 5.2: Subaerial morphology of the terminus of Mueller Glacier, February 2011. Fine-grained, glacio-fluvial sediment and coarse-grained, avalanche-derived sediment can be seen on the terminus. Exposed ice cliffs can be seen adjacent to Mueller lake, along the meltwater river and near the grey pond. 'Blue water' ponds can be seen on the SW of the terminus, which is lower in elevation than the rest of the terminus.

Variations in the terminus position between November 2009 and February 2011 are shown in Figure 5.3. The main ice cliff which terminates into the lake, adjacent to the meltwater river, retreated ~120 m between 2009 and 2010 and a further 30 m between 2010 and February 2011. The up-glacier end of the small embayment in the centre of the terminus, adjacent to the meltwater river, advanced ~64 m between 2010 and 2011. The bays at the south-west of the terminus enlarged to incorporate a number of surrounding supraglacial ponds into the lake.

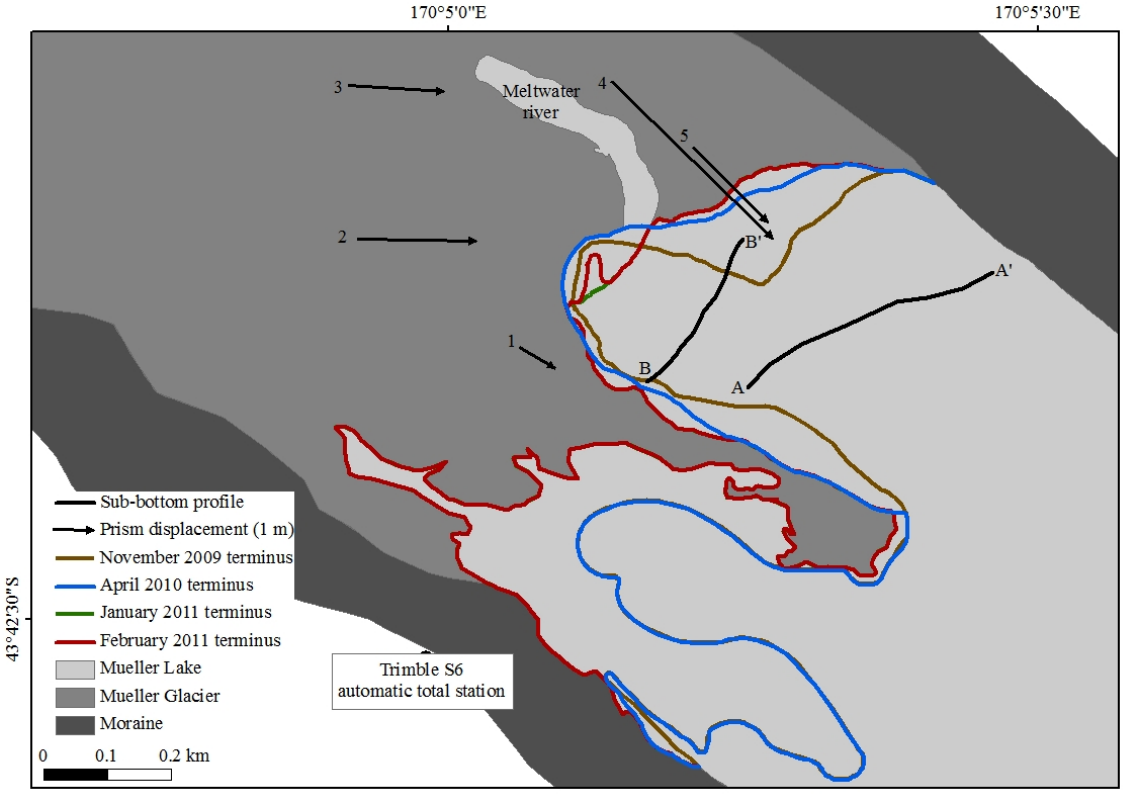

Figure 5.3: Variation in the terminus position of Mueller Glacier between November 2009 and February 2011, and the horizontal displacement of five prisms (numbered 1-5) on the terminus. The horizontal displacement (m) of each prism between the first and last survey, between 23 January and 18 February 2011, are shown by the black arrows (a 1 m scale arrow is shown in the legend). The location of the Trimble S6 automatic total station, used to survey the prisms, is also shown. Lines A-A' and B-B' show the location of sub-bottom sonar profiles shown in Figures 5.6 and 5.7.

5.6.2 Subaqueous morphology and lake size

The bathymetry of Mueller lake in 2009, 2010 and 2011 is shown in Figure 5.4. A 3D image of Mueller Lake in February 2011 is shown in appendix 1. Water depth in the lake is less than 10 m, at a distance of 50 m from the terminus and the lake floor slopes at 18˚ towards the deepest point of the lake (83 m, measured ~600 m in front of the terminus). Increases in lake depth, between 2009 and 2011 occurred adjacent to the terminus ice cliff (Figure 5.2) at the NW (increases of up to 47 m), along the peninsula extending from the centre of the terminus (increases of up to 30 m) and up-valley of the inflow of the Hooker River (increases of up to 40 m). Lake depth decreased, by up to 52

m, between 2009 and 2011 immediately in front of the inflow of the Hooker River, in the deepest section of the lake (~600 m in front of the terminus), and immediately in front of the meltwater stream that exits the glacier in the embayment in the centre of the terminus (Figure 5.2 and Figure 5.4A), as well as in isolated locations near the northern and southern lateral moraines. Between November 2009 and February 2011 the area covered by the lake increased by 17% from 8.33 x 10^5 m^2 to 9.73 x 10^5 m^2 while lake volume increased by 32% from 16.3 x 10^6 m^3 to 21.5 x 10^6 m^3. This is a 141% increase in area and a 842% increase in volume since 1994 (Watson, 1995). A digital elevation model (DEM) of difference of the volume of the lake between November 2009 and February 2011 is shown in Figure 5.5.

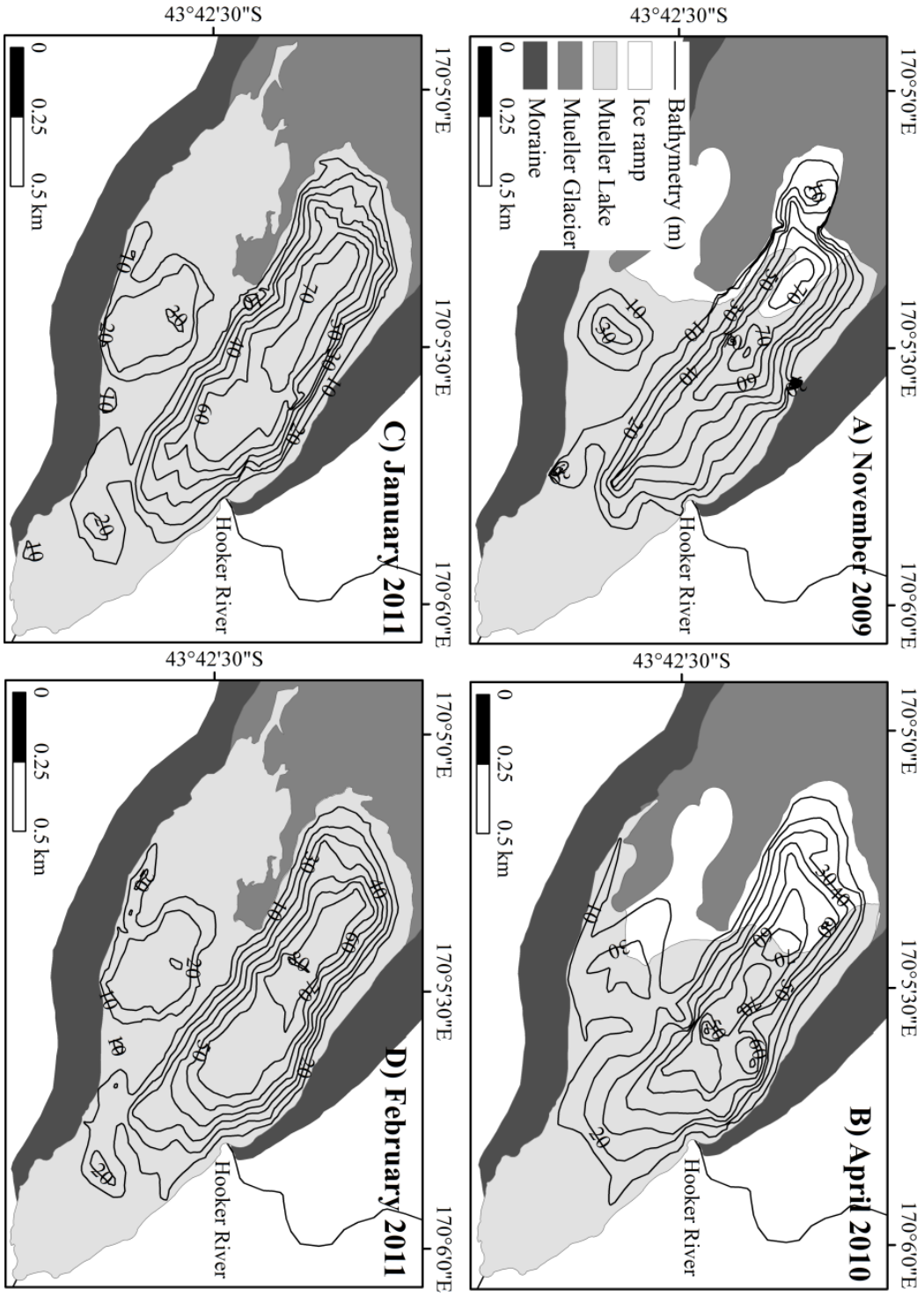

Figure 5.4: The bathymetry of Mueller lake between November 2009 and February 2011. The approximate outline of the subaqueous ice ramp in November 2009 and April 2010 is shown in (A) and (B). A DEM of difference between November 2009 and February 2011 is shown in Figure 5.5. Ice ramp data are not available for January and February 2011.

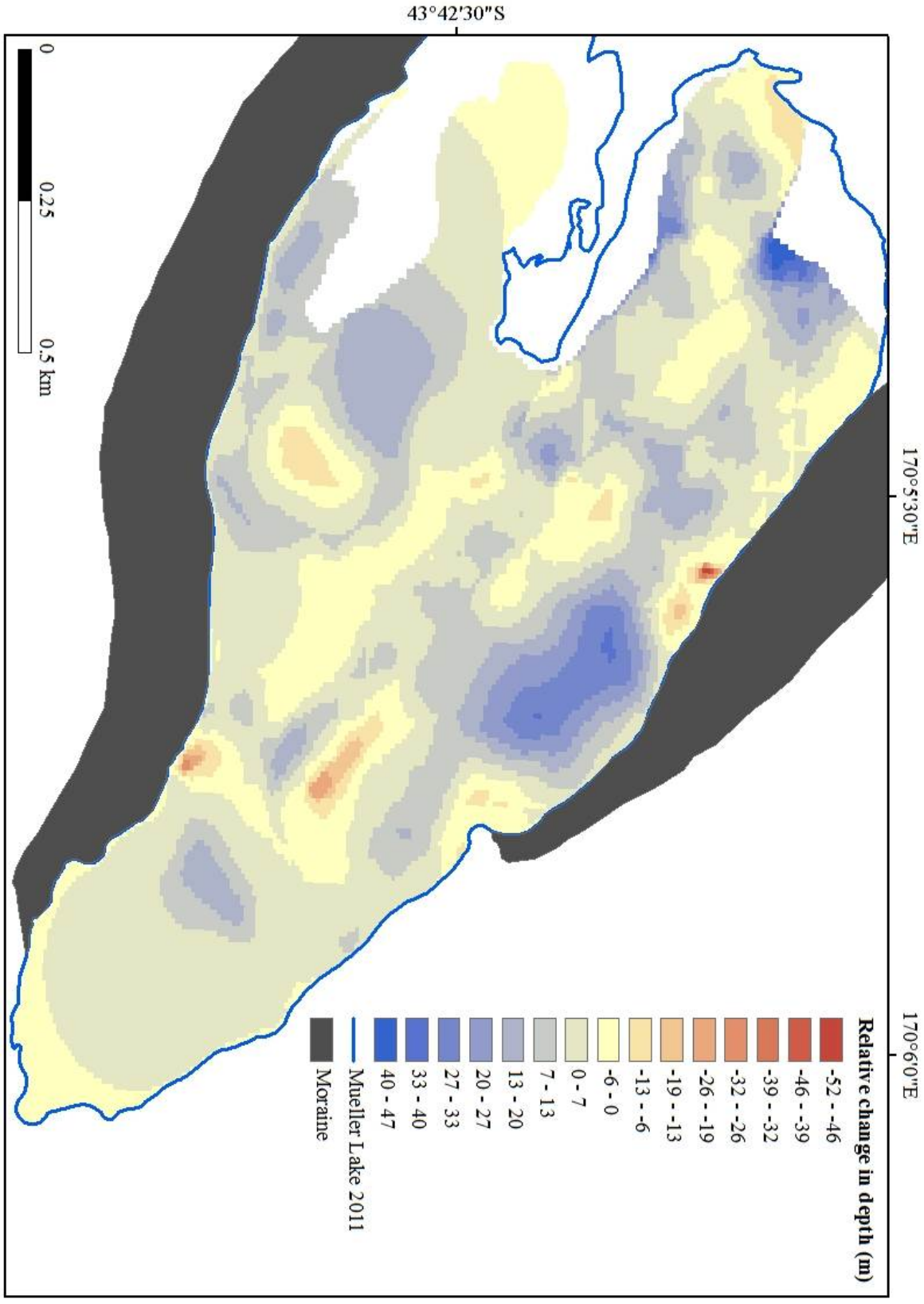

Figure 5.5: DEM of difference for Mueller lake between November 2009 and February 2011. Negative values (red) show a decrease in depth and positive values (blue) show an increase in depth.

Sub-bottom sonar data (Figures 5.6 and 5.7. The location of the profiles is shown in Figure 5.3) show that the lake floor within approximately 370 m of the terminus is underlain with ice, the extent of which is shown in Figure 5.4A and 5.4B. In November 2009 this ice ramp extended ~325 m from the NW of the terminus into the lake and had a surface area of approximately 0.16 km^2. By April 2010, the ramp had increased in length to ~370 m with an area to 0.23 km^2, due to subaerial calving on the NW of the terminus during the 2009/2010 summer (Figure 5.3). The longest section of the ice ramp was 510 m in April 2010. The sub-bottom sonar profiles (Figure 5.6 and 5.7) show that the ice ramp is overlain with a thick layer of sediment (up to 10 m) and contains bands of debris, similar to that seen in the terminal subaerial ice cliffs.

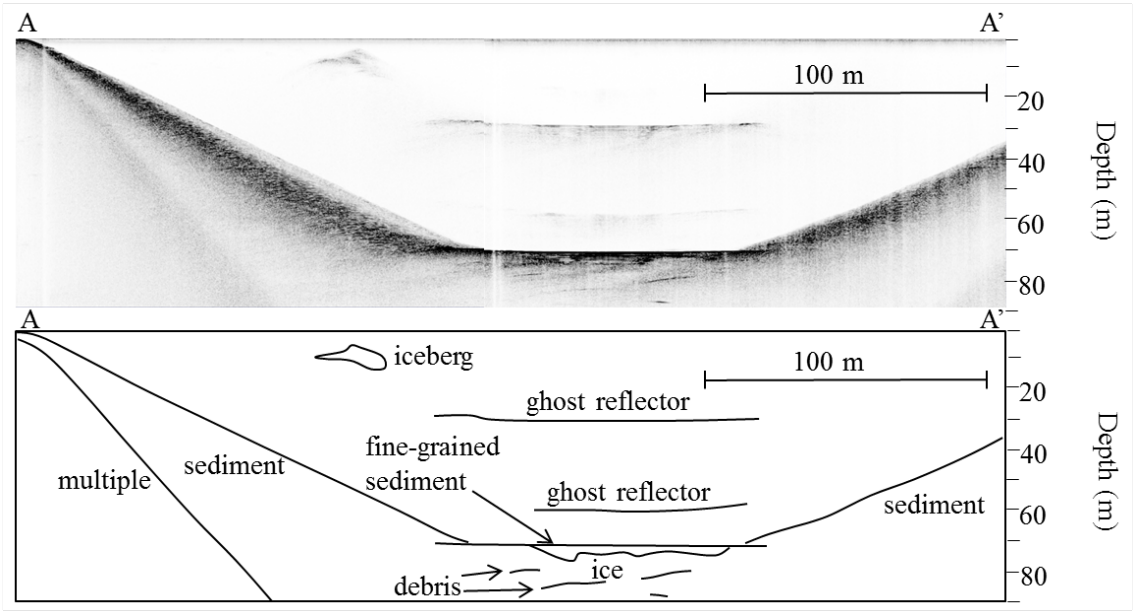

Figure 5.6: Sub-bottom profile image A-A' and interpretation from Mueller lake, April 2010. The location of the image is shown in Figure 5.3. The images show ice at the bottom of the lake, which is overlain with fine-grained sediment (as identified by the thin laminations). Debris bands can be seen in the ice. Sediment on the lake side's slopes down and overlaps the ice.

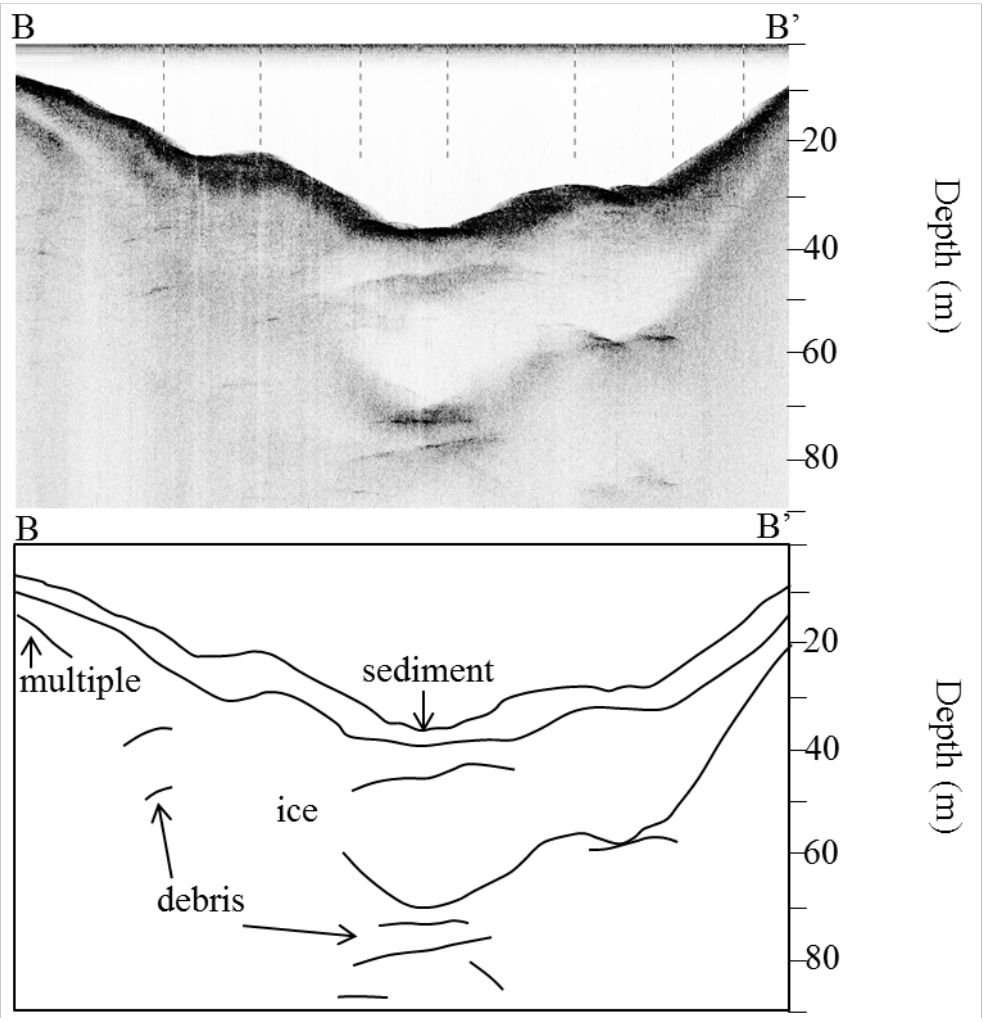

Figure 5.7: Sub-bottom profile image B-B' and interpretation from Mueller lake April 2010. The location of the image is shown in Figure 5.3. The images show the lake floor near the terminus, which is underlain with ice. A thick layer of sediment (~5-7 m) covers the ice and debris bands can be seen within the ice.

5.6.3 Vertical and horizontal terminus displacements

Horizontal and vertical displacements of the five prisms on the lower terminus of Mueller Glacier are shown in Table 5.1. The prisms moved down-glacier by up to 5.82 m (±0.02 m) (Figure 5.3) and were uplifted up to 1.43 m (±0.02 m) over the survey period (Figure 5.8). After initial uplifts of between 1.11 m and 1.43 m between the 23rd and 27th January, vertical displacement of the prisms was minimal, with some recorded displacements falling within the ±0.02 m error range. Vertical displacements do not show any significant response to precipitation or lake level (Figure 5.8). Although the largest vertical displacements occurred following 75.4 mm of precipitation over 14

hours and a ~660 mm rise in lake level on the 26th & 27th January, subsequent precipitation events or fluctuations in lake level did not show any significant response in vertical displacements. Similarly, no clear trend can be seen in horizontal displacements (Table 5.1) after precipitation and subsequent lake level rise, or following periods of little or no precipitation (Figure 5.8). Horizontal displacements, relative to the previous surveyed location, did reduce (from between 1.18 m and 2.29 m on the 4th February to between 0.04 m and 0.17 m on the 7th February; Table 5.1) during and after the large precipitation event on the 5th to the 7th February (300 mm over 40 hours). However, this trend was not repeated during any other precipitation events over the study period.

Table 5.1: Horizontal (H) and vertical (V) displacement (m) of prisms on the terminus of Mueller Glacier between 23 January and 18 February 2011 Data is non-cumulative and displacement is relative to the previous location. * is the first survey.

	Displacement (m)									
	Prism 1		Prism 2		Prism 3		Prism 4		Prism 5	
	H	V	H	V	H	V	H	V	H	V
23 Jan	*	*	*	*	*	*			*	*
24 Jan					2.94	0.32	*	*	2.56	0.31
27 Jan	2.48	1.41	2.97	1.43	7.17	1.15			7.01	1.11
31 Jan	1.78	0.08			3.02	0.03			3.10	0.01
1 Feb	1.07	-0.04			1.75	-0.01			1.78	-0.03
3 Feb	1.96	0.0			3.42	-0.01			3.49	-0.03
4 Feb	1.18	-0.04			2.19	-0.02			2.29	-0.01
5 Feb	0.42	0.00			0.77	0.00			0.85	-0.01
7 Feb	0.04	-0.02							0.17	-0.11
16 Feb	0.63	-0.08							1.24	-0.23
17 Feb	0.28	0.09							0.56	-0.05
18 Feb					0.89	-0.25	5.82	1.04	1.77	-0.06

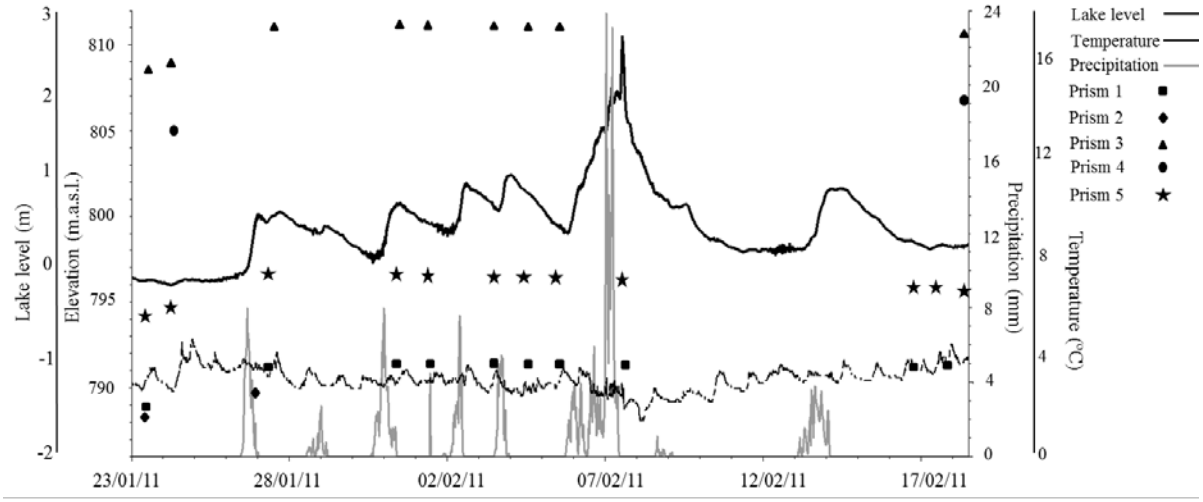

Figure 5.8: Relative lake level, precipitation (from the climate station on the south-western side of the lake, shown in Figure 5.1), water temperature (at depth data logger, shown in Figure 5.1) and the vertical displacement of the five prisms on the lower terminus of Mueller Glacier, between 23 January to 18 February 2011. The symbols for each prism represent survey dates.

Subaerial topography (Figure 5.2) and water depth (Figure 5.4) data show that between 2009 and 2011 the terminus of Mueller Glacier was close to the flotation thickness (92 m), h_f, as calculated from:

$$h_f = \frac{\rho_w}{\rho_i} d \qquad 5.1$$

where d is water depth, ρ_w is water density (1000 kg m^{-3}) and ρ_i is the density of ice (900 kg m^{-3}). Variations in elevation over the subaerial section of the glacier (Figure 5.2) put the glacier at approximately 72-89% of flotation. Prisms 1 (117 m ice thickness) and 2 (106 m ice thickness) were closest to the flotation thickness (92 m) and also recorded the largest vertical displacement between the start and end of the study period (Table 5.1).

5.6.4 Water temperature

Data collected from the lake mooring show temperatures throughout the water column typically fluctuate in unison, with variations of ~1 ºC occurring over 1 or 2 days within 100 m of the glacier terminus (Figure 5.9). The lake was generally thermally stratified over the study period. Strong cooling typically occurred following large precipitation events, except in two periods, when a 1 ºC drop in temperature was not associated with a large precipitation event (grey lines in Figure 5.9).

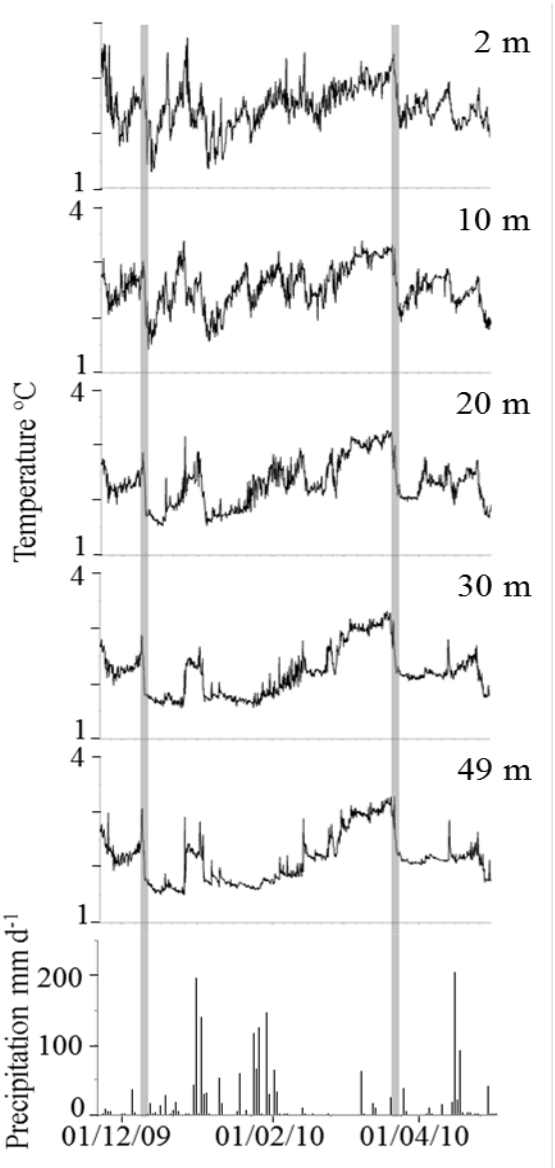

Figure 5.9 (previous page): Lake temperature and precipitation in Mueller lake from 22 November 2009 to 30 April 2010. The first five graphs show water temperature at different depths approximately 100 m in front of the terminus and the bottom graph shows precipitation (mm d^{-1}) recorded at *Aoraki*/Mount Cook Village. Strong cooling typically occurred following a large precipitation event. The two grey lines show periods where a 1˚C drop in temperature was not associated with a large precipitation event.

5.7 Discussion

Mueller Glacier retreated ~150 m between November 2009 and February 2011 (Figure 5.3), while the volume of Mueller lake increased by 32%. In November 2009 an ice ramp extended ~325 m into the lake from the terminus in the NW and had a surface area of ~0.16 km^2. Subaerial calving on the NW of the terminus during the 2009/2010 summer increased the length of the ramp to ~370 m and the area to 0.23 km^2 in April 2010. The longest section of the ice ramp was 510 m in April 2010. During January and February 2011 the terminus of the glacier was uplifted by up to 1.43 m, with horizontal, down-glacier displacements of up to 5.82 m.

5.7.1 Subaqueous morphology

Bathymetric and sub-bottom data show that the subaqueous morphology of Mueller lake changed between November 2009 and February 2011, with both increases and decreases in water depth throughout the lake. The main areas where lake depth increased included areas adjacent to the terminus (depth increases of up to 47 m), along the peninsula extending from the centre of the terminus (increases of up to 30 m) and up-valley of the inflow of the Hooker River (increases of up to 40 m). Subaqueous melt rates in Mueller lake are likely to be significantly reduced due to sediment on the ice ramp and lake floor and cold water temperatures (between 1.5˚C and 2.5˚C). Based on the water depth increases reported (between 30 and 50 m), subaqueous melt rates would need to be around 100 mmd^{-1} between November 2009 and February 2011 to result in the measured depth increases. Based on Röhl's (2005) calculations of subaqueous ice melt under debris at Tasman Glacier, melt rates of between 0.06 and 0.39 mm d^{-1} could be expected for ice under 2 m of debris, in water temperatures of between 1˚C and 1.5˚C. Röhl's (2005) melt rates are considerably lower than those required to result in the increases in depth seen in Mueller lake between 2009 and 2011. Although Röhl's (2005) melt rates could be considered a minimum for Mueller lake, because debris cover on the lake floor is thicker than 2 m (Figures 5.6 and 5.7) and water temperatures are higher than 1˚C and 1.5˚C, it is unlikely that subaqueous melting was the dominant process of mass loss in Mueller lake between 2009 and 2011. Thus, increases in depth near the ice cliff and peninsula can largely be attributed to subaqueous calving, which can remove much larger volumes of ice than subaqueous melting alone. Sub-bottom data show ice in the lake floor in these areas and large icebergs were also observed

emerging from the lake in these areas in December 2009 and April 2010 (C. Hobbs, pers. comm. 2010), which is evidence that subaqueous calving was active. Sub-bottom sonar data do not show ice in or on the lake floor near the inflow of the Hooker River, therefore, lake depth increases in this area are not thought to be the result of subaqueous calving or melting, but instead the result of sliding and slumping of the unconsolidated moraine wall that form the sides of the lake (e.g. Hicks *et al.*, 1990).

Decreases in lake depth occurred mainly in the deepest sections of the lake basin, immediately in front of the meltwater stream that exits the glacier in the embayment in the centre of the terminus, isolated areas adjacent to the moraine walls, and immediately in front of the inflow of the Hooker River. Sediment supply to these areas is likely to be high due to the proximity of high, unstable moraine walls surrounding the lake, and rivers with high suspended sediment concentrations flowing into the lake. Mass movements from the unstable moraine walls, are likely to have redistributed sediment on the lake side's downslope to the deeper sections of the lake basin, resulting in a decrease in lake depth. Decreases in lake depth around the Hooker River and the meltwater river flowing from Mueller Glacier are likely to be the result of sedimentation by the settling out of suspended sediment and bed load. Both rivers have high suspended sediment loads (Griffiths, 1981) and contribute to high suspended sediment levels within the lake. As these rivers enter the lake a portion of the suspended sediment settles out creating fine-grained sediment fans (e.g. Powell & Molnia, 1989; Hicks *et al.*, 1990). Thus the decreases in lake depth in Mueller lake can be attributed to sedimentation via mass movement, fluvial deposition and sediment settling out of suspension.

We propose four controls to explain the changes in subaqueous morphology of Mueller lake between November 2009 and February 2011, including; 1) subaqueous melting; 2) the removal of the subaerial section of the ice cliff resulting in mass loss above the waterline exceeding subaqueous mass loss; 3) subaqueous calving caused by buoyant forces acting on the subaqueous ice ramp, and; 4) sedimentation. As discussed earlier, subaqueous melting is not thought to be the primary control on subaqueous morphology changes, as the estimated subaqueous melt rates are not high enough to result in the

measured depth increases. The subaqueous section of the glacier enlarged over the study period due to the retreat of the subaerial section of the terminus (150 m) with subaerial retreat exceeding subaqueous retreat (Figure 5.4). This resulted in the maintenance of the subaqueous ice ramp extent. Warm surface water temperatures near the terminus (between 0.85˚C and 4.7˚C, Figure 5.9) may have enhanced melting at the waterline, weakening the subaerial ice cliff, and resulting in subaerial calving (Figure 5.3). Decreases in water temperature near the terminus between November 2009 and April 2010 which were not associated with precipitation events (grey lines in Figure 5.9), may indicate these subaerial calving events, where icebergs in the lake cooled the surrounding water (Churski, 1973). Subaqueous calving was observed after the subaerial section of the glacier had retreated between November 2009 and April 2010; 3 days prior to the April 2010 survey subaqueous icebergs were seen emerging from the lake near the ice cliffs in the centre of the terminus (C. Hobbs, pers. comm. 2010). High precipitation events, such as between the 5th and 7th February 2011 (300 mm of precipitation resulting in a ~2.7 m rise in lake level), however did not appear to have a direct influence on the subaqueous ice ramp as no subaqueous calving events or icebergs in the lake were observed. Sedimentation was responsible for water depth decreases near the inflow of the meltwater river and Hooker River and in the deepest section of the lake over the study period. Based on the observed changes and processes operating in the lake, it can be surmised that the evolution in subaqueous morphology was the result of a combination of removal of the subaerial section of ice and subsequent subaqueous calving, along with sedimentation.

5.7.2 Horizontal and vertical displacements on the terminus

Horizontal displacements on the lower 300 m of Mueller Glacier show that the glacier is not stagnant around the lake margin, with displacements between the start and end of the survey ranging from 0.45 m to 5.82 m (Table 5.1). No correlation can be seen between horizontal displacements, lake level fluctuations or precipitation events (Table 5.1 and Figure 5.8). However, displacements did decrease following the large (300 mm in 40 hours) precipitation event of 5-7 February 2011. This could be attributed to increased basal sliding up-glacier caused by rising subglacial water pressure, increasing velocities at the terminus (Kamb *et al.*, 1994; Benn *et al.*, 2007b; Boyce *et al.*, 2007). The precipitation events during January and February (Figure 5.8) may not have been

large enough to result in such a response. Kirkbride and Warren (1997) found that Maud Glacier showed a strong correlation between lake level and ice velocity when the lake level was rising or stationary but not when lake level was falling. No clear correlation can be seen between vertical displacement, lake level or precipitation (Figure 5.8). Although, the largest vertical displacement (that occurred between the 23rd and 27th January 2011) did coincide with a rise in lake level (~660 mm over 10 hours) which followed five days of stable lake level and a precipitation event on the 26th and 27th of January (75.4 mm over 14 hours, Figure 5.8). Subsequent variations in lake level however, did not result in a response in vertical displacements. The largest horizontal displacements occurred at the same time as the highest vertical displacements (between the 23rd and 27th January 2011).

Evidence for the uplift of the terminus in 2011 comes from measured vertical displacement (Table 5.1). Vertical displacement of the five prisms between the first and last survey ranged from 0.88 m to 1.43 m, with a large displacement occurring between the 23rd and 27th January 2011 (Figure 5.8 and Table 5.1). These displacements are considerably larger than the errors associated with the data (±0.02 m). After the 27th January, vertical displacement was minimal. Terminus outlines in Figure 5.3 also show that the terminus advanced approximately 64 m in the small embayment in the centre of the terminus between 2010 and 2011. If a simple calculation is made using the average horizontal displacement from this study (Table 5.1), a horizontal displacement of ~30 m could be expected between the 2010 and February 2011 surveys. This only accounts for half of the surveyed advancement in the embayment. Lake level data do not show a difference in lake level which is significant enough to account of the advancement between the two surveys; in other words, lake level did not decrease between the two surveys to expose the area above lake level. Therefore, this advancement may be the result of the bottom of the ice-cored (Figure 5.7) shallow bay being uplifted, and exposed above the lake level.

Two possible causal mechanisms for the vertical displacement of the terminus are: 1) subglacial topography forcing the terminus upwards as it flows over a topographic high or; 2) the terminus approached or reached flotation thickness (e.g. Boyce *et al.*, 2007).

The main vertical displacement occurred over 5 days in early January 2011, when between 2.48 and 7.17 m of horizontal displacement was recorded (Table 5.1). Based on this time period, and the amount of horizontal displacement, it is unlikely that the horizontal movement of the glacier would be large enough to allow subglacial topography to influence the subaerial elevation of the glacier. Geophysical data from the terminus of the glacier would however be necessary to confirm this assertion. Flotation calculations presented earlier, however, show that the terminus was close to flotation thickness over the study period. Although, supraglacial and englacial debris would affect the buoyancy of the terminus as rock debris has a greater density than that of ice (2000-4000 kg m^3 compared to 900 kg m^3 which is typically assumed for glacier ice) (Tweed, 2000). This results in the debris adding mass or effectively 'weighting down' the glacier, and thus, deeper water depths are needed for the glacier to reach flotation thickness. Due to the thick layer of supraglacial debris on Mueller Glacier, and the englacial debris in the ice, it is likely that the flotation thickness would be higher than that calculated from equation 1 (92 m). The glacier would therefore be closer to this flotation thickness. Thus, the vertical displacement of the terminus in January and February 2011 was likely the result of the terminus approaching flotation thickness.

5.8 Conclusion

This study has examined the temporal evolution of the subaerial and subaqueous morphology of the terminus of Mueller Glacier, which retreated ~150 m between November 2009 and February 2011, with a volume increase of its proglacial lake of 32%. Data from the study indicate that buoyant forces may act on subaqueous ice ramps, to result in subaqueous calving. In addition, data show that changes in the subaqueous morphology are controlled by a combination of subaerial retreat and subsequent subaqueous calving, along with sedimentation. Subaqueous melting is minimal due to the debris cover. Horizontal and vertical displacements of these glaciers may also not be directly connected to precipitation and lake level fluctuations but have the potential to be driven by the terminus approaching flotation thickness. The development and maintenance of the extent of subaqueous ice ramps is intrinsically

linked with retreat of the subaerial section, as subaerial retreat has been shown to drive subaqueous retreat. This study has contributed to the quantitative dataset on subaqueous ice ramps, and increased understanding on the dominant processes controlling their evolution in debris-covered, lake-calving glaciers. In doing so, understanding of the processes responsible for, and which contribute to, overall glacial retreat and proglacial lake development debris-covered, lake-calving glaciers, has been improved.

5.9 Acknowledgements

This work was funded by the Ryoichi Sasakawa Young Leaders Fellowship Fund. We would like to thank Charlie Hobbs for invaluable local knowledge and equipment, the Department of Conservation for allowing this work and the New Zealand Alpine Club. Field assistance from Jess Costall, Alastair Clement, Jingjing Wang, Sam Benny, Rob Eastham, Rob Dykes and David Feek was also greatly appreciated. Critical reviews from Roman Motyka and an anonymous reviewer significantly improved the manuscript and were greatly appreciated.

Chapter 6: Calving retreat and proglacial lake growth at Hooker Glacier, Southern Alps, New Zealand

6.1 Introduction

Chapter 5 examined the temporal evolution of the subaqueous morphology of Mueller Glacier in relation to changes in the subaerial morphology. The dominant processes that control the evolution of ice ramps in debris-covered, lake-calving glaciers include a combination of subaerial retreat and subsequent subaqueous calving, along with sedimentation. The development and maintenance of the extent of subaqueous ice ramps is intrinsically linked with subaerial retreat. Predictions of glacier retreat should therefore consider subaqueous morphologies. Two retreat scenarios, one of which is based on the maintenance of a subaqueous ice ramp, are applied to Hooker Glacier in this chapter. Hooker Glacier is the focus of this study as valley profile data up-glacier of the 2011 terminus is published. No such data are available for Mueller, Murchison, or the Godley Valley glacial valleys.

Parts of this chapter are contained within the manuscript: Robertson, C.M., Brook, M.S., Holt, K.A., Fuller, I.C. and Benn, D.I., Calving retreat and proglacial lake growth at Hooker Glacier, Southern Alps, New Zealand, which has been accepted for publication in *New Zealand Geographer*. The manuscript examines past retreat of the glacier and proposes two scenarios for twenty-first century retreat. Firstly, chapter 3 is expanded by quantifying retreat rates for the glacier between 1965 and 2011 and concurrent expansion of Hooker Lake (section 6.6). Two retreat scenarios are then applied; one assuming that calving rates are driven by the rate of waterline melt, while the second one is based on the calving rate-water depth relationship (section 6.6). Proglacial lake growth is also extrapolated into the future (section 6.6). The results of these scenarios are then discussed and compared with neighbouring glaciers, while additional factors that may also influence future retreat are identified (section 6.7). The scenario that best accounts for subaqueous morphologies, and therefore the effect of an

ice ramp extending from the terminus of a glacier, is also identified (section 6.7). The study illustrates once again that glacier retreat differs between glaciers within a single mountain belt (chapter 3) even when predicted into the future, and comes full circle by applying retreat scenarios that consider how subaqueous morphologies influence subaerial retreat and vice versa.

6.2 Abstract

Hooker Glacier, in the central Southern Alps of New Zealand, has undergone significant downwasting and recession (~2.14 km) during the last two centuries. High retreat rates (51 m a^{-1} 1986 to 2001, 43 m a^{-1} 2001 to 2011) have produced a large (1.22 km^2) proglacial lake. We present two retreat scenarios for Hooker Glacier. A fast retreat scenario predicts the glacier terminus will stabilise ~3 km up-valley of the current lake outlet around 2028, when ice velocity equals calving rate. A slow retreat scenario predicts the glacier will retreat ~3 km up-valley by 2038.

Key words: calving retreat, Hooker Glacier, proglacial lake.

6.3 Introduction

Alpine glaciers are considered to be sensitive indicators of climate (Chinn *et al.*, 2005; Oerlemans, 2005), with climate warming, following the end of the Little Ice Age (LIA) in the mid-nineteenth century, causing a general global pattern of glacier recession (Brown *et al.*, 2010). With the rate of warming projected to increase during the twenty-first century (Solomon *et al.*, 2007), a general acceleration of glacier retreat appears the likely scenario. However, in reality glacier behaviour is often incongruous with these expected general patterns, and glaciers in regions such as maritime western Scandinavia (Winkler *et al.*, 2009), Iceland (Dowdeswell *et al.*, 1997), and the Southern Alps of New Zealand (Chinn *et al.*, 2005), have in fact undergone phases of advance over the last four decades. Furthermore, glaciers within the same mountain range do not always display the same advance and retreat patterns (Granshaw & Fountain, 2006). This may

be due to variations in long-profile gradient, amount of debris cover, geometry, size and presence or absence of a proglacial lake adjacent to the glacier terminus (Salinger *et al.*, 2008). The latter factor is highly important at a number of glaciers, particularly in the central Southern Alps of New Zealand (Kirkbride, 1993; Chinn, 1996; Warren & Kirkbride, 2003; Röhl, 2005; Quincey & Glasser, 2009; Dykes *et al.*, 2011), the Himalaya (Watanabe *et al.*, 1995; Benn *et al.*, 2000; Benn *et al.*, 2001; Watanabe *et al.*, 2009; Thompson *et al.*, 2012) and the European Alps (Haeberli *et al.*, 2001; Huggel *et al.*, 2002; Diolaiuti *et al.*, 2005; Diolaiuti *et al.*, 2006). The presence of an ice-contact proglacial lake at a glacier terminus is important because such 'calving' glaciers can become partially decoupled from climate-forcing, allowing factors other than mass balance to control rates of retreat or advance (Benn *et al.*, 2007b).

Glaciers to the west of the Main Divide of the Southern Alps (e.g. Franz Josef and Fox glaciers) have shown a pattern of advance and retreat over the last century, due to steep long-profiles, debris-free surfaces and large accumulation areas relative to their ablation areas (e.g. Purdie *et al.*, 2008). Their termini have responded to changes in regional atmospheric circulation in less than a decade (Herman *et al.*, 2011). In contrast, to the east of the Main Divide the lake-calving glaciers of *Aoraki*/Mt Cook National Park are longer, have low-gradient long-profiles, and debris-covered ablation zones, which insulate the ice beneath, diminishing surface melt (Quincey & Glasser, 2009). Due to these factors, these glaciers have much longer terminus response times, and are still responding to post-LIA warming via gradual downwasting (Herman *et al.*, 2011), occurring in addition to calving (the mechanical loss of ice from the terminus). Hence, while the response of west coast glaciers to climate variability is well established (e.g. Hooker & Fitzharris, 1999), and terminus variations have been predicted by numerical modelling (Anderson *et al.*, 2006), the future terminus fluctuations of the large lake-calving glaciers of *Aoraki*/Mt Cook National Park remains equivocal. Furthermore, research in the National Park has traditionally been limited to Tasman Glacier (e.g. Röhl, 2006; Quincey & Glasser, 2009; Dykes *et al.*, 2011), with other glaciers such as Hooker Glacier receiving less attention, usually as a minor part of a broader study (e.g. Warren & Kirkbride, 1998; Röhl, 2006). The last detailed study of Hooker Glacier was in 1996 (e.g. Hochstein *et al.*, 1998).

Late twentieth and twenty-first century retreat in the central Southern Alps has already been quantified in order to provide a broader picture of contemporary glacier recession (Chapter 3). In order to expand and extend this work, we focus more specifically on Hooker Glacier, with a more detailed analysis of past retreat which is used to predict future glacier retreat. Hooker Glacier is a debris-covered, lake-calving glacier that has undergone significant downwasting and recession during the twentieth and twenty-first centuries. The aims of the study are to use a suite of aerial photographs and satellite images to quantify the changing rate of retreat at Hooker Glacier between 1965 and 2011 in order to propose tentative scenarios for the twenty-first century retreat of Hooker Glacier; and identify factors that may impact on future calving retreat of the glacier. Retreat scenarios are based on 1) waterline melting, and 2) the water depth – calving rate relationship. Waterline melting causes the development of thermal erosional notches, which promote calving of the subaerial ice cliff (Röhl, 2006). The water depth – calving rate $(U_c\text{-}D_w)$ relationship, established empirically from other lake-calving glaciers (Funk & Röthlisberger, 1989; Warren *et al.*, 1995b), assumes that calving rates will increase as a glacier retreats back into a bedrock overdeepening, increasing water depths. The relationship does not require consideration of the processes operating at the terminus (Kirkbride & Warren, 1999) and varies between regions, within regions (see Chapter 3) and over time for a single glacier (van der Veen, 2002).

6.4 Study area

Hooker Glacier (Figure 6.1) is a 12.3 km long compound valley glacier, descending from 3000 m a.s.l to 876 m a.s.l (Hochstein *et al.*, 1998), with a surface area of 17 km^2 (including the tributaries of the Sheila, Empress and Noeline glaciers). The glacier lies in the valley on the western side of *Aoraki*/Mt Cook. Twenty five per cent of the glacier surface is covered with supraglacial debris ~3 m thick (Chinn, 1996), with the lowermost 1.5 km of the glacier having a surface gradient of only 3.5º (Röhl, 2005). Since reaching its LIA maximum during the mid-late 19th century (Gellatly, 1985; Schaefer *et al.*, 2009), Hooker Glacier downwasted along its centreline at a rate of up to 1 m a^{-1} between 1915 and 1986. Downwasting diminished to only ~0.3 m a^{-1} over the following decade until 1996 (Hochstein *et al.*, 1998), presumably as debris thickness

increased and the long-profile gradient decreased. Downwasting and melting of exposed ice on the terminus prior to 1982 led to the development of a proglacial lake (Figure 6.2) in the late 20th century (Chinn, 1999; Kirkbride & Warren, 1999). Kirkbride (1993) proposed that the development of an unconfined aquifer on the lower terminus, in conjunction with glacier thinning, increased the buoyancy of ice blocks along the glacier margins. This induced fracturing, enhancing melt by allowing further water infiltration, resulting in the development of large meltwater channels (Kirkbride, 1993). These channels then coalesced to form a proglacial lake soon after 1982, effectively 'drowning' the terminus (Kirkbride, 1993).

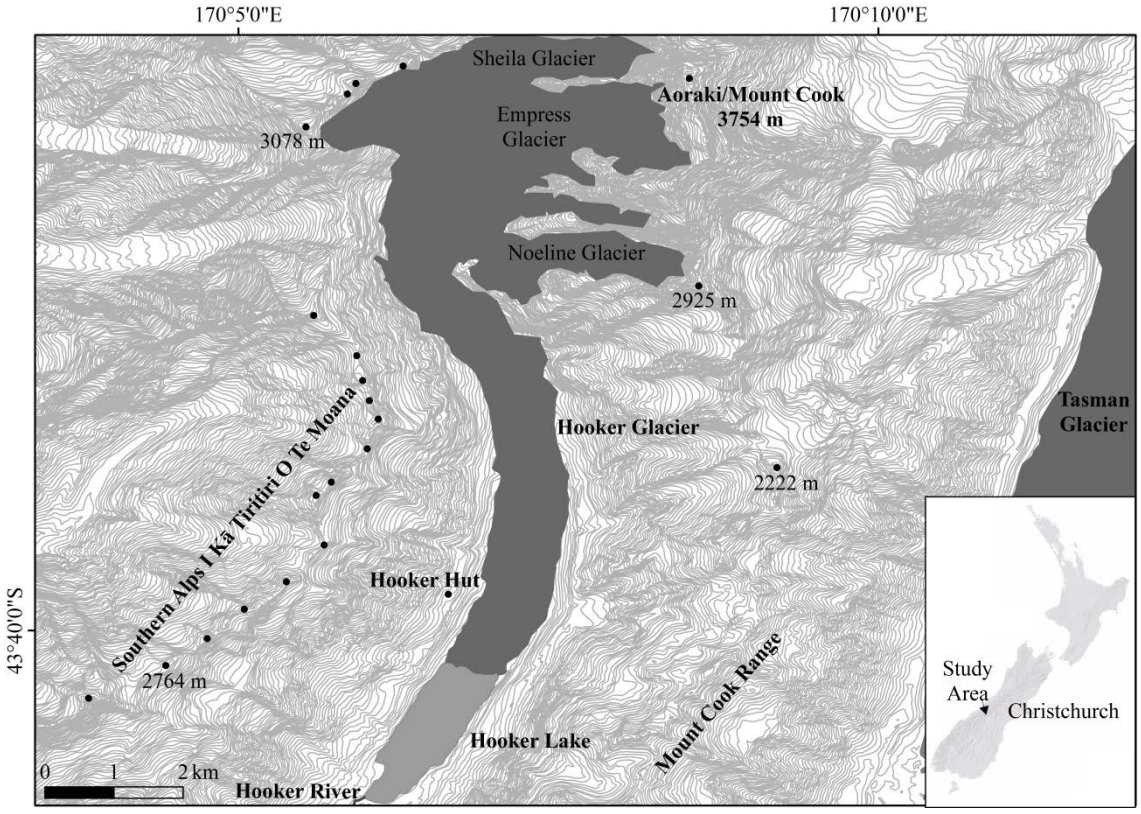

Figure 6.1: Map showing the location of Hooker Glacier and Lake in the central Southern Alps, New Zealand. Black dots denote the Main Divide of the Southern Alps. Sheila, Empress and Noeline glaciers, tributaries of Hooker Glacier, are also shown.

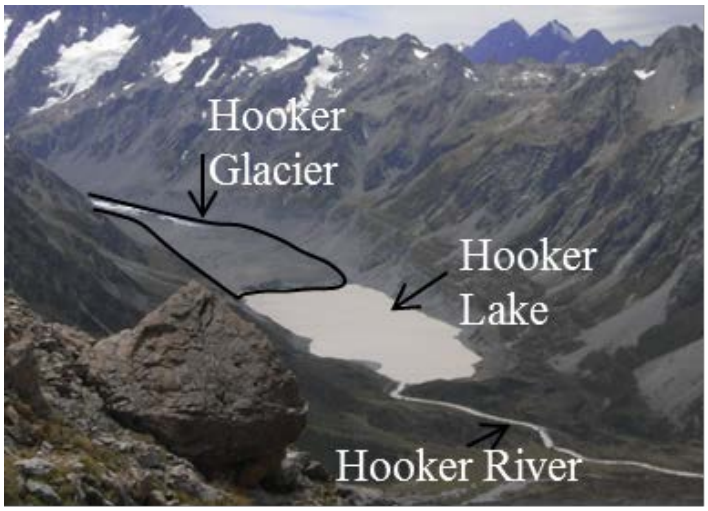

Figure 6.2: Hooker Glacier terminating into Hooker Lake (view to the northeast). Hooker River exits the lake near the bottom of the photo (source: C. Robertson, 26 January 2011).

Processes of mass loss at the terminus transitioned from melting to calving in the early 1990s (Hochstein *et al.*, 1998; Warren & Kirkbride, 1998), and contemporary retreat of the glacier is thought to now be largely independent of regional climatic signals (Chinn, 1996; Hoelzle *et al.*, 2007). Retreat rates decreased between the early 1980s and 1996 from 70 m a^{-1} to 30 m a^{-1} (Hochstein *et al.*, 1998; Warren & Kirkbride, 1998) but then increased between 2001 and 2003 with rates of 79 m a^{-1} reported (Röhl, 2006). Glacial retreat via subaerial calving led to a proglacial lake with a surface area of 1.22 km^2, a volume of 0.05 km^3 and a maximum depth of 140 m in 2009 (Chapter 4).

6.5 Methods

Terminus positions of Hooker Glacier from 1965 to 1986 were acquired from 5 aerial photographs, while 6 multispectral satellite images were used for the periods between 2001 and 2008, and 2010 and 2011. In addition, the terminus position in 2009 was surveyed in the field by global positioning system (GPS), with an accuracy typically within ± 5 m (Garmin Ltd, 2007). Satellite images were acquired from the Advanced

Spaceborne Thermal Emission and Reflection Radiometer (ASTER) and Landsat satellite sources. All images were geo-referenced using ground control points (stable, recognisable features present in all images) to register the selected images against topographic data from Land Information New Zealand Topo50-BX15 (New Zealand Transverse Mercator 2000). The images were registered using the rotation, sampling and translation warping (RST) method resulting in the root mean square error for each image being smaller than a single pixel (Jensen, 1997). Terminus positions and lake areas were generated by manual digitisation in ESRI ArcMap software. Retreat rates were calculated by measuring the perpendicular distance between terminus profiles at a series of locations along the terminus front. These measurements were averaged and the mean rate of change from this information was then used to represent the rate of change during the measured periods. From these data, future twenty-first century calving retreat scenarios were created, with the basis for these retreat scenarios explained further in the results section (6.6). Bathymetric data of Hooker Lake was collected in November 2009 using a Humminbird 323 DualBeam Plus dual frequency echo-sounder (frequencies of 200 kHz and 83 kHz). Data were collected over intersecting transects at ~100 m spacings, with depth sounding positions recorded via handheld GPS with an accuracy of ± 5 m (Garmin Ltd, 2007). The echo-sounder was calibrated against known depths within the lake to give an accuracy of less than 1 m. Data were interpolated using triangular irregular network (TIN) modelling, from which smoothed bathymetric contours were produced in ESRI ArcMap.

6.6 Results

Hooker Glacier has retreated 2.14 km up-valley from its LIA terminal moraine since 1965 (Figure 6.3). Results show that lake expansion (Figure 6.4) has followed a steadily increasing trend after the coalescence of supraglacial and ice-marginal ponds between 1982 and 1986, confirming Kirkbride's (1993) theory. Since formation of the proglacial lake, terminus retreat rates (U_r) have ranged from approximately -3 m a^{-1} (an advance) between May 2006 and May 2008, to 153 m a^{-1} between November 2009 and February 2010 (Table 6.1). As a consequence of this retreat, the surface area of Hooker Lake also increased overall, forming a lake of 1.28 km^2 in 2011 (Figure 6.4). The glacier now

calves into Hooker Lake via a linear (in plan form) subaerial ice cliff (Figure 6.5), with the lake occupying the bottom of a steep-sided U-shaped glacial valley, with the lake floor shoaling towards the Hooker River outlet (Figure 6.6). From the deepest point in the lake (140 m, 390 m in front of the terminus) the lake floor shallows rapidly towards the terminus at an angle of approximately 20˚. Towards the centre of the lake, the lake floor is flat with a change in elevation of only 20 m over a distance of 270 m.

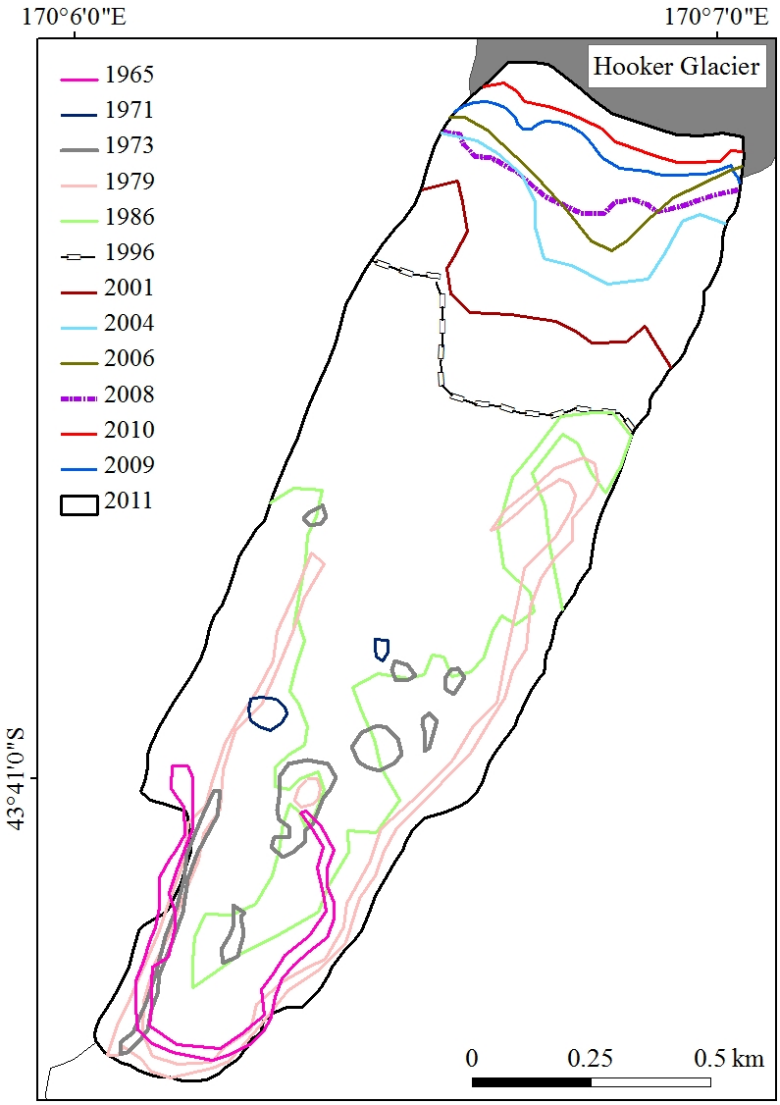

Figure 6.3: Terminus positions of Hooker Glacier, 1965 to 2011. Supraglacial and ice-marginal ponds, which developed between 1965 and the early 1980s, coalesced in 1982. Since 1965 the terminus of Hooker Glacier has retreated 2.14 km up-valley from its LIA terminal moraine. The 1996 terminus position is from Hochstein *et al.* (1998).

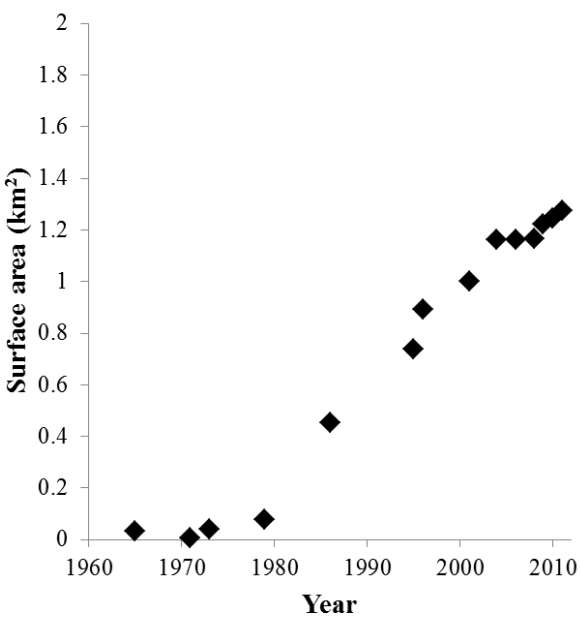

Figure 6.4: Surface area of Hooker Lake between 1965 and 2011. Growth in lake surface area has followed a steadily increasing trend after the coalescence of supraglacial and ice-marginal ponds in 1982 and subsequent high retreat rates.

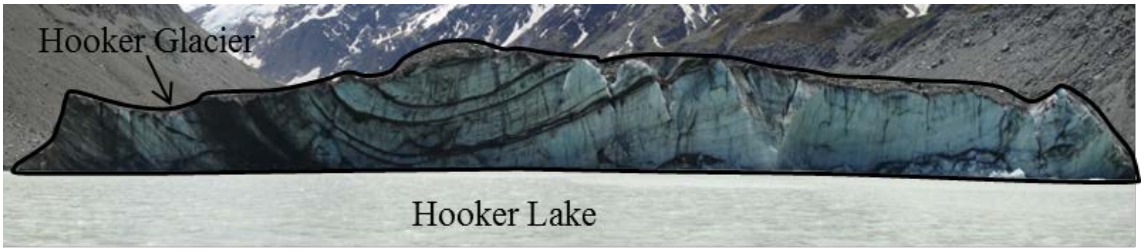

Figure 6.5: Ice cliff at the terminus of Hooker Glacier (source: C. Robertson, 23 November 2009). Note the layers of debris in the subaerial ice cliff which provide pre-existing weaknesses in the glacier which can be exploited to result in calving. The calving terminus is comprised of a vertical subaerial ice cliff (approximately 30 m high), which then forms a low gradient subaqueous ice ramp sloping away from the terminus into the lake.

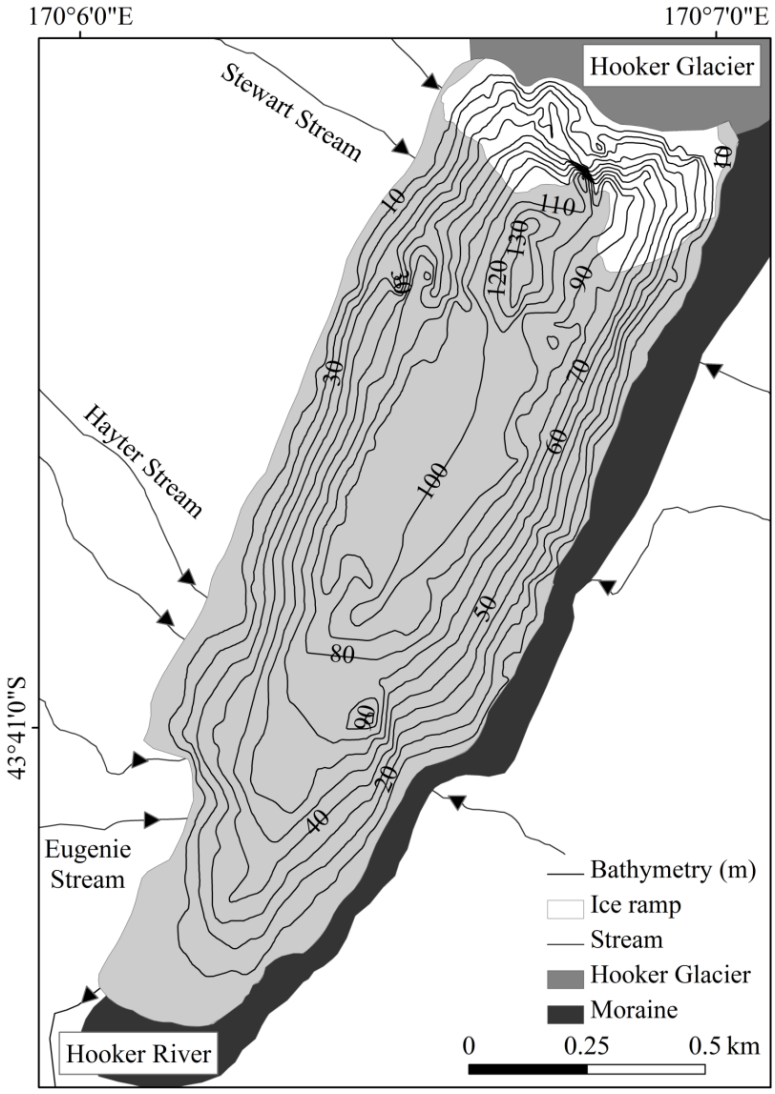

Figure 6.6: Hooker Lake bathymetry and the location of an ice ramp which was identified in 2009 (Chapter 4).

The retreat rates (Figure 6.3 and U_r in Table 6.1) only give a simple insight into actual calving rates, because they ignore factors such as ice velocity and ice melt. To address this, two further approaches were used. The first estimates calving rates (U_c m a^{-1}) from the difference between glacier velocity (U_i) at the terminus and the rate of change in glacier length (∂L) over a given period of time (∂t):

$$U_c = U_i - \frac{\partial L}{\partial t} \qquad 6.1$$

An ice velocity of 30 m a^{-1} was used, and is the mean annual ice velocity near the 2011 terminus measured by Röhl (2005) between 2001 and 2002. Results (U_c m a^{-1}) are reported in Table 6.1. A further approach, following Warren and Kirkbride (2003), was to incorporate melting of the calving face into calving rate calculations, and these results ($U_c + U_m$) are included in Table 6.1. A mean annual melt rate of bare ice at the terminus of 14 m a^{-1} was used, which was the estimate of Röhl (2005). Using these calculations, calving rates ($U_c + U_m$) ranged from ~2 m a^{-1}, between February 1979 and February 1986, to ~135 m a^{-1}, between November 2009 and February 2010. A comparison of U_r, U_c and $U_c + U_m$ is given in Figure 6.7 which shows the variation between the three methods.

Table 6.1: Hooker Glacier full width retreat data between 1979 and 2011. ∂L_{max} is maximum retreat, ∂L_{mean} is mean retreat, U_r is retreat rate (∂L_{mean} multiplied by t to determine the annual rate), U_c is calving rate, $U_c + U_m$ is calving rate + melt at the calving cliff, D_w is water depth. Negative values indicate a width-averaged advance of the glacier.

Survey interval	Time interval (t) in days	∂L_{max} m	∂L_{mean} m	U_r m a^{-1}	U_c m a^{-1}	$U_c + U_m$ m a^{-1}	D_w m
14/02/79-01/02/86	2544	241	86	12	12	2	-
01/02/86-01/02/96	3652	1369	623	62	32	46	90
01/02/96-31/03/01	1885	204	154	30	0	14	100
31/03/01-28/04/04	1124	269	164	54	23	37	130
28/04/04-04/05/06	736	122	61	30	0	14	120
04/05/06-13/05/08	740	100	-6	-3	-32	46	120
13/05/08-24/11/09	560	150	83	54	24	38	70
24/11/09-19/02/10	87	59	36	153	121	135	-
19/02/10-16/02/11	362	84	55	55	25	39	-
01/02/86-31/03/01	5537	1573	776	51	21	35	-
31/03/01-16/02/11	3609	514	429	43	13	27	-

Water depths (D_w) reported in Table 6.1 are based on the deepest area adjacent to the terminus. These water depths allow an estimation of a water depth-calving rate relationship (U_c-D_w) at Hooker Glacier, by comparing spatial changes in lake bathymetry with temporal changes in the calving ice cliff position. The relationship at Hooker Glacier can be represented as:

$$U_c = 43.4 + -0.1\ D_w \qquad 6.2$$

This equation is a least-squared linear regression (r^2 =0.03) using the data reported in Table 6.1 between 1986 and 2009. The relationship between water depth and calving rate at Hooker Glacier does not follow the generally accepted trend of calving rates increasing as the glacier retreats into deeper water, as have been generally reported elsewhere (e.g. Funk & Röthlisberger, 1989; Warren *et al.*, 1995b). Additional data may however be required to pick up any correlation.

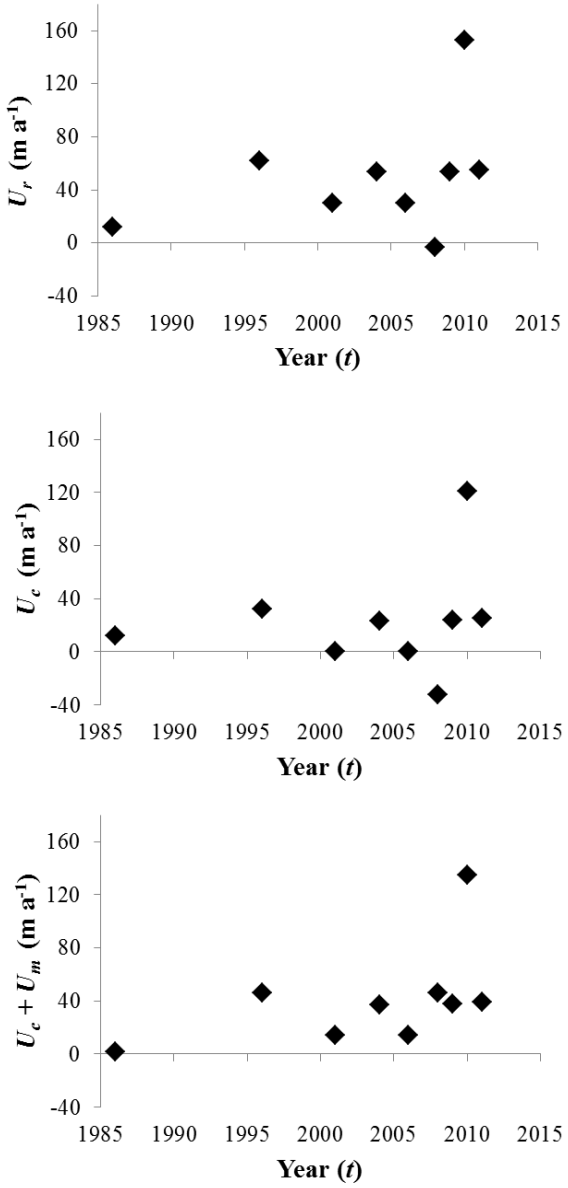

Figure 6.7: Retreat rates and calving rates of Hooker Glacier between 1986 and 2011. U_r is retreat rate (mean retreat along the terminus multiplied by time), U_c is calving rate, $U_c + U_m$ is calving rate + melt at the calving cliff. Values are reported in Table 6.1.

Following Kirkbride and Warren (1999) and Dykes and Brook (2010), two future retreat scenarios for Hooker Glacier are presented in Figure 6.8. The first scenario assumes that the calving rate will be driven by the rate of waterline melt. A calving rate of 45.5 m a^{-1} has been assumed in this scenario, which is based on calving being driven by waterline melting and subsequent thermo-erosional notch development, calculated by Röhl (2005)

for the period 2001 to 2002. This scenario predicts that Hooker Glacier will retreat, reaching a stable terminus more than 3 km up-valley of the current lake outlet when $U_i=U_c$. Annual ice velocity at Hooker Hut (~3 km up-valley of the lake outlet) is approximately 36 m a^{-1} (Röhl, 2005). It is projected that the glacier will retreat 3 km up-valley by approximately 2028, in water ~156 m deep.

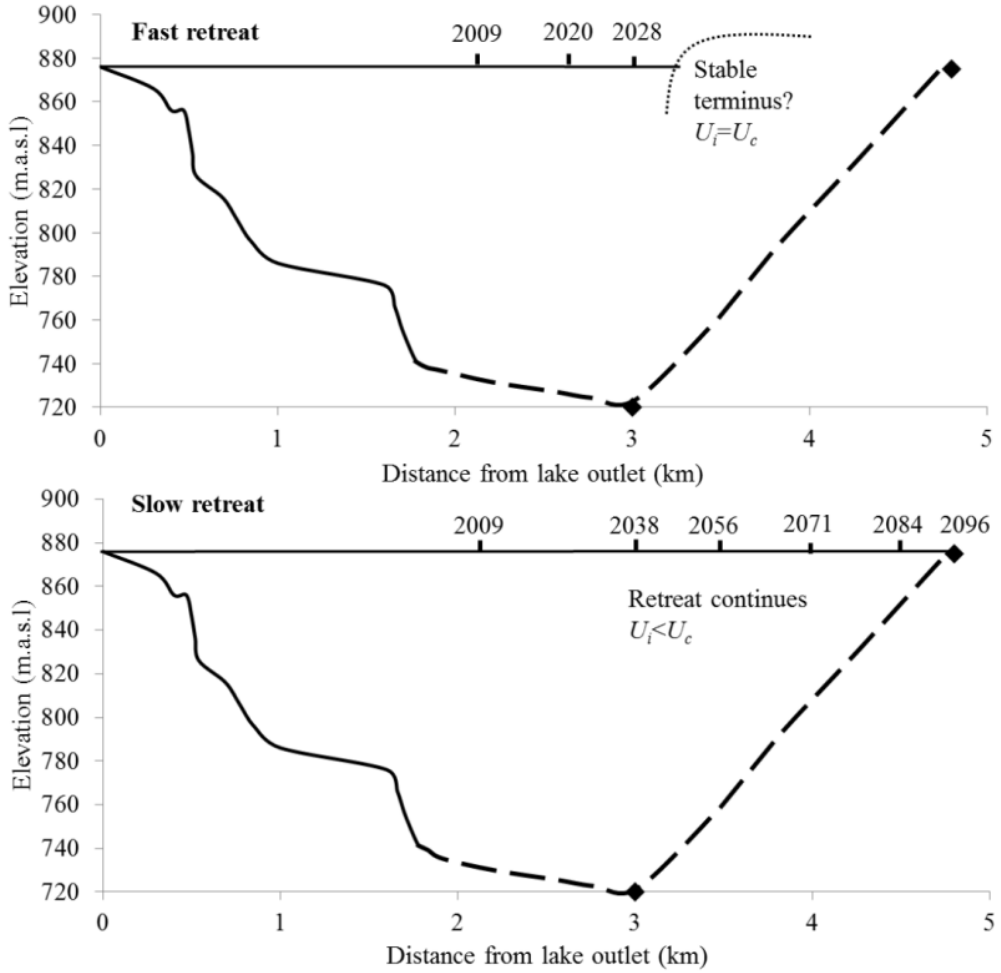

Figure 6.8: Predicted retreat scenarios for Hooker Glacier. The profiles have a vertical exaggeration of approximately 12. The subglacial bedrock profile (dashed line) is inferred from Hochstein *et al.*'s (1998) ice thickness data, and is measured at 3 km and 4.8 km up-valley of the Hooker Lake outlet. The fast retreat scenario is based on waterline melt from Röhl (2005) and predicts the glacier terminus will stabilise > 3 km up-valley of the current lake outlet after 2028, when ice velocity equals calving rate. The slow retreat scenario, based on the calving rate-water depth relationship (established by Funk & Röthlisberger, 1989; Warren *et al.*, 1995b), predicts the glacier will retreat ~4.8 km up-valley where it will stabilise as bedrock outcrops at lake level by 2096.

A second retreat scenario which applies the U_c-D_w relationship to Hooker Glacier is shown in Figure 6.8. The scenario assumes that the glacier will retreat up-valley at a rate (calculated from equation 6.2) relative to the mean water depth at the terminus (based on the approximated valley floor topography shown in Figure 6.8), until it gets to the point where the valley floor is at the same elevation as the current lake level (876 m a.s.l). When the glacier reaches this point, the effect the proglacial lake has on the terminus will be significantly diminished as the glacier will begin to withdraw from Hooker Lake. This withdrawal will reduce calving retreat rates and allow the terminus to stabilise. Bedrock outcrops at the level of the current lake approximately 4.8 km up-valley from the lake outlet (Hochstein *et al.*, 1998), as shown in Figure 6.8. At these (slower) retreat rates, the glacier terminus will recede to this location in approximately 2096.

Extrapolation of lake expansion up-valley of the 2011 terminus (Figure 6.4) estimates that the surface area of Hooker Lake could be 1.98 km^2 once the glacier retreats 3 km up-valley from the lake outlet in the first retreat scenario. When the glacier reaches the bedrock at 4.8 km in 2096 in the second retreat scenario, the surface area of the lake is estimated to be 3.12 km^2. These surface areas follow the trend of lake surface area growth as shown in Figure 6.4.

6.7 Discussion

6.7.1 Retreat rates

Rates of retreat of Hooker Glacier since the late 1970s have varied, with U_c-U_m ranging from 2 m a^{-1}, prior to 1982, to 135 m a^{-1} between 2009 and 2010. A significant increase in U_c-U_m occurred in the mid-1980s when rates increased from 2 m a^{-1}, between 1979 and 1986, to 46 m a^{-1}, between 1986 and 1996. This increase was likely the result of the coalescence of a single proglacial lake in 1982 which increases melting of exposed ice and hence retreat rates (e.g. Kirkbride, 1993). A direct comparison between calving and retreat rates reported here and rates calculated in other studies of Hooker Glacier is difficult due to variations in survey periods. Hochstein *et al.* (1998) reported a retreat

rate of 30 m a^{-1} for the period between 1982 and 1996 and also during 1998. Retreat rates calculated in this study which cover those periods differ with rates of between 2 m a^{-1} and 46 m a^{-1} (Table 6.1). Both sets of retreat rates incorporate ice velocity and ice melt rates, although these rates differ, with Hochstein *et al.* (1998) using an ice velocity of 5 m a^{-1} and a melt rate of 40 m a^{-1} compared with an ice velocity of 30 m a^{-1} and a melt rate of 14 m a^{-1} incorporated in this study. Therefore the difference in retreat rates between the two studies is likely to be the result of a combination of different ice velocities and melt rates incorporated into the calculations and variations in the survey periods used. Although there are similar difficulties in comparing retreat rates between this study and that of Dykes and Brook (2010), it is clear that retreat rates at Tasman Glacier during the early 21st century have been higher than those at Hooker Glacier. These difference may be the result of an increase in glacier velocities at Tasman Glacier after 2006, which may have increased calving rates as the glacier counteracted the increase in velocity by increasing calving rates, along with the expansion of supraglacial lakes on the terminus of Tasman Glacier after 2000 (e.g. Quincey & Glasser, 2009; Dykes & Brook, 2010).

6.7.2 Retreat scenarios

The first retreat scenario (based on the rate of waterline melting) predicts higher calving rates, and hence glacier retreat rates, and indicates that the terminus of the glacier will retreat 3 km up-valley of the lake outlet by 2028. This contrasts with the second scenario (U_c-D_w) which predicts slower retreat rates and that the glacier will reach 3 km up-valley in 2038 (Figure 6.8). For Tasman Glacier, Kirkbride and Warren (1999) and Dykes and Brook (2010) found that the retreat scenario based on the U_c-D_w relationship predicted faster retreat than the scenario that was based on waterline melting of the ice cliff. In contrast, for Hooker Glacier, the second model (based on the U_c-D_w relationship) predicts slower future retreat rates (between 30 and 40 m a^{-1} for water depths between 31 and 156 m) than the first scenario (45.5 m a^{-1}), which is based solely on waterline melting.

The relationship between U_c and D_w in Hooker Glacier does not appear to follow the trend at other glaciers worldwide (e.g. Funk & Röthlisberger, 1989; Warren *et al.*, 1995b). This trend is of increasing calving rates with increasing water depth. As water depths have increased at Hooker Glacier with progressive retreat, there has been no real trend, either positive or negative, in calving rates, reflected in the low r^2 value (0.03) from equation 6.2. One possible explanation for this is the way in which water depths at the terminus are estimated. When past terminus positions are overlaid on post-retreat lake bathymetry (e.g. Figure 6.3 overlain on Figure 6.6), it is simply assumed that the subaqueous terminal ice cliff is vertical. Therefore the water depth, as read off the post-retreat bathymetry map, was the water depth adjacent to the terminus at that point in time. This assumption however, does not consider the presence of a subaqueous ice ramp extending from the terminus into the lake. A subaqueous ice ramp decreases the water depth at the terminus as the subaerial ice cliff does not extend vertically down to the bed of the valley, but instead to the ice ramp, which may extend from the terminus as little as 1 m below lake level. Thus, if an ice ramp is present, the water depth adjacent to the terminus, as read off the post-retreat bathymetry map, would be incorrect. An ice ramp extending 320 m from Hooker Glacier into Hooker Lake was identified in 2009 (Figure 6.6) (Chapter 4). The length of the ramp and calculated subaerial calving rates prior to 2009 (Table 6.1) indicate that the ramp had been present in the lake for at least a few years. Thus, water depths measured at the terminus positions in Figure 6.3 would be much deeper than the actual depth adjacent to the terminus at that time. The first retreat scenario overcomes this issue, and is perhaps more applicable to Hooker Glacier because of this, as it assumes that the effective water depth adjacent to the terminus remains constant, due to preservation of a subaqueous ice ramp (e.g. Kirkbride & Warren, 1999). There are still however, limitations to the application of both scenarios to Hooker Glacier.

It has been assumed in the predicted retreat scenarios that ice velocities will stay at the 2001-2002 rates, as there is currently no method for accurately predicting future velocities. This assumption, however, ignores the possibility that velocities may respond to calving, which has been termed the ‘master versus slave’ debate (Benn *et al.*, 2007b). According to the ‘calving as master’ side of the debate, ice velocities will increase up-glacier in response to calving losses at the terminus (Meier, 1997). The acceleration

causes the glacier to thin, which decreases effective basal pressure, and increases flow, producing a negative feedback on retreat rates (Meier, 1994). If ice velocities at Hooker Glacier increase as a result of calving losses, retreat rates may reduce, increasing the time it takes the glacier to retreat to the point where bedrock outcrops at current lake level, 4.8 km up-valley, and starts to separate from Hooker Lake.

An annual melt rate of the terminal ice cliff of 14 m a^{-1} was incorporated into both scenarios (Table 6.1), and is based on Röhl (2005), who measured melt rates at Tasman Glacier and then extrapolated these rates to Hooker Glacier, based on differences in altitude and climate. Röhl's (2005) estimated melt rate was however, considerably lower than the melt rate calculated by Hochstein *et al.* (1998) for Hooker Glacier, using the Russel-Head (1980) relationship. Hochstein *et al.* (1998) incorporated water temperature data and calculated a melt rate of 40 m a^{-1}. If this melt rate was incorporated into the scenarios, the calving rates (U_c + U_m) would be much faster than the values given in Table 6.1. For example, the calving rate between 2001 and 2011 would increase to 53 m a^{-1} from 27 m a^{-1}.

The topography of the valley floor up-glacier of the 2009 terminus will also influence calving retreat rates, with the subglacial long-profile topography (e.g. Hochstein *et al.*, 1998) unlikely to be as simple as that portrayed by the current data (Figure 6.8). Bedrock steps between the current terminus and 4.8 km up-valley would alter the potential water depth and, in turn, the second retreat scenario, which is based on water depth. In addition, the valley floor may actually be deeper than known depths at the two measured points (e.g. 3 and 4.8 km up-glacier), as is typical in alpine valley systems (MacGregor *et al.*, 2000). These bedrock overdeepenings would increase the predicted water depth in the lake which may impact the U_c-D_w relationship at Hooker Glacier. Based on this relationship, if water depths were deeper adjacent to the terminus, calving rates could be higher than those reported in Table 6.1. This would increase the rate the glacier retreated up-valley and result in the glacier reaching the point where bedrock outcrops at lake level sooner than predicted in Figure 6.8.

Although thick debris cover and a lack of high-resolution satellite images of Hooker Glacier make it difficult to examine crevasses on the glacier surface, the location, timing and magnitude of calving will be determined by these pre-existing weaknesses (Benn *et al.*, 2007b). A high concentration of crevasses in the terminal zone will encourage higher calving rates by providing weaknesses in the ice that can be exploited. If there are a low number of crevasses or crevasses do not penetrate the full thickness of the glacier (Benn *et al.*, 2007b), calving rates may be slower than those calculated. In addition, if the terminus of Hooker Glacier became buoyant, calving rates would likely increase, speeding up retreat of the glacier. Conditions for buoyancy could be met if thinning of the glacier caused the ice to become less than the ice thickness required for flotation. This would cause the terminus to up-warp and fail via calving at the up-glacier limit of buoyant ice, increasing retreat rates (e.g. Warren *et al.*, 2001). Although the thick cover of supraglacial debris adds mass to the terminus, further disintegration of this cover, similar to that seen in the late 1970s and early 1980s (e.g. Kirkbride, 1993; Hochstein *et al.*, 1998), could encourage melting of exposed ice and thus cause glacier thinning. Increased ice velocities, in response to calving, could also encourage glacier thinning (Meier, 1994; 1997).

6.8 Conclusions

Calving retreat rates of Hooker Glacier between the late 1970s and 2011 have varied between 2 m a^{-1} to 135 m a^{-1}, with a significant increase caused by the coalescence of a single proglacial lake occurring after 1982. Retreat rates calculated here differ from those presented by Hochstein *et al.* (1998) due to variations in ice velocity and melt rates used in each study. Although, retreat rates at Hooker Glacier are considerably lower than those at Tasman Glacier, both glaciers had an increase in calving rates between 2006 and 2008 when glacier velocity and ice melt were considered. Two potential retreat scenarios have been presented for Hooker Glacier based on currently available data. A slow-retreat scenario (based on the U_c-D_w relationship for Hooker Glacier) predicts that by 2096, Hooker Glacier will have retreated 4.8 km up-valley, where bedrock outcrops at the current lake level. The glacier will then begin to retreat away from Hooker Lake. A fast-retreat scenario, based on waterline melting, sees

Hooker Glacier stabilise when ice velocity equals calving rates which will occur when the glacier retreats more than 3 km up-valley from the Hooker Lake outlet after 2028. There are a myriad of factors however which may influence the future retreat of Hooker Glacier, including crevasses and glacier buoyancy, which cannot be incorporated into the presented scenarios. This is due primarily to a lack of data and inability to predict future crevasse propagation and buoyancy accurately. These scenarios differ to those presented for Tasman Glacier (Kirkbride & Warren, 1999; Dykes & Brook, 2010), which show that the U_c-D_w relationship predicts fast retreat, while calving rates driven by waterline melting predicts slow retreat of the glacier. Although there is no current theoretical model which fully accounts for calving rates at water-terminating glaciers (Benn *et al.*, 2007b), it appears that the application of the fast-retreat scenario (waterline melting) overcomes some of the difficulties associated with water depths at the terminus and accounts for the effect of an ice ramp extending from the terminus.

6.9 Acknowledgements

This work was funded by the Ryoichi Sasakawa Young Leaders Fellowship Fund (to CMR). We would like to thank the Department of Conservation for allowing field-based work and Rob Dykes, Jingjing Wang, Rob Eastham and David Feek for field assistance. Satellite images and aerial photographs were generously provided by Trevor Chinn, Stefan Winkler and Wolfgang Rack.

Chapter 7: Synthesis and Conclusions

7.1 Introduction

The potential impact that subaqueous mass loss may have on glacier mass balance and volume reduction is unclear, primarily due to a lack of quantitative data. Therefore, in order to fully understand the potential contribution subaqueous calving and melting may make to freshwater glacier mass loss, it is important to understand how subaqueous extensions of glacier fronts ("ice ramps") are created and maintained. The primary aim of the study was to improve the understanding of the controls on subaqueous ice ramp development and evolution at debris-covered, lake-calving margins. As subaqueous morphology and thus subaqueous mass loss appear to be closely linked to subaerial retreat it was crucial to analyse the evolution of subaqueous and subaerial margins concurrently. In order to do this, the study investigated the temporal evolution and subaqueous morphology of the termini of Mueller, Hooker, Tasman, Murchison, Classen, Grey, Maud and Godley glaciers in *Aoraki*/Mount Cook National Park. These eight glaciers provided an excellent opportunity to study the evolution of glaciers that are in close proximity to each other, yet represent different stages on the glacier retreat-proglacial lake development continuum.

Underpinning the aim of this study was the need to complete a comprehensive review of current literature of lake-calving glaciers (chapter 2). The review highlighted that many models fail to comprehensively incorporate mass loss from subaqueous ice ramps due to a paucity of quantitative data. It also highlighted that it is illusory to expect a universally applicable calving law to exist, given the myriad of factors influencing calving. No research to date had investigated subaqueous ice ramps, even though the potential for ice ramps to extend from glaciers had been suggested and the lack of data acknowledged. The review highlighted that, due to the feedback between the proglacial water body and glacier dynamics, and, glacier dynamics and calving, it was important to understand why and how subaqueous ice ramps develop and evolve. The review also highlighted the lack of up-to-date data available for debris-covered lake-calving glaciers in *Aoraki*/Mount Cook National Park.

To gain a better understanding of the lake-calving glaciers in *Aoraki*/Mount Cook National Park and how subaqueous ice ramps might affect glacial retreat, a comprehensive examination of terminus retreat and proglacial lake development since 1965, and the processes responsible for that retreat was imperative (objective 1, chapter 3). The investigation quantified retreat rates and lake surface areas over different timescales in Mueller and Murchison glaciers and lakes, where retreat had not been quantified before, and Hooker, Classen, Grey, Maud and Godley glaciers and lakes, where retreat calculations were updated and extended. A four-stage temporal and spatial evolutionary model of the glaciers and proglacial lakes in the Park was identified. Stage one involved the appearance and growth of supraglacial lakes and/or meltwater channels, which then transition to a single coalesced lake (stage two). Stage three represented stable expansion of the single coalesced lake with stage four characterised by a decrease in retreat rates as the valley's bedrock profile comes close to lake level as glacier retreat proceeds up-valley. Based on this four-stage evolutionary model, retreat rates and proglacial lake growth trends, Mueller, Hooker and Murchison glaciers were found to be in stage three, while Classen, Godley, Grey and Maud glaciers were approaching or entering stage four.

To gain a better understanding of the subaqueous environment and ice ramps, the subaqueous termini of Mueller, Hooker and Tasman glaciers were examined in greater detail (chapter 4). The three glaciers provided an excellent opportunity to examine subaqueous morphologies of glaciers that are within the same stage of glacier retreat and proglacial lake expansion (chapter 3) within a single mountain belt. The objective of mapping and comparing the subaqueous termini of the glaciers was to identify key characteristics of each subaqueous margin, and to determine what processes control the development and evolution of the subaqueous termini (objective 2 and 3). The difference between subaerial retreat and subaqueous retreat was identified as a key control in the initial development and the ice ramp extent maintenance. In order to maintain a 'steady-state' situation in ice ramp extent, subaerial retreat needed to be matched by retreat of the subaqueous ice ramp. Debris cover on the ice ramp was also a controlling factor, by greatly reducing melting and therefore thinning which, in turn, decreased buoyant forces acting to break up the ramps. Debris cover on an ice ramp enabled the ramps to remain intact hundreds of metres (>510 m) in front of the

terminus. This research found that these ice ramps evolve over time as variables of glacier dynamics and water-body properties change and influence subaerial retreat and therefore it cannot be assumed that if an ice ramp does not exist at a particular time, that the glacier is unable to support such a feature.

Although chapter 4 identified a number of key controls on the development and evolution of subaqueous termini. Mueller Glacier was studied over a 16 month period (chapter 5) to examine the temporal evolution of both the subaerial and subaqueous sections of the terminus and to identify the key controls for the observed changes (objective 4). The study found the development and maintenance of the extent of subaqueous ice ramps is intrinsically linked with the retreat of the subaerial section, as subaerial retreat drives subaqueous retreat. Retreat of the subaerial section of these glaciers allows buoyant forces to act on subaqueous ice ramps, which may result in subaqueous calving. Changes in the subaqueous morphology of debris-covered, lake-calving glaciers are controlled by a combination of subaerial retreat and subsequent subaqueous calving, along with sedimentation. Subaqueous melting at debris-covered glaciers is also minimal due to the effect of debris cover. Horizontal and vertical displacements of these glaciers may also not be directly connected to precipitation and lake level fluctuations but have the potential to be driven by the terminus approaching flotation thickness. These findings contribute to the 'master versus slave' debate as subaqueous retreat is driven by subaerial retreat which may influence, or respond to, glacier dynamics. Retreat or disintegration of a subaqueous ice ramp, driven by subaerial retreat, may cause a change in the basal conditions and potentially subglacial drainage systems, which may influence ice velocities.

In Chapter 6, conceptual models of future glacier retreat were presented for Hooker Glacier based on extending the retreat rate and proglacial lake growth calculations from chapter 3, and subaqueous terminal morphology data from 2009 presented in chapter 4. Chapter 6 built on these previous chapters by applying retreat scenarios that considered how subaqueous morphologies influenced subaerial retreat and vice-versa. A slow-retreat scenario (based on the U_c-D_w relationship) predicted that Hooker Glacier will retreat 4.8 km up-valley, and away from Hooker Lake by 2096. A fast-retreat scenario (based on waterline melting) predicted that Hooker Glacier will stabilise more than 3

km up-valley from the Hooker Lake outlet after 2028. A number of other factors were also identified that may influence the future retreat of Hooker Glacier, including crevasses and glacier buoyancy (objective 5). Retreat predictions varied depending on the data that were input into the scenario and it was vital to incorporate valley topography data into the retreat scenarios in order to increase the accuracy of the predicted future extent of the glacier. A retreat scenario based on waterline melting appeared to overcome issues associated with the use of water depth in calculations by accounting for a subaqueous ice ramp extending from the terminus.

This study has found that glacier retreat and concurrent proglacial lake expansion can vary significantly within a single mountain belt, and therefore cannot be solely attributed to climate-forcing. In order to understand what controls glacier retreat however, it is vital to understand the subaqueous morphology of glaciers, how these evolve over time and what controls this evolution. It has been found that the evolution of subaqueous ice ramps is intrinsically linked to subaerial retreat as subaerial retreat increases buoyant forces acting on an ice ramp leading to subaqueous calving. It has been found, for the first time, that temporal changes in subaqueous morphology are driven by subaerial calving, subsequent subaqueous calving, and sedimentation. The study has provided the first detailed data set on subaqueous ice ramps extending from glaciers anywhere in the world. This contribution has significantly increased the quantitative data available on subaqueous morphologies and how these are affected by subaerial retreat. Therefore, due to the connection between subaqueous ice ramps and subaerial retreat, retreat predictions must consider subaqueous morphologies in order to more accurately predict glacier retreat and mass loss from a glacier. Subaqueous morphologies appear to be best addressed in retreat predictions through the incorporation of quantitative subaqueous morphology data and waterline melt rates. The identification of subaqueous ice ramps extending from lake-calving glaciers in *Aoraki*/Mount Cook National Park, along with the examination of controls on ice ramp development and evolution is the first study of its kind. The study contributes significantly to the understanding of subaqueous morphologies, potential mass loss from these sections of the glacier and hence, glacier retreat. These subaqueous datasets, in addition to retreat rate and lake growth data lead to a better understanding of how subaqueous sections influence overall glacial retreat. The methods developed in this

study and the conclusions reached may also be broadly applicable to studies of other lake-calving glaciers around the world, although each glacier system must be understood as being unique, responding to a unique array of variables.

7.2 Avenues for future research

Research into calving glaciers over the past half century has primarily focused on subaerial calving. This focus has been on subaerial calving rates, types of subaerial calving, the forcing behind the rapid increase in mass loss from calving termini, and whether the mass loss will continue in the near future and, if so, at what rate. This research has been driven by the need to improve our understanding of how mass loss at these glaciers will impact society through sea level rise, water availability, and natural hazards. Calving glacier research is now benefitting from improvements in data collection and interpretation methods such as the availability of satellite images, the frequency of which these are taken and increases in the resolution of such imagery. The development of sub-bottom sonar, ground/ice-penetrating radar (GPR) (e.g. Hoch *et al.*, 2011) and remotely operated vehicles (ROV) (e.g. Cadena, 2011), have also increased the range of possible research. Nevertheless, research at calving glaciers remains extremely hazardous due to the unpredictable nature of calving events. More recently, research at calving glaciers has focused on the following: subaqueous melt rates (Xu *et al.*, 2011); the seismicity of calving (Veitch & Nettles, 2011; Dykes *et al.*, 2012); how glaciers are, and may continue to, respond to climate change (Hart *et al.*, 2011; Post *et al.*, 2011; Radić & Hock, 2011; Scherler & Strecker, 2011; Jacob *et al.*, 2012; Nick *et al.*, 2012); interactions between glaciers and proglacial lakes (Tsutaki *et al.*, 2012); the conditions which supraglacial lakes form under (Salerno *et al.*, 2012); and assessing techniques to examine glaciers (Gjermundsen *et al.*, 2011; Heid & Kääb, 2011).

The outcomes of this study have provided important observations of subaqueous morphology development and evolution and how these sections of the glacier may influence glacier retreat at debris-covered, lake-calving glaciers. However, it is recognised that this work is only a step along the way to fully understanding the

processes that operate to develop and alter subaqueous ice ramps and how these ice ramps influence overall glacier retreat. Hence, there remain many aspects that would benefit from further, focused study. Exploring the following avenues of future research would contribute to the studies currently being undertaken into calving glaciers and in particular how subaqueous sections of glaciers will contribute to retreat and mass loss in the future. Further research will also led to a more comprehensive understanding of the processes that control subaqueous morphologies over different timescales, subaqueous morphology development and evolution in other glacial regions, as well as the future retreat of debris-covered, lake-calving glaciers in *Aoraki*/Mount Cook National Park.

1. Detailed studies of the development and evolution of subaqueous ice ramps at a number of glaciers over an extended period of time. These studies need to include measurements of calving, lake level, temperature, precipitation inputs, glacier velocity, buoyancy and debris cover. Central to this research is the need to record subaqueous and subaerial calving events concurrently to quantify mass loss and the frequency of these events. High resolution, high frequency photography and video, captured from multiple viewpoints, could be used to record calving events. Field-based measurements would also be important to quantify the size of the calving events and to aid volumetric estimates. Side-scan sonar (e.g. Turner *et al.*, 2012) would be an ideal technique for 'viewing' the subaqueous section of the glacier and changes in this area following subaqueous calving in conjunction with high resolution bathymetric and sub-bottom surveys to identify where icebergs had originated from. Airborne GPR surveys may also allow data to be collected without researchers entering the highly hazardous 'calving zone'. Airborne GPR has been used in other glaciated regions (Machguth *et al.*, 2006; Kim *et al.*, 2010); however, the effectiveness of this method to collect data 'through a water body' would need to be tested against lake-based methods (e.g. sub-bottom sonar). High resolution measurements of ice ramps and associated variables over long timespans (years) will allow for a better understanding of what variables control ramp evolution and final disintegration.

2. Subaqueous melt rates remain poorly defined in glaci-lacustrine environments. Subaqueous melting remains the most difficult process to investigate due to access issues, the lack of a suitable measurement technique, debris cover and the hazardous nature of the lake above subaqueous ice (due to subaqueous calving). Quantifying melting of subaqueous margins however, remains an important component in understanding subaqueous ice ramps, as quantifying mass loss via subaqueous melting will allow measured changes in lake bathymetry to be more accurately assigned to subaqueous calving or melting. Rignot *et al.* (2010) and Xu *et al*. (2012) have gone some way to quantifying subaqueous melt rates at tidewater glaciers in Greenland by measuring ocean currents, temperatures and salinity and applying numerical models. Similar techniques could be applied to freshwater, lake-terminating glaciers. Another technique that could be tested is the placement of pressure sensors in subaqueous ice in proglacial lakes to measure sub-millimetre changes in the overlying thickness of ice. A system which incorporated this technique was used by Bøggild *et al.* (2004) to measure ice ablation on the surface of a glacier in inaccessible locations. If debris cover is present this would need to be removed prior to the placement of sensors but could then be replaced to enable measurements of melt under debris. A ROV could assist with the removal of debris and the placement of the sensors. Similar techniques could be applied to the subaerial ice cliff, if a small section of the cliff descended vertically under the lake level.

3. The uncertainty of the physical nature and location of pre-existing weaknesses in a glacier is a constraining factor when predicting future glacier retreat. Crevasses and englacial debris bands have been identified as important components in glacier retreat as they act as pre-existing weaknesses, which can be exploited, resulting in calving. A crevasse-depth calving criterion (developed by Benn *et al.*, 2007b) partly addresses the role of crevasses in glacier retreat, however it has a number of short-falls including the overestimation of glacier length where second-order processes (subaqueous melting and force imbalances at the ice cliff) play a significant role in calving. Thus, there is still a need to consider quantitative data from the specific glacier when predicting future retreat. Shean and Marchant (2010) used a combination of seismic, GPR, direct-current resistivity and gravity surveys in

Antarctica to give independent but complementary datasets that significantly improved internal composition interpretation. GPR surveys could be completed from the air (with GPR antenna attached to a helicopter) as this allows vast amounts of data to be collected over short time period (when compared to a ground-based survey) and would also allow surveys to be completed in areas that are difficult to access on foot (e.g. Eisenburger *et al.*, 2009; Catapano *et al.*, 2012). Seismographs could also be deployed to record crevasse propagation within a glacier. Dalban Canassy *et al.* (2012) used seismographs on Triftgletscher, Switzerland to monitor crevasse propagation, although further work needs to be completed to overcome difficulties when differentiating between icefalls and fracture propagation. Further improvements could be made with the incorporation of precise data on the location and extent of crevasses and debris bands into retreat scenarios.

4. Geophysical data up-glacier of the current termini of Mueller, Hooker, Murchison, Classen, Grey, Maud and Godley glaciers. Valley long-profiles may also influence retreat rates (e.g. in the calving rate–water depth relationship) and thus the time it may take a glacier to retreat to the bedrock outcrop. One study has collected glacier thickness measurements on Hooker Glacier (e.g. Hochstein *et al.*, 1998), however these data are very limited (e.g. 3 and 4.8 km up-valley of the lake outlet). In order to accurately predict potential future retreat of the glaciers, data of glacier thicknesses and bedrock profiles under the glaciers are needed. Work is currently being completed which incorporates ice thickness modelling in the central Southern Alps (Anderson & Mackintosh, 2012). However field-based work is also required to collect high-resolution subglacial bedrock profiles. Airborne GPR surveys would overcome access difficulties on these debris-covered glaciers, although difficulties with using GPS in the narrow sky-view valleys would need to be overcome. A combination of seismic, GPR, direct-current resistivity and gravity surveys could also be applied. These data would assist in determining the nature of the valley floor under the glaciers and enable predictions to be made as to how far the glacier may retreat before the lake level is at the same elevation as the bedrock.

5. Bathymetric data of Murchison, Classen, Grey/Maud and Godley proglacial lakes. Murchison Lake has never been surveyed and so no bathymetric data are available. Bathymetric data from Classen, Grey/Maud and Godley lakes, collected in the mid-1990s is now out-of-date due to the significant (> 1 km) retreat of these glaciers since that time. Bathymetric data are needed to examine the current subaqueous terminal morphologies of these glaciers and to compare these to the morphology in the mid-1990s. This comparison will increase the understanding of how and why subaqueous morphologies, and in particular ice ramps, evolve over time. Bathymetric data will also improve predicted retreat scenarios, particularly when the calving rate–water depth relationship is applied. Application of a real-time dynamic mapping engine integrating GPS, echo-sounding and swath data would enable high-resolution 3-dimensional maps to be created in real-time. Real-time analysis of data would ensure that areas of interest were adequately surveyed. Classification of subaqueous debris could also be made from this data. Remote sensing methods such as air-borne laser scanning (e.g. Gao, 2011) are not suitable due to the high turbidity and suspended sediment concentration in proglacial lakes.

7.3 Concluding remarks

This study identified and described subaqueous ice ramps extending from debris-covered, lake-calving glaciers in *Aoraki*/Mount Cook National Park, and discussed the controls on ice ramp development and evolution. The study has made a significant contribution to our understanding of how subaqueous extensions of calving glacier termini are created and evolve and how subaqueous sections of glaciers are connected to glacier retreat, and therefore volume reduction of glaciers. It has also made a significant contribution to the quantitative dataset available on subaqueous morphologies.

Additional research on subaqueous ice ramps at other calving termini, how these evolve over time, and interact with other glaciological processes such as basal sliding, will further enhance our understanding of the processes that control their development. The quantification of subaqueous melt also remains elusive. Retreat predictions that

incorporate subaqueous ice ramps could be further enhanced with the incorporation of data on glacier structures, such as pre-existing weaknesses, and predictions for glaciers in *Aoraki*/Mount Cook National Park would be enhanced with up-to-date bathymetry and valley profile data.

Enhancing our knowledge of mass loss processes at calving glaciers will improve our understanding of how glaciers and ice caps may be affected by climate change in the future. Increasing this understanding will reduce uncertainty surrounding future sea level rise, water availability issues and natural hazards, which may affect the environments in which people live.

Chapter 8: References

Allen, S. K., Schneider, D., & Owens, I. (2009). First approaches towards modelling glacial hazards in the Mount Cook region of New Zealand's Southern Alps. *Natural Hazards and Earth System Sciences, 9*(2), 481-499.

Alley, R. B. (1991). Sedimentary processes may cause fluctuations of tidewater glaciers. *Annals of Glaciology, 15*, 119-124.

Alley, R. B., Dupont, T. K., Parizek, B. R., & Anandakrishnan, S. (2005). Access of surface meltwater to beds of sub-freezing glaciers: preliminary insights. *Annals of Glaciology, 40*, 8-14.

Alley, R. B., Horgan, H. J., Joughin, I., Cuffey, K. M., Dupont, T. K., Parizek, B. R., Anandakrishnan, S., & Bassis, J. (2008). A simple law for ice-shelf calving. *Science, 322*(5906), 1344 (doi: 1310.1126/science.1162543).

Anderson, B., Lawson, W., Owens, I., & Goodsell, B. (2006). Past and future mass balance of Ka Roimata o Hine Hukatere (Franz Josef Glacier). *Journal of Glaciology, 52*(179), 597-607.

Anderson, B., & Mackintosh, A. (2012). Controls on mass balance sensitivity of maritime glaciers in the Southern Alps, New Zealand: The role of debris cover. *Journal of Geophysical Research, 117*(F1).

Anderton, P. W. (1975). Tasman Glacier 1971-73 *Hydrological Research: Annual Report No. 33*. Wellington, New Zealand: Ministry of Works and Development, National Water and Soil Conservation Organisation.

Ashley, G. M. (1995). Glaciolacustrine environments. In J. Menzies (Ed.), *Modern and past glacial environments*. London: Butterworth-Heinemann.

Barry, R. G. (2006). The status of research on glaciers and global glacier recession: a review. *Progress in Physical Geography, 30*(3), 285-306.

Bartholomew, I., Nienow, P., Sole, A., Mair, D., Cowton, T., & King, M. A. (2012). Short-term variability in Greenland Ice Sheet motion forced by time-varying meltwater drainage: Implications for the relationship between subglacial drainage system behavior and ice velocity. *Journal of Geophysical Research, 117*(F3).

Bassis, J. N. (2011). The statistical physics of iceberg calving and the emergence of universal calving laws. *Journal of Glaciology, 57*(201), 3-16.

Beletsky, D., Hawley, N., Rao, Y. R., Vanderploeg, H. A., Beletsky, R., Schwab, D. J., & Ruberg, S. A. (2012). Summer thermal structure and anticyclonic circulation of Lake Erie. *Geophysical Research Letters, 39*(L06605).

Benn, D. I., Hulton, N. R. J., & Mottram, R. H. (2007a). 'Calving laws', 'sliding laws' and the stability of tidewater glaciers. *Annals of Glaciology, 46*(1), 123-130.

Benn, D. I., Warren, C. R., & Mottram, R. H. (2007b). Calving processes and the dynamics of calving glaciers. *Earth-Science Reviews, 82*(3-4), 143-179.

Benn, D. I., Wiseman, S., & Hands, K. A. (2001). Growth and drainage of supraglacial lakes on debris-mantled Ngozumpa Glacier, Khumbu Himal, Nepal. *Journal of Glaciology, 47*(159), 626-638.

Benn, D. I., Wiseman, S., & Warren, C. R. (2000). Rapid growth of a supraglacial lake, Ngozumpa Glacier, Khumbu Himal, Nepal *Debris Covered Glaciers (Proceedings of a workshop held at Seattle, Washington, USA, September 2000)* (pp. 288): IAHS Publ. no 264.

Bindschadler, R. (1980). The predicted behaviour of Griesgletscher and its possible threat to a nearby dam. *Zeitschrift fuer Gletscherkunde und Glazialgeologie, 16*, 45-59.

Bindschadler, R., & Rasmussen, L. A. (1983). Finite difference model predictions of the drastic retreat of Columbia Glacier, Alaska. *United States Geological Survey Professional Paper 1258-D*.

Bindschadler, R. A. (1983a). The importance of pressurized subglacial water in separation and sliding at the glacier bed. *Journal of Glaciology, 29*(101), 3-19.

Bindschadler, R. A. (1983b). The predicted behaviour of Griesgletscher, Wallis, Switzerland, and its possible threat to a nearby dam. *Annals of Glaciology, 4*, 295.

Björnsson, H., Pálsson, F., & Gudmundsson, S. (2001). Jökulsárlón at Breidamerkursandur, Vatnajökull, Iceland: 20th century changes and future outlook. *Jökull, 50*, 1-18.

Black Laser Learning (2006). *Not in the manual guide to subbottom profiler surveys*: Black Laser Learning.

Blair, R. W. J. (1994). Moraine and Valley Wall Collapse due to Rapid Deglaciation in Mount Cook National Park, New Zealand. *Mountain Research and Development, 14*(4), 347-358.

Bøggild, C. E., Olesen, O. B., Ahlstrøm, A. P., & Jørgensen, P. (2004). Automatic glacier ablation measurements using pressure transducers. *Journal of Glaciology, 50*, 303-304.

Boyce, E. S., Motyka, R. J., & Truffer, M. (2007). Flotation and retreat of a lake-calving terminus, Mendenhall Glacier, Southeast Alaska, USA. *Journal of Glaciology, 53*(181), 211-224.

Brazier, V., Owens, I. F., Soons, J. M., & Sturman, A. (1992). Report on the Franz Josef Glacier. *Zeitschrift für Geomorphologie Supplementband, 86*, 35-49.

Bronge, C. (1999). Hydrology of Tierney Creek, Vestfold Hills, Antarctica. *Polar Record, 35*, 139-148.

Brown, C. S., Meier, M. F., & Post, A. (1982). Calving speed of Alaska tidewater glaciers, with application to Columbia Glacier. *U.S. Geological Survey Professional Paper, 1258-C*.

Brown, J., Harper, J., & Humphrey, N. (2010). Cirque glacier sensitivity to 21st century warming: Sperry Glacier, Rocky Mountains, USA. *Global and Planetary Change, 74*(2), 91-98.

Brunt, K. M., Okal, E. A., & MacAyeal, D. R. (2011). Antarctic ice-shelf calving triggered by the Honshu (Japan) earthquake and tsunami, March 2011. *Journal of Glaciology, 57*(205), 785-788.

Budd, W. F., Keage, P. I., & Blundy, N. A. (1979). Empirical studies of ice sliding. *Journal of Glaciology, 23*, 157-170.

Cadena, A. (2011). Design and implementation of cooperative autonomous underwater vehicles for Antarctic exploration. In W. W. Hou & R. Arnone (Eds.), *Ocean Sensing and Monitoring III* (Vol. 8030, pp. 80300F-80300F-80312): Proceedings of the SPIE.

Calmanti, S., Motta, L., Turcoc, M., & Provenzale, A. (2007). Impact of climate variability on Alpine glaciers in northwestern Italy. *International Journal of Climatology, 27*(15), 2041-2053.

Campbell, W. J. (1973). Structure and inferred circulation of South Cascade Lake, Washington, U.S.A. *International Association of Scientific Hydrology, publication 95*, 259-262.

Canassy, P. D., Bauder, A., Dost, M., Fah, R., Funk, M., Margreth, S., Muller, B., & Sugiyama, S. (2011). Hazard assessment investigations due to recent changes in Triftgletscher, Bernese Alps, Switzerland. *Natural Hazards and Earth System Sciences, 11*(8), 2149-2162.

Carbonell, M., & Bauer, A. (1968). Exploitation des couvertures photographiques aériennes répétées du front des glaciers vélant dans Disko Bugt et Umanak Fjord, juin-juillet 1964. *Meddeleser om Grønland, Kommissionen for widenskabelige Undersøgelser i Grønland, 173*(5).

Catapano, I., Crocco, L., Krellmann, Y., Triltzsch, G., & Soldovieri, F. (2012). A tomographic approach for helicopter-borne ground penetrating radar imaging. *IEEE Geoscience and Remote Sensing Letter, 9*(3), 378-382.

Chen, X., Shearer, P. M., Walter, F., & Fricker, H. A. (2011). Seventeen Antarctic seismic events detected by global surface waves and a possible link to calving events from satellite images. *Journal of Geophysical Research-Solid Earth, 116*, 16.

Chikita, K., Jha, J., & Yamada, T. (1999). Hydrodynamics of a supraglacial lake and its effect on the basin expansion: Tsho Rolpa, Rolwaling Valley, Nepal Himalaya. *Arctic, Antarctic, and Alpine Research, 31*(1), 58-70.

Chinn, T. J. H. (1996). New Zealand glacier responses to climate change of the past century. *New Zealand Journal of Geology and Geophysics, 39*, 415-428.

Chinn, T. J. H. (1999). New Zealand glacier response to climate change of the past 2 decades. *Global and Planetary Change, 22*, 155-168.

Chinn, T. J. H., Winkler, S., Salinger, J., & Haakensen, N. (2005). Recent glacier advances in Norway and New Zealand: A comparison of their glaciological and meteorological causes. *Geografiska Annaler, 87A*(1), 141-157.

Chinn, T. J. H., & Woods, A. D. H. (1984). *Hydrology and glaciology, Dry Valleys, Antarctica: annual for 1981-82* (Vol. Report WS 1017). Christchurch: Ministry of Works and Development.

Churski, Z. (1973). Hydrographic features on the proglacial area of Skeidarárjökull. *Geographia Polonica, 26*, 209-254.

Clague, J. J., & Evans, S. G. (2000). A review of catastrophic drainage of moraine-dammed lakes in British Columbia. *Quaternary Science Reviews, 19*, 1763-1783.

Clarke, G. K. C., Marshall, S. J., Hillaire-Marcel, C., Bilodeau, G., & Veiga-Pires, C. (1999). A glaciological perspective on Heinrich events. In P. U. Clark, R. S. Webb & L. D. Keigwin (Eds.), *Mechanisms of global climate change at Millennial time scales* (pp. 243-262): American Geophysical Union Monograph 112.

Cohen, D., Iverson, N. R., Hooyer, T. S., Fischer, U. H., Jackson, M., & Moore, P. L. (2005). Debris-bed friction of hard-bedded glaciers. *Journal of Geophysical Research, 110*(F2), F02007.

Cox, S. C., & Allen, S. K. (2009). Vampire rock avalanches of January 2008 and 2003, Southern Alps, New Zealand. *Landslides, 6*(2), 161-166.

Cox, S. C., & Barrell, D. J. A. (2007). *Geology of the Aoraki area. Institute of Geological and Nuclear Sciences 1:250 000 geological map 15. 1 sheet + 71 p.* Lower Hutt, New Zealand: GNS Science.

Cox, S. C., Ferris, B. G., & Allen, S. K. (2008). Vampire rock avalanches, Aoraki/Mount Cook National Park, New Zealand. *GNS Science Report, 2008/10*, 1-34.

Cuevas, J. G., Calvo, M., Little, C., Pino, M., & Dassori, P. (2010). Are diurnal fluctuations in streamflow real? *Journal of Hydrology and Hydromechanics, 58*(3), 149-162.

Cutler, P. M., Mickelson, D. M., Colgan, P. M., MacAyeal, D. R., & Parizek, B. R. (2001). Influence of the Great Lakes on the dynamics of the southern Laurentide ice sheet: numerical experiments. *Geology, 29*, 1039-1042.

Dalban Canassy, P., Faillettaz, J., Walter, F., & Huss, M. (2012). Seismic activity and surface motion of a steep temperate glacier: a study on Triftgletscher, Switzerland. *Journal of Glaciology, 58*(209), 513-528.

Derbyshire, E. (1974). The Bathymetry of Jökulsárlon, South-East Iceland. *The Geographical Journal, 140*(2), 269-274.

Diolaiuti, G., Citterio, M., Carnielli, T., D'Agata, C., Kirkbride, M. P., & Smiraglia, C. (2006). Rates, processes and morphology of freshwater calving at Miage Glacier (Italian Alps). *Hydrological Processes, 20*, 2233-2244.

Diolaiuti, G., D'Agata, C., Smiraglia, C., Kirkbride, M. P., Citterio, M., Benn, D. I., & Nicholson, L. (2009). Calving phenomena at the Miage Glacier (Mont Blanc). *News Bulletin of the International Glaciological Society, 151*(3), 24.

Diolaiuti, G., Kirkbride, M. P., Smiraglia, C., Benn, D. I., D'Agata, C., & Nicholson, L. (2005). Calving processes and lake evolution at Miage glacier, Mont Blanc, Italian Alps. *Annals of Glaciology, 40*, 207-214.

Dowdeswell, J. A., Hagen, J. O., Bjørnsson, H., Glazovsky, A. F., Harrison, W. D., Holmlund, P., Jania, J., Koerner, R. M., Lefauconnier, B., Ommanney, C. S. I., & Thomas, R. H. (1997). The mass balance of circum-Arctic glaciers and recent climate change. *Quaternary Research, 48*, 1-14.

Drewry, D. (1986). *Glacial Geologic Processes*. London, UK: Edward Arnold.

Duck, R. W., & Herbert, R. A. (2006). High-resolution shallow seismic identification of gas escape features in the sediments of Loch Tay, Scotland: tectonic and microbiological associations. *Sedimentology, 53*, 481-493.

Duck, R. W., & McManus, J. (1985). Short-term bathymetric changes in an ice-contact proglacial lake. *Norsk Geografisk Tidsskrift, 39*, 39-45.

Dykes, R., & Brook, M. (2010). Terminus recession, proglacial lake expansion and 21st century calving retreat of Tasman Glacier, New Zealand. *New Zealand Geographer, 66*, 203-217.

Dykes, R., Brook, M. S., & Winkler, S. (2010). The contemporary retreat of Tasman Glacier, Southern Alps, New Zealand, and the evolution of Tasman proglacial lake since AD 2000. *Erdkunde, 64*(2), 141-154.

Dykes, R., Lube, G., & Brook, M. (2012). Coseismic initiated calving at a freshwater-terminating glacier: Tasman Glacier, New Zealand. *Geophysical Research Abstracts, 14*(EGU2012-6884).

Dykes, R. C., Brook, M. S., Robertson, C. M., & Fuller, I. C. (2011). Twenty-first century calving retreat of Tasman Glacier, Southern Alps, New Zealand. *Arctic, Antarctic and Alpine Research, 43*(1), 1-10.

EdgeTech (2005). *Discover sub-bottom profiler processor software, technical and user's manual, Revision 2.2*. Massachusetts: EdgeTech.

Eijpen, K. J., Warren, C. R., & Benn, D. I. (2003). Subaqueous melt rates at calving termini: a laboratory approach. *Annals of Glaciology, 36*, 179-183.

Eisenburger, D., Lentz, H., & Jenett, M. (2009). *Helicopter-borne GPR systems: A way from ice thickness measurements to geological applications.* Paper presented at the IEEE International Conference on Ultra-Wideband (ICUWB2008), Vol 3, 10-12 Sept, 2008.

Elsberg, D., Zirnheld, S., Echelmeyer, K., Trabant, D., & Krimmel, R. (2003). The slow advance of a tidewater glacier: Hubbard Glacier, Alaska. *Annals of Glaciology, 36*, 45-50.

Engel, Z., Sobr, M., & Yerokhin, S. A. (2012). Changes of Petrov glacier and its proglacial lake in the Akshiirak massif, central Tien Shan, since 1977. *Journal of Glaciology, 58*(208), 388-398.

Evans, H. E. (1984). *Mechanisms of Creep Failure*. Amsterdam: Elsevier.

Fastook, J. L., & Schmidt, W. F. (1982). Finite element analysis of calving from ice fronts. *Annals of Glaciology, 3*, 103-106.

Fischer, M. P., Alley, R. B., & Engelder, T. (1995). Fracture toughness of ice and firn determined from the modified ring test. *Journal of Glaciology, 41*, 383-394.

Fischer, M. P., & Powell, R. D. (1998). A simple model for the influence of push-moraine banks on the calving and stability of glacial tidewater termini. *Journal of Glaciology, 44*, 31-41.

Fitzharris, B., Lawson, W., & Owens, I. (1999). Research on glaciers and snow in New Zealand. *Progress in Physical Geography, 23*(4), 469-500.

Fleisher, P. J., Franz, J. M., & Gardner, J. A. (1993). Bathymetry and sedimentary environments in proglacial lakes at the Eastern Bering Piedmont Glacier of Alaska. *Journal of Geological Education, 41*, 267-274.

Funk, M., & Röthlisberger, H. (1989). Forecasting the effects of a planned reservoir which will partially flood the tongue of Unteraargletscher in Switzerland. *Annals of Glaciology, 13*.

Gao, J. (2011). Lasar scanning applications in fluvial studies. *Progress in Physical Geography, 35*, 782-809.

Garmin Ltd (2007). *Owner's Manual eTrex HC series*. Kansas, USA: Garmin International, Inc.

Gellatly, A. F. (1985). Historical Records of Glacier Fluctuations in Mt Cook National Park, New Zealand: A Century of Change. *The Geographical Journal, 151*(1), 86-99.

Gilbert, R. (1971). Observations on ice-dammed Summit Lake, British Columbia, Canada. *Journal of Glaciology, 10*(60), 351-356.

Gilbert, R., & Desloges, J. R. (1987). Sediments of ice-dammed, self draining Ape Lake, British Columbia. *Canadian Journal of Earth Sciences, 24*(9), 1735-1747.

Gilbert, R., & Lamoureux, S. (2004). Processes affecting deposition of sediment in a small, morphologically complex lake. *Journal of Paleolimnology, 31*(1), 37-48.

Gilbert, R., & Shaw, J. (1981). Sedimentation in proglacial Sunwapta Lake, Alberta. *Canadian Journal of Earth Sciences, 18*(1), 81-93.

Gjermundsen, E. F., Mathieu, R., Kääb, A., Chinn, T. J. H., Fitzharris, B., & Hagen, J. O. (2011). Assessment of multispectral glacier mapping methods and derivation of glacier area changes, 1978-2002, in the central Southern Alps, New Zealand, from ASTER satellite data, field survey and existing inventory data. *Journal of Glaciology, 57*(204), 667-683.

Glasser, N. F., Harrison, S., Jansson, K. N., Anderson, K., & Cowley, A. (2011). Global sea-level contribution from the Patagonian Icefields since the Little Ice Age maximum. *Nature Geoscience, 4*, 303-307.

Goldthwait, R. P., McKellar, I., & Cronk, C. (1963). Fluctuations of Crillon Glacier system, southeast Alaska. *International Association of Scientific Hydrologists Bulletin, 8*, 62-74.

Granshaw, F. D., & Fountain, A. G. (2006). Glacier change (1958-1998) in the North Cascades National Park Complex, Washington, USA. *Journal of Glaciology, 52*(177), 251-256.

Griffiths, G. A. (1981). Some suspended sediment yields from South Island catchments, New Zealand. *JAWRA Journal of the American Water Resources Association, 17*(4), 662-671.

Griffiths, G. A., & McSaveney, M. J. (1983). Distribution of mean annual precipitation across some steepland regions of New Zealand. *New Zealand Journal of Science, 26*, 197-209.

Gustavson, T. C. (1975a). Bathymetry and Sediment Distribution in Proglacial Malaspina Lake, Alaska. *Journal of Sedimentary Petrology, 45*(2), 450-461.

Gustavson, T. C. (1975b). Sedimentation and physical limnology in proglacial Malaspina Lake, southeastern Alaska. In A. V. Jopling & B. C. McDonald (Eds.), *Glaciofluvial and Glaciolacustrine* (pp. 249-273). Tulsa, Oklahoma, USA: Society of Economic Paleontologists and Mineralogists, Special Publication No. 23.

Haeberli, W. (1977). Experience with glacier calving and air-bubbling in high alpine water reservoirs. *Journal of Glaciology, 19*(81), 589-594.

Haeberli, W., Kääb, A., Mühll, D. V., & Teysseire, P. (2001). Prevention of outburst floods from periglacial lakes at Grubengletscher, Valais, Swiss Alps. *Journal of Glaciology, 47*, 111-122.

Haeberli, W., & Roethlisberger, H. (1976). Beobahtungen zum Mechanismus und zu den Auswirkungen von Kalbungen am Grubengletscher (Saastal, Schweiz). *Zeitschrift fuer Gletscherkunde und Glazialgeologie, 11*, 221-228.

Hagen, J. O., Melvold, K., Pinglot, F., & Dowdeswell, J. A. (2003). On the net mass balance of the glaciers and ice caps in Svalbard, Norwegian Arctic. *Arctic, Antarctica and Alpine Research, 35*(2), 264-270.

Hambrey, M. J., & Ehrmann, W. (2004). Modification of sediment characteristics during glacial transport in high-alpine catchments: Mount Cook area, New Zealand. *Boreas: An International Journal of Quaternary Research, 33*(4), 300-318.

Hambrey, M. J., & Muller, F. (1978). Structures and Ice deformation in the White Glacier, Axel Heiberg Island, North West Territories, Canada. *Journal of Glaciology, 20*, 41-66.

Hambrey, M. J., Quincey, D. J., Glasser, N. F., Reynolds, J. M., Richardson, S. D., & Clemmens, S. (2008). Sedimentological, geomorphological and dynamic context of debris-mantled glaciers, Mount Everest (Sagarmatha) region, Nepal. *Quaternary Science Reviews, 27*(25-26), 2361-2389.

Hanson, B., & Hooke, R. L. (2000). Glacier calving: a numerical model of forces in the calving-speed/water-depth relation. *Journal of Glaciology, 46*(153), 188-196.

Haresign, E. C. (2004). *Glacio-limnological interactions at lake-calving glaciers.* Unpublished PhD thesis, University of St Andrews, St Andrews.

Haresign, E. C., & Warren, C. R. (2005). Melt rates at calving termini: a study at Glaciar Léon, Chilean Patagonia. In C. Harris & J. B. Murton (Eds.), *Cryospheric Systems: Glaciers and Permafrost* (Vol. 242, pp. 99-110). London: Geological Society Special Publication.

Harris, P. W. V. (1976). The seasonal temperature-salinity structure of a glacial lake: Jokulsarlon, South-East Iceland. *Geografiska Annaler, 58*(4), 329-336.

Harrison, S., Glasser, N. F., Winchester, V., Haresign, E., Warren, C. R., & Jansson, K. N. (2006). A glacial lake outburst flood associated with recent mountain glacier retreat, Patagonian Andes. *Holocene, 16*(4), 611-620.

Hart, J. K., Rose, K. C., Waller, R. I., Vaughan-Hirsch, D., & Martinez, K. (2011). Assessing the catastrophic break-up of Briksdalsbreen, Norway, associated with rapid climate change. *Journal of the Geological Society, 168*, 673-688.

Hay, J. E., & Fitzharris, B. (1988). The synoptic climatology of ablation on a New Zealand glacier. *International Journal of Climatology, 8*(2), 201-215.

Heid, T., & Kääb, A. (2011). *Evaluation of existing image matching methods for deriving glacier surface displacements globally from optical satellite imagery.* Paper presented at the Abstract C11D-0696 presented at 2011 Fall Meeting, AGU, San Francisco, California, 5-9 December.

Herman, F., Anderson, B., & Leprince, S. (2011). Mountain glacier velocity variation during a retreat/advance cycle quantified using sub pixel analysis of ASTER images. *Journal of Glaciology, 57*(202), 197-207.

Hessell, J. W. D. (1983). Climatic effects on the recession of the Franz Josef Glacier. *New Zealand Journal of Science, 26*, 315-320.

Hicks, D. M., McSaveney, M. J., & Chinn, T. J. H. (1990). Sedimentation in Proglacial Ivory Lake, Southern Alps, New Zealand. *Arctic and Alpine Research, 22*(1), 26-42.

Hindmarsh, R. C. A. (2012). An observationally validated theory of viscous flow dynamics at the ice-shelf calving front. *Journal of Glaciology, 58*(208), 375-387.

Hoch, A. M., Velez, J. A., Tsoflias, G. P., Stearns, L. A., & van der Veen, C. J. (2011). Multi-channel cooherent radar depth sounding of Jakobshavn Isbrae and its catchment. *IEEE National Radar Conference Proceedings*, 1135-1137.

Hochstein, M. P., Claridge, D., Henrys, S. A., Pyne, A., Leary, S. F., & Nobes, D. C. (1995). Downwasting of the Tasman Glacier, South Island, New Zealand: changes in the terminus region between 1971 and 1993. *New Zealand Journal of Geology and Geophysics, 38*, 1-16.

Hochstein, M. P., Watson, M. I., Nobes, D. C., & Owens, I. (1998). Rapid melting of the terminal section of the Hooker Glacier (Mt Cook National Park, New Zealand). *New Zealand Journal of Geology and Geophysics, 41*, 203-218.

Hoelzle, M., Chinn, T. J. H., Stumm, D., Paul, F., Zemp, M., & Haeberli, W. (2007). The application of glacier inventory data for estimating past climate change effects on mountain glaciers: A comparison between the European Alps and the Southern Alps of New Zealand. *Global and Planetary Change, 56*, 69-82.

Holdsworth, G. (1973). Ice calving into proglacial Generator Lake, Baffin Island, North West Territories, Canada. *Journal of Glaciology, 12*, 235-250.

Hooker, B. L., & Fitzharris, B. B. (1999). The correlation between climatic parameters and the retreat and advance of Franz Josef Glacier, New Zealand. *Global and Planetary Change, 22*(1-4), 39-48.

Howarth, P. J., & Price, R. J. (1969). The Proglacial Lakes of Breidamerkurjökull and Fjallsjökull, Iceland. *The Geographical Journal, 135*(4), 573-581.

Howat, I. M., Joughin, I., Tulaczyk, S., & Gogineni, S. (2005). Rapid retreat and acceleration of Helheim Glacier, east Greenland. *Geophysical Research Letters, 32*(22).

Hubbard, B., Heald, A., Reynolds, J. M., Quincey, D. J., Richardson, S. D., Luyo, M. Z., Portilla, N. S., & Hambrey, M. J. (2005). Impact of a rock avalanche on a

moraine-dammed proglacial lake: Laguna Safuna Alta, Cordillera Blanca, Peru. *Earth Surface Processes and Landforms, 30*, 1251-1264.

Huggel, C., Haeberli, W., Kääb, A., Bieri, D., & Richardson, S. D. (2004). An assessment procedure for glacial hazards in the Swiss Alps. *Canadian Geotechnical Journal, 41*, 1068-1083.

Huggel, C., Kääb, A., Haeberli, W., Teysseire, P., & Paul, F. (2002). Remote-sensing based assessment of hazards from glacier lake outbursts: a case study in the Swiss Alps. *Canadian Geotechnical Journal, 36*, 316-330.

Hughes, T. (1986). The Jakobshanvs effect. *Geophysical Research Letters, 13*(1), 46-48.

Hughes, T. (1992). Theoretical calving rates from glaciers along ice walls grounded in water of variable depths. *Journal of Glaciology, 38*(129), 282-294.

Hughes, T. (1996). Can Ice Sheets Trigger Abrupt Climatic Change? *Arctic and Alpine Research, 28*(4), 448-465.

Hughes, T. (1998). *Ice Sheets*. Oxford: Oxford University Press.

Hughes, T. (2002). Calving bays. *Quaternary Science Reviews, 21*(1-3), 267-282.

Hughes, T. J., & Nakagawa, M. (1989). Bending shear: the rate-controlling mechanism for calving ice walls. *Journal of Glaciology, 35*(120), 260-266.

Hulton, N. R., Purves, R. S., McCulloch, R. D., Sugden, D. E., & Bentley, M. J. (2002). The Last Glacial Maximum and deglaciation in southern South America. *Quaternary Science Reviews, 21*(1-3), 233-241.

Hunter, L. E., & Powell, R. D. (1998). Ice foot development at temperate tidewater margins in Alaska. *Geophysical Research Letters, 25*(11), 1923-1926.

Iken, A. (1977). Movement of a large ice mass before breaking off. *Journal of Glaciology, 19*(81), 595-605.

Iken, A. (1981). The effect of subglacial water pressure on the sliding velocity of a glacier in an idealised numerical model. *Journal of Glaciology, 27*(97), 407-421.

Iken, A., & Bindschadler, R. A. (1986). Combined measurements of subglacial water pressure and surface velocity of Findelengletscher, Switzerland: conclusions about drainage system and sliding mechanism. *Journal of Glaciology, 32*(110), 101-119.

Iken, A., & Truffer, M. (1997). The relationship between subglacial water pressure and velocity of Findelengletscher, Switzerland, during its advance and retreat. *Journal of Glaciology, 43*, 328-338.

Jacob, T., Wahr, J., Pfeffer, W. T., & Swenson, S. (2012). Recent contributions of glaciers and ice caps to sea level rise. *Nature, 482*, 514-518.

Jacobs, S. S., Helmer, H. H., Doake, C. S. M., Jenkins, A., & Frolich, R. M. (1992). Melting of ice shelves and the mass balance of Antarctica. *Journal of Glaciology, 38*, 375-387.

Jakobsson, M. (1999). First high-resolution chirp sonar profiles from the central Arctic Ocean reveal erosion of Lomonosov Ridge sediments. *Marine Geology, 158*, 111-123.

Jania, J. (1986). Dynamics of the Spitsbergen tidewater glaciers fronts. *Geographia, Studia et dissertationes, 9*, 78-100.

Jenkins, A. (2011). Convection-driven melting near the grounding lines of ice shelves and tidewater glaciers. *Journal of Physical Oceanography, 41*(12), 2279-2294.

Jensen, J. R. (1997). *Remote sensing of the environment: an earth resource perspective*. Upper Saddle River, NJ: Pearson Prentice Hall.

Josberger, E. G. (1978). A laboratory and field study of iceberg deterioration. In A. A. Husseiny (Ed.), *Iceberg utilization* (pp. 245-264). Iowa, USA: Proceedings of

the First International Conference and Workshops on Iceberg Utilization, Iowa, USA, October 2-6 1977.

Joughin, I., Waleed, A., & Fahnestock, M. (2004). Large fluctuations in speed on Greenland's Jakobshavn Isbrae glacier. *Nature, 432*, 608-610.

Kääb, A., & Reichmuth, T. (2005). Advance mechanisms of rock glaciers. *Permafrost and Periglacial Processes, 16*(2), 187-193.

Kamb, B., Engelhardt, H., Fahnestock, M., Humphrey, N. F., Meier, M. F., & Stone, D. (1994). Mechanical and hydrologic basis for the rapid motion of a large tidewater glacier. *Journal of Geophysical Research, 99 (B8)*(15), 231-244.

Kehle, R. O. (1964). Deformation of the Ross Ice Shelf, Antarctica. *Geological Society of America Bulletin, 75*, 259-286.

Kehrl, L. M., Hawley, R. L., Powell, R. D., & Brigham-Grette, J. (2011). Glacimarine sedimentation processes at Kronebreen and Kongsvegen, Svalbard. *Journal of Glaciology, 57*(205), 841-847.

Kenneally, J. P., & Hughes, T. J. (2002). The calving constraints on inception of Quaternary ice sheets. *Quaternary International, 95-96*, 43-53.

Kenneally, J. P., & Hughes, T. J. (2006). Calving giant icebergs: old principles, new applications. *Antarctic Science, 18*(3), 409-419.

Kennett, M., Laumann, T., & Kjøllmoen, B. (1997). Predicted response of the calving glacier Svartisheibreen, Norway, and outbursts from it, to future changes in climate and lake level. *Annals of Glaciology, 24*, 16-20.

Kershaw, J. A., Clague, J. J., & Evans, S. G. (2005). Geomorphic and sedimentological signature of a two-phase outburst flood from moraine-dammed Queens Bess Lake, British Columbia. *Earth Surface Processes and Landforms, 30*, 1-25.

Kim, K. Y., Lee, J., Hong, M. H., Hong, J. K., & Shon, H. (2010). Helicopter-borne and ground-towed radar surveys of the Fourcade Glacier on King George Island, Antarctica. *Exploration Geophysics, 41*(1), 51-60.

Kirkbride, M. P. (1993). The temporal significance of transitions from melting to calving termini at glaciers in the central Southern Alps of New Zealand. *The Holocene, 3*(3), 232-240.

Kirkbride, M. P., & Warren, C. R. (1997). Calving processes at a grounded ice cliff. *Annals of Glaciology, 24*, 116-121.

Kirkbride, M. P., & Warren, C. R. (1999). Tasman Glacier, New Zealand: 20th-century thinning and predicted calving retreat. *Global and Planetary Change, 22*, 11-28.

Kohler, A., Chapuis, A., Nuth, C., Kohler, J., & Weidle, C. (2012). Autonomous detection of calving-related seismicity at Kronebreen, Svalbard. *Cryosphere, 6*(2), 393-406.

Komori, J. (2008). Recent expansions of glacial lakes in the Bhutan Himalayas. *Quaternary International, 184*, 177-186.

Lafferty, B., Quinn, R., & Breen, C. (2006). A side-scan sonar and high-resolution Chirp sub-bottom profile study of the natural and anthropogenic sedimentary record of Lower Lough Erne, northwestern Ireland. *Journal of Archaeological Science, 33*, 756-766.

Laumann, T., & Wold, B. (1992). Reactions of a calving glacier to large changes in water level. *Annals of Glaciology, 16*, 158-162.

Leonard, G. H., Wright, J. W., & Haskell, T. G. (2011). *Measurement of coastal sea ice vertical and horizontal displacements using a differential GPS and total station measurement array.* Paper presented at the Snow and Ice Research Group (NZ) Annual Workshop, 9-11 February 2011, Fox Glacier Township.

Liverman, D. G. E. (1987). Sedimentation in ice-dammed Hazard Lake, Yukon. *Canadian Journal of Earth Sciences, 24*, 1797-1806.

MacGregor, K. R., Anderson, R. S., Anderson, S. P., & Waddington, E. D. (2000). Numerical simulations of glacial-valley longitundinal profile evolution. *Geology, 28*(77), 1031-1034.

Machguth, H., Eisen, O., Paul, F., & Hoelzle, M. (2006). Helicopter-borne snow profiling on alpine glaciers with GPR. *Geophysical Research Abstracts, 8*(07411).

Mangerud, J., Jakobsson, M., Alexanderson, H., Astakhov, V., Clarke, G. K., Henriksen, M., Hjort, C., Krinner, G., Lunkka, J. P., Moller, P., Murray, A., Nikolskaya, O., Saarnisto, M., & Svendsen, J. I. (2004). Ice-dammed lakes and rerouting of the drainage of northern Eurasia during the Last Glaciation. *Quaternary Science Reviews, 23*(11-13), 1313-1332.

Mann, D. H. (1986). Reliability of a fjord glacier's fluctuations for palaeoclimatic reconstructions. *Quaternary Research, 25*, 10-24.

Martin, S., Josberg, E., & Kaufmann, P. (1978). Wave-induced heat transfer to an iceberg. In A. A. Husseiny (Ed.), *Iceberg utilization* (pp. 260-263). New York: Pergamon Press.

Mattson, L. E., Gardner, J. S., & Young, G. J. (1993). Ablation on debris covered glaciers: an example from the Rakhiot Glacier, Punjab, Himalaya *Snow and Glacier Hydrology (Proceedings of the Kathmandu Symposium, November 1992)* (Vol. IAHS Publication no. 218, pp. 289-296).

McKillop, R. J., & Clague, J. J. (2006). A procedure for making objective preliminary assessments of outburst flood hazard from moraine-dammed lakes in southwestern British Columbia. *Natural Hazards, 41*(131-157).

McKillop, R. J., & Clague, J. J. (2007). Statistical, remote sensing-based approach for estimating the probability of catastrophic drainage from moraine-dammed lakes in southwestern British Columbia. *Global and Planetary Change, 56*, 153-171.

McSaveney, M. J. (2002). Recent rockfalls and rock avalanches in Mount Cook National Park, New Zealand. In S. G. Evans & J. DeGraff, V (Eds.), *Catastrophic landslides: effects, occurrence, and mechanisms* (illustrated ed.): Geological Society of America.

Meier, M. F. (1958). The mechanics of crevasse formation. *IAHS Publication 46*, 500-508.

Meier, M. F. (1994). Columbia Glacier during rapid retreat: interactions between glacier flow and iceberg calving dynamics. In N. Reeh (Ed.), *Workshop on the Calving Rate of West Greenland Glaciers in Response to Climate Change* (pp. 63-83). Copenhagen: Danish Polar Center Report.

Meier, M. F. (1997). The iceberg discharge process: observations and inferences drawn from the study of Columbia Glacier. In C. J. Van der Veen (Ed.), *Calving Glaciers: Report of a Workshop, February 28 - March 2, 1997* (pp. 109-114). Byrd Polar Research Centre Report No. 15: The Ohio State University, Columbus, Ohio.

Meier, M. F., & Post, A. (1987). Fast Tidewater Glaciers. *Journal of Geophysical Research, 92*(B9), 9051-9058.

Meier, M. F., Rasmussen, I. A., Krimmel, R. M., Olsen, R. W., & Frank, D. (1985). Photogrammetric determination of surface altitude, terminus position, and ice velocity of Columbia Glacier, Alaska. *U.S. Geological Survey Professional Paper, 1258-F*.

Mercer, J. H. (1961). The response of fjord glaciers to change in firn limit. *Journal of Glaciology, 10*, 850-858.

Mikesell, T. D., van Wijk, K., Haney, M. M., Bradford, J. H., Marshall, H. P., & Harper, J. T. (2012). Monitoring glacier surface seismicity in time and space using Rayleigh waves. *Journal of Geophysical Research, 117*(F2).

Motyka, R. J. (1997). Deep-water calving at Le Conte Glacier, Southeast Alaska. In C. J. van der Veen (Ed.), *Calving Glaciers: Report of a Workshop, Feb 28 March 2, 1997* (pp. 115-118). Columbus, Ohio: Byrd Polar Research Centre Report No. 15: The Ohio State University.

Motyka, R. J., Hunter, L., Echelmeyer, K. A., & Connor, C. (2003a). Submarine melting at the terminus of a temperate tidewater glacier, LeConte Glacier, Alaska, USA. *Annals of Glaciology, 36*, 57-65.

Motyka, R. J., O'Neel, S., Connor, C., & Echelmeyer, K. A. (2003b). Twentieth century thinning of Mendenhall Glacier, Alaska, and its relationship to climate, lake calving, and glacier run-off. *Global and Planetary Change, 35*, 93-112.

Motyka, R. J., O'Neel, S., Connor, C. L., & Echelmeyer, K. (2003c). Twentieth century thinning of Mendenhall Glacier, Alaska, and its relationship to climate, lake calving and glacier runoff. *Global and Planetary Change, 35*, 93-112.

Mullins, H. T., & Halfman, J. D. (2001). High-Resolution Seismic Reflection Evidence for Middle Holocene Environmental Change, Owasco Lake, New York. *Quaternary Research, 55*(3), 322-331.

Nansen, F. (1919). *The First Crossing of Greenland* (H. M. Gepp, Trans.). London: Longmans, Green and Co.

Naruse, R., & Skvarca, P. (2000). Dynamic features of thinning and retreating Glaciar Upsala, a lacustrine calving glacier in Southern Patagonia. *Arctic, Antarctic, and Alpine Research, 32*(4), 485-491.

Neshyba, S., & Josberger, E. G. (1980). On the estimation of Antarctic iceberg melt rate. *Journal of Physical Oceanography, 10*(10), 1681-1685.

Nick, F. M. (2006). *Modelling the behavior of tidewater glaciers.* Unpublished PhD thesis, University of Utrecht.

Nick, F. M., Luckman, A., Vieli, A., van der Veen, C. J., van As, D., van De Wal, R. S. W., Pattyn, F., Hubbard, A. L., & Floricioiu, D. (2012). The response of Petermann Glacier, Greenland, to large calving events, and its future stability in the context of atmospheric and oceanic warming. *Journal of Glaciology, 58*(208), 229-239.

Nick, F. M., & Oerlemans, J. (2006). Dynamics of tidewater glaciers: comparison of three models. *Journal of Glaciology, 52*, 183-190.

Nick, F. M., van der Veen, C. J., & Oerlemans, J. (2007). Controls on advance of tidewater glaciers: Results from numerical modelling applied to Columbia Glacier. *Journal of Geophysical Research, 112*.

Nixon, W. A., & Schulson, E. M. (1987). A micromechanical view of the fracture toughness of ice. *Journal de Physique, 48*, 313-319.

Nye, J. F. (1952). The mechanics of glacier flow. *Journal of Glaciology, 2*, 82-93.

Nye, J. F. (1957). The distribution of stress and velocity in glaciers and ice sheets. *Proceedings of the Royal Society of London, Series A 239*, 113-133.

O'Neel, S., Marshall, H. P., McNamara, D. E., & Pfeffer, W. T. (2007). Seismic detection and analysis of icequakes at Columbia Glacier, Alaska. *Journal of Geophysical Research-Earth Surface, 112*(F3), 14.

O'Neel, S., Pfeffer, W. T., Krimmel, R., & Meier, M. F. (2005). Evolving force balance at Columbia Glacier, Alaska, during its rapid retreat. *Journal of Geophysical Research, 110*(F03012).

Oerlemans, J. (2005). Extracting a climate signal from 169 glacier records. *Science, 308*, 675-677.

Østrem, G. (1959). Ice melting under a thin layer of moraine, and the existence of ice cores in moraine ridges. *Geografiska Annaler, 41*, 228-230.

Pantin, H. M., & Wright, I. C. (1994). Submarine hydrothermal activity within the offshore Taupo Volcanic Zone, Bay of Plenty continental shelf, New Zealand. *Continental Shelf Research, 14*, 1411-1438.

Paul, F. (2011). Sea-level rise: Melting glaciers and ice caps. *Nature Geoscience, 4*, 71-72.

Payne, A. J., Vieli, A., Shepherd, A. P., Wingham, D. J., & Rignot, E. (2004). Recent dramatic thinning of largest west Antarctic ice stream triggered by oceans. *Geophysical Research Letters, 31*.

Pelto, M. S., & Warren, C. R. (1991). Relationship between tidewater glacier calving velocity and water depth at the calving front. *Annals of Glaciology, 15*, 115-118.

Petrovic, J. J. (2003). Review Mechanical properties of ice and snow. *Journal of Materials Science, 38*(1), 1-6.

Pillewizer, W. (1965). Bewegungsstudien an einem arktischen Gletscher. *Polarforschung, Jahrg. 34, 1964, 5*(34), 247-253.

Popovnin, V. V., & Rozova, A. V. (2002). Influence of sub debris thawing on ablation and runoff of the Djankuat Glacier in the Caucasus. *Nordic Hydrology, 33*, 79-94.

Post, A. (1975). *Preliminary Hydrography and Historic Terminal Changes of Columbia Glacier, Alaska*: U.S.G.S Hydrologic Investigations Atlas HA-559.

Post, A., O'Neel, S., Motyka, R. J., & Streveler, G. (2011). A complex relationship between calving glaciers and climate. *EOS Transactions American Geophysical Union, 92*(37), 305.

Powell, R. D. (1983). Glacial-marine sedimentation processes and lithofacies of temperate tidewater glaciers, Glacier Bay, Alaska. In B. F. Molnia (Ed.), *Glacial Marine Sedimentation* (pp. 185-232). New York: Plenum Press.

Powell, R. D. (1991). Grounding-line systems as second-order controls on fluctuations of tidewater termini of temperate glaciers. In J. B. Anderson & G. M. Ashley (Eds.), *Glacial Marine Sedimentation; Paleoclimatic Significance* (pp. 75-93). Boulder, USA: Geological Society of America Special Paper 261.

Powell, R. D., & Molnia, B. F. (1989). Glacimarine sedimentary processes, facies and morphology of the south-southeast Alaska shelf and fjords. *Marine Geology, 85*, 359-390.

Pralong, A., & Funk, M. (2005). Dynamic damage model of crevasses opening and application to glacier calving. *Journal of Geophysical Research, 110*.

Pralong, A., Funk, M., & Lüthi, M. P. (2003). A description of crevasse formation using continuum damage mechanics. *Annals of Glaciology, 37*, 77-82.

Pritchard, H. D., & Vaughan, D. G. (2007). Widespread acceleration of tidewater glaciers on the Antarctic Peninsula. *Journal of Geophysical Research, 112*.

Purdie, H. L., Brook, M. S., & Fuller, I. C. (2008). Seasonal variation in ablation and surface velocity on a temperate maritime glacier: Fox Glacier, New Zealand. *Arctic, Antarctic and Alpine Research, 40*(1), 140-147.

Purdie, J. (1996). *Ice loss at the terminus of the Tasman Glacier*. Unpublished MSc thesis, University of Otago, Dunedin.

Purdie, J., & Fitzharris, B. (1999). Processes and rates of ice loss at the terminus of Tasman Glacier, New Zealand. *Global and Planetary Change, 22*(1-4), 79-91.

Quincey, D. J., & Glasser, N. F. (2009). Morphological and ice-dynamical changes on the Tasman Glacier, New Zealand, 1990-2007. *Global and Planetary Change 68*(3), 185-197.

Quincey, D. J., Lucas, R. M., Richardson, S. D., Glasser, N. F., Hambrey, M. J., & Reynolds, J. M. (2005). Optical remote sensing techniques in high-mountain environments: application to glacial hazards. *Progress in Physical Geography, 29*(4), 475-505.

Quincey, D. J., Richardson, S. D., Luckman, A., Lucas, R. M., Reynolds, J. M., Hambrey, M. J., & Glasser, N. F. (2007). Early recognition of glacial lake hazards in the Himalaya using remote sensing datasets. *Global and Planetary Change, 56*, 137-152.

Radić, V., & Hock, R. (2011). Regionally differentiated contribution of mountain glaciers and ice caps to future sea-level rise. *Nature Geoscience, 4*, 91-94.

Raper, S. C. B., & Braithwaite, R. J. (2005). The potential for sea level rise: New estimates from glacier and ice cap area and volume distributions. *Geophysical Research Letters, 32*(L05502).

Raymond, C. F. (1996). Shear margins in glaciers and ice sheets. *Journal of Glaciology, 42*(140), 90-102.

Reeh, N. (1968). On the calving of ice from floating glaciers and ice shelves. *Journal of Glaciology, 7*, 215-232.

Reid, J. R., & Callender, E. (1965). Origin of Debris-covered Icebergs and Mode of Flow of Ice into "Miller Lake", Martin River Glacier, Alaska. *Journal of Glaciology, 5*(40), 497-503.

Reynolds, J. M. (1999). Glacier hazard assessment at Tsho Rolpa, Rolwaling, central Nepal. *Quaternary Journal of Engineering Geology, 32*, 209-214.

Reznichenko, N., Davies, T. R. H., & Alexander, D. J. (2011). Effects of rock avalanches on glacier behaviour and moraine formation. *Geomorphology, 132*(3-4), 327-338.

Richards, J., Moore, R. D., & Forrest, A. L. (2011). Late-summer thermal regime of a small proglacial lake. *Hydrological Processes, DOI: 10.1002/hyp.8360*.

Richardson, S. D., & Reynolds, J. M. (2000). An overview of glacial hazards in the Himalayas. *Quaternary International, 65/66*, 31-47.

Rignot, E., & Kanagaratnam, P. (2006). Changes in the velocity structure of the Greenland Ice Sheet. *Science, 311*, 986-990.

Rignot, E., Koppes, M., & Velicogna, I. (2010). Rapid submarine melting of the calving faces of West Greenland glaciers. *Nature Geoscience, 3*, 187-191.

Rignot, E., Rivera, A., & Casassa, G. (2003). Contribution of the Patagonia Icefields of South America to sea level rise. *Science, 302*(5644), 434-437.

Rist, M. A., & Murrell, S. A. F. (1994). Ice triaxial deformation and fracture. *Journal of Glaciology, 40*, 305-318.

Rist, M. A., Sammonds, P. R., Murrell, S. A. F., Meredith, P. G., Doake, C. S. M., Oerter, H., & Matsuki, K. (1999). Experimental and theoretical fracture mechanisms applied to Antarctic ice fracture and surface crevassing. *Journal of Geophysical Research, Series B 104*, 2973-2987.

Rist, M. A., Sammonds, P. R., Murrell, S. A. F., Meredith, P. G., Oerter, H., & Doake, C. S. M. (1996). Experimental fracture and mechanical properties of Antarctic ice: preliminary results. *Annals of Glaciology, 23*, 284-292.

Rivera, A., Lange, H., Aravena, J. C., & Casassa, G. (1997). The 20th-century advance of Glaciar Pio XI, Chilean Patagonia. *Annals of Glaciology, 24*, 66-71.

Robe, R. Q. (1978). Upwelling by icebergs. *Nature, 271*(687).

Robin, G. d. Q. (1974). Depth of water filled crevasses that are closely spaced. *Journal of Glaciology, 13*, 543.

Röhl, K. (1999). *Sedimentation Processes in the Proglacial Tasman Lake.* Unpublished Postgraduate Diploma of Science thesis, University of Otago, Dunedin.

Röhl, K. (2005). *Terminus disintegration of debris-covered, lake-calving glaciers.* Unpublished PhD thesis, University of Otago, Dunedin.

Röhl, K. (2006). Thermo-erosional notch development at fresh-water-calving Tasman Glacier, New Zealand. *Journal of Glaciology, 52*(177), 203-213.

Röhl, K. (2008). Characteristics and evolution of supraglacial ponds on debris-covered Tasman Glacier, New Zealand. *Journal of Glaciology, 54*(188), 867-880.

Rott, H., Stuefer, M., Siegel, A., Skvarca, P., & Eckstaller, A. (1998). Mass fluxes and dynamics of Moreno Glacier, Southern Patagonia Icefield. *Geophysical Research Letters, 25*(9), 1407-1410.

Russell-Head, D. S. (1980). The melting of free-drifting icebergs. *Annals of Glaciology, 1*, 119-122.

Sakai, A., Nishimura, K., Kadota, T., & Takeuchi, N. (2009). Onset of calving at supraglacial lakes on debris-covered glaciers of the Nepal Himalaya. *Journal of Glaciology, 55*(193), 909-917.

Sakai, A., Takeuchi, N., Fujita, K., & Nakawo, M. (2000). Role of supraglacial ponds in the ablation process of a debris-covered glacier in the Nepal. *IAHS Publication 264 (Symposium at Seattle 2000 - Debris-Covered Glaciers)*, 119-130.

Sakai, A., Yamada, T., & Chikita, K. (2001). Thermal regime of a moraine-dammed glacial lake, Tsho Rolpa, in Rolwaling Himal, Nepal Himalayas. *Bulletin of Glaciological Research, 18*, 37-44.

Salerno, F., Thakuri, S., D'Agata, C., Smiraglia, C., Manfredi, E. C., Viviano, G., & Tartari, G. (2012). Conditions of formation of glacial lakes in Mt Everest region. *Geophysical Research Abstracts, 14*(EGU2012-2046).

Salinger, J., Chinn, T. J. H., Willsman, A., & Fitzharris, B. (2008). Glacier response to climate change. *Water & Atmosphere, 16*(3), 16-17.

Salinger, M. J., Heine, M. J., & Burrows, C. J. (1983). Variations of the Stocking (Te Wae Wae) Glacier, Mount Cook, and climatic relationships. *New Zealand Journal of Science, 26*, 321-338.

Scambos, T. A., Hulbe, C., Fahnestock, M., & Bohlander, J. (2000). The link between climate warming and break-up of ice shelves in the Antarctic Peninsula. *Journal of Glaciology, 46*(154), 516-530.

Schaefer, J. M., Denton, G., Kaplan, M., Putnam, A., Finkel, R. C., Barrell, D. J. A., Andersen, B. G., Schwartz, R., Mackintosh, A., Chinn, T. J. H., & Schluchter, C. (2009). High-Frequency Holocene Glacier Fluctuations in New Zealand Differ from the Northern Signature. *Science, 324*(5927), 622-625.

Scherler, B. B., & Strecker, M. R. (2011). Spatially variable response of Himalayan glaciers to climate change affected by debris cover. *Nature Geoscience, 4*, 156-159.

Schock, S. G., LeBlanc, L. R., & Mayer, L. A. (1989). Chirp subbottom profiler for quantitative sediment analysis. *Geophysics, 54*(4), 445-450.

Schomacker, A. (2010). Expansion of ice-marginal lakes at the Vatnajökull ice cap, Iceland, from 1999 to 2009. *Geomorphology, 119*, 232-236.

Schweizer, J., & Iken, A. (1992). The role of bed separation and friction in sliding over an undeformable bed. *Journal of Glaciology, 38*(128), 77-92.

Shean, D. E., & Marchant, D. R. (2010). Seismic and GPR surveys of Mullins Glacier, McMurdo Dry Valleys, Antarctica: ice thickness, internal structure and implications for surface ridge formation. *Journal of Glaciology, 56*(195), 48-64.

Shepherd, A. W., Wallis, D., Giles, D., Laxon, K., & Sundal, S. A. V. (2010). Recent loss of floating ice and the consequent sea level contribution. *Geophysical Research Letters, 37*(L13503).

Shulmeister, J., Davies, T., Evans, D. J. A., Hyatt, O. M., & Tovar, D. S. (2009). Catastrophic landslides, glacier behaviour and moraine formation: a view from an active plate margin. *Quaternary Science Reviews, 28*(11-12), 1085-1096.

Siegert, M. J., & Dowdeswell, J. A. (1995). Modelling ice-sheet sensitivity to Late Weichselian environments in the Svalbard-Barents Sea Region. *Journal of Quaternary Science, 10*, 33-43.

Siegert, M. J., & Dowdeswell, J. A. (2004). Numerical reconstructions of the Eurasian Ice Sheet and climate during the Late Weichselian. *Quaternary Science Reviews, 23*, 1273-1283.

Sikonia, W. G. (1982). Finite-element glacier dynamics model applied to Columbia Glacier, Alaska. *U.S. Geological Survey Professional Paper, 1258-B*.

Skvarca, P., De Angelis, H., Naruse, R., Warren, C. R., & Aniya, M. (2002). Calving rates in fresh water: new data from southern Patagonia. *Annals of Glaciology, 34*, 379-384.

Skvarca, P., Rott, H., & Nagler, T. (1995). Drastic retreat of Upsala Glacier, Southern Patagonia, revealed by ERS-1 images and field survey. *SELPER, 11*, 51-55.

Smiraglia, C., Motta, M., Vassena, G., & Diolaiuti, G. (2004). Dry calving processes at the ice cliff of an Antarctic local glacier: the study case of Strandline Glacier (Northern Victoria Land, Antarctica). *Annals of Glaciology, 39*, 201-208.

Solomon, S., Qin, D., Manning, M., Chen, Z., Marquis, M., Averyt, K. B., Tignor, M., & Miller, H. L. (2007). *Climate Change 2007: The Physical Science Basis. Contribution of Working Group I to the Fourth Assessment Report of the Intergovernmental Panel on Climate Change*. Cambridge: Cambridge University Press.

Stokes, C. R., & Clark, C. D. (2004). Evolution of late glacial ice-marginal lakes on the northwestern Canadian Shield and their influence on the location of the Dubawnt Lake palaeo-ice stream. *Palaeogeography, Palaeoclimatology, Palaeoecology, 215*, 155-171.

Straneo, F., Curry, R. G., Sutherland, D. A., Hamilton, G. S., Cenedese, C., Våge, K., & Stearns, L. A. (2011). Impact of fjord dynamics and glacial runoff on the circulation near Helheim Glacier. *Nature Geoscience, 4*, 322-327.

Sugiyama, S., Skvarca, P., Naito, N., Enomoto, H., Tsutaki, S., Tone, K., Marinsek, S., & Aniya, M. (2011). Ice speed of a calving glacier modulated by small fluctuations in basal water pressure. *Nature Geoscience, 4*(9), 597-600.

Syvitski, J. P. M. (1989). On the deposition of sediment within glacier-influenced fjords: oceanographic controls. *Marine Geology, 85*, 301-329.

Tarr, R. S. (1909). The Yakutat Bay region, Alaska *U.S. Geological Survey. Professional Paper 64*.

Theakstone, W. H. (1989). Further catastrophic break up of a calving glacier: observations at Austerdalsisen, Svartisen, 1983-1987. *Geografiska Annaler, 71A*(3-4), 245-253.

Theakstone, W. H., & Knudsen, N. T. (1986). Recent changes of a calving glacier, Austerdalsisen, Svartisen, Norway. *Geografiska Annaler, 68*(4), 303-316.

Thompson, S. S., Benn, D. I., Dennis, K., & Luckman, A. (2011). A rapidly growing moraine-dammed glacial lake on Ngozumpa Glacier, Nepal. *Geomorphology*(doi: 10.1013/j.geomorph.2011.08.015).

Thompson, S. S., Benn, D. I., Dennis, K., & Luckman, A. (2012). A rapidly growing moraine-dammed glacial lake on Ngozumpa Glacier, Nepal. *Geomorphology, 145*(doi: 10.1013/j.geomorph.2011.08.015), 1-11.

Tinti, S., Maramai, A., & Cerutti, A. V. (1999). The Miage Glacier in the Valley of Aosta (Western Alps, Italy) and the Extraordinary Detachment which Occurred on August 9, 1996. *Phys. Chem. Earth (A), 24*(2), 157-161.

Tsutaki, S., Fujita, K., Yamaguchi, S., Sakai, A., Nuimura, T., Komori, J., Takenaka, S., & Tshering, P. (2012). Dynamic interactions between glacier and glacial lake in the Bhutan Himalaya. *Geophysical Research Abstracts, 14*(EGU2012-7687).

Tsutaki, S., Nishimura, D., Yoshizawa, T., & Sugiyama, S. (2011). Changes in glacier dynamics under the influence of proglacial lake formation in Rhonegletscher, Switzerland. *Annals of Glaciology, 52*(58), 31-36.

Turner, A. J., Woodward, J., Dunning, S. A., Shine, A. J., Stokes, C. R., & Cofaigh, C. O. (2012). Geophysical surveys of the sediments of Loch Ness, Scotland: implications for the deglaciation of the Moray Firth Ice Stream, British-Irish Ice Sheet. *Journal of Quaternary Science, 27*(2), 221-232.

Tweed, F. S. (2000). Jökulhlaup initiation by ice-dam flotation: the significance of glacier debris content. *Earth Surface Processes and Landforms, 25*(1), 105-108.

van der Veen, C. J. (1996). Tidewater calving. *Journal of Glaciology, 42*(141), 375-385.

van der Veen, C. J. (1997). Backstress: what it is and how it affects glacier flow. In C. J. Van der Veen (Ed.), *Calving Glaciers: Report of a Workshop, Feb 28-March 2, 1997* (pp. 173-180). Columbus, Ohio: Byrd Polar Research Centre Report No. 15, The Ohio State University.

van der Veen, C. J. (1998a). Fracture mechanics approach to penetration of bottom crevasses on glaciers. *Cold Regions Science and Technology, 27*, 213-223.

van der Veen, C. J. (1998b). Fracture mechanics approach to penetration of surface crevasses on glaciers. *Cold Regions Science and Technology, 27*, 31-47.

van der Veen, C. J. (1999a). Crevasses on glaciers. *Polar Geography, 23*, 213-245.

van der Veen, C. J. (1999b). *Fundamentals of Glacier Dynamics*. Rotterdam: Balkema.

van der Veen, C. J. (2002). Calving glaciers. *Progress in Physical Geography, 26*(1), 96-122.

van der Veen, C. J., Plummer, J. C., & Stearns, L. A. (2011). Controls on the recent speed-up of Jakobshavn Isbræ, West Greenland. *Journal of Glaciology, 57*(204), 770-782.

van der Veen, C. J., & Whillans, I. M. (1989). Force Budget: I. Theory and Numerical Methods. *Journal of Glaciology, 35*(119), 53-60.

Vaughan, D. G. (1993). Relating the occurrence of crevasses to surface strain rates. *Journal of Glaciology, 39*, 255-266.

Veitch, S. A., & Nettles, M. (2011). *Temporal variation in source characteristics of glacial earthquakes.* Paper presented at the Abstract C13A-0724 presented at 2011 Fall Meeting, AGU, San Francisco, California, 5-9 December.

Venteris, E. R. (1997). Evidence for bottom crevasse formation on Columbia Glacier, Alaska. In C. J. van der Veen (Ed.), *Calving Glaciers: Report of a Workshop, February 28 - March 2, 1997* (pp. 118-185). Byrd Polar Research Centre Report No. 15: The Ohio State University, Columbus, Ohio.

Venteris, E. R. (1999). Rapid tidewater glacier retreat: a comparison between Columbia Glacier, Alaska and Patagonian calving glaciers. *Global and Planetary Change, 22*(1-4), 131-138.

Vieli, A., Funk, M., & Blatter, H. (2000). Tidewater glaciers: frontal flow acceleration and basal sliding. *Annals of Glaciology, 31*, 217-221.

Vieli, A., Funk, M., & Blatter, H. (2001). Flow dynamics of tidewater glaciers: a numerical modelling approach. *Journal of Glaciology, 47*, 595-606.

Vieli, A., Jania, J., & Kolondra, L. (2002). The retreat of a tidewater glacier: observations and model calculations on Hansbreen, Spitsbergen. *Journal of Glaciology, 48*, 592-600.

Vincent, C., Auclair, S., & Le Meur, E. (2010). Outburst flood hazard for glacier-dammed Lac de Rochemelon, France. *Journal of Glaciology, 56*(195), 91-100.

Vuichard, D., & Zimmermann, M. (1987). The 1985 catastrophic drainage of a moraine-dammed lake, Khumbu Himal, Nepal: cause and consequences. *Mountain Research Development, 7*(2), 91-110.

Walter, F., Amundson, J. M., O'Neel, S., Truffer, M., Fahnestock, M., & Fricker, H. A. (2012). Analysis of low-frequency seismic signals generated during a multiple-iceberg calving event at Jakobshavn Isbræ, Greenland. *Journal of Geophysical Research, 117*(F1).

Warren, C. R. (1991). Terminal environment, topographic control and fluctuations of West Greenland Glaciers. *Boreas, 20*(1), 1-15.

Warren, C. R. (1992). Iceberg calving and the glacioclimatic record. *Progress in Physical Geography, 16*(3), 253-282.

Warren, C. R. (1999). Calving speed in freshwater at Glaciar Ameghino, Patagonia. *Zeitschrift Für Gletscherkunde Und Glazialgeologie, 35*(1), 21-34.

Warren, C. R., & Aniya, M. (1999). The calving glaciers of southern South America. *Global and Planetary Change, 22*(1-4), 59-77.

Warren, C. R., Benn, D. I., Winchester, V., & Harrison, S. (2001). Buoyancy-driven lacustrine calving, Glaciar Nef, Chilean Patagonia. *Journal of Glaciology, 47*(156), 135-146.

Warren, C. R., Glasser, N. F., Harrison, S., Winchester, V., Kerr, A. R., & Rivera, A. (1995a). Characteristics of tide-water calving at Glacier San-Rafael, Chile. *Journal of Glaciology, 41*(138), 273-289.

Warren, C. R., Greene, D. R., & Glasser, N. F. (1995b). Glaciar Upsala, Patagonia: rapid calving retreat in fresh water. *Annals of Glaciology, 21*(311-316).

Warren, C. R., & Hulton, N. R. (1990). Topographic and glaciological controls on Holocene icesheet margin dynamics, central West Greenland. *Annals of Glaciology, 14*, 307-310.

Warren, C. R., & Kirkbride, M. P. (1998). Temperature and bathymetry of ice-contact lakes in Mount Cook National Park, New Zealand. *New Zealand Journal of Geology and Geophysics, 41*, 133-143.

Warren, C. R., & Kirkbride, M. P. (2003). Calving speed and climatic sensitivity of New Zealand lake-calving glaciers. *Annals of Glaciology, 36*, 173-178.

Watanabe, T., Kameyama, S., & Sato, T. (1995). Imja Glacial dead-ice melt rates and changes in a supra-glacial lake, 1989-1994, Khumbu Himal, Nepal: danger of lake drainage. *Mountain Research and Development, 15*, 293-300.

Watanabe, T., Lamsal, D., & Ives, J. D. (2009). Evaluating the growth characteristics of a glacial lake and its degree of danger of outburst flooding: Imja Glacier, Khumbu Himal, Nepal. *Norwegian Journal of Geography, 63*, 255-267.

Watson, M. I. (1995). *Geophysical and glaciological studies of the Tasman and Mueller Glaciers.* Unpublished MSc thesis, University of Auckland, Auckland, New Zealand.

Weber, L. J., & Nixon, W. A. (1996). Fracture toughness of freshwater ice-Part I: Experimental technique and results. *ASME Journal of Offshore Mechanics and Arctic Engineering, 118*, 135-140.

Weeks, W. F., & Campbell, W. J. (1973). Icebergs as a freshwater source: an appraisal. *Journal of Glaciology, 12*, 207-223.

Weertman, J. (1973). Can a water filled crevasse reach the bottom surface of a glacier? *IAHS Publication 95*, 139-145.

Wetzel, R. G. (2001). *Limnology; lake and river ecosystems* (Third ed.). United States of America: Elsevier Science (USA).

Whillans, I. M., Jackson, M., & Tseng, Y.-H. (1993). Velocity pattern in a transect across Ice Stream B, Antarctica. *Journal of Glaciology, 39*, 562-572.

Whillans, I. M., & van der Veen, C. J. (1997). The role of lateral drag in the dynamics of Ice Stream B, Antarctica. *Journal of Glaciology, 43*, 231-237.

White, M. S., Xenopoulos, M. A., Metcalfe, R. A., & Somers, K. M. (2010). On the role of natural water level fluctuation in structuring littoral benthic macroinvertebrate community composition in lakes. *Limnology and Oceangraphy, 55*(6), 2275-2284.

Wilhelm, F. (1963). Beobachtungen ü ber Geschwindigkeitsänderungen und Bewegungstypen beim Eismassentransport arktischer Gletscher. *International Association of Scientific Hydrology Publication 61 (General Assembly of Berkeley 1963 - Snow and Ice)*, 261-271.

Willis, M. J., Melkonian, A. K., Pritchard, M. E., & Ramage, J. M. (2012). Ice loss rates at the Northern Patagonian Icefield derived using a decade of satellite remote sensing. *Remote Sensing of Environment, 117*, 184-198.

Winkler, S. (2004). Lichenometric dating of the 'Little Ice Age' maximum in Mt Cook National Park, Southern Alps, New Zealand. *The Holocene, 14*(6), 911-920.

Winkler, S., Elvehøy, H., & Nesje, A. (2009). Glacier fluctuations of Jostedalsbreen, western Norway, during the past 20 years: the sensitive response of maritime mountain glaciers. *The Holocene, 19*(3), 389-414.

Xu, Y., Rignot, E., Menemenlis, D., & Koppes, M. (2011). *Modeling of subaqueous melting of Greenland tidewater glaciers using an ocean general circulation model.* Paper presented at the Abstract C22A-04 presented at 2011 Fall Meeting, AGU, San Francisco, California, 5-9 December.

Xu, Y., Rignot, E., Menemenlis, D., & Koppes, M. (2012). Numerical experiments on subaqueous melting of Greenland tidewater glaciers in response to ocean warming and enhanced subglacial drainage. *Annals of Glaciology, 53*(60), 229-234.

Yamada, T. (1998). *Glacier lake and its outburst flood in the Nepal Himalaya*: Tokyo, Japanese Society of Snow and Ice. Data Center for Glacier Research. (Monograph 1.).

Yamada, T., & Sharma, C. K. (1993). Glacier lakes and outburst floods in the Nepal Himalaya. *International Association of Hydrological Sciences Publication, 218 (Symposium at Kathmandu 1992 - Snow and Glacier Hydrology)*, 319-330.

Zhou, X.-h., Jiang, X.-j., & Shi, Y.-z. (2007). Application of side scan sonar and sub-bottom profile in the checking of submerged pipeline in Hangzhou Bay. *Hydrographic Surveying and Charting, 04*.

Zweck, C., & Huybrechts, P. (2003). Modeling the marine extent of Northern Hemisphere ice sheets during the last glacial cycle. *Annals of Glaciology, 37*, 173-180.

Chapter 9: Appendices

The following appendices contain additional data and information on the specific methods and equipment used within this study. The DRC 16 form 'Statement of Contribution of Doctoral Thesis containing publications' for chapters that have been submitted as a paper to a scientific journal are also included. These forms relate to chapters three to six.

Appendix 1: 3D model of Mueller lake, February 2011

Appendix 2A: Sub-bottom profiler image from Tasman Lake

Appendix 2B: Sub-bottom profiler image from Mueller lake

Appendix 3: Further information on the methodologies and equipment used

EdgeTech 216S sub-bottom profiler

Humminbird 323 DualBeam PLUS dual frequency echo-sounder

RTK-dGPS and handheld GPS

Onset Tidbit temperature loggers and thermistor

Onset U20-001-01 HOBO Depth Data Logger

Trimble S6 automatic total station

Additional methods that were tested

Coverage and sources of aerial photographs and satellite images

Appendix 4: DRC 16 form for chapter 3

Robertson, C.M., Brook, M.S., Fuller, I.C., Holt, K.A. and Benn, D.I., Glacier retreat and proglacial lake expansion in *Aoraki*/Mount Cook National Park, New Zealand. *Geomorphology.*

Appendix 5: DRC 16 form for chapter 4

Robertson, C.M., Benn, D.I., Brook, M.S., Fuller, I.C. and Holt, K.A., 2012, Subaqueous calving margin morphology at Mueller, Hooker and Tasman glaciers in *Aoraki*/Mount Cook National Park, New Zealand. *Journal of Glaciology*, 58(212), 1037-1046.

Appendix 6: DRC 16 form for chapter 5

Robertson, C.M., Brook, M.S., Fuller, I.C., Benn, D.I. and Holt, K.A., Temporal evolution of the calving terminus at Mueller Glacier, *Aoraki*/Mount Cook National Park, New Zealand. *Geografiska Annaler*.

Appendix 7: DRC 16 form for chapter 6

Robertson, C.M., Brook, M.S., Holt, K.A., Fuller, I.C. and Benn, D.I., in press, Calving retreat and proglacial lake growth at Hooker Glacier, Southern Alps, New Zealand. *New Zealand Geographer.*

Appendix 1: 3D model of Mueller lake, February 2011

The image shows a 3D model of Mueller lake based on bathymetry data collected in February 2011. The blank areas within the lake are gravel islands. The scale is given in m a.s.l with lake level (the 0 m bathymetry contour) at 765 m a.s.l.

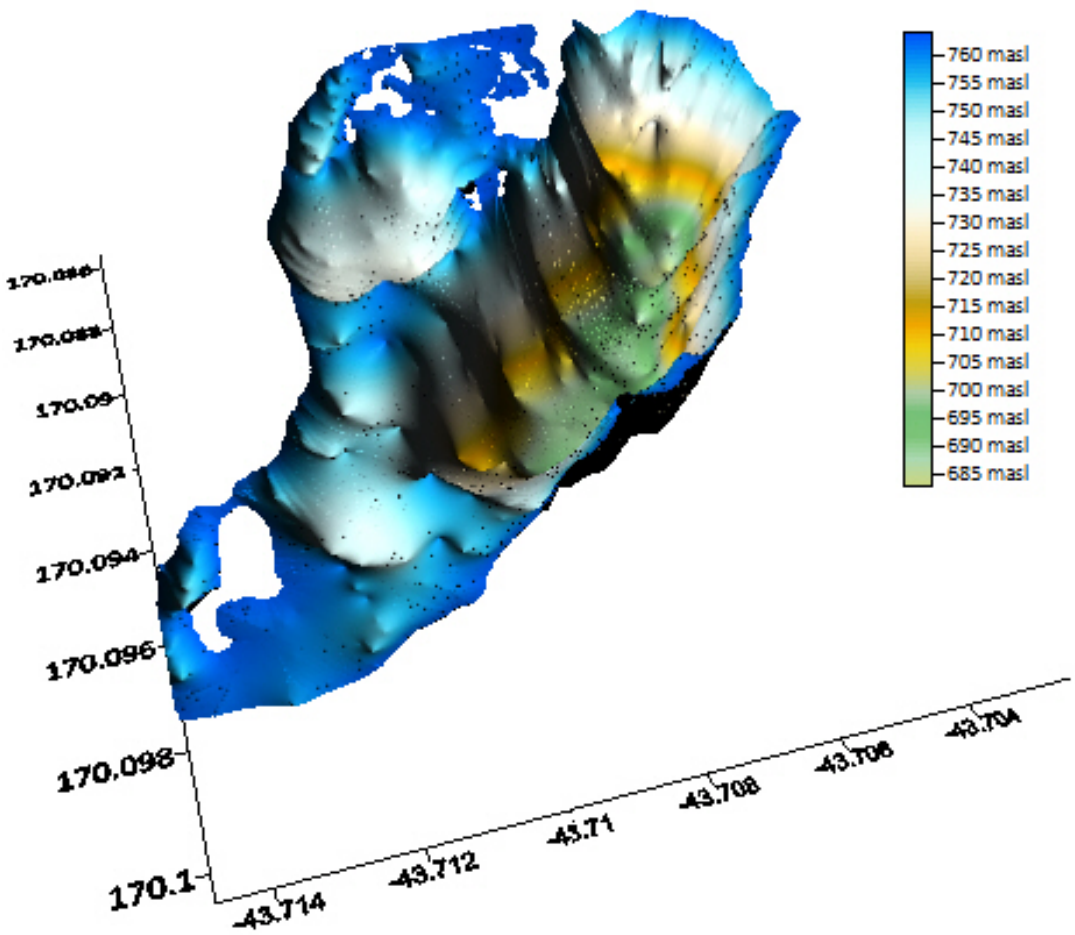

Appendix 2A: Sub-bottom profiler image from Tasman Lake

The sub-bottom profile image from Tasman Lake in 2008 shows the ice ramp which extends from Tasman Glacier abutting the lateral moraine on the western side of Tasman Lake. The data were collected approximately 20-30 m in front of the terminus, 50-75 m from the lateral moraine.

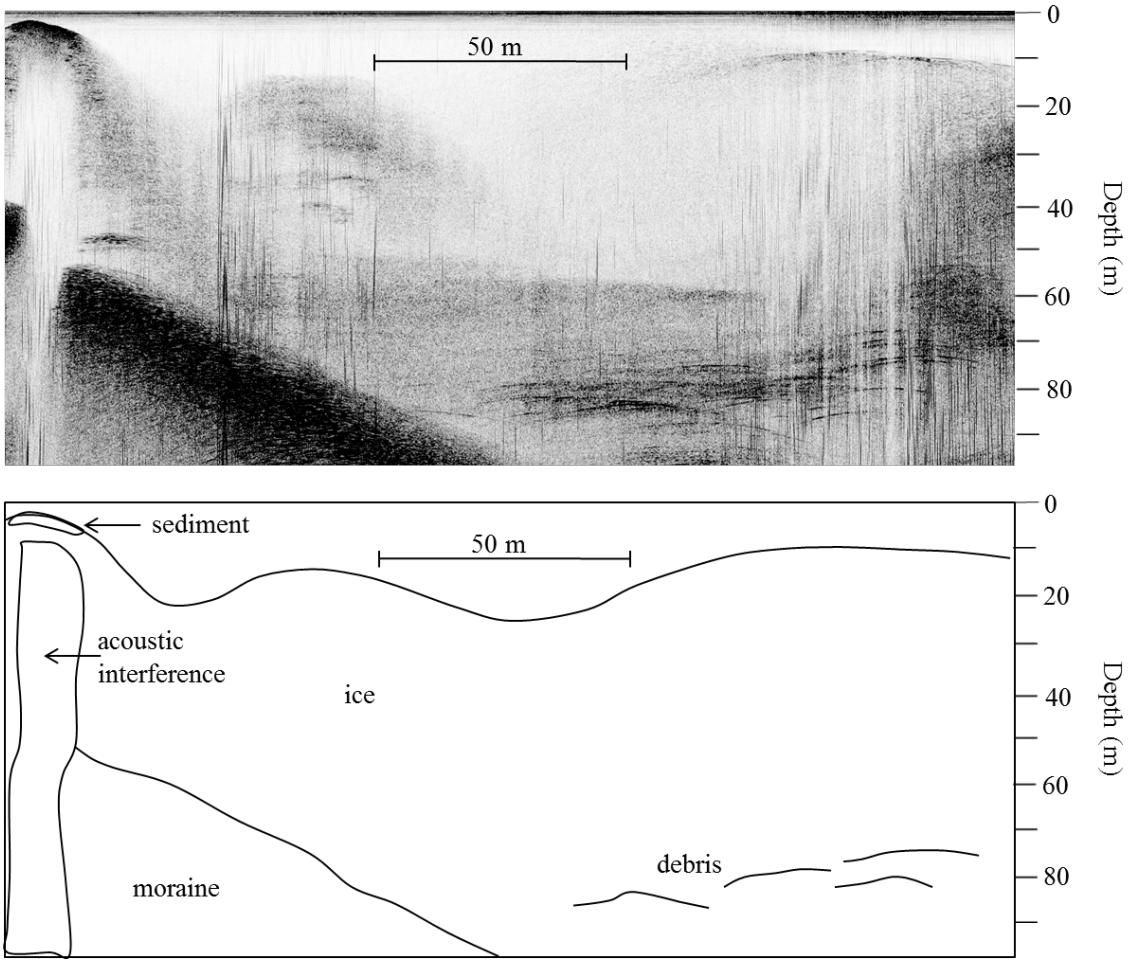

9

Appendix 2B: Sub-bottom profiler image from Mueller lake

The sub-bottom profile image from Mueller lake in 2009 shows a fine-grained sediment-filled basin in the SW of the lake. The data were collected approximately 50 m in front of the terminus.

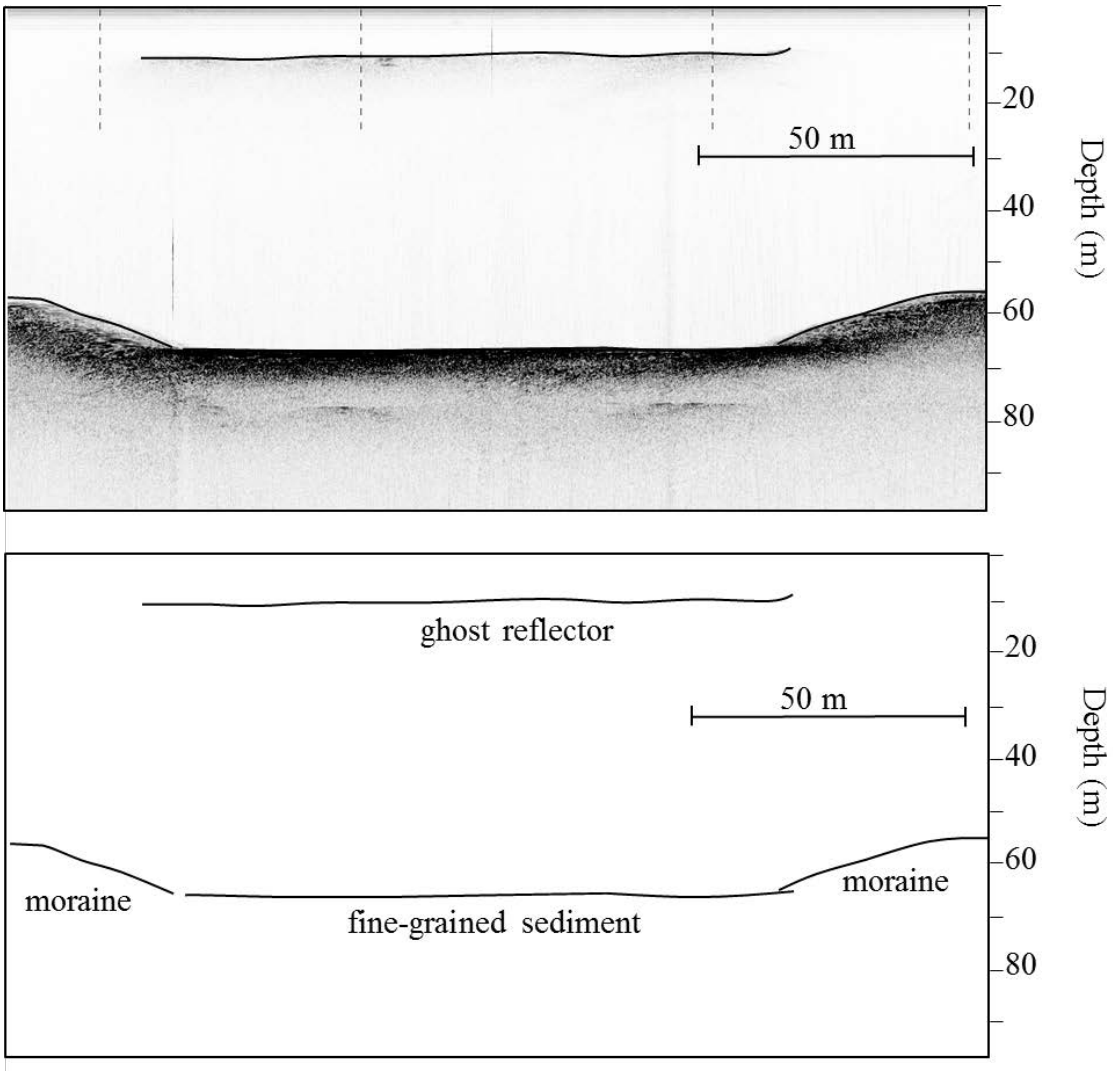

Appendix 3: Further information on the methodologies and equipment used

Outlined below is specific information about the methods and equipment used throughout this study. As chapters 3 to 6 are based on manuscripts submitted for publication as journal articles, detailed explanations of why particular methods and equipment were chosen and the strengths and weaknesses of the methods and equipment were restricted. The methods and equipment discussed include an EdgeTech 216S sub-bottom profiler, a Humminbird 323 DualBeam Plus dual frequency echo-sounder, RTK-dGPS and handheld GPS, Onset Tidbit temperature loggers and a thermistor, a Onset U20-001-01 HOBO Depth Data Logger, a Trimble S6 automatic total station and a Lighter-than-air-Helikite. Sources of aerial photographs and satellite images used throughout the study are also included.

EdgeTech 216S sub-bottom profiler

The portable, hydro-dynamically stable, sub-bottom profiler operates by remotely determining the acoustic attenuation of lake or ocean sediments by transmitting an FM pulse (also known as CHIRP [Compressed High Intensity Radar Pulse] or Klauder wavelets) linearly over an area (Schock *et al.*, 1989; EdgeTech, 2005). The FM pulse penetrates the sediment and returns to the minicomputer which converts the signal into a real-time grey-scale profile. Individual features can be identified as different facies give varied acoustic returns. The sonar works on a frequency range of 2-16 kHz and gives a vertical resolution of 60-100 mm (EdgeTech, 2005). It is capable of working in water depths of up to 300 m. The EdgeTech 216S sub-bottom profiler was used in Mueller, Hooker and Tasman lakes to identify ice ramps extending from the termini of these glaciers and ice in the sediment on the lake floor. Sub-bottom profilers have not been used for this type of work before. They have however, been widely employed in geological surveys for sediment analysis, gas identification and hazard assessment as well as for engineering works and archaeological investigations (Jakobsson, 1999; Duck & Herbert, 2006; Lafferty *et al.*, 2006; Zhou *et al.*, 2007; Turner *et al.*, 2012). The profiler was attached to a minicomputer and Toughbook laptop on the survey boat by a 30 m, heavy duty cable. In Tasman Lake, where the first survey was completed, the

profiler was towed approximately 20 m behind the boat. Trimble Real-Time Kinematic differential Global Positioning System (RTK-dGPS) was used to locate this survey with a rover attached to the top of the profiler (Figure 9.1). After this survey it was decided that due to mobility issues, the profiler would be towed within 10 m of the boat (Figure 9.2). This made surveying in small bays where icebergs were present possible without the profiler cable becoming snagged and increased mobility. Further use and experimentation with the position of the profiler proved that the profiler could be towed beside the boat, held in place by rope (Figures 9.3 and 9.4), with no loss of signal or interference from the boat. When the aluminium boat was used, the profiler needed to be slightly further away from the boat (approximately 300 mm) to ensure it did not bang against the side of the boat. This made it considerably easier to survey within small bays and to turn the boat, and also to mark the position of the profiler traces with handheld GPS as the GPS unit could be held above the profiler.

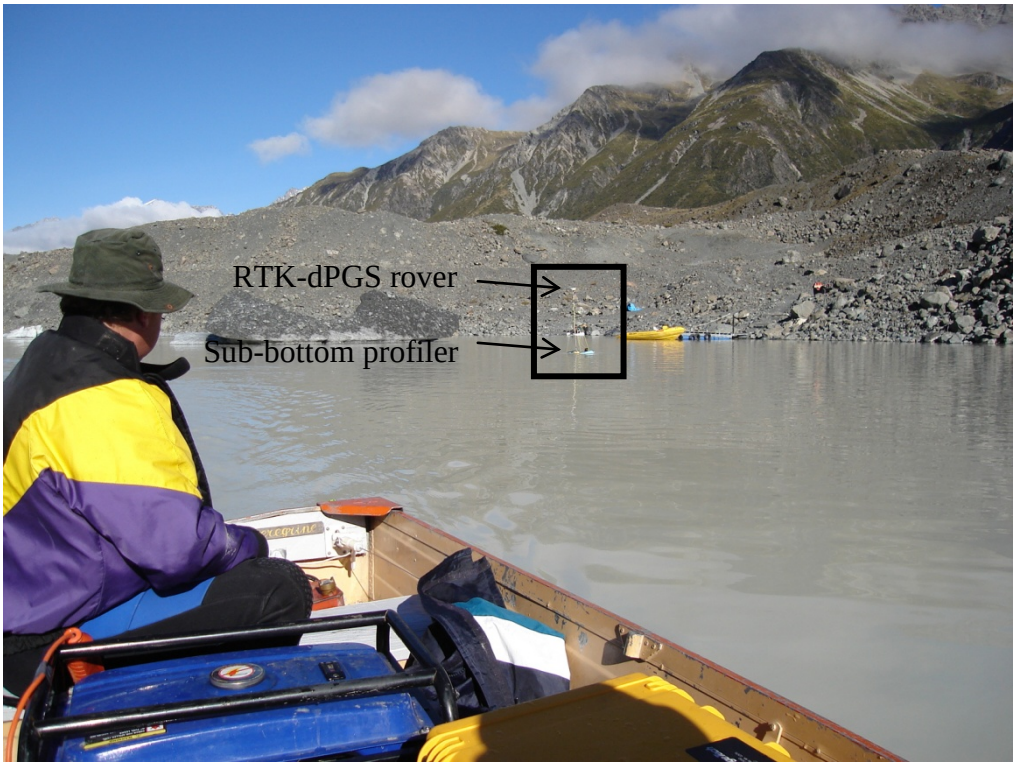

Figure 9.1: The EdgeTech 216S sub-bottom profiler being towed approximately 20 m behind the boat in Tasman Lake (source: C. Robertson, 2 April 2008). A RTK-dGPS rover attached to the top of the profiler to locate the survey.

Figure 9.2: The EdgeTech 216S sub-bottom profiler being towed approximately 10 m behind the boat in front of the terminus ice cliff of Hooker Glacier (source: R. Dykes, 29 November 2009).

Figure 9.3: EdgeTech 216S sub-bottom profiler towed beside the boat in Mueller lake (source: C. Robertson, 15 April 2010). The ballast (green tubes) which was attached to the profiler can be seen sitting above the water. The minicomputer and Toughbook used in conjunction with the profile can also been seen. Figure 9.4 shows a more detailed view of these components.

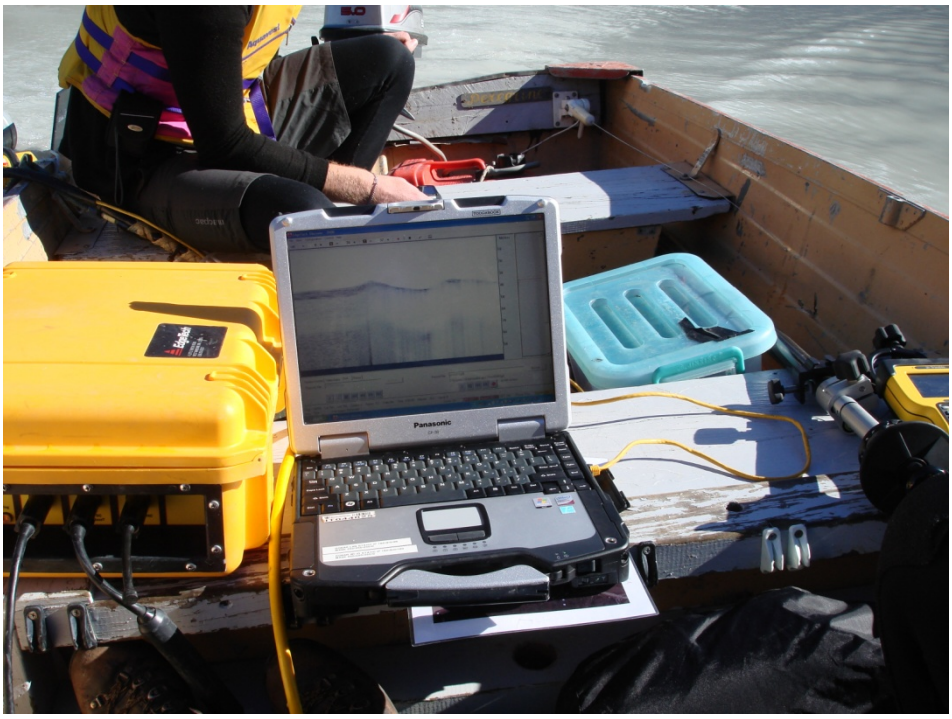

Figure 9.4: Minicomputer and Toughbook laptop used with the EdgeTech 216S sub-bottom profiler (source: C. Robertson, 15 April 2010). The profiler is attached to the yellow box (minicomputer) by a cable, with the minicopter then being connected to the Toughbook laptop. A profiler image can be seen on the Toughbook screen. The minicomputer is powered by batteries contained in the green plastic box.

The EdgeTech 216S sub-bottom profiler has a number of advantages over conventional sub-bottom systems, including: greater penetration of sediment and thus higher resolution (due to the tapered wave form spectrum; EdgeTech, 2005), and greater precision of sediment classification (particularly between ice and sediment) as the amplitude, phase and energy parameters of the FM pulse can be precisely controlled (EdgeTech, 2005). Another advantage was the ease of use and user-friendly display software. Real-time processing and image display meant that areas of interest could be identified and resurveyed if necessary.

One disadvantage of the sub-bottom profiling system is interference caused by gas or sediment in the water column. Gas blocks the FM pulse and prevents the sub-bottom signal from returned to the minicomputer (Black Laser Learning, 2006). This is termed

acoustic blanking (Duck & Herbert, 2006). Air is one of the strongest reflectors that can block the signal. Acoustic blanking was experienced in Mueller, Hooker (Figure 9.5) and Tasman lakes during the surveys caused by both air bubbles in the water column and gas in the lake floor. Air bubbles in ice on the lake bed also frequently blocked the signal penetrating into the sediments below the ice. Duck and Herbert (2006) also experienced issues with gas in the water column in Loch Tay, Scotland. Pantin and Wright (1994) found that gas in the water column or water inhomogeneities caused acoustic scattering of the sub-bottom signal, which prevented a clear signal and therefore picture forming on the minicomputer. Acoustic scattering was a particular problem in the *Aoraki*/Mount Cook proglacial lakes when lake conditions were rough or choppy, with swells of as little as 200 mm causing interference (Figure 9.6). Scattering of the signal made interpretation of the data very difficult as the picture create was not clear therefore data with this scattering were largely dismissed.

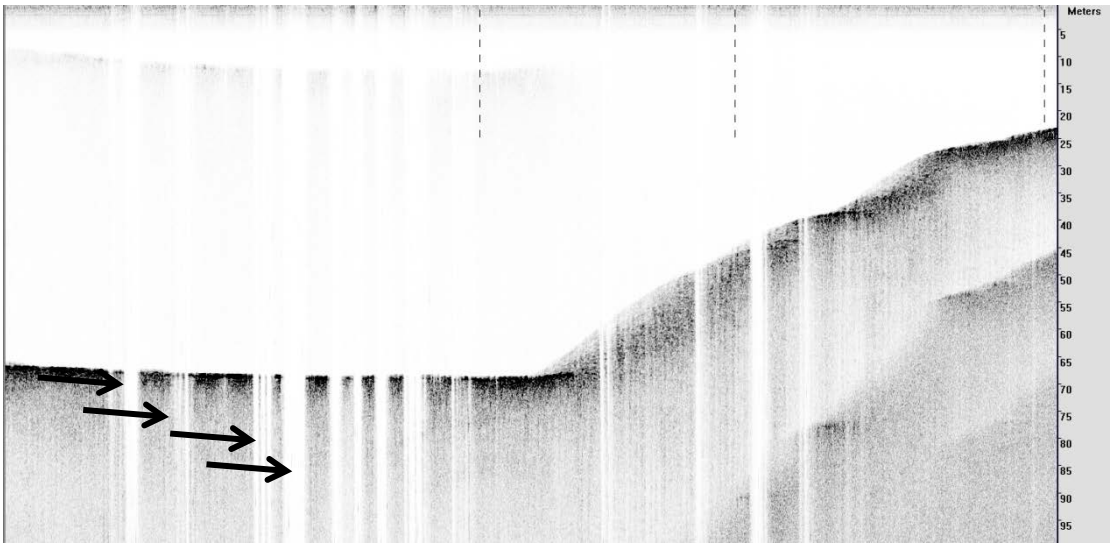

Figure 9.5: An example of a sub-bottom profiler image from Hooker Lake which shows a considerable amount of acoustic blanking (shown by the arrows), the result of the signal being blocked by gas in the water column or lake bed.

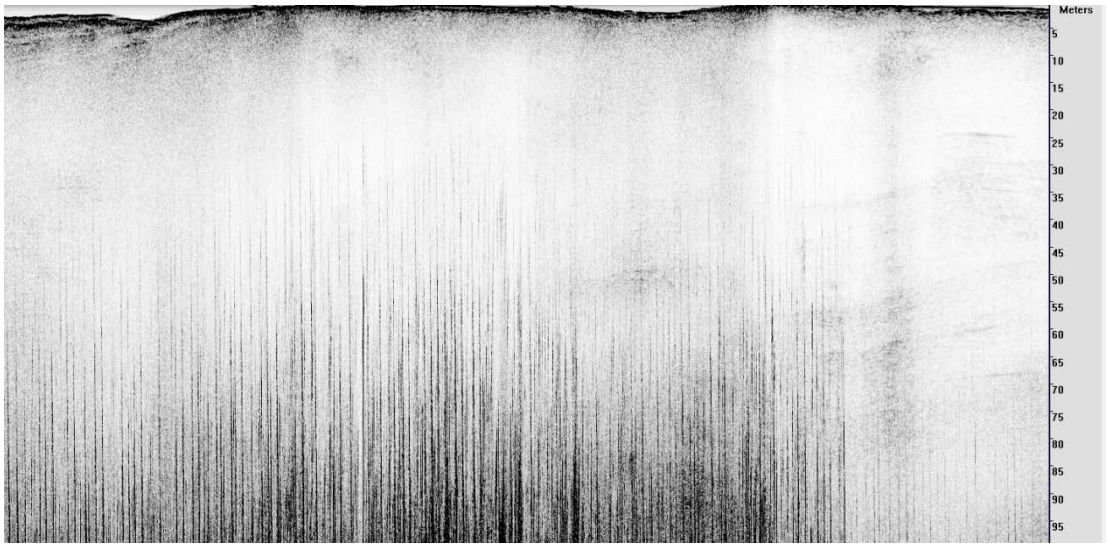

Figure 9.6: An example of a sub-bottom profiler image from Mueller lake which shows acoustic scattering (the heavily lined part of the image) caused by gas in the water column or water inhomogeneities. Acoustic scattering prevents the image being analysed and interpreted due to the quality of the image.

A second disadvantage of the EdgeTech 216S sub-bottom profiler was its appropriateness for use in proglacial lakes. The profile is designed to be towed close to the lake bed with an optimum height above the bed of 3 to 5 m (EdgeTech, 2005). Surveys near the terminus in the proglacial lakes were particularly hazardous due to the high risk of calving, both subaerially and subaqueously. Towing the sonar 3-5 m above the lake bed in the lakes was deemed a very high risk due to the potential need to make a quick exit from the area if calving did occur. Towing the sonar within 3-5 m of the lake of the bed would have slowed this exit considerably. In addition, the boats that were used in the lakes were not capable of towing the profiler close to the lake bed safely. Therefore the profiler was modified by removing 70 kg of lead in the base and attaching ballast to make the profiler float, with the base of the profiler submerged approximately 150 mm under the surface of the lake (Figure 9.3). Towing the sonar just below the surface of the lake and not within the optimal height above the lake bed may however, have reduced the vertical resolution. Due to the large spatial extend of the lakes that surveys were carried out in and the depths within the lakes (up to 240 m) the potential decrease in vertical resolution was deemed acceptable.

Humminbird 323 DualBeam PLUS dual frequency echo-sounder

A Humminbird 323 DualBeam PLUS dual frequency echo-sounder operates by sending a signal which, when it comes into contact with a structure (e.g. the lake bed), rebounds and returns an echo to the echo-sounder unit attached to the boat. The signal is then processed to display a real-time image on the echo-sounder screen. The echo-sounder operates at frequencies of 200 kHz and 83 kHz and sends out two beams, a narrow, precise 20˚ beam and a wide 60˚ beam, providing both precision and a wide survey area. The echo-sounder can work in water up to 300 m deep. A Humminbird 323 DualBeam PLUS dual frequency echo-sounder was used in Mueller and Hooker lakes to measure lake bathymetry by attaching it to the back of a boat which followed intersecting transects across the lake. Transects were approximately 100 m apart and a depth reading was recorded approximately every 50 m along each transect. Depths measured by the echo-sounder were calibrated against known depths within the lake to give an accuracy of less than 1 m. Echo-sounders are the most common tool used to map bathymetry and have been employed in many proglacial lakes worldwide (Hochstein *et al.*, 1995; Naruse & Skvarca, 2000; Benn *et al.*, 2001; Warren *et al.*, 2001; Motyka *et al.*, 2003b; Haresign, 2004; Diolaiuti *et al.*, 2005; Boyce *et al.*, 2007; Dykes *et al.*, 2011; Kehrl *et al.*, 2011; Engel *et al.*, 2012; Thompson *et al.*, 2012).

Advantages of the Humminbird 323 DualBeam PLUS dual frequency echo-sounder include the real-time image displayed on the screen of the surveyed area, that it is very user friendly and it continuously sends signals to measure depth. The unit is also very small and does not require a large number of batteries to power it. There are however, a number of disadvantages to this particular echo-sounder. The unit does not record the data, therefore data must be manually read off the unit and recorded elsewhere. This must be done as soon as the data is displayed on the screen as the echo-sounder has no memory and continuously updates depth readings as the boat moves. There is also a limited ability to change the settings of the echo-sounder. For example, both 20˚ and 60˚ beams are used continuously with the user only being able to change the screen setting to view separate returned signals or a combination of the two.

RTK-dGPS and handheld GPS

Trimble Real-Time Kinematic differential Global Positioning System (RTK-dGPS) and a Garmin eTrex handheld GPS were used to locate surveys both on the glaciers and proglacial lakes in *Aoraki*/Mount Cook National Park. Unfortunately, the use of RTK-dGPS was limited to Tasman Lake due to the narrow sky-views at Mueller and Hooker lakes which prevented the base unit connected to an adequate number of satellites. In Tasman Lake, RTK-dGPS was used to locate the sub-bottom profiler surveys by attaching a rover unit to the profiler, while a base station was established on a topographic high near the southern end of the lake. Handheld GPS were used on Mueller and Hooker lakes to locate sub-bottom profiler surveys, bathymetry surveys, and to map lake extend. When completing the sub-bottom surveys, points were marked on the survey images where a GPS reading was taken, this was approximately every 30-50 m along the survey transects. For bathymetry surveys, GPS readings were taken approximately every 50 m along the survey transect and the depth at that point, as measured by the echo-sounder, was recorded. These readings were recorded manually. The handheld GPS was very user friendly, however, the precision of measurements were not as high (± 5 m) as those measurements made with the RTK-dGPS (± 60 mm). Although high-resolution data from RTK-dGPS would have been ideal, the constraints of the environment prevented this from being used at all locations. Handheld GPS have been used in numerous other studies (Dykes *et al.*, 2011)

Onset Tidbit temperature loggers and thermistor

Onset Tidbit temperature loggers were used to continuously record water temperature in Mueller and Hooker lakes. Onset Tidbit temperature loggers are commonly used to measure temperature within lakes (e.g. Gilbert & Lamoureux, 2004; Richards *et al.*, 2011; Beletsky *et al.*, 2012). A stationary lake mooring, which consisted of two buoys, an anchor (a concrete block), and a floating rope with 5 tidbits attached, was deployed in each lake approximately 100 m in front of the terminus in approximately 50 m of water (Figure 9.7). The tidbits were spaced at depths approximately 2 m, 10 m, 20 m, 30 m and 49 m down from the surface of the lake. The rope which the tidbits were attached to had some slack in it in order to compensate for fluctuations in lake level. The tidbits recorded temperatures every 3 hours. The lake mooring in Hooker Lake was unable to

be found and was later discovered to have snapped and floated down the lake, beaching on the southern lake shore. A local tramper found the buoys on the lake shore and said no tidbits were attached to the rope. The advantages of the tidbits are the ability to change and set the frequency with which they recorded water temperature, their long battery life (up to 5 years) and the high accuracy of the measurements (0.2˚C over the range of O˚C to 50˚C). The tidbits were also very small which made attaching them to the lake mooring rope easy. A number of disadvantages of the lake mooring system used include the breakage of the mooring in Hooker Lake, the anchor sinking in Mueller lake, which prevented the system being recovered in April 2010, and then subsequently, the anchor coming free from the sediment in which it was stuck and moving around the lake in January 2011.

Figure 9.7: The two buoys of the stationary lake mooring which 5 Onset Tidbit temperature loggers were attached to in Hooker Lake (source: C. Robertson, 28 November 2009).

Spot temperature measurements were also made in Mueller and Hooker lakes with a thermister (YSI Model 58 dissolved oxygen meter and 5739 series dissolved oxygen

probe) attached to a 50 m cable. The thermistor was sourced from the Ecology Group at Massey University. Spot measurements were taken throughout the lake at depths of 0.10 m, 5 m, 15 m, 30 m and 50 m below the surface of the lake in November 2009 and April 2010 and every 1 m in Mueller lake in January and February 2011. The temperatures were recorded manually and located with handheld GPS. The depth of measurements was limited to the length of the cable. A thermistor with a longer cable (i.e. 140 m, the maximum depth of Hooker Lake) could not be sourced, despite thorough investigations throughout New Zealand. One advantage of the thermistor used was that it was very reactive to changes in water temperature and required only a short period of time (2-3 minutes) to adjust from high air temperatures to lake temperatures when it was placed in the lake.

Onset U20-001-01 HOBO Depth Data Logger

An Onset U20-001-01 HOBO Depth Data Logger was deployed in Mueller lake to record lake level. The logger was deployed in a sheltered bay in the southeast of the lake in approximately 1.5 m of water and recorded data every 5 minutes. The logger was placed in a plastic basket to protect it from impacts and anchored to the lake shore (Figure 9.8). The depth data logger works by measuring changes in pressure of the overlying water. HOBO software then converted this pressure data to water depth data. The data was corrected for barometric pressure with data from the NIWA automatic climate station at *Aoraki*/Mount Cook Village. One advantage of the Onset U20-001-01 HOBO Depth Data Logger is that it can be set up and deployed for long periods of time due to the long battery life and large internal memory. It is also straightforward to set up multiple data recording periods and remove data from the logger, simply by putting it into a coupler attached to a laptop. The logger was however difficult to deploy due to the need to be very careful when placing it onto the lake bed. It had to be lowered into the lake from a boat to avoid any bumps or knocks that could damage it. Recovery was also difficult as the basket sunk slightly into soft sediment on the lake bed. Onset U20-001-01 HOBO Depth Data Loggers have been used in numerous other studies to monitor lake level (e.g. Cuevas *et al.*, 2010; White *et al.*, 2010).

Figure 9.8: The plastic basket the Onset U20-001-01 HOBO Depth Data Logger was deployed in to protect it from impacts (source: C. Robertson, 18 February 2011). This photograph was taken after the logger had been recovered in February 2011. Fine sediment can be seen on the basket from where it sunk into the sediment on the lake floor.

Trimble S6 automatic total station

A Trimble S6 automatic total station was utilised to measure horizontal (*x*,*y*) and vertical (*z*) glacier displacement and to collect topographic data on the surface of Mueller Glacier as it was not possible to employ RTK-dGPS. The total station was established on Kea Point, ~150 m above Mueller Glacier (figure 9.9 and 9.10) and each survey was locked into the same baseline by surveying stationary features (e.g. information boards, wooden platform and a seat) at the beginning of each survey along with fixing the total station over the same peg for all surveys. The automatic total station allowed the position of features on the glacier to be accurately viewed and measured (distance and angle of the feature from the total station) within a local grid which could then be converted into latitude and longitude coordinates. The precision of the measurements was very high with precision within 05" over a maximum distance of 919 m giving an error of 0.02 m in positional accuracy, at the furthest point. Electronic

distance measurements were corrected for barometric pressure and temperature with data from the National Institute of Water and Atmospheric Research (NIWA) automatic climate station at Mount Cook Village (-43.736 ºS 170.096 ºE). The total station also corrected vertical angle measurements for curvature and refraction. One disadvantage of the total station system was the slow speed in which it took to locate and measure a feature on the glacier. Due to the distances between the surveyed features and the total station and high heat shimmer on the glacier it was not possible to use the automatic find function. In addition, surveys were restricted to areas within line-of-sight of the S6.

Figure 9.9: The Trimble S6 automatic total station (black box) established on Kea Point, ~150 m above Mueller Glacier, from where the photograph is taken (source: C. Robertson, 5 January 2011).

Figure 9.10: The Trimble S6 automatic total station established on Kea Point, ~150 m above Mueller Glacier (source: A. Clement, 21 January 2011).

In order to measure horizontal and vertical displacements an array of five reflective prisms were used. The prisms were attached to large, stable boulders by heavy-duty glue (Figure 9.11) and directed towards Kea Point, on the lower 400 m of the terminus. Distance and angles between the total station and prisms were measured on twelve different days during January and February 2011. This set-up removed the need to have a person on the glacier (as would be required with manual RTK-dGPS) and resulted in only one person being needed to make the measurements remotely from Kea Point. Low cloud cover and strong heat shimmer on the glacier however, prevented a reflection

being returned from the prisms to the total station on some days. A similar total station and reflective prism set-up was successfully used in Antarctica by Leonard (Leonard *et al.*, 2011) to measure vertical and horizontal displacements of coastal sea ice.

Figure 9.11: The author beside a reflective prism that has just been attached to a large, stable, flat boulder on the surface of Mueller Glacier (source: A. Clement, 20 January 2011). The reflective face of the prism is directed towards Kea Point. The photograph is taken looking up-glacier.

Topographic data were collected using the automatic total station to map the surface of the glacier terminus. Two people were needed to collect this data. One person walked around on the glacier terminus, placing a reflective prism attached to a pole, on breaks in slope within and between morphological units and on geographic features, while a second person, stationed at Kea Point, located the reflective prism through the S6. 1500 data points (x,y,z) were collected in February 2011. Again, due to the distance between the S6 and the reflective prism on the glacier and shiny, reflective boulders on the

glacier surface, the automatic find and follow mode on the S6 could not be used. This method was slower than using a RTK-dGPS rover as the reflective prism had to be located and 'locked' into view at each survey point. In addition, some areas could not be surveyed including the area of the glacier near the lateral moraines, as the prism on the glacier was not in line-of-sight with the S6 on Kea Point.

Additional methods that were tested

A Lighter-than-air-Helikite with a digital camera was tested to take photographs of the terminus of Mueller Glacier (Figure 9.12). The technique however, was unsuccessful. An array of ground control points (GCP) were marked on the terminus of the glacier with large triangles of blue tarpaulin and orange spray-paint crosses and located with GPS. With the camera set on continuous shoot, the Helikite was deployed and manoeuvred across the terminus. When the photographs were reviewed however, it was found that the majority of the photos did not contain a single GCP (Figure 9.13). Of the few photographs that did contain GCPs (Figure 9.14), it was not possible to determine what GCP was in the photograph and therefore the location of the photograph. Further testing was needed to determine the best method for marking GCPs, which could have involved numbering the GCPs. These numbers however would need to be large enough to see in a photograph taken approximately 50-100 m above the ground and spaced very closely to ensure every photograph contained at least two GCPs. Due to the large spatial area of the terminus of Mueller Glacier, the time it would have taken to adequately mark hundreds of GCPs and the value of the data gathered, it was deemed inappropriate to continue with this method. Another major disadvantage of the Lighter-than-air-Helikite was the need for perfect wind conditions throughout the flight. Once the camera was attached to the kite, the wind needed to be strong enough to lift the helikite off the ground as the helium in the kite was not adequate to lift the camera, even though the weight of the camera was below the maximum weight the kite was designed to lift, according to the manufacturer's instructions. However, in strong winds the kite became very difficult to control once it was a more than 5 m off the ground. In addition, if there was a decrease in wind strength while the kite was in the air, it would descend very quickly to the ground, and if not caught, the camera would make a hard landing on the

ground. The fluctuating wind conditions at Mueller Glacier at the time of the survey made moving the kite around on the terminus very difficult.

Figure 9.12: An example of a photograph taken from a camera attached to the Lighter-than-air-Helikite (source: C. Robertson, 22 November 2009). The image contained a GCP (orange cross in the lower right hand corner) and could also be located (due to the inclusion of the boat and pond). The orange boat is approximately 3 m long.

Figure 9.13: An example of a photograph taken from the Lighter-than-air-Helikite that did not contained a GCP and therefore could not be located (source: C. Robertson, 22 November 2009). The large boulders in the upper and lower centre of the photograph are approximately 5 m in diameter.

Figure 9.14: An example of a photograph taken from the Lighter-than-air-Helikite that contained two GCPs (orange cross in the upper right corner and blue tarpaulin in the lower left corner) (source: C. Robertson, 22 November 2009). The photo could not be located as it was unclear what GCP the two are in the photo. The large boulder in the upper right of the photograph is approximately 5 m in diameter.

Coverage and sources of aerial photographs and satellite images

Aerial photographs and satellite images used to map glacier terminus positions and proglacial lake extents were from a variety of sources. Table 9.1 gives details of what images were used, what glaciers and lakes each image covered and where the image was sourced from.

Table 9.1: Date, type, coverage and source of aerial photographs and satellite images used in this study. New Zealand Aerial Mapping photographs were sourced from Trevor Chinn, Wanaka, New Zealand. The Landsat image was sourced from NASA and the Advanced Spaceborne Thermal Emission and Reflections (ASTER) images were sourced from Wolfgang Rack at the University of Canterbury, New Zealand.

Image date	Image type	Coverage	Source
17 March 1965	Aerial photo	Mueller and Hooker	New Zealand Aerial Mapping
25 February 1965	Aerial photo	Murchison	New Zealand Aerial Mapping
25 February 1965	Aerial photo	Classen, Grey, Maud and Godley	New Zealand Aerial Mapping
3 April 1971	Aerial photo	Mueller and Hooker	New Zealand Aerial Mapping
3 April 1971	Aerial photo	Classen, Grey, Maud and Godley	New Zealand Aerial Mapping
3 April 1971	Aerial photo	Murchison	New Zealand Aerial Mapping
1 March 1973	Aerial photo	Mueller and Hooker	New Zealand Aerial Mapping
1 March 1973	Aerial photo	Murchison	New Zealand Aerial Mapping
24 March 1974	Aerial photo	Classen, Grey, Maud and Godley	New Zealand Aerial Mapping

Image date	Image type	Coverage	Source
14 February 1979	Aerial photo	Mueller and Hooker	New Zealand Aerial Mapping
February 1986	Aerial photo	Murchsion	New Zealand Aerial Mapping
February 1986	Aerial photo	Mueller and Hooker	New Zealand Aerial Mapping
February 1986	Aerial photo	Classen, Grey, Maud and Godley	New Zealand Aerial Mapping
31 March 2001	Satellite image	Mueller, Hooker, Murchison, Classen, Grey, Maud and Godley	Landsat
12 July 2002	Satellite image	Murchison	ASTER
28 April 2004	Satellite image	Hooker	ASTER
4 May 2006	Satellite image	Mueller and Hooker	ASTER
9 May 2006	Satellite image	Murchison	ASTER
11 April 2007	Satellite image	Murchison	ASTER
18 July 2007	Satellite image	Classen, Grey and Maud	ASTER
13 May 2008	Satellite image	Mueller and Hooker	ASTER
18 October 2008	Satellite image	Murchison	ASTER
21 December 2008	Satellite image	Classen, Grey, Maud and Godley	ASTER
19 February 2010	Satellite image	Hooker	ASTER
15 April 2010	Satellite image	Murchison	ASTER
16 February 2011	Satellite image	Hooker	ASTER

MASSEY UNIVERSITY
GRADUATE RESEARCH SCHOOL

STATEMENT OF CONTRIBUTION TO DOCTORAL THESIS CONTAINING PUBLICATIONS

(To appear at the end of each thesis chapter/section/appendix submitted as an article/paper or collected as an appendix at the end of the thesis)

We, the candidate and the candidate's Principal Supervisor, certify that all co-authors have consented to their work being included in the thesis and they have accepted the candidate's contribution as indicated below in the *Statement of Originality*.

Name of Candidate: Clare Robertson

Name/Title of Principal Supervisor: Dr. Ian Fuller

Name of Published Research Output and full reference:
Robertson, C.M., Brook, M.S., Fuller, I.C., Holt, K.A. and Benn, D.I., Glacier retreat and proglacial lake expansion in *Aoraki*/Mount Cook National Park, New Zealand. *Geomorphology.*

In which Chapter is the Published Work: Chapter 3

Please indicate either:

- The percentage of the Published Work that was contributed by the candidate:

  and / or

- Describe the contribution that the candidate has made to the Published Work:

  The candidate completed all the work contained in the manuscript herself, while the co-authors have acted in a supervisory role and assisted in editing.

Candidate's Signature _____ Date _____

Principal Supervisor's signature _____ Date _____

MASSEY UNIVERSITY
GRADUATE RESEARCH SCHOOL

STATEMENT OF CONTRIBUTION TO DOCTORAL THESIS CONTAINING PUBLICATIONS

(To appear at the end of each thesis chapter/section/appendix submitted as an article/paper or collected as an appendix at the end of the thesis)

We, the candidate and the candidate's Principal Supervisor, certify that all co-authors have consented to their work being included in the thesis and they have accepted the candidate's contribution as indicated below in the *Statement of Originality*.

Name of Candidate: Clare Robertson

Name/Title of Principal Supervisor: Dr. Ian Fuller

Name of Published Research Output and full reference:
Robertson, C.M., Benn, D.I., Brook, M.S., Fuller, I.C. and Holt, K.A., in press, Subaqueous calving margin morphology at Mueller, Hooker and Tasman glaciers in *Aoraki*/Mount Cook National Park, New Zealand. *Journal of Glaciology.*

In which Chapter is the Published Work: Chapter 4

Please indicate either:

- The percentage of the Published Work that was contributed by the candidate:

  and / or

- Describe the contribution that the candidate has made to the Published Work:

  The candidate completed all the work contained in the manuscript herself, while the co-authors have acted in a supervisory role and assisted in editing.

Candidate's Signature _____ Date _____

Principal Supervisor's signature _____ Date _____

MASSEY UNIVERSITY
GRADUATE RESEARCH SCHOOL

STATEMENT OF CONTRIBUTION TO DOCTORAL THESIS CONTAINING PUBLICATIONS

(To appear at the end of each thesis chapter/section/appendix submitted as an article/paper or collected as an appendix at the end of the thesis)

We, the candidate and the candidate's Principal Supervisor, certify that all co-authors have consented to their work being included in the thesis and they have accepted the candidate's contribution as indicated below in the *Statement of Originality*.

Name of Candidate: Clare Robertson

Name/Title of Principal Supervisor: Dr. Ian Fuller

Name of Published Research Output and full reference:
Robertson, C.M., Brook, M.S., Fuller, I.C., Benn, D.I. and Holt, K.A., Temporal evolution of the calving terminus at Mueller Glacier, *Aoraki*/Mount Cook National Park, New Zealand. *Geografiska Annaler.*

In which Chapter is the Published Work: Chapter 5

Please indicate either:

- The percentage of the Published Work that was contributed by the candidate:

  and / or

- Describe the contribution that the candidate has made to the Published Work:

The candidate completed all the work contained in the manuscript herself, while the co-authors have acted in a supervisory role and assisted in editing.

Candidate's Signature _____ Date _____

Principal Supervisor's signature _____ Date _____

MASSEY UNIVERSITY
GRADUATE RESEARCH SCHOOL

STATEMENT OF CONTRIBUTION TO DOCTORAL THESIS CONTAINING PUBLICATIONS

(To appear at the end of each thesis chapter/section/appendix submitted as an article/paper or collected as an appendix at the end of the thesis)

We, the candidate and the candidate's Principal Supervisor, certify that all co-authors have consented to their work being included in the thesis and they have accepted the candidate's contribution as indicated below in the *Statement of Originality*.

Name of Candidate: Clare Robertson

Name/Title of Principal Supervisor: Dr. Ian Fuller

Name of Published Research Output and full reference:
Robertson, C.M., Brook, M.S., Holt, K.A., Fuller, I.C. and Benn, D.I., Calving retreat and proglacial lake growth at Hooker Glacier, Southern Alps, New Zealand. *New Zealand Geographer*.

In which Chapter is the Published Work: Chapter 6

Please indicate either:

- The percentage of the Published Work that was contributed by the candidate:

  and / or

- Describe the contribution that the candidate has made to the Published Work:

The candidate completed all the work contained in the manuscript herself, while the co-authors have acted in a supervisory role and assisted in editing.

Candidate's Signature _____ Date _____

Principal Supervisor's signature _____ Date _____